

AD-A244 668



**NAVAL POSTGRADUATE SCHOOL**  
**Monterey, California**

✓  
②



**THESIS**

ENHANCED CONDENSATION OF R-113 ON A  
SMALL BUNDLE OF HORIZONTAL TUBES

by

ROBERT WALTER MAZZONE

December, 1991

Co-Advisor  
Co-Advisor

Paul J. Marto  
Stephen B. Memory



92-01763

Approved for public release; distribution is unlimited

92 1 21 073

Unclassified

security classification of this page

REPORT DOCUMENTATION PAGE				
1a Report Security Classification <b>Unclassified</b>			1b Restrictive Markings	
2a Security Classification Authority			3 Distribution/Availability of Report	
2b Declassification/Downgrading Schedule			Approved for public release; distribution is unlimited.	
4 Performing Organization Report Number(s)			5 Monitoring Organization Report Number(s)	
6a Name of Performing Organization Naval Postgraduate School		6b Office Symbol (if applicable) 34	7a Name of Monitoring Organization Naval Postgraduate School	
6c Address (city, state, and ZIP code) Monterey, CA 93943-5000			7b Address (city, state, and ZIP code) Monterey, CA 93943-5000	
8a Name of Funding/Sponsoring Organization		8b Office Symbol (if applicable)	9 Procurement Instrument Identification Number	
8c Address (city, state, and ZIP code)			10 Source of Funding Numbers	
			Program Element No	Project No
			Task No	Work Unit Accession No
11 Title (include security classification) <b>ENHANCED CONDENSATION OF R-113 ON A SMALL BUNDLE OF HORIZONTAL TUBES</b>				
12 Personal Author(s) <b>ROBERT WALTER MAZZONE</b>				
13a Type of Report Master's Thesis		13b Time Covered From To	14 Date of Report (year, month, day) December, 1991	15 Page Count 235
16 Supplementary Notation The views expressed in this thesis are those of the author and do not reflect the official policy or position of the Department of Defense or the U.S. Government.				
17 Cosati Codes			18 Subject Terms (continue on reverse if necessary and identify by block number)	
Field	Group	Subgroup	Heat Transfer, Condensation, R-113, Inundation, Tube Bundle	
19 Abstract (continue on reverse if necessary and identify by block number)				
<p>Condensation of R-113 was studied using an evaporator/condenser test platform. The condenser section contained four horizontal tubes (nominal outer diameter 15.9 mm) forming a vertical in-line column with a pitch-to-diameter ratio of 2.25 and a condensing length of 1.2 m. The condenser tubes could be operated either individually (ie. as a single tube apparatus) or as a small tube bundle. This allowed investigation of the effects of condensate inundation on different types of condenser tubes. Tubes tested were smooth copper tubes, copper/nickel KORODENSE roped tubes, KORODENSE tubes wrapped with wire, and copper/nickel finned tubes (26 fpi). The outside heat transfer coefficient, <math>h_o</math>, was calculated by experimentally determining the overall heat transfer coefficient, <math>U_o</math>, and then using a modified Wilson Plot procedure. Great care was taken to ensure the results were not vitiated by the presence of noncondensibles.</p> <p>Results obtained with the smooth copper tubes are in agreement with published data and verify satisfactory operation of the test platform. Furthermore, problems associated with the apparatus encountered by previous workers were successfully overcome. In comparison to the top smooth tubes, the copper/nickel top KORODENSE tube yielded about a 22% increase in <math>h_o</math>. When different diameters of wire were wrapped around the copper/nickel KORODENSE tubes, an optimum pitch-to-wire diameter of 7 was found yielding almost a 90% increase in <math>h_o</math>, compared to the top smooth tube. This marked increase is presumably due to surface tension effects thinning the condensate film. The copper/nickel finned tubes gave the best enhancement (approximately a 7 fold increase). Comparison of the data obtained from the top copper/nickel finned tubes agreed well with the model of Beatty and Katz.</p> <p>The effect of condensate inundation was to reduce <math>h_o</math> for the lower tubes compared to the top tube in the bundle. Comparison of <math>h_o</math> for the second tube compared to the top tube showed that the effects of condensate inundation are reduced most by wrapping the KORODENSE tubes with fine wire.</p>				
20 Distribution/Availability of Abstract			21 Abstract Security Classification	
<input checked="" type="checkbox"/> unclassified unlimited <input type="checkbox"/> same as report <input type="checkbox"/> DTIC users			Unclassified	
22a Name of Responsible Individual Paul J. Marto			22b Telephone (include Area code) (408) 646-2768	22c Office Symbol 54Ss

DD FORM 1473, 84 MAR  
security classification of this page

83 APR edition may be used until exhausted

All other editions are obsolete

Unclassified

Approved for public release; distribution is unlimited.

ENHANCED CONDENSATION OF R-113 ON A  
SMALL BUNDLE OF HORIZONTAL TUBES

by

ROBERT WALTER MAZZONE

Lieutenant, United States Navy

B.A., University of California, San Diego, 1971

Ph.D., State University of New York at Buffalo, 1975

Submitted in partial fulfillment of the  
requirements for the degree of

MASTER OF SCIENCE IN MECHANICAL ENGINEERING

from the

NAVAL POSTGRADUATE SCHOOL


December, 1991

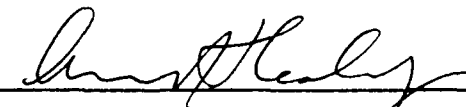
Author:

  
ROBERT WALTER MAZZONE

Approved by:

  
Paul J. Marto, Co-Advisor

  
Stephen B. Memory, Co-Advisor

  
Anthony J. Healey, Chairman,  
Department of Mechanical Engineering

## ABSTRACT

Condensation of R-113 was studied using an evaporator/condenser test platform. The condenser section contained four horizontal tubes (nominal outer diameter 15.9 mm) forming a vertical in-line column with a pitch-to-diameter ratio of 2.25 and a condensing length of 1.2 m. The condenser tubes could be operated either individually (ie. as a single tube apparatus) or as a small tube bundle. This allowed investigation of the effects of condensate inundation on different types of condenser tubes. Tubes tested were smooth copper tubes, copper/nickel KORODENSE roped tubes, KORODENSE tubes wrapped with wire, and copper/nickel finned tubes (26 fpi). The outside heat transfer coefficient,  $h_o$ , was calculated by experimentally determining the overall heat transfer coefficient,  $U_o$ , and then using a modified Wilson Plot procedure. Great care was taken to ensure the results were not vitiated by the presence of noncondensibles.

Results obtained with the smooth copper tubes are in agreement with published data and verify satisfactory operation of the test platform. Furthermore, problems associated with the apparatus encountered by previous workers were successfully overcome. In comparison to the top smooth tubes, the copper/nickel top KORODENSE tube yielded about a 22% increase in  $h_o$ . When different diameters of wire were wrapped around the copper/nickel KORODENSE tubes, an optimum pitch-to-wire diameter of 7 was found yielding almost a 90% increase in  $h_o$ , compared to the top smooth tube. This marked increase is presumably due to surface tension effects thinning the condensate film. The copper/nickel finned tubes gave the best enhancement (approximately a 7 fold increase). Comparison of the data obtained from the top copper/nickel finned tubes agreed well with the model of Beatty and Katz.

The effect of condensate inundation was to reduce  $h_o$  for the lower tubes compared to the top tube in the bundle. Comparison of  $h_o$  for the second tube compared to the top tube showed that the effects of condensate inundation are reduced most by wrapping the KORODENSE tubes with fine wire.



<b>Accession For</b>	
NTIS GRA&I	<input checked="" type="checkbox"/>
DTIC TAB	<input type="checkbox"/>
Unannounced	<input type="checkbox"/>
Justification	
By _____	
Distribution/	
Availability Codes	
Dist	Avail and/or Special
A-1	<div style="border: 1px solid black; width: 50px; height: 50px; margin: 0 auto;"></div>

## TABLE OF CONTENTS

I. INTRODUCTION .....	1
A. BACKGROUND .....	1
B. OBJECTIVES. ....	2
C. SPECIFIC OBJECTIVES .....	3
II. LITERATURE SURVEY .....	4
A. INTRODUCTION .....	4
B. CONDENSATION OF REFRIGERANTS ON SMOOTH TUBES .....	4
C. ENHANCEMENT OF FILM CONDENSATION .....	5
1. Condensation on Single Enhanced Tubes: Theoretical Models .....	5
2. Condensation on Single Enhanced Tubes: Experimental Results .....	9
3. Summary of Single Enhanced Tube Condensation .....	11
4. Condensation on Enhanced Tube Bundles: Theoretical Models .....	12
5. Condensation in Enhanced Tube Bundles: Experimental Studies .....	13
6. Summary of Enhanced Tube Bundle Condensation .....	15
III. EXPERIMENTAL APPARATUS .....	16
A. TEST PLATFORM .....	16
1. Condenser Section .....	16
2. Evaporator Section .....	20
3. Coolant System .....	20
4. Instrumentation .....	21
B. CLEANING AND DECONTAMINATION PROCEDURES .....	22
IV. EXPERIMENTAL PROCEDURES .....	25
A. GENERAL PROCEDURES .....	25
1. Tube Bundle .....	25
2. Single Tube Experiments .....	26
B. SPECIFIC EXPERIMENTS .....	26
1. Baseline Experiments .....	26
2. Enhancement of Inside Heat Transfer Coefficient .....	27

3. Enhancement of Outside Heat Transfer Coefficient. ....	29
V. DATA REDUCTION .....	32
A. DATA ACQUISITION .....	32
B. DATA REDUCTION .....	33
C. MODIFIED WILSON PLOT .....	39
VI. RESULTS AND DISCUSSION .....	41
A. DECONTAMINATION .....	42
B. OVERALL HEAT TRANSFER COEFFICIENT .....	43
1. Smooth Copper Tubes .....	43
2. Copper/Nickel KORODENSE Tubes .....	53
3. Wire Wrapped KORODENSE Tubes .....	62
4. KORODENSE Tubes Wrapped with 0.049" Wire .....	76
5. Copper/Nickel Finned Tubes .....	76
C. OUTSIDE HEAT TRANSFER COEFFICIENT .....	83
1. Smooth Copper Tubes .....	83
2. KORODENSE Tubes .....	94
3. Wire Wrapped KORODENSE Tubes .....	112
4. KORODENSE Tubes Wrapped with 0.049" Wire .....	112
5. Copper/Nickel Finned Tubes .....	123
D. IMPLICATIONS OF PRESENT WORK .....	138
VII. CONCLUSIONS .....	142
A. GENERAL .....	142
B. OVERALL HEAT TRANSFER COEFFICIENT .....	142
C. OUTSIDE HEAT TRANSFER COEFFICIENT .....	142
D. EFFECTS OF CONDENSATE INUNDATION .....	142
VIII. RECOMMENDATIONS .....	144
A. GENERAL RECOMMENDATIONS .....	144
B. EXPERIMENTAL RECOMMENDATIONS .....	144
APPENDIX A. FLOWMETER CALIBRATION .....	145

APPENDIX B. EMF VERSUS TEMPERATURE .....	151
APPENDIX C. PROPERTIES OF ETHYLENE GLYCOL/WATER MIXTURE	153
APPENDIX D. PHYSICAL AND THERMODYNAMIC PROPERTIES OF R-113 .....	158
APPENDIX E. SAMPLE CALCULATION .....	164
APPENDIX F. UNCERTAINTY ANALYSIS FOR $U_o$ .....	171
APPENDIX G. PROGRAM LISTING .....	178
LIST OF REFERENCES .....	213
INITIAL DISTRIBUTION LIST .....	220

## LIST OF TABLES

Table 1. THERMOCOUPLE CHANNEL ASSIGNMENTS. ....	32
Table 2. SUMMARY OF EXPERIMENTAL RUNS .....	41
Table 3. SUMMARY OF AREA RATIO CALCULATIONS .....	141
Table 4. MASS FLOW RATE (KG/SEC) AT 0 AND 24 C. ....	145
Table 5. FLOWMETER CALIBRATION REGRESSION RESULTS. ....	146
Table 6. LEADING COEFFICIENTS FOR CONVERSION OF EMF TO TEMPERATURE. ....	151
Table 7. EMF AND TEMPERATURES FOR RUN 1 DATA SET SM06. ....	164
Table 8. SUMMARY OR RESULTS FOR SAMPLE UNCERTAINTY ANALYSIS. ....	177



## LIST OF FIGURES

Figure 1.	Schematic diagram of test platform. ....	17
Figure 2.	Photograph of the evaporator/condenser test platform. ....	18
Figure 3.	Schematic diagram of condenser showing shroud. ....	19
Figure 4.	Twisted tape insert and HEATEX radial mixing element. ....	28
Figure 5.	Copper/nickel finned tube, Korodense tube, Wire wrapped tube. ....	31
Figure 6.	HITRAN correlation for 13.26 mm elements ....	36
Figure 7.	HITRAN correlation for 10.16 mm elements ....	37
Figure 8.	Bundle run on smooth copper tubes without inserts. ....	45
Figure 9.	Single tube run on smooth copper tubes without inserts. ....	46
Figure 10.	Smooth copper tubes with tape insert operated as a bundle. ....	47
Figure 11.	Data from Mabrey,[Ref. 2]. ....	48
Figure 12.	Smooth copper tubes with tape insert operated individually. ....	49
Figure 13.	Smooth copper tubes with HEATEX inserts. Bundle operation. ....	51
Figure 14.	Smooth copper tubes with HEATEX installed. Individual operation. ..	52
Figure 15.	Repeat run on smooth copper tubes with HEATEX insert. ....	54
Figure 16.	Repeat run on smooth copper tube with HEATEX. Individual runs. ..	55
Figure 17.	Effect of tube inserts on $U_o$ . ....	56
Figure 18.	KORODENSE tubes with no insert, bundle operation. ....	58
Figure 19.	KORODENSE tubes operated individually, no inserts installed. ....	59
Figure 20.	KORODENSE tubes with tape inserts, bundle operation. ....	60
Figure 21.	KORODENSE tubes with tape inserts, individual operation. ....	61
Figure 22.	KORODENSE tubes with HEATEX inserts, bundle operation. ....	63
Figure 23.	KORODENSE tubes with HEATEX inserts, individual operation. ....	64
Figure 24.	Effect of tube inserts on $U_o$ . ....	65
Figure 25.	Effect of wire diameter on $U_o$ for tube A. ....	66
Figure 26.	Effect of wire diameter on $U_o$ for tube B. ....	67
Figure 27.	Effect of wire diameter on $U_o$ for tube C. ....	68
Figure 28.	Effect of wire diameter on $U_o$ for tube D. ....	69
Figure 29.	Effect of no wire on $U_o$ for all tubes. ....	71
Figure 30.	Effect of 0.029" wire on $U_o$ for all tubes. ....	72
Figure 31.	Effect of 0.049" wire on $U_o$ for all tubes. ....	73

Figure 32. Effect of 0.0675" wire on $U_o$ for all tubes. . . . .	74
Figure 33. $U_o$ as a function of wire diameter for the four tubes. . . . .	75
Figure 34. 0.049" wire wrapped KORODENSE tubes, bundle operation, expt. 1. . .	77
Figure 35. 0.049" wire wrapped KORODENSE tubes, bundle operation, expt. 2. . .	78
Figure 36. 0.049" wire wrapped KORODENSE tubes, individual runs, expt. 1. . .	79
Figure 37. 0.049" wire wrapped KORODENSE tubes, individual runs, expt. 2. . .	80
Figure 38. Copper/nickel finned tubes, no insert, bundle operation. . . . .	81
Figure 39. Copper/nickel finned tubes, no insert, individual operation. . . . .	82
Figure 40. Copper/nickel finned tubes, tape insert, bundle operation. . . . .	84
Figure 41. Copper/nickel finned tubes, tape insert, individual operation. . . . .	85
Figure 42. Copper/nickel finned tubes, HEATEX insert, bundle operation. . . . .	86
Figure 43. Copper/nickel finned tubes, HEATEX insert, individual operation. . . .	87
Figure 44. Summary of effect of tube inserts on $U_o$ . . . . .	88
Figure 45. Smooth Copper tubes, tape insert, bundle operation. . . . .	90
Figure 46. Smooth Copper tubes, tape insert, individual operation. . . . .	91
Figure 47. Smooth Copper tubes, HEATEX insert, bundle operation. . . . .	92
Figure 48. Smooth Copper tubes, HEATEX insert, individual operation. . . . .	93
Figure 49. Effect of tape insert on $h_o$ and $h_i$ . . . . .	95
Figure 50. Effect of HEATEX insert on $h_o$ and $h_i$ . . . . .	96
Figure 51. Local $h_o$ for tape insert. . . . .	97
Figure 52. Local $h_o$ for HEATEX element. . . . .	98
Figure 53. Average $h_o$ for tape insert. . . . .	99
Figure 54. Average $h_o$ for HEATEX element. . . . .	100
Figure 55. KORODENSE tubes, tape insert, bundle operation. . . . .	102
Figure 56. KORODENSE tubes, tape insert, individual operation. . . . .	103
Figure 57. KORODENSE tubes, HEATEX insert, bundle operation. . . . .	104
Figure 58. KORODENSE tubes, HEATEX insert, individual operation. . . . .	105
Figure 59. Effect of tape insert on $h_o$ and $h_i$ . . . . .	106
Figure 60. Effect of HEATEX insert on $h_o$ and $h_i$ . . . . .	107
Figure 61. Local $h_o$ for tape insert. . . . .	108
Figure 62. Local $h_o$ for HEATEX element. . . . .	109
Figure 63. Average $h_o$ for tape insert. . . . .	110
Figure 64. Average $h_o$ for HEATEX element. . . . .	111
Figure 65. Effect of wire diameter on $h_o$ for tube A. . . . .	113
Figure 66. Effect of wire diameter on $h_o$ for tube B. . . . .	114

Figure 67. Effect of wire diameter on $h_o$ for tube C. ....	115
Figure 68. Effect of wire diameter on $h_o$ for tube D. ....	116
Figure 69. Effect of no wire on $h_o$ for all tubes. ....	117
Figure 70. Effect of 0.029" wire on $h_o$ for all tubes. ....	118
Figure 71. Effect of 0.049" wire on $h_o$ for all tubes. ....	119
Figure 72. Effect of 0.0675" wire on $h_o$ for all tubes. ....	120
Figure 73. 0.049" wire wrapped KORODENSE tubes, bundle operation, expt. 1. .	121
Figure 74. 0.049" wire wrapped KORODENSE tubes, bundle operation, expt. 2. .	122
Figure 75. 0.049" wire wrapped KORODENSE, individual runs, expt. 1. ....	124
Figure 76. 0.049" wire wrapped KORODENSE, individual runs, expt. 2. ....	125
Figure 77. Average $h_o$ wire wrapped KORODENSE, expt. 1. ....	126
Figure 78. Average $h_o$ wire wrapped KORODENSE, expt. 2. ....	127
Figure 79. Local $h_o$ wire wrapped KORODENSE, expt. 1. ....	128
Figure 80. Local $h_o$ wire wrapped KORODENSE, expt. 2. ....	129
Figure 81. $h_o$ for copper/nickel finned tubes, tape insert. ....	130
Figure 82. $h_o$ for copper/nickel finned tubes, HEATEX insert. ....	131
Figure 83. Average $h_o$ for Cu/Ni finned tubes, tape insert. ....	133
Figure 84. Average $h_o$ for Cu/Ni finned tubes, HEATEX insert. ....	134
Figure 85. Local $h_o$ for Cu/Ni finned tubes, tape insert. ....	135
Figure 86. Local $h_o$ for Cu/Ni finned tubes, HEATEX insert. ....	136
Figure 87. Experimental data (tape insert) vs. Beatty/Katz model. ....	139
Figure 88. Experimental data (HEATEX insert) vs. Beatty/Katz model. ....	140
Figure 89. Calibration for flowmeter A. ....	147
Figure 90. Calibration for flowmeter B. ....	148
Figure 91. Calibration for flowmeter C. ....	149
Figure 92. Calibration for flowmeter D. ....	150
Figure 93. EMF versus temperature. ....	152
Figure 94. Density of ethylene glycol/water mixture. ....	154
Figure 95. Kinematic viscosity of ethylene glycol/water mixture. ....	155
Figure 96. Thermal heat capacity of ethylene glycol/water mixture. ....	156
Figure 97. Thermal conductivity of ethylene glycol/water mixture. ....	157
Figure 98. Heat capacity versus temperature for R-113. ....	159
Figure 99. Viscosity as a function of temperature for R-113. ....	160
Figure 100. Thermal Conductivity of R-113 as function of temperature. ....	161
Figure 101. Density as a function of temperature for R-113. ....	162

Figure 102. Latent heat versus temperature for R-113. ....	163
Figure 103. Computer printout of results for run 1 data set SM06. ....	170

## NOMENCLATURE

### Standard Symbols

$A$	area, $m^2$
$b$	fin spacing, m
$C_b$	parameter defined in Eq (2-11)
$C_p$	specific heat, J/kg K
$D$	diameter, m
$e$	fin height, m
$g$	gravitational acceleration, $m/s^2$
$h$	heat transfer coefficient, $W/m^2 K$
$h_b$	heat transfer coefficient in flooded portion of finned tube, $W/m^2 K$
$h_h$	heat transfer coefficient in unflooded region of finned tube, $W/m^2 K$
$h_f$	heat transfer coefficient for fins in unflooded region, $W/m^2 K$
$k$	thermal conductivity, $W/m K$
$L$	length, m
$\bar{L}$	average condensing length defined by Eq (2-4)
$m$	mass flow rate, kg/s
$N$	number of tubes in a vertical column
$Nu$	Nusselt number
$Pr$	Prandtl number
$q$	heat transfer rate, W
$q''$	heat flux, $W/m^2$
$R$	radius, m
$R_f$	fouling resistance, $K/W$
$R_w$	wall resistance, $K/W$
$Re$	Reynolds number
$Re_f$	film Reynolds number
$T$	temperature, K
$t$	fin thickness, m
$U$	overall heat transfer coefficient, $W/m^2 K$

$V$  velocity, m/s

#### Greek Symbols

$\delta$  tape thickness, m  
 $\eta$  fin efficiency  
 $\xi$  aspect ratio of condensate surface, Eq (2-13)  
 $\Theta_m$  rotation angle normal to fin surface  
 $\mu$  dynamic viscosity, kg/m s  
 $\rho$  density, kg/m<sup>3</sup>  
 $\sigma$  surface tension, N/m  
 $\phi_f$  flooding angle defined in Eq (2-7)

#### Subscripts

c coolant  
eq equivalent  
ef effective  
f film  
fs fin sides  
ft fin tips  
i inside or inlet  
o outside or outlet  
r root  
sat saturation

## I. INTRODUCTION

### A. BACKGROUND

In the last few years, budgetary considerations have led to a reduction in the funding level available for new vessel construction for the US Navy. In construction of ships, weight can often be equated to cost. This has led the Navy to look at various ways by which the weight of auxiliary systems can be reduced.

Of particular interest to the Navy has been the issue of reduced weight and therefore cost of refrigeration systems. Two major components of refrigeration systems are the evaporator and condenser. If the weight of these two components can be reduced, then the overall weight and presumably cost, can also be reduced.

Condenser weight can be significantly reduced by the proper selection of materials for condenser construction. A major weight savings comes from changing the material which is used for construction of the condenser tubes. As an example, the DDG-51 was originally intended to have a refrigeration condenser made of titanium finned tubes. This would provide a substantial weight savings and a reduced cost (presumably). However, the system was not installed on the current flight of ships. Rather, traditional copper/nickel finned tubes were utilized for the refrigeration condenser.<sup>1</sup>

In re-designing refrigeration condensers, changes in condenser tube material based solely on weight consideration should not be the only consideration. The reason for this is that a lightweight material may not have heat transfer characteristics which are comparable to copper or even copper/nickel. Therefore, condenser tube designs have to be developed to maintain or even enhance heat transfer or else the condenser will have to be enlarged. This enlargement is necessary in order to provide the requisite surface area to maintain the required level of heat transfer.

Copper/nickel finned condenser tubes have been used in refrigeration condensers onboard US Navy ships for many years. However, the use of titanium, as was planned for the DDG-51 class ships, holds the promise of providing substantial weight savings (not to mention improved corrosion resistance on the tube side). Unfortunately, titanium has a thermal conductivity which is substantially less than that of copper or copper/nickel. The question which must therefore be addressed is whether titanium

---

<sup>1</sup> According to Mr. John Goodhue, NAVSEA code SEA 56Y15, the reason the units were not installed was that they could not be ready to support proposed construction dates for flight one.

condenser tubes can be constructed in such a manner as to maintain heat transfer (due to enhancement) despite the lower value of thermal conductivity.

A major problem along these lines is how to measure the performance of various types of condenser tubes. Typically, this is done with single tubes or small tube bundles. These tubes tend to be relatively short. Often, the experimental apparatus bears little resemblance to a shipboard condenser. Thus, any results become suspect when they are extended to the real situation.

In order to examine heat transfer characteristics of various designs of condenser tubes, the best means is to construct a test platform composed of an evaporator and condenser with a size comparable to that of a shipboard system. Unfortunately, this is seldom feasible due to costs involved and the size of the plants. However, it is possible to construct a reasonably large scale test platform in which tube performance can be evaluated. This evaluation must include both single tube performance as well as tube bundle operation. The reason for this is that condensate forming on one tube falls onto lower tubes. This effect, known as condensate inundation, can result in decreased heat transfer on lower tubes due to a thickening of the condensate layer. Hence, another aspect which must be considered is whether condenser tube geometry can be changed in such a manner as to reduce the adverse effects of condensate inundation. This could help make up for decreased thermal conductivity associated with lightweight materials such as titanium.

The construction of a suitable condenser/evaporator test platform was begun at the Naval Postgraduate School by Zebrowski [Ref. 1]. The construction and initial operation of the test platform was completed by Mabrey [Ref. 2] in 1988. Mabrey conducted experiments using R-113 and R-114 on smooth copper tubes as well as copper/nickel finned tubes (26 fpi). During the course of his experiments, an orange-peel or dimpled appearance was observed on the smooth copper tubes. Additionally, the copper/nickel finned tubes showed a buildup of "material" between the fins. This material was believed to be ice although this was not proved. The cause of the orange-peel appearance was also never identified.

## **B. OBJECTIVES.**

This thesis concentrates on the condenser section of the test platform with specific interest in the condensation of R-113. R-113 was chosen for this study because of convenience, i.e., it is a liquid at atmospheric pressure. The condenser section consists of four horizontal tubes mounted in a vertical in-line column. The nominal diameter of



the tubes is 16 mm with a condensing length of 1.2 m. While the condensing medium used in this study was R-113, the condensation of many different types of fluids can be evaluated. In addition, the condenser can be used to study heat transfer on almost any type of condenser tube subject to the nominal outer diameter and condensing length restrictions indicated.

The main objective of this thesis was to resolve the contamination problem found by Mabrey [Ref. 2], and to make the test platform operational. It was felt that such a system, once operational, could be used to study heat transfer using condenser tubes made of various materials and geometries. In addition, since the tubes are arranged in a vertical in-line column, the effect of condensate inundation could also be studied.

### **C. SPECIFIC OBJECTIVES**

The specific objectives of this study were as follows:

1. Resolve the contamination problem reported by Mabrey [Ref. 2]
2. Establish baseline condensation data by examining the condensation of R-113 on smooth copper tubes.
3. Examine the heat transfer characteristics of R-113 on various tube geometries
4. Investigate the effects of condensate inundation

## II. LITERATURE SURVEY

### A. INTRODUCTION

Condensation occurs when vapor molecules come into contact with a surface which has a temperature below the vapor saturation temperature. This vapor, coming into contact with the cooler surface, forms a liquid which can accumulate in two ways. If the liquid wets the entire surface, a continuous film of liquid is formed. On the other hand, if the liquid fails to wet the entire surface, droplets are formed. These two types of condensation are referred to as filmwise and dropwise condensation respectively. Dropwise condensation yields larger heat transfer coefficients but is difficult to maintain [Ref. 3]. All condensers today are therefore designed to operate with film condensation conditions.

In 1916, Nusselt [Ref. 4] reasoned that as vapor condenses on a cooler surface, such as a horizontal tube, a continuous film of condensate will form. This film grows in thickness as the condensate flows around the tube under the influence of gravity. Hence, the thickness of the condensate is not uniform around a horizontal tube. Since the condensate acts as a resistance to heat transfer, Nusselt argued that the local heat transfer coefficient will be a maximum at the top of the tube where the film thickness is least and decreases around the tube as the condensate thickness increases.

### B. CONDENSATION OF REFRIGERANTS ON SMOOTH TUBES

Goto et al. [Ref. 5] examined film condensation of various refrigerants, including R-113, on smooth copper tubes. Their results showed values for the vapor-side heat transfer coefficient on the order of 1.2 to 1.5  $kW/m^2 K$  for a wall-film temperature difference of 3 to 25 K. Furthermore, their results were about 10% below that predicted by Nusselt theory.

Masuda and Rose [Ref. 6,7] reported that condensation of R-113 on smooth copper tubes yielded an outside heat transfer coefficient of about 1500  $W/m^2 K$  for wall-film temperature differences of 12 to 20 K. Their results showed good agreement with Nusselt theory.

Marto et al. [Ref. 8] showed that for condensation of R-113 on smooth copper tubes, the vapor-side heat transfer coefficient was on the order of 1000  $W/m^2 K$  for a temperature drop across the film of 20 to 25 K. Their values were also in good agreement with Nusselt theory.

### C. ENHANCEMENT OF FILM CONDENSATION

The most commonly used procedure for enhancement of film condensation is through the use of integral-fin tubes. With this type of condenser tube, two distinct regions exist; namely, a flooded and an unflooded region. Typically, as fluid condenses on a finned surface, it is pulled from the fin tip to the fin root by surface tension forces. Gravity then causes the fluid between fins to drain to the bottom of the tube where it drains off. Hence, condensation on a finned tube involves a combination of surface tension and gravity forces. It is the added surface tension which tends to enhance heat transfer over smooth tubes by thinning the condensate film at the fin tip.

Since the present study uses R-113 as the working fluid, the remainder of this chapter will focus on previous experiments which have used low surface tension fluids such as refrigerants. For additional information involving other fluids, the reader is referred to recent review articles by Marto [Ref. 9,10], Webb [Ref. 11] and Sukhatme [Ref. 12].

#### 1. Condensation on Single Enhanced Tubes: Theoretical Models

The first theoretical model of condensation on finned tubes was published by Beatty and Katz [Ref. 13]. Their theoretical model is given by:

$$h_{BK} = \eta_f h_f \frac{A_f}{A_{ef}} + h_u \frac{A_u}{A_{ef}} \quad (2-1)$$

Here  $\eta_f$  is the fin efficiency,  $A_f$  is the fin surface area,  $A_u$  is the unfinned surface area, and  $A_{ef}$  is the effective total surface area. The above equation can be simplified to:

$$h_{BK} = 0.689 \left[ \frac{k_f^3 \rho_f^2 g h_{fg}}{\mu_f \Delta T D_{eq}} \right]^{\frac{1}{4}} \quad (2-2)$$

where the equivalent diameter is given by:

$$\left( \frac{1}{D_{eq}} \right)^{\frac{1}{4}} = 1.30 \eta_f \frac{A_f}{A_{ef}} \frac{1}{\bar{L}^{1/4}} + \frac{A_o}{A_{ef}} \frac{1}{D_r^{1/4}} \quad (2-3)$$

In this equation,

$$\bar{L} = \frac{\pi(D_o^2 - D_r^2)}{4D_o} \quad (2-4)$$

and

$$A_{ef} = \eta_f A_f + A_u \quad (2-5)$$

The equation for the heat transfer coefficient is a Nusselt-type condensation equation based on the equivalent diameter for a finned tube. This equation predicted the experimental results obtained by Beatty and Katz to within  $\pm 20\%$ .

There are several important limitations to the Beatty and Katz model [Ref. 13]. It does not distinguish between fin tips and fin flanks, essentially assuming that the fins have no thickness. Therefore the model is not suitable for trapezoidal fins. A second, and perhaps more significant limitation is that the Beatty and Katz model fails to take into account surface tension effects. Instead, the model assumes that the flow of the condensate film is simply a function of gravity. While this may not pose a serious limitation when low surface tension fluids such as refrigerants are examined, this assumption can become critical when condensation of high surface tension fluids such as steam are investigated.

Another limitation of the Beatty and Katz model is that it does not take into account condensate flooding. Rudy and Webb [Ref. 14] argued that the flooded portion of the tube was ineffective in condensation. They therefore proposed that the Beatty and Katz model be modified by:

$$h_{RW} = h_{BK} \frac{\phi_f}{\pi} \quad (2-6)$$

where  $\phi_f$ , the flooding angle, is defined as:

$$\phi_f = \cos^{-1} \left[ \left[ \frac{2\sigma \cos \psi}{\rho g b R_o} \right] - 1 \right] \quad (2-7)$$

where  $R_o$  is the outside radius,  $\psi$  is the fin tip half angle and  $\sigma$  is the fluid surface tension. It is interesting to note that this modification resulted in an underprediction of Rudy and Webb's R-11 condensation data by about 35%.

Webb et al. [Ref. 15] next argued that surface tension drainage must be considered in the model. They derived the equation:

$$h_f = 0.943 \left[ \frac{k_f^3 \rho h_{fg}}{\mu_f \Delta T} \right]^{\frac{1}{4}} \left[ \frac{2\sigma}{e^2} \left( \frac{1}{t} + \frac{1}{b} \right) \right]^{\frac{1}{4}} \quad (2-8)$$

where  $e$  is the fin height,  $t$  is the fin thickness and  $b$  is the width of the space between the fins. Substitution into the Beatty and Katz expression yielded agreement with experimental data of  $\pm 10\%$ .

Owen et al. [Ref. 16] argued that the Rudy and Webb [Ref. 15] model had to be corrected in order to account for heat transfer in the flooded part of the tube. Owen et al. proposed the equation:

$$h_o = h_{BK} \frac{\phi_f}{\pi} + h_b \left( 1 - \frac{\phi_f}{\pi} \right) \quad (2-9)$$

where  $h_o$  is the average outside heat transfer coefficient and  $h_b$  is the heat transfer coefficient in the flooded region of the tube. This value was estimated using a one-dimensional radial conduction model. This corrected model of Owen et al. resulted in agreement of  $\pm 30\%$  with earlier experimental data.

In 1985, Webb et al. [Ref. 17] proposed a model that included heat transfer in the flooded region as well as surface tension drainage on the fin flanks and gravity drainage on the interfin surface. Their model equation for the average heat transfer coefficient is:

$$h_w = (1 - C_B) \left[ h_h \frac{A_r}{A} + h_f \eta_f \frac{A_f}{A} \right] + C_B h_B \quad (2-10)$$

In this expression,  $h_h$  is the heat transfer coefficient for the unflooded root surface between the fins and  $h_f$  is the heat transfer coefficient on the fin flanks in the unflooded area, and  $h_b$  is the heat transfer coefficient in the condensate flooded region. The term  $C_B$  is the fraction of finned tube surface flooded by condensate, or,

$$C_B = 1 - \frac{\phi_f}{\pi} \quad (2-11)$$

where  $\phi_f$  is the flooding angle given in equation (2-7).

In the Webb et al. [Ref. 17] expression for the average heat transfer coefficient,  $h_h$ ,  $h_f$  and  $h_b$  are defined mathematically as follows:

$$h_h = 1.514 \left[ \frac{\mu_f^2}{k_f^2 \rho_f^2 g} Re_f \right]^{-\frac{1}{3}} \quad (2-12)$$

where  $Re_f$  is the condensate film Reynolds number.

$$h_f = 2.149 \frac{k_f}{S_m} \left[ \frac{\sigma \rho_f h_{fg} \Theta_m S_m}{\mu_f k_f \Delta T} \frac{(\xi + 1)}{(\xi + 2)^3} \right]^{\frac{1}{4}} \quad (2-13)$$

where  $S_m$  is the length of the convex surface and  $\Theta_m$  is the rotation angle normal to the fin surface [Ref. 18]. The term  $\xi$  is a parameter that characterizes the aspect ratio of the condensate surface.

Finally,  $h_b$  is defined as:

$$h_b = \frac{\phi k}{e} \quad (2-14)$$

This complex model of Webb et al. was able to predict heat transfer coefficients to within  $\pm 20\%$  of experimental data obtained with R-11.

Honda and Nozu [Ref. 19] and Honda et al. [Ref. 20] have proposed the most comprehensive model to date. This model treats the heat transfer problem as one involving vapor-to-coolant heat transfer through a finned tube wall. In this model, trapezoidal fins were divided into flooded (f) and unflooded (u) regions. Equation (2-7) was used to determine the flooding angle. Condensate flow in between the fins was assumed to be driven by gravity whereas for the fin surface, condensate flow was assumed to be driven by both surface tension forces and gravity. The condensate film thickness on the fin surface was arbitrarily divided into a thick region, where no heat transfer occurred, and a thin film region. The equation of the condensate film thickness was solved numerically.

Honda and Nozu [Ref. 19] showed that the average Nusselt number could be written in terms of relevant parameters for the flooded (f) and unflooded (u) regions as:

$$Nu_d = \frac{h d_o}{k_l} = \frac{Nu_{du} \eta_u (1 - \tilde{T}_{wu}) \tilde{\phi}_f + Nu_{df} \eta_f (1 - \tilde{T}_{wf}) (1 - \tilde{\phi}_f)}{(1 - \tilde{T}_{wu}) \tilde{\phi}_f + (1 - \tilde{T}_{wf}) (1 - \tilde{\phi}_f)} \quad (2-15)$$

Here,  $\tilde{T}_{wu}$  and  $\tilde{T}_{wf}$  are the dimensionless average wall temperatures at the fin root and  $\tilde{\phi}_f$  is defined as:

$$\tilde{\phi}_f = \frac{\phi_f}{\pi} \quad (2-16)$$

It should be pointed out that  $\bar{T}_{w,u}$  and  $\bar{T}_{w,f}$  are determined by solving a circumferential wall heat conduction equation. This wall temperature variation must be considered since heat transfer rates through flooded and unflooded regions are very different.

Honda and Nozu [Ref. 19] used their model to predict average heat transfer coefficients. These predictions were compared to experimental data on eleven different fluids and twenty-two tubes. The predicted values matched most experimental values to within  $\pm 20\%$ .

## **2. Condensation on Single Enhanced Tubes: Experimental Results**

The first experiments conducted on enhanced tubes were performed by Katz and colleagues [Ref. 21,22, 13 ]. These authors looked at condensation of R-12 and R-22 on smooth and finned tubes. Their results showed a significant enhancement in heat transfer for finned tubes.

In 1971, Karkhu and Borovkov [Ref. 23] examined condensation of R-113 on five finned tubes. Their results showed that the rate of condensation for these tubes with trapezoidal fins could be increased by 50 to 100% over smooth tubes.

Arai et al. [Ref. 24] and Kisaragi et al. [Ref. 25] studied the condensation of R-12 and R-113 respectively on finned tubes with spiral grooves cut along the length of the tube. Arai et al. showed that grooves with a pitch of 0.7 mm gave the best enhancement in heat transfer. Kisaragi and co-workers also compared grooved finned tubes with tubes on which the fins had been covered with a porous coating. In comparison to the finned tube, a two fold enhancement was seen with the grooved finned tube while a four fold enhancement was obtained with the finned porous coated tube.

Carnavos [Ref. 26] performed one of the first detailed studies of condensation of R-11 on enhanced copper tubes. In this study, eleven different tubes were tested. The tubes included finned tubes as well as finned tubes which had an axial spiral groove cut along their length. Various sizes and shapes of fins were included. Enhancements of 4 to 6 were seen when compared to smooth tubes.

Rudy [Ref. 27] and Webb et al. [Ref. 15] reported experimental data obtained for R-11 condensing on copper tubes with different fin geometries. Their results showed that increasing the fin density from 748 to 1378 fpm resulted in about a 70% increase in heat transfer presumably due to an increased surface area.

Honda et al. [Ref. 28] studied condensation of R-113 on copper finned tubes of various fin density. Their results showed a 6 to 9 fold enhancement for R-113 condensation for finned tubes when compared to smooth tubes. A similar study by Kabov [Ref. 29] examined the condensation of R-12 and R-22 on tubes with different fin

densities His results also showed that the degree of enhancement is determined by fin spacing.

Masuda and Rose [Ref. 6] examined heat transfer for the condensation of R-113 on low integral-fin copper tubes. Fourteen different fin spacings (0.25 to 20 mm) were examined. The optimal fin spacing was 0.5 mm which resulted in a 7.3 fold enhancement in the vapor-side heat transfer coefficient.

Lin and Berghmans [Ref. 30] examined condensation of R-11, R-113, and R-114 on an enhanced tube. This enhanced tube, known commercially as "EVERFIN", is made of trapezoidal fins (1378 fpm) with a spacing between the fins of 0.064 mm.<sup>2</sup> This tube gave an 8 to 10 fold increase in the vapor-side heat transfer coefficient when compared to a smooth tube.

Condensation of R-11 on a variety of enhanced copper tubes has been reported recently by Sukhatme et al. [Ref. 31]. All tubes had trapezoidal shaped integral fins. The fin density, fin height and fin-tip half angle were systematically varied in order to determine the optimal values which would result in maximum enhancement. The maximum enhancement obtained by these authors was about 10.3 relative to smooth tubes. This enhancement corresponded to a fin spacing of 0.35 mm, a fin height of 1.22 mm and a fin-tip half angle of 10 degrees. In addition, a set of specially enhanced tubes were tested by these authors. These tubes had axial grooves cut into them with the trapezoidal fins present. An enhancement of 12.3 was obtained with these specially enhanced tubes when compared to smooth tubes.

Marto et al. [Ref. 8] studied condensation of R-113 on a variety of copper integral-fin tubes with rectangularly shaped fins. The optimum fin spacing was found to lie between 0.25 and 0.5 mm. The vapor-side heat transfer coefficient was enhanced on the order of 4 to 7 fold.

Michael et al. [Ref. 32] continued the studies of Marto et al. [Ref. 8] by looking at the effect of root diameter on the condensation of R-113 on integral-fin tubes. They found that the root diameter had only a negligible effect on heat transfer enhancement. In addition, these investigators found that the optimal fin spacing was about 0.5 mm. They obtained an enhancement of 5 to 6.

---

<sup>2</sup> While the authors quote a fin spacing of 0.064 m, this value seems too small. The schematic diagram of the fins together with other dimensions published by these authors tend to suggest that the correct fin spacing is 0.64 mm. This value is more in line with values quoted by other authors.



In comparing enhancements reported by various authors, a word of caution is required. In calculating values for the vapor-side heat transfer coefficients, the surface area to be used in this calculation must be defined. This area can be based on outside or envelope diameter, root diameter or total fin area. The great majority of authors define this area by the outside diameter of the tube as opposed to the root diameter. In the various sources cited above, this has been the case. That is, the surface area has been defined by the outside tube diameter.

While it is clear that integral-fin tubes can result in an enhancement of the vapor-side heat transfer coefficient, other alternatives exist. As an example, Fujii et al. [Ref. 33] studied the condensation of R-11 on smooth tubes which were wrapped with fine wire. These authors found an optimal pitch-to-wire diameter ratio of 2 which resulted in an enhancement of 2.5 in the vapor-side heat transfer coefficient when compared to copper smooth tubes. These authors argued that the enhancement in the heat transfer coefficient was due to a thinning of the condensate film. The reason that the condensate film thickness is reduced is that the presence of the wire creates a low pressure region in the film near the base of the wires. This low pressure region is due to the concave shape of the condensate film next to the wire. As a result, condensate film is pulled along the tube wall towards the wire. This results in a thinning of the condensate film between the wires.

### **3. Summary of Single Enhanced Tube Condensation**

It is clear from the preceding discussion that theoretical models, despite their degree of sophistication, still only match experimental data to within  $\pm 20\%$ . This suggests that the process of condensation on enhanced tubes is extremely complex and far from being fully understood.

In terms of experimental data involving condensation of refrigerants on enhanced tubes, several comments need to be made. The experiments reported here have shown that integral-fin tubes can give enhancements of the vapor-side heat transfer coefficient on the order of 7 to 12. The magnitude of this enhancement depends upon such factors as fin shape, fin spacing, and fin height. Trapezoidal shaped fins with a spacing of 0.5 mm give the highest enhancements.

Unfortunately, the above experiments were all performed on enhanced tubes made of copper. In Naval refrigeration systems, where seawater is used as the coolant, corrosion is of major concern. This necessitates the need for copper nickel or titanium condenser tubes in order to minimize corrosion. However, as can be seen from the foregoing summary of the literature, essentially no work has been done on the

condensation of refrigerants on copper/nickel or titanium finned tubes. Since both copper/nickel and titanium condenser tubes have a lower thermal conductivity than copper, one must wonder what effect this will have on the vapor-side heat transfer coefficient. Clearly, experiments using these tubes must be carried out.

#### 4. Condensation on Enhanced Tube Bundles: Theoretical Studies

Condensation in tube bundles presents an entirely different situation than condensation on single tubes. In a tube bundle, two conflicting factors come into play. First, condensate forming on an upper tube drains off this tube onto lower tubes within the bundle. This increases the thickness of the condensate layer on lower tubes which further increases the resistance of these tubes to heat transfer. This effect is referred to as condensate inundation.

Condensate falling from one tube to another can have a second effect. As droplets fall from one tube to the next, ripples and splashing (turbulence) are induced in the condensate film. This can actually enhance heat transfer on the lower tubes.

Vapor velocity can also be a significant factor in tube bundle condensation. As the vapor travels into the tube bundle and condenses, the local velocity decreases. This decrease in local velocity leads to a decrease in the heat transfer coefficient similar to an inundation effect since vapor shear effects that thin the condensate film are reduced.

In analyzing condensation in horizontal tube bundles, Nusselt [Ref. 4] assumed that all condensate flowed from one tube to another as a continuous laminar sheet. He showed that the ratio of the average heat transfer coefficient for a vertical column of horizontal tubes with respect to the top tube could be expressed as:

$$\frac{\bar{h}_N}{h_1} = N^{-\frac{1}{4}} \quad (2-17)$$

where  $N$  is the number of tubes in the vertical column. A local coefficient can also be calculated for the  $N$ th tube using Nusselt theory. This coefficient is given by:

$$\frac{h_N}{h_1} = N^{\frac{3}{4}} - (N-1)^{\frac{3}{4}} \quad (2-18)$$

Kern [Ref. 34] proposed a less conservative approach. He argued that droplets of condensate falling from one tube to another causes ripples which disturb the condensate film, thereby diminishing the effect of condensate inundation. His mathematical model took the form:

$$\frac{\bar{h}_N}{h_1} = N^{-\frac{1}{6}} \quad (2-19)$$

The local value of  $h$  for the  $N$ th tube can be expressed as:

$$\frac{h_N}{h_1} = N^{\frac{5}{6}} - (N-1)^{\frac{5}{6}} \quad (2-20)$$

In 1972, Eissenberg [Ref. 35] proposed that condensate may not drain only in a vertical direction, but rather, may be diverted sideways, presumably due to local vapor flow conditions. This so-called "side drainage" model predicts a less severe effect of inundation yields:

$$\frac{\bar{h}_N}{h_1} = 0.60 + N^{-\frac{1}{4}} \quad (2-21)$$

At the present time, numerous investigations have been carried out in an attempt to better understand the phenomenon of condensate inundation. However, the data are scattered and as a consequence, no successful theoretical model of condensate inundation exists [Ref. 3]. However, for design purposes, Butterworth [Ref. 36] has recommended that the Kern model be used.

### 5. Condensation in Enhanced Tube Bundles: Experimental Studies

Young and Wohlenberg [Ref. 37] examined the condensation of R-12 on a vertical column of smooth horizontal tubes. These investigators found that the effect of the number of tubes in the vertical column is less than that predicted by Nusselt.

Katz et al. [Ref. 38] investigated the condensation of R-12 on a vertical column of six horizontal finned tubes. Their results also showed a less severe inundation effect than predicted by the model of Nusselt.

Smirnov and Lukanov [Ref. 39] used R-11 to study condensation on 20 horizontal rows of finned tubes arranged in a triangular fashion. Their results showed a dramatic reduction in heat transfer for the first five tubes. However, after this, the heat transfer coefficient remained almost constant for the rest of the tubes in the column.

Honda et al. [Ref. 40] have studied the condensation of R-113 on a vertical column of horizontal low finned tubes. An inundation tube was used to simulate additional rows of tubes. These authors described four modes of condensate flow; namely, droplet mode, column mode, column and sheet mode, and sheet mode. Unfortunately,

these authors did not calculate the heat transfer coefficient so that no comparison with theoretical models is possible.

Webb and Murawski [Ref. 41] examined the condensation of R-11 on a column of enhanced condenser tubes. The tubes tested were a standard 1024 fpi tube, a GEWA-SC tube, a Turbo-C tube and a TRED-D tube. The GEWA-SC tube is a 1024 fpi tube but the fins have a Y-shaped cross-section. The Turbo\_c and TRED-D tubes are similar to the 1024 fpi tube except that the fins have a saw-tooth shape. Webb and Murawski found that a standard 1024 fpm tube showed virtually no row (inundation) effect. However, when the experiments were conducted on Turbo-C, GEWA-SC and Tred-D tubes, row effects (ie., inundation effects) were seen. The inundation effect was greatest for the Tred-D tube which also had the lowest single tube performance. These investigators found values for the exponent in equations (2-17, 2-19, and 2-21) on the order of 0.12 to 0.26. Recall that Nusselt's theory used a value of 0.25.

More recently, Honda et al. [Ref. 42] studied the condensation of R-113 on an in-line horizontal tube bundle. The tubes tested consisted of either flat-sided (rectangular) annular fins or three dimensional trapezoidal fins. These authors found that the effects of condensate inundation were greatest for the three dimensional fin tubes. Unfortunately, these authors also had vapor velocities on the order of 3.4 m/s or greater. Therefore, it is difficult to compare their results directly to the theoretical models of Nusselt, Kern, or Eissenberg.

An interesting facet of the experiments of Honda et al. [Ref. 42] deserves mention. These investigators compared the effects of condensate inundation on the vapor-side heat transfer coefficient for smooth and finned copper tubes. Their results showed that despite condensate inundation, the heat transfer coefficient for the finned tubes was still substantially above that of the unfinned tubes. In addition, the decrease in the heat transfer coefficient with increasing row number was less with the finned tubes suggesting that the effects of condensate inundation were less severe with finned tubes than with unfinned tubes. Presumably, this result is due to the fact that condensate draining off of a finned tube drains in columns rather than continuous sheets. Lower tubes will therefore not be completely covered with condensate but instead will have unflooded regions.

Honda and Nozu [Ref. 43] examined the effects of condensate inundation on smooth and integral-fin copper tubes using a theoretical model derived recently by Honda et al. [Ref. 44] This model was a single tube model which was extended to include the effects of condensate inundation by realizing that condensate did not flow off tubes

as sheets but rather as columns. The model took account of the fact that regions which received drainage of condensate had different heat transfer coefficients than regions which did not. The results support the more recent experimental results of Honda et al. [Ref. 42]. The effect of inundation was less severe for the finned tubes than for the smooth tubes. The authors suggest that this is due to condensate being channeled on the finned tubes whereas for the smooth tubes, the entire tube surface becomes covered with a condensate film of varying thickness.

#### **6. Summary of Enhanced Tube Bundle Condensation**

Experimental data has shown that the Nusselt model for the effects of condensate inundation may be too conservative. Rather, most experimental data seems to fall between the Kern and Eissenberg predictions.

Other experimental data suggests that the effects of condensate inundation are less for finned tubes as opposed to smooth tubes. Presumably, this is due to the manner in which condensate flows from one finned tube to another. The presence of the fins seems to channel the flow of condensate leaving large areas relatively free of flooding from inundation.

As a final comment, the use of wire wrapped tubes provides an interesting alternative to the more conservative finned tube approach. However, the effects of refrigerant condensate inundation on wire wrapped tubes has yet to be examined.

### III. EXPERIMENTAL APPARATUS

#### A. TEST PLATFORM

Details of the design and construction of the condenser/evaporator test platform are provided by Zebrowski [Ref. 1] and Mabrey [Ref. 2]. Therefore, only a brief summary will be presented here.

The test platform is shown schematically in Figure 1 while a photograph of the unit is shown in Figure 2. The unit is made from rolled stainless steel plate (6.35 mm thick) and designed to withstand an absolute pressure of 308 kPa (approximately 3 bar).

##### 1. Condenser Section

The top section is the condenser. It is 1.3 m in length with an internal diameter of 0.61 m. The end plates are made of stainless steel plate (6.35 mm thickness) with a diameter of 0.71 m. They are connected to the condenser shell using a bolted flange assembly. A rubber gasket, 3.22 mm thick, provides a vacuum tight seal. The condenser unit has five viewports which allow the condensation process to be viewed.

Four test condenser tubes are contained in the condenser forming a vertical in-line column with a pitch-to-diameter ratio of 2.25. These are held in place at each end by a nylon block bolted to the end plate. A rubber gasket provides a vacuum tight seal. A stainless steel plate is fitted over the ends of the condenser tubes and bolted to the nylon block. O-rings are placed in between the nylon block and steel plate in order to provide a vacuum tight seal.

In order to provide a means of pressure control during testing of the condenser tubes, the test platform was fitted with five auxiliary condenser tubes. These auxiliary condenser tubes are constructed of 9.53 mm diameter copper tube, wound into coils. Each coil is supported by a stainless steel rod welded to one of the end plates. The auxiliary condenser coils enter and exit through this same condenser end plate.

A stainless steel shroud assembly, shown in Figure 3, is installed in the condenser unit. This shroud surrounds the test condenser tubes as well as the auxiliary condenser coils. A window, installed in the side of the shroud, allows visualization of the test condenser tubes through the viewports. The purpose of this shroud is to funnel vapor from the evaporator below, around the outside of the shroud and then vertically down past the condenser tubes. The velocity of the vapor past the condenser tubes was 0.1 m/s.

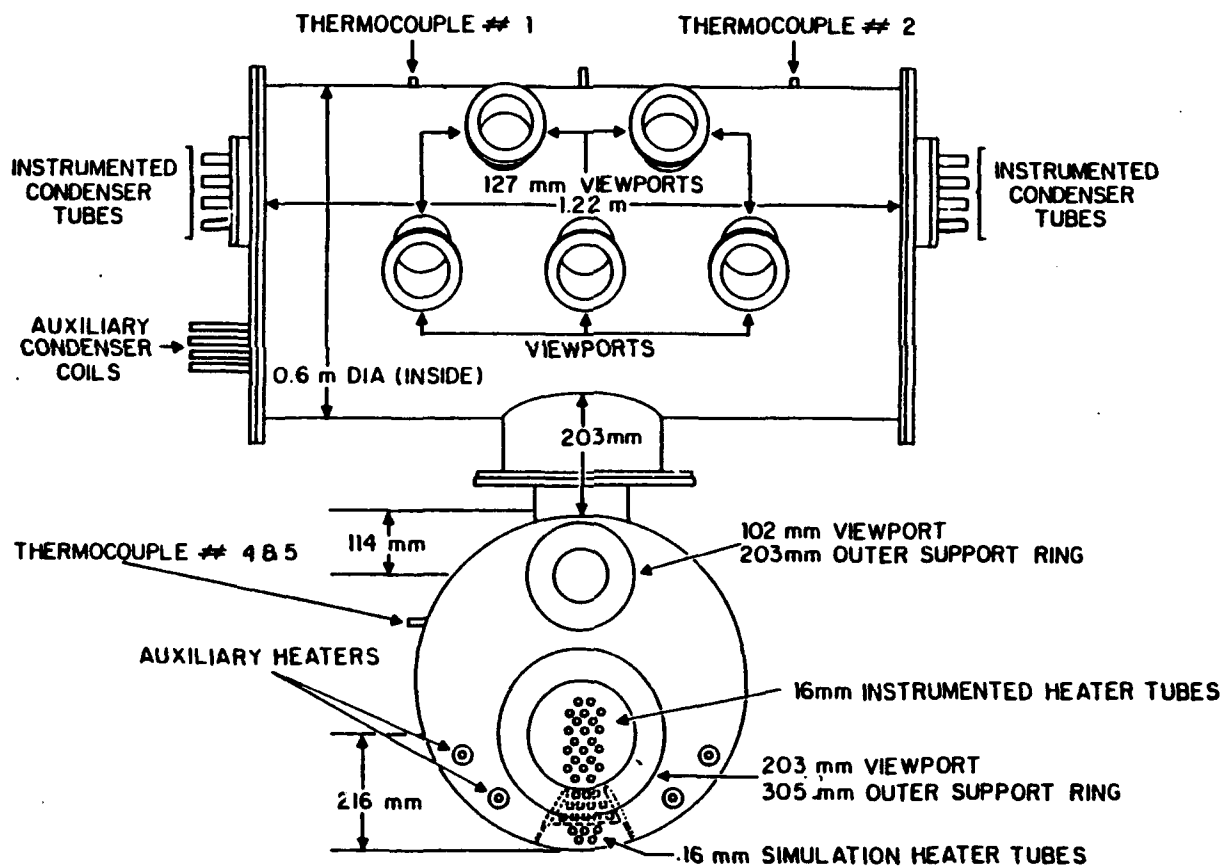


Figure 1. Schematic diagram of test platform.



Figure 2. Photograph of the evaporator/condenser test platform.



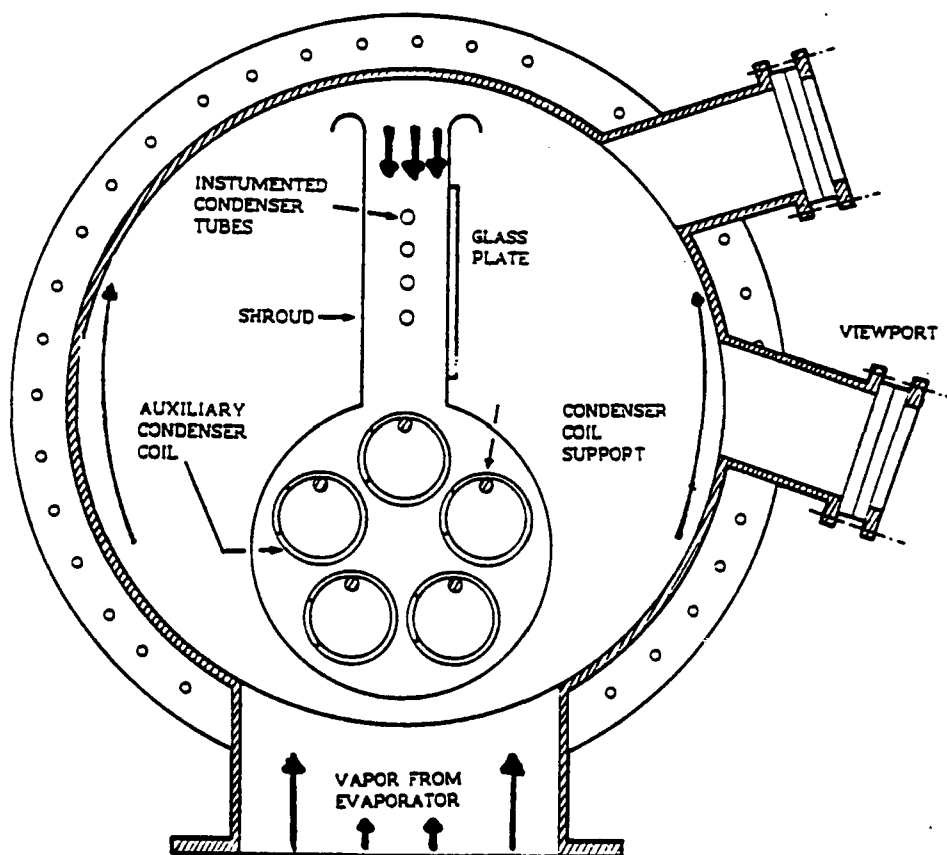


Figure 3. Schematic diagram of condenser showing shroud.

## 2. Evaporator Section

The flooded evaporator is formed from rolled stainless steel and has an internal diameter of 0.61 m with a width of 0.279 m. Two viewports allow visualization of the boiling process. This unit is connected to the condenser by a collar assembly 0.28 m in diameter and 0.203 m in length. The volume of liquid contained in the evaporator is approximately  $0.06 \text{ m}^3$ , just sufficient to cover the boiler tubes.

Vapor is produced in the evaporator using a combination of three groups of heaters. The first group is the main bundle and is composed of thirty-five tubes in a triangular pitch (pitch to diameter ratio of 1.2). Fifteen of these have heaters with a nominal rating of 1 kW each. Five of these heated tubes are instrumented with thermocouples to enable bundle boiling data to be obtained. In addition, unheated dummy tubes are used to guide the two phase flow within the bundle.

The second group of tubes is composed of five simulation heaters, each with a nominal rating of 4 kW. These are placed below the main bundle in order to simulate further rows of tubes.

The final group consists of four auxiliary heaters, each with a nominal rating of 4 kW. Two of these are placed on each side of the evaporator in order to keep the liquid pool at saturation conditions; this avoids any subcooling of the liquid. Power to all three sets of heaters is provided by three separate STACO 240V, 23.5kVA rheostat controllers.

For further information on the design and construction of the test platform, the reader is referred to Zebrowski [Ref. 1], Mabrey [Ref. 2], Murphy [Ref. 45], and Chilman [Ref. 46].

## 3. Coolant System

The coolant is a 54/46 by weight mixture of ethylene glycol and water. The coolant system consists of two main coolant pumps. These pumps are 0.5 hp constant speed pumps which take a suction from the main coolant sump. One pump is used to supply five rotameters. A ball valve, located at the entrance to each rotameter, is used to control the flow rate. Flow to each test condenser tube is supplied by an individual rotameter. The fifth rotameter is used to supply one of the auxiliary condenser coils. A needle valve is used to provide fine control of flow through the coil. This coil is normally used to control saturation pressure during experimental runs.

The second coolant pump is used to supply coolant flow to the remaining four auxiliary condenser coils. Flow through each coil is controlled by a needle valve located at the entrance to each coil. It should be noted that the four auxiliary cooling coils are

seldom needed during the condenser experiments; their primary purpose is for use during evaporator experiments. (see Chilman [Ref. 46]).

In addition to supplying the four auxiliary condenser coils, the second coolant pump also provides coolant flow to a refrigerant storage tank and to a cold trap located at the top of the condenser. The storage tank can be used to store refrigerant during condenser or evaporator tube changeout. The cold trap is placed in-line between the condenser and a vacuum pump. Vapor from the condenser is drawn through the cold trap which is cooled by the ethylene glycol/water mixture. This process is used to remove noncondensibles from the condenser while preventing loss of refrigerant to the atmosphere.

Flow of the coolant mixture from the auxiliary condenser cooling coils, storage tank, and cold trap are returned to the sump tank. Coolant flow from the test condenser tubes empties into a common header which then empties into the same coolant sump tank.

In order to keep the coolant mixture temperature approximately constant, it is cooled by an eight ton refrigeration system located outside the building. This system continually recirculates the coolant using a 0.75 hp pump. Coolant temperature can be maintained at any temperature from ambient temperature (approximately 20 °C) down to -20 °C.

#### **4. Instrumentation**

Prior to entering each condenser tube, the coolant flows through a mixing chamber. The inlet temperature is measured using a single copper/constantan type-T thermocouple. Coolant flows from each condenser tube through an outlet mixing chamber. Outlet coolant temperatures are then measured using two thermocouples for each tube. An average outlet temperature is then taken for each tube. All thermocouples had been previously calibrated by Mabrey [Ref. 2].

Refrigerant temperatures were measured at several different locations in the evaporator/condenser test platform using similar single thermocouples. Vapor temperature was measured in two separate locations at the top of the condenser and one location just above the liquid level. Refrigerant liquid temperature was measured at both the top and bottom of the tube bundle. The thermocouples were inserted into stainless steel housings (with copper tips) which were installed in the condenser/evaporator test platform.

## B. CLEANING AND DECONTAMINATION PROCEDURES

As mentioned earlier, there was a contamination problem with the test platform during the work of Mabrey [Ref. 2]. Therefore, the experimental apparatus was initially disassembled and cleaned in accordance with the following procedure.

Prior to removing the evaporator, all heaters and thermocouples were disconnected. The lagging around the mating flange was then removed. A Porta-lift was connected to the evaporator mating flange in order to support the weight of the evaporator prior to removing the bolts holding the evaporator and condenser together. After supporting the evaporator, the bolts were removed and the evaporator lowered from the condenser unit.

Referring to Figure 2, the condenser unit is capped at each end by a steel end plate. The left end plate supports the auxiliary condenser units and is therefore removed after the right end plate. The test condenser tubes must be removed prior to the disassembly of the condenser. The assembly which holds the condenser tubes in place is composed of a nylon plate bolted to the condenser end plate. A gasket insures a tight seal between the nylon and condenser end plates. A stainless steel plate is bolted against the nylon plate with O-rings in between which ensure an air tight seal between the environment and the inside of the condenser.

The plates holding the test condenser tubes in place must be removed prior to removal of the condenser end plates. The stainless steel plates at both ends are removed by unbolting the retaining nuts. The nuts holding the nylon plate in place are then removed. A rubber mallet is used to tap out the test condenser tubes from the left end of the platform. This causes the right end nylon plate to move away from the right condenser end plate. Screwdrivers can then be used to pry the nylon end plate away from the condenser.

The condenser end plates can be removed after the test condenser tubes have been removed. As a word of caution, these end plates weigh in excess of 100 pounds. Therefore, they must be supported during the removal process. In these studies, a Porta-lift was used for this purpose. The right condenser end plate was removed first, followed by the left end plate. Prior to removal of the left end plate, the shroud assembly had to be removed. This was facilitated by first removing the thermocouple probes which penetrate the top of the condenser unit. The shroud was then pulled out of the condenser.

If the auxiliary condenser tubes are to be removed, then the the left condenser end plate will have to be removed. This is because the five auxiliary condenser tubes are attached to the left end plate. The location of the test platform in relation to the coolant

sump is such that this end can not be removed with the evaporator/condenser test platform in its present location. Rather, if the left head must be removed, the entire test platform must be rotated 180 degrees about a vertical axis.

Initial inspection of the condenser unit showed only one small area of discoloration which surrounded the middle viewport. No other obvious signs of contamination were evident. The condenser and evaporator were both cleaned using "3-D Supreme Cleaning Agent", a commercially available product which leaves no residue. All components were rinsed with fresh water, dried, then given a final cleaning with acetone. The auxiliary condenser coils were cleaned and decontaminated in the same manner.

The copper condenser tubes also appeared somewhat discolored. These were cleaned using "Shower Power", a commercially available cleaning agent. Prior to installation into the condenser unit, they were given a final cleaning with acetone to ensure removal of any residue left over from the cleaning procedure.

During the reassembly, all gaskets were replaced. Prior to replacement of the evaporator unit, a test blank was installed on the condenser and a vacuum test successfully performed. After this test was completed, the test blank was removed and the evaporator reinstalled. All penetrations were reconnected, the boiling tube bundle reinstalled and another vacuum test performed.

Prior to charging the system with R-113, the ethylene glycol/water coolant pumps were energized and flow started through the test condenser tubes. For this initial test, smooth copper tubes were used. The temperature of the coolant was  $-15^{\circ}\text{C}$ . Since Mabrey [Ref. 2] had noted that during condensation, a thickening between the fins of copper/nickel finned tubes was occurring which suggested ice formation, it was felt that water vapor might be present in the test platform since it had been open to the atmosphere. Therefore, by running the coolant mixture at this temperature through the condenser tubes, if no condensation was seen, this would rule out the presence of water vapor. During this initial run, no condensation was seen on any tubes. In addition, the orange peel appearance noted by Mabrey on the smooth copper tubes was not in evidence.

After checking the evacuated system for possible contamination, the test platform was charged with fresh R-113. Coolant flow was again started. This time an orange peel, or dimpled appearance could be seen on the top condenser tube. This suggested some type of contamination layer.

Power ( $\sim 20$  kW) was applied to the heaters while the coolant temperature was raised to  $\sim 0^{\circ}\text{C}$ . The orange peel appearance on the top tube was still present. Measurements of the vapor temperature at the top and bottom of the condenser showed approximately a  $20^{\circ}\text{C}$  differential, signifying the presence of significant amounts of noncondensable gases. These gases enter with the refrigerant and are released into the condenser when the liquid is boiled.

A vacuum pump, connected to the top of the condenser was used to remove these noncondensable gases. When this was done, the temperature differential between the top and bottom of the condenser decreased to less than  $0.5^{\circ}\text{C}$ . The orange peel appearance quickly disappeared and all four condenser tubes demonstrated good filmwise condensation. Based on these observations, it was standard practice to degas the system for at least four hours after the system was open to the atmosphere or fresh R-113 was added to the evaporator.

## **IV. EXPERIMENTAL PROCEDURES**

### **A. GENERAL PROCEDURES**

The experimental procedure was identical for all experiments. The coolant pumps were energized and flow started through one of the auxiliary condensers. Flow was also started through the four test condenser tubes at a nominal coolant velocity of 0.2 m/s. The auxiliary heaters were set at 3 kW, the instrumented tube bundle set at 3.5 kW, and the simulation heaters set at 1.5 kW.

The vapor temperature at the bottom and the top of the condenser was allowed to rise to 47.5 °C which corresponds to the saturation temperature of R-113 at atmospheric pressure. The rate of temperature rise was controlled to approximately 0.3 degrees per minute by adjusting the rate of coolant flow through the auxiliary condenser. During the heat up period, a vacuum pump, connected to the top of the condenser via the cold trap, was run continuously in order to remove any noncondensibles. The absence of noncondensibles was indicated when the vapor temperature difference between the top and bottom of the condenser unit was less than 0.5 °C.

When the vapor temperature was about 45 °C, coolant velocity was adjusted to between 1 and 1.2 m/s for the four condenser tubes. The heater power levels were then readjusted in order to maintain a relatively constant condenser pressure while leaving one auxiliary condenser coil on-line. At lower coolant velocities, condenser pressure was maintained using the auxiliary condenser coils. The power settings for the heaters were not altered during the course of the experiment.

During all experimental runs, the vapor temperature at the top and bottom of the condenser unit was maintained between 46.5 and 48.5 °C which corresponds to a condenser pressure of approximately one atmosphere. Pressure control was accomplished by adjusting coolant flow through the auxiliary condenser tubes.

#### **1. Tube Bundle**

Once the vapor temperature was between 46.5 and 48.5 °C, coolant flow was adjusted to the desired coolant velocity for the four test condenser tubes. Here, the desired coolant velocity is an input to the computer program. The program then calculates the required flowmeter setting using the calibration curves (Appendix A). The initial coolant velocity used was 0.2 m/s. After setting the flow rate, the temperature difference between the inlet and outlet of all four condenser tubes was monitored using the com-

puter program, DRPCON7. Approximately ten minutes was required for this temperature differential to stabilize. Once stable, a data set was taken. This procedure was repeated in increments of 0.1 m/s up to a maximum of 1.2 m/s. The procedure was then repeated by decreasing the flow in 0.1 m/s increments down to 0.2 m/s. Two data sets were obtained at each coolant velocity. It should be mentioned that for the copper/nickel finned tubes, the range of flow settings was changed. The minimal flow setting was 0.6 m/s while the maximum flow setting was 2.0 m/s. The reasons for this change are discussed in "3. Enhancement of Outside Heat Transfer Coefficient." on page 30.

## **2. Single Tube Experiments**

After completion of the tube bundle runs, the experiment was repeated for each individual tube starting with the lowest tube (tube D). Flow through the tubes above the test tube was stopped and flow through the tube of interest was set for a velocity of 0.2 m/sec. The vapor pressure was again maintained using an auxiliary condenser coil. During this time, the upper tubes were continuously observed for condensate formation. No single tube data was obtained until condensate formation on the upper tubes had ceased. This typically required twenty to thirty minutes.

Once the coolant temperature rise had stabilized, a data set was obtained. Following this, the coolant flow rate was increased in 0.1 m/s increments up to the maximum flow velocity. A data set was obtained at each flow velocity. Throughout the experiment, tubes above the test tube were visually monitored to ensure that no condensate formation occurred. The flow velocity was then decreased in 0.1 m/s increments down to the minimum coolant flow velocity, with a data set obtained at each flow velocity. This procedure was repeated for each test condenser tube in the bundle.

## **B. SPECIFIC EXPERIMENTS**

### **1. Baseline Experiments**

The purpose of the baseline experiments was to validate the performance of the condenser/evaporator test platform by comparing data to that of Mabrey [Ref. 2]. These initial baseline experiments were performed using smooth copper tubes (inside diameter of 13.26 mm, outside diameter of 15.88 mm, thermal conductivity of 386 W/m K). The condensing length of the tubes was 1.219 m. The tubes were supplied by Wolverine Tube Co.



## 2. Enhancement of Inside Heat Transfer Coefficient

The main purpose of this study was to obtain accurate values of the outside heat transfer coefficient,  $h_o$ . In order to obtain accurate values for  $h_o$ , the resistance to heat transfer on the inside of the tube  $\frac{1}{h_i A_i}$  needs to be minimized. The reason that this resistance must be minimized is that if the inside resistance is a large part of the overall vapor-to-coolant resistance, then  $h_o$  will become inaccurate. In order to minimize the inside resistance, one must enhance the inside heat transfer coefficient.

The inside heat transfer coefficient is influenced by the type of coolant flow through the tubes. In the test platform, the coolant is a 54/46 percent (by weight) ethylene glycol/water mixture. At temperatures below 0 °C, this fluid is extremely viscous with Reynolds numbers in the range of 300 to 2800, suggesting laminar flow. When the coolant flow is laminar, the inside heat transfer coefficient is low. However, if this laminar flow can be mixed, then the inside resistance can be decreased and the heat transfer coefficient increased. This can be accomplished through the use of radial mixing elements. Radial mixing elements have the effect of mixing the thermal boundary layer (formed on the inside of the tube) with the colder core flow thereby improving heat transfer. It should be noted that a penalty in using such elements is an increased pressure drop which must always be kept in mind in practical applications. However, for the purposes of this study, increased pressure drop was not important.

In this thesis, two types of mixing elements were investigated. The first was a twisted tape insert made of copper [Ref. 47,48]. This tape insert had a thickness of 0.559 mm with a pitch for a 180 degree twist of three times the inner tube diameter.

The second type of insert used in this study was a commercially available product referred to as HEATEX radial mixing elements.<sup>3</sup> These elements are manufactured from stainless steel and consist of a number of small flexible loops (petals) of steel wire attached to a central wire core. These flexible petals are placed in the tube such that they face the oncoming flow. Their outside diameter is slightly larger than the inside diameter of the tube and are therefore kept in position with a "pinch" fit. The petals disturb the thermal boundary layer and promote fluid mixing. Figure 4 shows the two types of inserts. It should be noted that two different sizes of HEATEX were used since condenser tubes of two different inside diameters were examined.

---

<sup>3</sup> manufactured by CAL GAVIN Birmingham, England.



**Figure 4.** Twisted tape insert and HEATEX radial mixing element.

As part of the baseline experiments, the smooth copper tubes were also tested with no insert installed. Experiments were repeated on the smooth copper tubes using the twisted tape inserts as well as the HEATEX elements. This data was then used as a baseline for comparison with other types of condenser tubes. It should be mentioned that when no insert is present, the inside tube resistance to heat transfer is very large relative to the outside resistance. In some cases (typically when the coolant flow rate is low), this can produce a negative value for the outside heat transfer coefficient. This is simply the inaccuracy in the calculation of  $h_o$  when the inside resistance dominates and clearly demonstrates the need for an insert as mentioned above.

### **3. Enhancement of Outside Heat Transfer Coefficient.**

The overall heat transfer coefficient,  $U_o$ , is influenced by the outside as well as the inside heat transfer coefficient. The means by which the outside heat transfer coefficient is enhanced is by altering the outside geometry of the condenser tube.

Experiments to investigate enhancement of the outside heat transfer coefficient utilized three types of condenser tubes. The first type of tube tested was a copper/nickel finned tube (26 fins/inch). This tube has an inside diameter of 10.16 mm with a thermal conductivity of 43 W/m K. The tubes were manufactured by Wolverine Tube Co. These tubes were tested as a tube bundle as well as individually. Experiments were performed with no insert as well as with the twisted tape and HEATEX inserts. These tubes are shown in Figure 5. One point must be mentioned with regard to the finned tubes. The use of fins on the outside of the tube enhances the heat transfer considerably. Consequently, the inside resistance again becomes a large fraction of the overall resistance, even when inserts are used.

One additional point must be discussed with regard to the copper/nickel finned tubes. Because the size of the holes in the nylon end plates is fixed, the outside diameter of any tubes to be tested must be the same. In order to have these finned tubes the same outside diameter, the inside diameter had to be reduced. Since the inside tube diameter was smaller for the finned tubes, higher coolant velocities were obtained.

The second series of experiments used a copper/nickel KORODENSE tube also manufactured by Wolverine Tube Co. This tube, shown in Figure 5, has a shallow spiral groove along the entire condensing length with a pitch of 10 mm. As with the finned copper/nickel tubes, experiments were performed on these KORODENSE tubes with no insert as well as with the twisted tape and HEATEX inserts. The tubes were tested in a tube bundle as well as individually.

Fujii and co-workers [Ref. 33] have previously shown that the condensation of refrigerants can be enhanced by wrapping smooth condenser tubes with a small diameter wire. Therefore, a third series of experiments were performed in which copper/nickel KORODENSE tubes were tightly wound with wire as shown in Figure 5. Since these authors showed that there was an optimum wire size which gave the greatest enhancement of heat transfer (0.5 mm at a pitch of 3 mm), the KORODENSE tubes used in this study were wrapped with one of three different sizes of wire. The sizes used were 0.029" (0.736 mm) diameter stainless steel wire, 0.049" (1.244 mm) diameter stainless steel wire, and 0.0675" (1.715 mm) diameter copper wire. The wire lay in the shallow grooves of the KORODENSE tubes and was soldered to the tubes at the ends only. Although the wire was tightly wrapped around the tubes, it was not physically attached except at the ends. Experiments were carried out on each tube individually. Each tube was tested in all four locations within the bundle. This was done to see if position within the bundle (i.e. wake from tubes above) had any effect. Only the HEATEX inserts were used with these tubes.

Once an optimal wire diameter was determined, a fourth series of experiments was conducted. This series used the same four KORODENSE tubes, only this time each was wrapped with the same optimal diameter wire. The tests were done with the HEATEX elements installed. Experiments were conducted on the tubes individually in order to compare with the previously obtained single tube data. In addition, these wire wrapped tubes were tested as a tube bundle in order to investigate whether or not the wire wrap had any effect on condensate innundation.

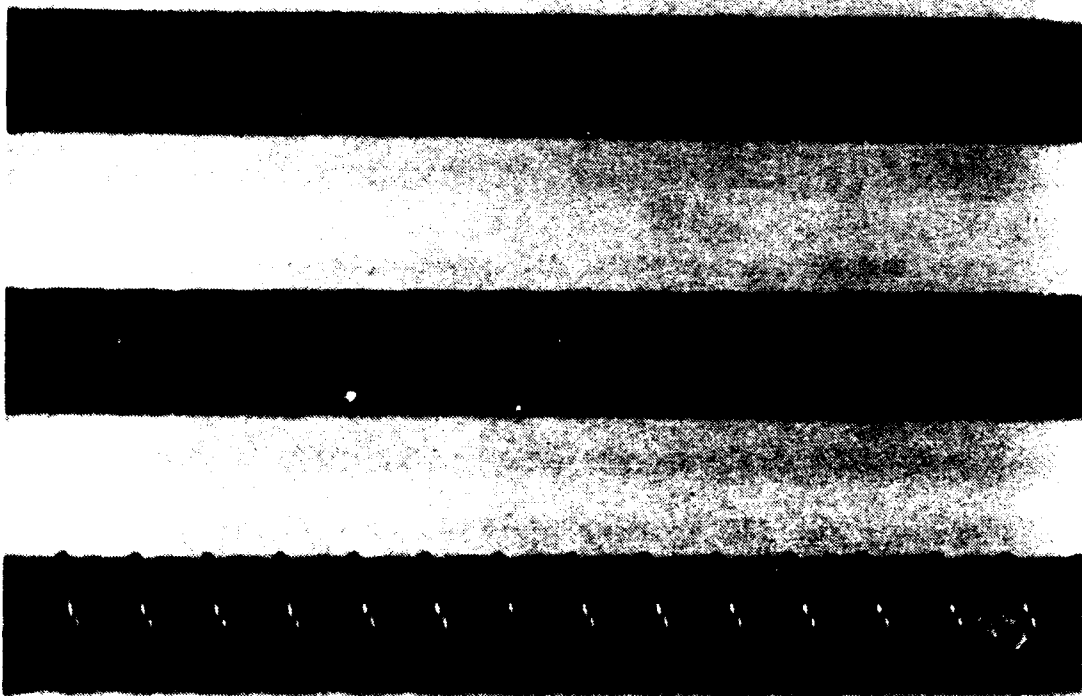


Figure 5. Copper/nickel finned tube, Korodense tube, Wire wrapped tube.

## V. DATA REDUCTION

### A. DATA ACQUISITION

The data acquisition system consisted of a Hewlett-Packard series 9000 computer coupled with a Hewlett-Packard model 3479A Data Acquisition system. The computer program used in this study was originally written by Mabrey [Ref. 2] but has been substantially modified in the course of this thesis. The data acquisition thermocouple channel assignments are shown in Table 1.

Table 1. THERMOCOUPLE CHANNEL ASSIGNMENTS.

Channel	Temperature Measured
0	Vapor (condenser top)
1	Vapor (condenser top)
—2	Vapor (top of liquid)
3	Liquid (top of bundle)
4	Liquid (top of bundle)
5	Liquid (bottom of pool)
6	Inlet tube 1
7	Inlet Tube 2
8	Inlet Tube 3
9	Inlet Tube 4
10, 11	Outlet Tube 1
12, 13	Outlet Tube 2
14, 15	Outlet Tube 3
16, 17	Outlet Tube 4

The computer program allows the user to acquire data, reprocess data, or plot data. During data acquisition the user selects the fluid velocity desired. Based on coolant inlet temperature, the coolant fluid properties and mass flow rates are calculated (see Appendix C). The program then uses equations derived from the flowmeter calibrations (Appendix A) in order to calculate the appropriate flowmeter settings.

Once the flowmeters are set for the required coolant velocity, the computer system displays the vapor temperature at the top and bottom of the condenser as well as the

coolant temperature rise for each condenser tube. When these temperature rises are stable (approximately 10 minutes), the user can terminate the display and acquire the data for that coolant flow velocity. While the temperature rises were stabilizing, coolant flow through an auxiliary condenser tube was adjusted in order to maintain constant pressure.

## B. DATA REDUCTION

The main function of the data reduction section of the computer program is to back out the outside heat transfer coefficient from an experimentally determined value of  $U_o$  and an assumed inside heat transfer coefficient correlation. This is accomplished in the following manner.

The data acquisition system measures the emf from the thermocouples listed in Table 1. These values of emf are converted to temperatures using correlations obtained from the temperature calibrations both contained in Appendix B. The volume flow rate of the ethylene glycol/water mixture is calculated based on the desired coolant velocity. The density, dynamic viscosity, thermal conductivity, heat capacity, and Prandtl number of the coolant are calculated using inlet temperatures (see Appendix C and Appendix E). From these quantities, the coolant mass flow rate and fluid velocity are calculated. The coolant Reynolds number for each condenser tube is also calculated. The heat transferred to the coolant is then found from

$$\dot{q} = \dot{m}C_p\Delta T \quad (5-1)$$

where  $\dot{m}$  is the mass flow rate and  $\Delta T$  is the coolant temperature rise. The outside heat flux,  $q''_o$ , is calculated by dividing  $\dot{q}$  by the surface area of the tube based on the outside tube diameter.

The overall heat transfer coefficient,  $U_o$ , is given by:

$$U_o = \frac{q''_o}{LMTD} \quad (5-2)$$

where LMTD is the log mean temperature difference defined as:

$$LMTD = \frac{\Delta T}{\ln \left[ \frac{T_{sat} - T_{c_i}}{T_{sat} - T_{c_o}} \right]} \quad (5-3)$$

The inside heat transfer coefficient (given as a dimensionless Nusselt number,  $Nu_c$ ) can then be calculated using one of three correlations. The choice of which correlation to use depends upon the type of insert installed inside the condenser tube. If no insert is installed, then  $Nu_c$  can be calculated from a correlation provided by Hausen [Ref. 49]<sup>4</sup> for developing laminar flow in a tube at constant wall temperature.

$$Nu_c = 3.66 + \left[ \frac{0.0668 \left( \frac{d_i}{l} \right) Re_{D,c} Pr_c}{1 + 0.04 \left[ \left( \frac{d_i}{l} \right) Re_{D,c} Pr_c \right]^{0.666}} \right] \quad (5-4)$$

If a twisted tape insert is installed, a correlation given by Hong and Bergles [Ref. 47] can be used to calculate  $Nu_c$  where

$$Nu_c = 5.172 \left[ 1 + 5.484 \times 10^{-3} Pr_c^{0.7} \left( \frac{Re_s}{y} \right)^{1.25} \right]^{0.5} \quad (5-5)$$

Here,  $y$  is the twist ratio (pitch over diameter).  $Re_s$  is the coolant Reynolds number, corrected for tape thickness.  $Re_s$  is given by:

$$Re_s = \frac{4\dot{m}}{\pi \mu (d_i - 4\delta)} \quad (5-6)$$

where  $\delta$  is the tape thickness. This correlation is valid for  $Re_s$  up to about 2300.

A number of correlations for determining the inside heat transfer coefficient have been published when using a wire matrix insert [Ref. 50,51,52, 53 ]. However, these correlations are specific for the type of mixing element used, and are especially dependent upon the loop density of the wire matrix.

The HEATEX mixing elements supplied by CAL GAVIN (nominal diameters of 13.26 and 10.16 mm) did not match the loop densities used by previous investigators. However, CAL GAVIN did supply experimental data for the heat transfer coefficient versus fluid velocity at three different temperatures for both sizes of elements. To convert this data into a usable correlation, the following procedure was developed.

---

<sup>4</sup> Calculations were performed for coolant flow through the smooth copper tubes at coolant velocities of 0.2 and 1.2 m/s. These calculations confirmed the coolant flow was not fully developed.



The correlations of Oliver and Aldington [Ref. 51, 52 ] took the form of

$$Nu = cRe^m Pr^n \quad (5 - 7)$$

where  $c$ ,  $m$ , and  $n$  are arbitrary constants which are dependent upon the type of insert used. It was assumed that a similar type of equation could be used in the present study by fitting the constants to the data (once non-dimensionalized) provided by CAL GAVIN.

The correlations of Oliver and Aldington [Ref. 51, 52 ] had Prandtl number raised to a power of 0.46. This was primarily to take into account temperature effects. Therefore, the same value was assumed in the present study. Values of  $Nu/Pr^{0.46}$  were plotted as functions of  $Re$  on a log-log basis. Figure 6 shows the data obtained for the 13.26 mm elements while Figure 7 shows the data obtained for the 10.16 mm elements. Based on the appearance of the non-dimensionalized data, a least squares linear regression was performed on each data set. The figures yield the values of the constants  $m$  and  $c$  (slope and intercept respectively) and provide the following correlations for the 13.26 and 10.16 mm elements respectively:

$$Nu_c = 0.226Re^{0.65} Pr^{0.46} \quad (5 - 8)$$

and

$$Nu_c = 0.065Re^{0.76} Pr^{0.46} \quad (5 - 9)$$

Once  $Nu_c$  was obtained from equations (5-4, 5-5 5-8 or 5-9), the inside heat transfer coefficient was calculated from:

$$h_i = \frac{Nu_c k_c}{d_i} \quad (5 - 10)$$

# HEATEX CORRELATION (13.26 MM)

$$NU = 0.226(RE^{.65})(PR^{.46})$$

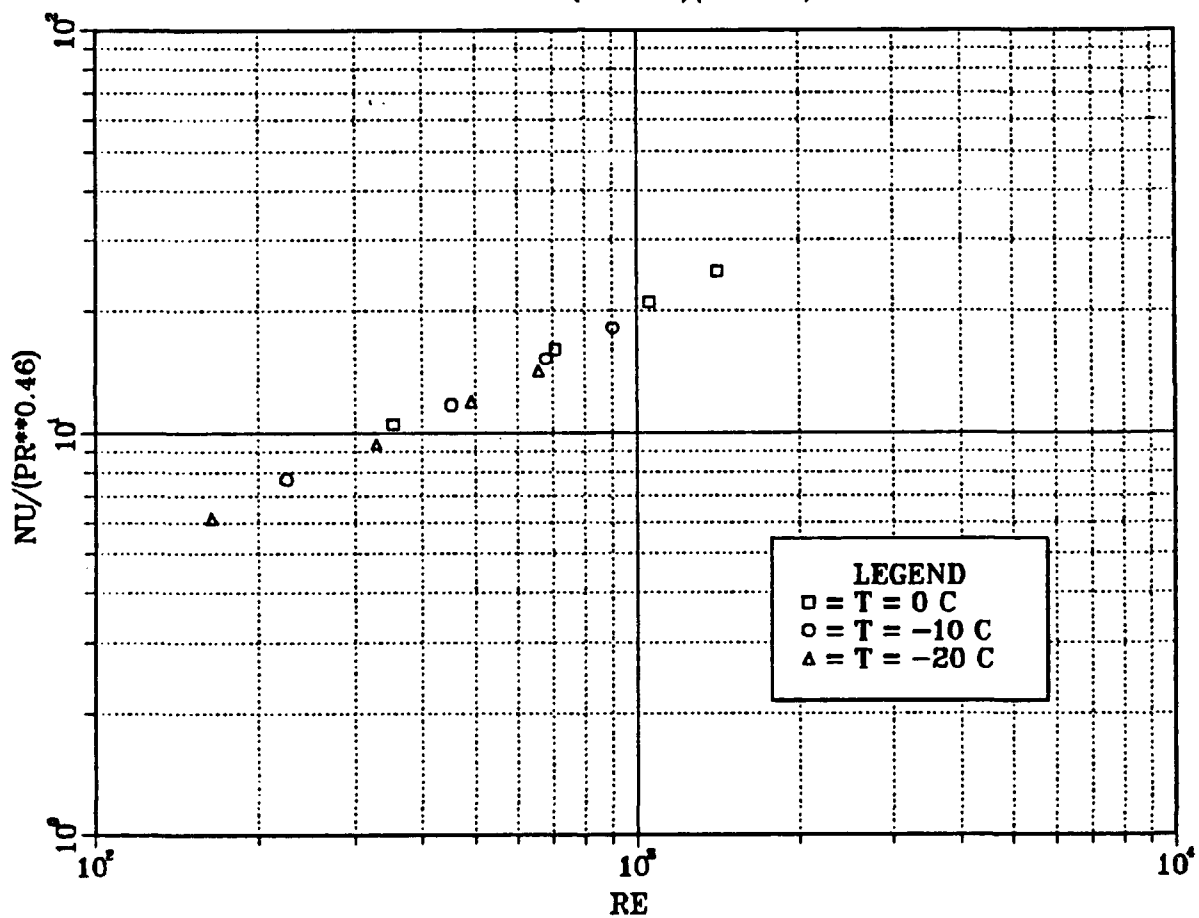


Figure 6. HITRAN correlation for 13.26 mm elements

# HEATEX CORRELATION (10.15 MM)

$$NU = 0.067(RE^{.76})(PR^{.46})$$

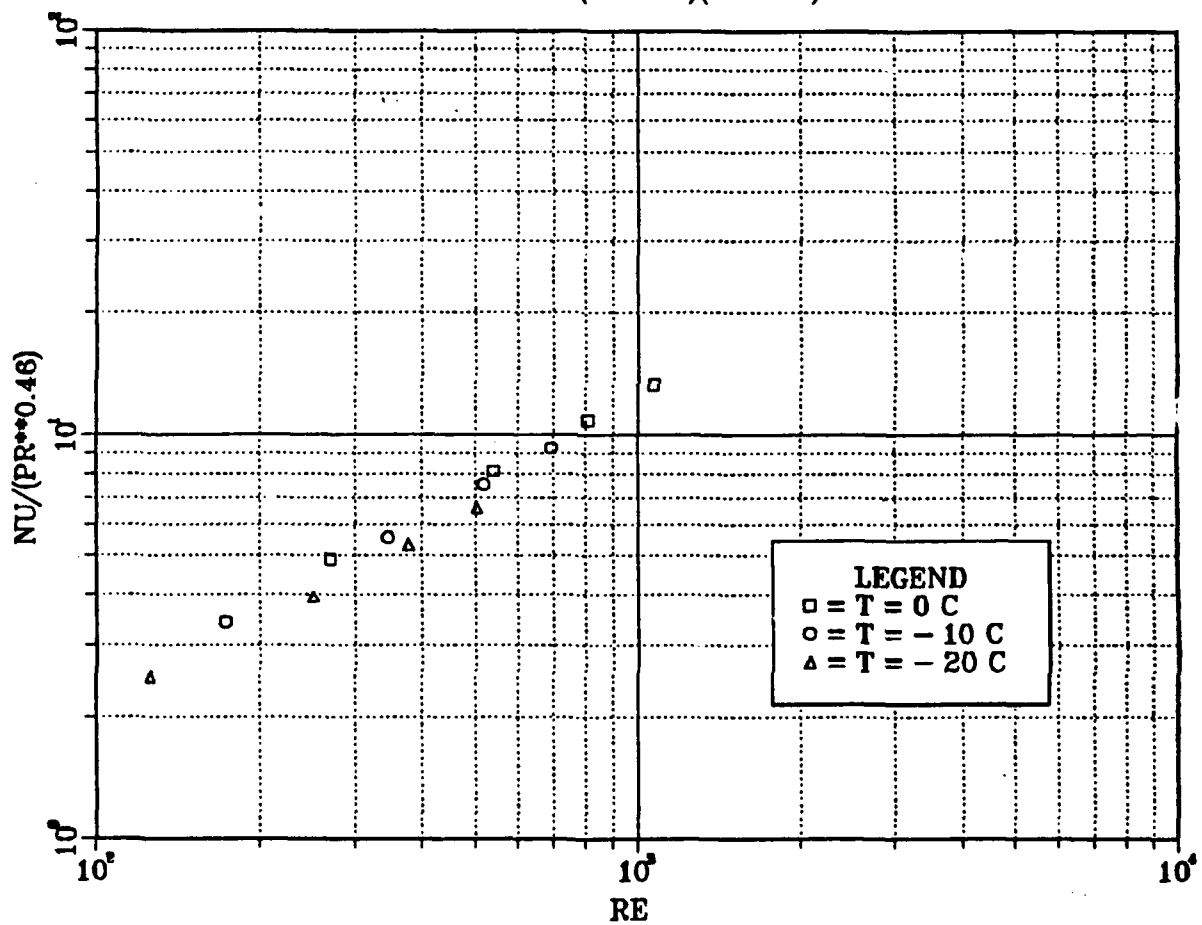


Figure 7. HITRAN correlation for 10.16 mm elements

The overall heat transfer coefficient,  $U_o$  is found from the summation of resistances to heat transfer across the whole tube:

$$\frac{1}{U_o A_o} = \frac{1}{h_o A_o} + R_f + R_w + \frac{1}{h_i A_i} \quad (5-11)$$

where  $R_f$  and  $R_w$  are the fouling and wall resistances respectively. In order to find  $h_o$  equation (5-11) can be rearranged to give:

$$h_o = \frac{1}{\frac{1}{U_o} - R_w A_o - R_f A_o - \frac{1}{h_i} \left( \frac{A_o}{A_i} \right)} \quad (5-12)$$

In all experiments, the tubes were meticulously cleaned and therefore, the fouling resistance,  $R_f$ , was neglected.

In order to better assess the calculated experimental value of the outside heat transfer coefficient, some form of comparison with prediction must be made. In this case, the experimentally obtained value of  $h_o$  was compared with Nusselt theory. However, because the wall temperatures are not known a priori, an iteration must be used to determine this predicted value of  $h_o$ . An initial value of  $h_o$  was estimated and based on this estimate, a wall temperature was calculated using the equation:

$$T_{wall} = T_{sat} - \frac{q''_o}{h_o} \quad (5-13)$$

The condensate film properties are then calculated using a reference temperature given by:

$$T_{film} = \frac{1}{3} T_{sat} + \frac{2}{3} T_{wall} \quad (5-14)$$

Once these condensate fluid properties are known (Appendix D), the theoretical outside heat transfer coefficient can be calculated from Nusselt theory [Ref. 4]:

$$h_o = 0.655 \left[ \frac{g k_f^3 \rho_f^2 h_{fg}}{\mu_f d_o q''_o} \right]^{\frac{1}{3}} \quad (5-15)$$

This calculated value is then compared to the initial guess. The error between the initial guess and the calculated value are compared. If the error is greater than 0.1%, the

"guessed" value for  $h_o$  is updated and the iteration continued. This process is repeated until the error between the calculated and guessed values is less than 0.1%.

### C. MODIFIED WILSON PLOT

The outside and inside heat transfer coefficients could be determined directly by measuring the vapor temperature, the tube wall temperature, and the coolant temperature rise. Of these, the most difficult temperature to measure directly is the tube wall temperature. This would require the use of instrumented tubes with thermocouples embedded in the tube wall. Unfortunately, the manufacture of such instrumented tubes is both costly and time consuming, especially when large numbers of tubes are to be tested.

An alternative to the use of instrumented tubes is to employ the "Modified Wilson Plot" procedure. This procedure has been outlined in detail by Marto [Ref. 10]. The modified Wilson plot procedure relies upon the overall heat transfer coefficient being reliably measured from experimental data. A summation of heat transfer resistances from vapor-to-coolant is then expressed as:

$$\frac{1}{U_o} = \frac{1}{h_o} + R_f A_o + R_w A_o + \frac{1}{h_i} \left( \frac{A_o}{A_i} \right) \quad (5-16)$$

As mentioned above, the fouling resistance is assumed to be negligible. This summation of resistances can be rearranged into a linear equation:

$$\left[ \frac{1}{U_o} - R_w A_o \right] = \left( \frac{A_o}{A_i} \right) \frac{1}{h_i} + \frac{1}{h_o} \quad (5-17)$$

In looking at the correlations given above for  $h_o$  and  $h_i$ , it can be seen that they all employ a leading coefficient. As an example, Nusselt theory, (equation 5-15) can be expressed in the form:

$$h_o = \alpha F \quad (5-18)$$

where:

$$F = \left[ \frac{g k_f^3 \rho_f^2 h_{fg}}{\mu_f d_o q''_o} \right]^{\frac{1}{3}} \quad (5-19)$$

In a similar manner, the equations for the inside heat transfer coefficients (equations 5-4, 5-5, 5-8, and 5-9) can also be transformed into the form:

$$h_i = C\Omega \quad (5-20)$$

where the form of  $\Omega$  would depend on which type of tube insert was being used. As an example, using equation 5-5,  $\Omega$  would become:

$$\Omega = \frac{k_c}{d_i} \left[ 1 + 5.484 \times 10^{-3} Pr_c^{0.7} \left( \frac{Re_s}{y} \right)^{1.25} \right]^{0.5} \quad (5-21)$$

The linearized version of the summation equation (equation 5-17) can then be rearranged to give:

$$\left[ \frac{1}{U_c} - R_w A_o \right] F = \frac{A_o F}{C\Omega A_i} + \frac{1}{\alpha} \quad (5-22)$$

This is a linear equation with two unknowns, namely,  $C$  and  $\alpha$ . Letting

$$Y = \left[ \frac{1}{U_c} - R_w A_o \right] F \quad (5-23)$$

and

$$X = \frac{A_o F}{A_i \Omega} \quad (5-24)$$

we can obtain a simplified linear equation:

$$Y = mX + b \quad (5-25)$$

where

$$m = \frac{1}{C} \quad (5-26)$$

and

$$b = \frac{1}{\alpha} \quad (5-27)$$

Since  $\Omega$  and  $F$  are both temperature dependent, an iterative solution procedure must be used. This is accomplished by applying a least squares fit to the linear equation.

It should be pointed out that the accuracy of the modified Wilson plot procedure relies heavily on the number of data points taken as well as the range of coolant velocities used.

## VI. RESULTS AND DISCUSSION

A summary of the experimental runs performed in this thesis is presented in Table 2. The abbreviation "SM" is for the smooth copper tubes, "KD" is for the KORODENSE tubes, and "CF" is for the copper/nickel finned tubes.

**Table 2. SUMMARY OF EXPERIMENTAL RUNS**

Data Set	Tube type	Insert	Comments
SM01	Copper	Tape	Test run
SM02	Copper	Tape	Test run
SM03	Copper	HEATEX	Test HEATEX correlation
SM05	Copper	HEATEX	Tube A insert bad
SM06	Copper	HEATEX	
SM07	Copper	Tape	
KD01	KORODENSE	Tape	1st test of KORODENSE
KD02	KORODENSE	None	
KD03	KORODENSE	HEATEX	
KD04	KORODENSE	Tape	
KD05	KORODENSE	HEATEX	Wire wrapped
KD06	KORODENSE	HEATEX	Wire wrapped
KD07	KORODENSE	HEATEX	Wire wrapped
KD08	KORODENSE	HEATEX	Wire wrapped
KD09	KORODENSE	HEATEX	0.049" Wire, bad insert
KD10	KORODENSE	HEATEX	0.049" Wire
KD11	KORODENSE	HEATEX	0.049" Wire
KD12	KORODENSE	HEATEX	0.049" Wire
CF01	Cu/Ni fin	Tape	dropwise condensation
CF02	Cu/Ni fin	Tape	Test run
CF03	Cu/Ni fin	Tape	
CF04	Cu/Ni fin	HEATEX	
CF05	Cu/Ni fin	None	

## A. DECONTAMINATION

Prior to charging the system with R-113, the system was evacuated to approximately 15 inHg and left for 24 hours. For this initial test, smooth copper tubes were used. The ethylene glycol coolant pumps were energized and flow started through the test condenser tubes. The temperature of the ethylene glycol was  $-15^{\circ}\text{C}$ . No condensation was seen on any tubes. In addition, the orange peel appearance noted by Mabrey [Ref. 2] was not observed.

After checking the evacuated system for possible contamination, the test platform was charged with fresh R-113. Coolant flow was again started. No orange peel, or dimpled appearance could be seen on the top condenser tube.

Power ( $\sim 20$  kW) was applied to the heaters while the coolant temperature was raised to  $\sim 0^{\circ}\text{C}$ . An orange peel appearance was noted for the top tube. Measurements of the vapor temperature at the top and bottom of the condenser showed approximately a  $20^{\circ}\text{C}$  differential.

A vacuum pump, connected to the top of the condenser, was used to remove any noncondensable gases. When this was done, the temperature differential decreased to less than  $0.5^{\circ}\text{C}$ . The orange peel appearance quickly disappeared from the top condenser tube. This suggests that at least part of the contamination problem reported by Mabrey was due to the presence of noncondensibles.

In a subsequent series of experiments conducted on a set of titanium finned tubes, a foreign substance appeared to build up on the tubes during the experimental run. This occurred despite continuous operation of the vacuum pump. The tubes were removed from the condenser and inspected. The foreign material had an oily feel to it and an odor similar to that of ethylene glycol.

The titanium finned tubes had smooth extensions (6" in length) attached to their ends using epoxy. These extensions penetrated the nylon block and steel plate and provided the smooth surface necessary for the O-rings to give an airtight seal between the condenser and the atmosphere. When these tubes were removed from the condenser, it was noted that the extensions on two of the tubes had come loose. The condenser was opened for inspection. Upon removal of the end plate and shroud assembly, pools of ethylene glycol were seen inside the condenser shell and on the auxiliary condenser tubes. In addition, ethylene glycol was found around the shroud assembly. The entire condenser and evaporator assembly were therefore dismantled and cleaned in accordance with the procedures outlined in "Experimental Apparatus".



After reassembly of the condenser and evaporator, the smooth copper tubes were cleaned and reinstalled. Operation of the test platform failed to show any orange-peel or dimpled appearance on the tubes. In addition, all tubes demonstrated good filmwise condensation.

It should be mentioned that in subsequent tests, copper/nickel finned tubes were installed in the condenser. However, unlike the titanium finned tubes, the smooth extensions on these tubes were soldered. During system operation, no foreign material was noted between the fins. Condensate retention between the fins was negligible. The tubes demonstrated good film wise condensation.

In summary, it is believed that the contamination problems noted by Mabrev [Ref. 2] were due to two problems. The first problem was the presence of noncondensibles during operation of the condenser. This resulted in the relatively low values for overall heat transfer as well as the fact that the top tube, which would be most affected by the noncondensibles, had the lowest heat transfer. Secondly, while it can not be proved conclusively, the author believes that ethylene glycol may also have been present in the system for certain tubes and that this is what was the material noted in between the fins by Mabrev.

## **B. OVERALL HEAT TRANSFER COEFFICIENT**

In the following sections, the results pertaining to the overall heat transfer coefficient are presented. It is important to keep in mind that this value is experimentally determined and does not rely on any correlations other than for the fluid properties. In addition, it should be mentioned that in the following graphs, tube A is the top tube in the bundle, tube B the second, tube C the third, and tube D the bottom tube.

### **1. Smooth Copper Tubes**

Figure 8 shows the overall heat transfer coefficient,  $U_o$ , plotted as a function of coolant velocity. The tubes did not contain any inserts. Note the low values for  $U_o$ . These values are almost constant for velocities over the range of 0.2 to 0.7 m/s. In this series of experiments, Reynolds numbers were typically of the order of 300 to 2300 indicating that flow is laminar. Without any insert to promote mixing, one would therefore expect relatively low values for  $U_o$ . This is because, in laminar flow, the inside resistance to heat transfer is relatively large and therefore leads to a lower value for heat transfer. Finally, there is essentially no difference between the tubes at low coolant velocities. This suggests that with these relatively low condensation rates, inundation is not a significant factor. At higher flow rate, it can be seen that the values for heat transfer

start increasing and that differences between the tubes become more apparent. As coolant velocity is increasing, flow is beginning to become turbulent. This reduces the inside resistance to heat transfer which leads to an increase in the overall heat transfer. As heat transfer increases, the effects of inundation become more apparent. This is presumably due to the outside resistance becoming more important as the inside resistance becomes less important.

The results obtained when these smooth copper tubes were tested individually is shown in Figure 9. Here, all the tubes behave similarly. In addition, comparison with Figure 8 shows that the values of  $U_o$  for the tubes when tested individually are approximately the same as for the top tube during the bundle run as one would expect.

The results for the same run with tape inserts installed are shown in Figure 10. It can be seen that  $U_o$  increases as coolant velocity increases. The values are clearly greater than when no insert is used (approximately 50% greater) indicating the advantage gained when enhancing the inside heat transfer coefficient in situations where coolant flow is laminar. The effect of condensate inundation on the overall heat transfer coefficient is also clearly seen. Here, condensate inundation results in approximately a 15% decrease in  $U_o$  when the top tube is compared to the second tube. Interestingly, there appears to be little difference in the values for  $U_o$  for tubes B, C, and D indicating that the condensate film is of similar thickness for these tubes. The data for a similar run performed by Mabrey [Ref. 2] is shown in Figure 11. The data obtained in the present study is almost twice the values reported by Mabrey. In addition, the present data shows that the top tube has the highest heat transfer which is to be expected assuming noncondensibles are not present. This was not the case in Mabrey's work.

The results for these same tubes when operated individually are shown in Figure 12. All the curves are essentially the same with values for  $U_o$  corresponding to that obtained for the top tube during the bundle run. The maximum variation is about 12%.

The next series of experiments were performed on the smooth copper tubes with the HEATEX elements installed. Figure 13 shows the results of these experiments when the tubes were operated as a bundle. As with the experiments performed with the twisted tape inserts, there is an increase in  $U_o$  as coolant velocity is increased. In this case the increase is 100% in comparison to the case with no insert! Also, as in the previous experiment, condensate inundation appears to result in about a 15% decrease in  $U_o$  for the second tube compared to the top tube. There appears to be little difference in the heat transfer coefficients for tubes B, C, and D, although some effect may be ar-

## UZERO SMOOTH COPPER TUBES

SM04, R-113, NO INSERT, SINGLE

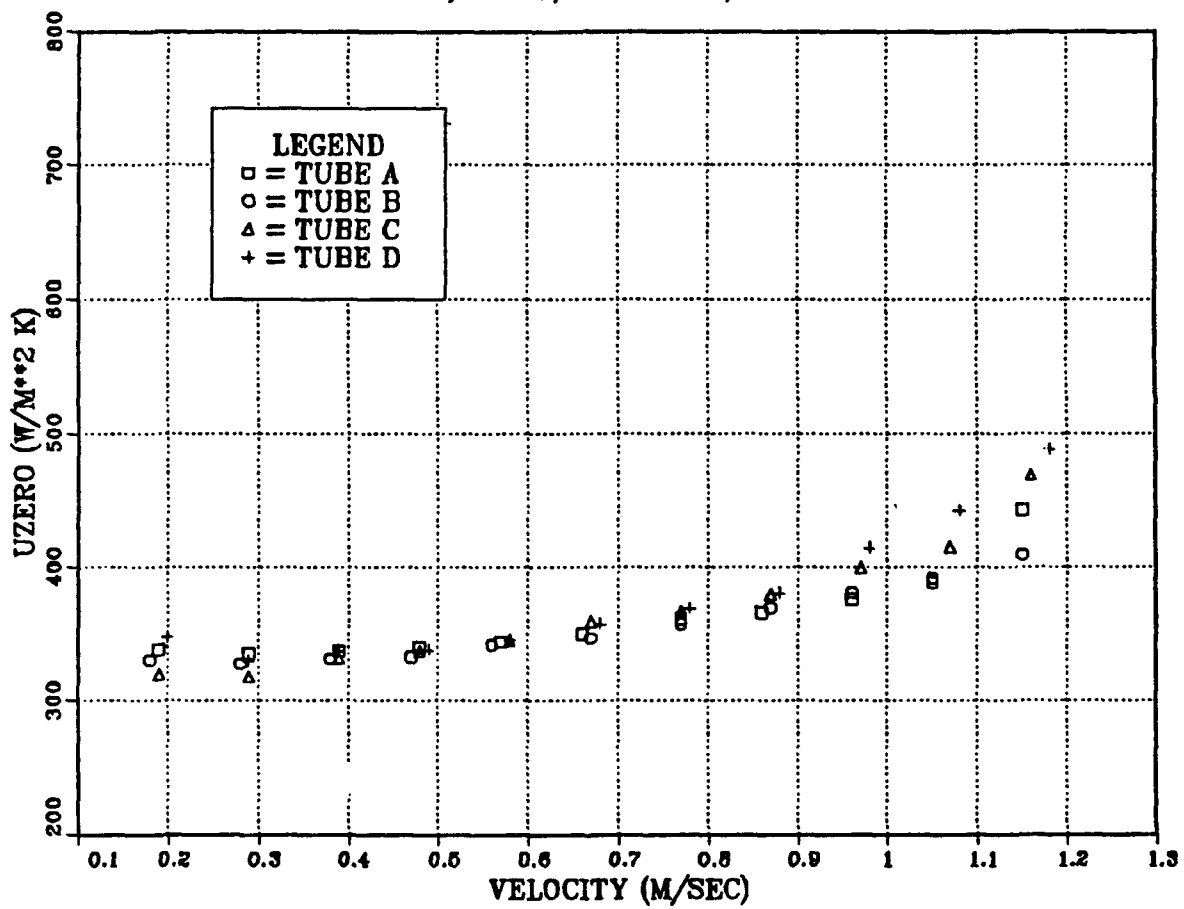


Figure 8. Bundle run on smooth copper tubes without inserts.

## UZERO SMOOTH COPPER TUBES

SM04, R-113, BUNDLE, NO INSERT

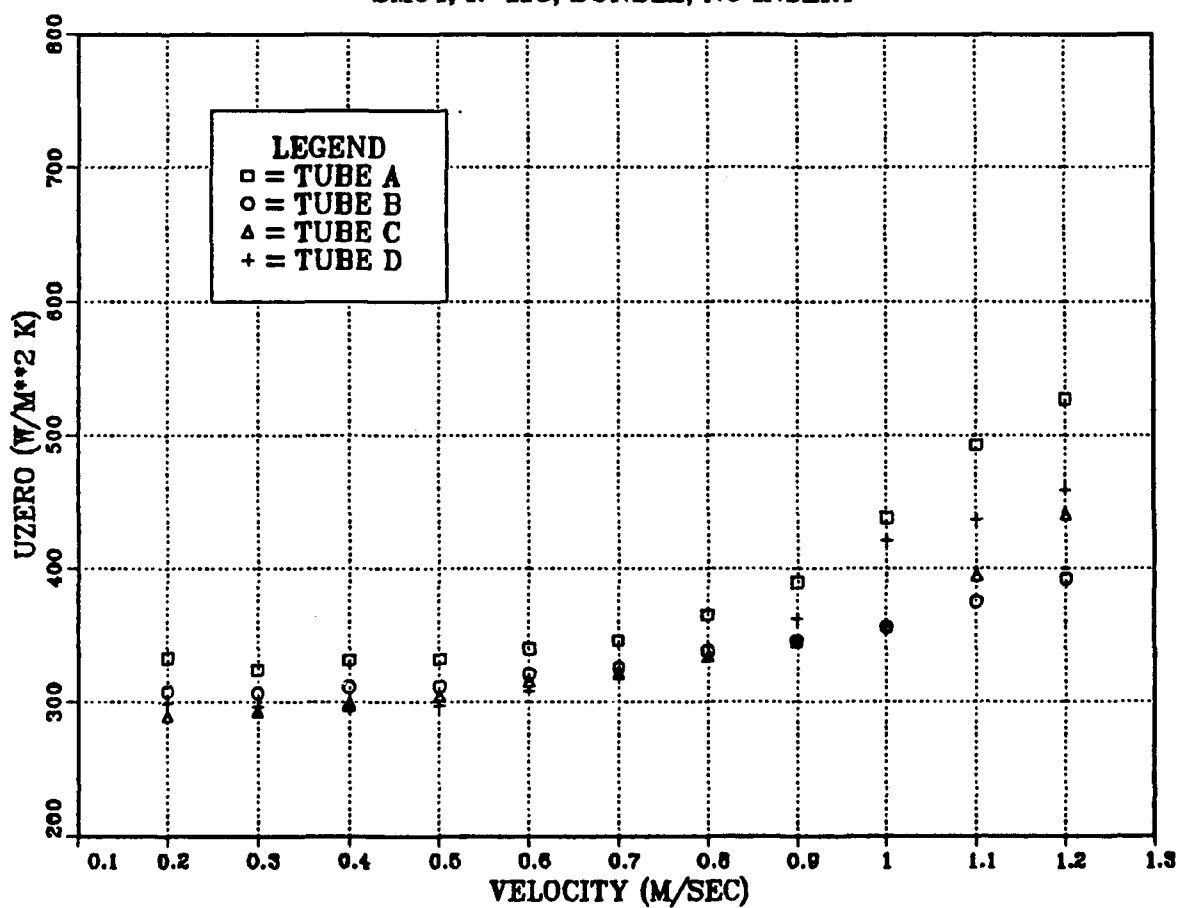


Figure 9. Single tube run on smooth copper tubes without inserts.

## UZERO SMOOTH COPPER TUBES

SM07, R-113, BUNDLE, TAPE INSERT

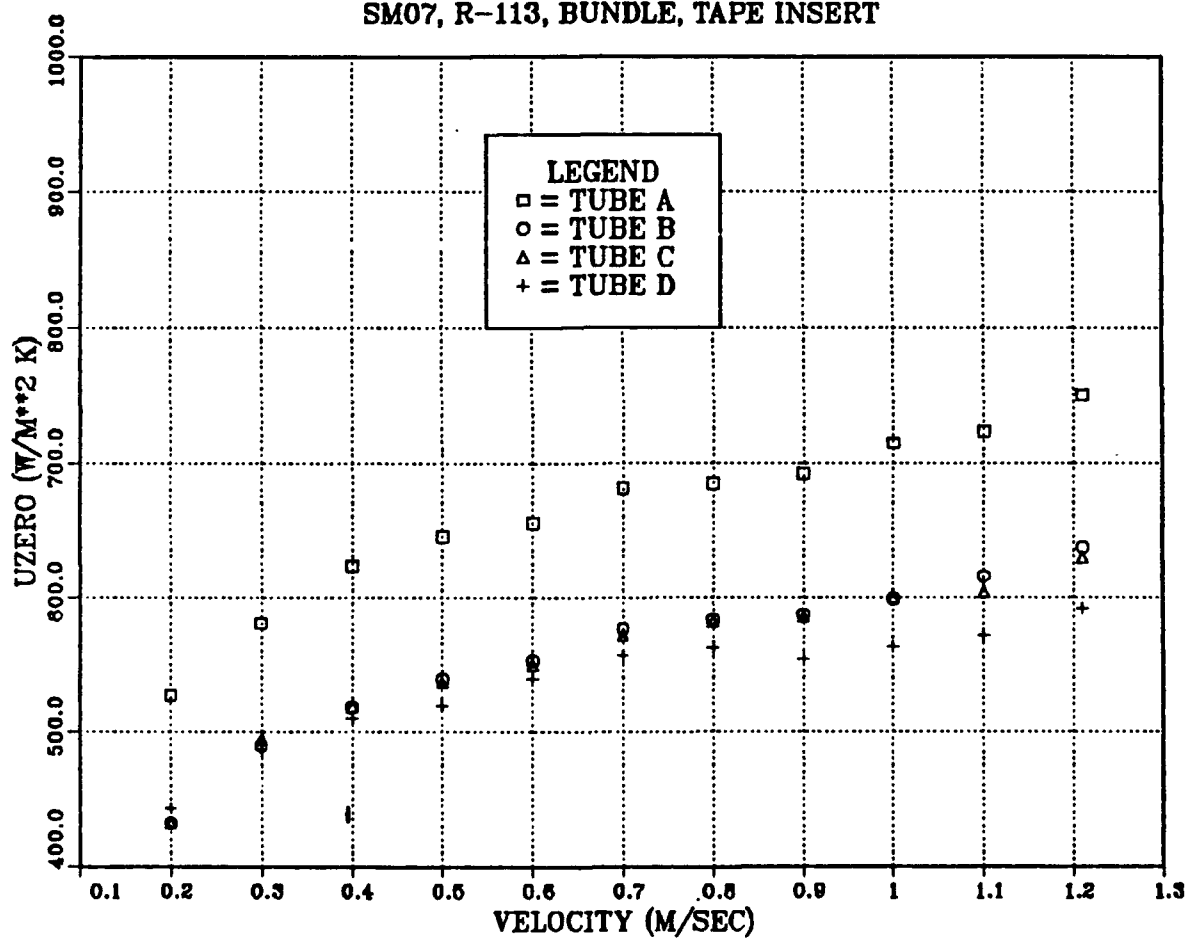


Figure 10. Smooth copper tubes with tape insert operated as a bundle.

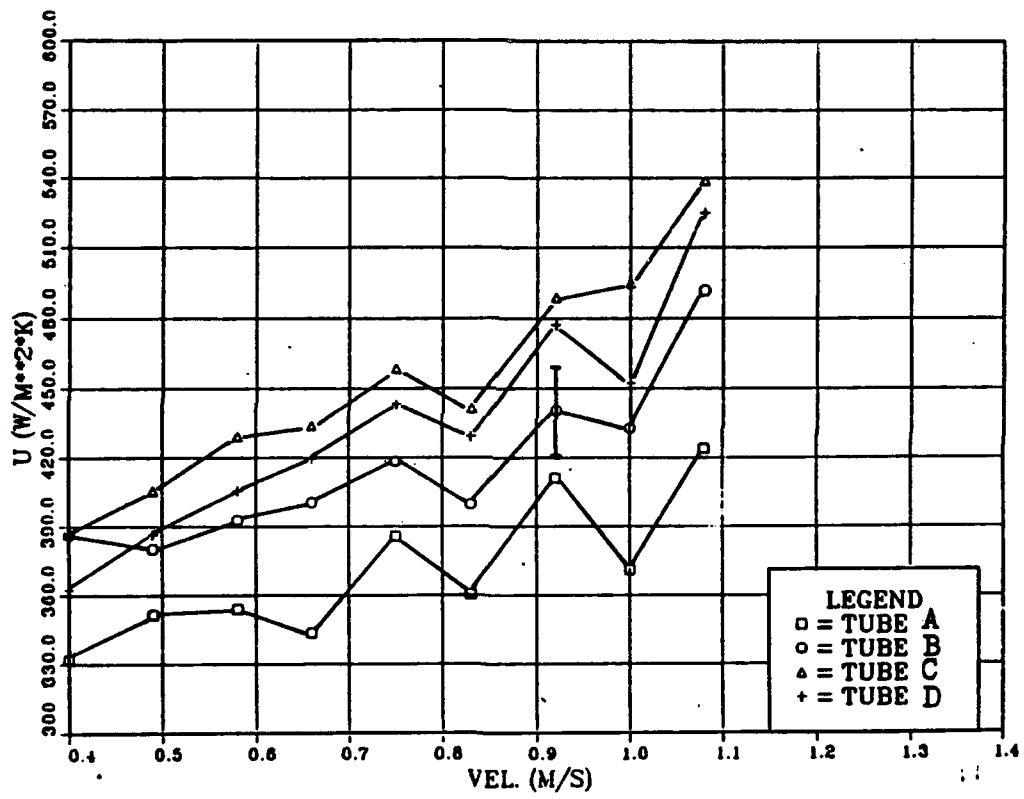


Figure 11. Data from Mabrey [Ref. 2]

## UZERO SMOOTH COPPER TUBES

SM07, R-113, SINGLE, TAPE INSERT

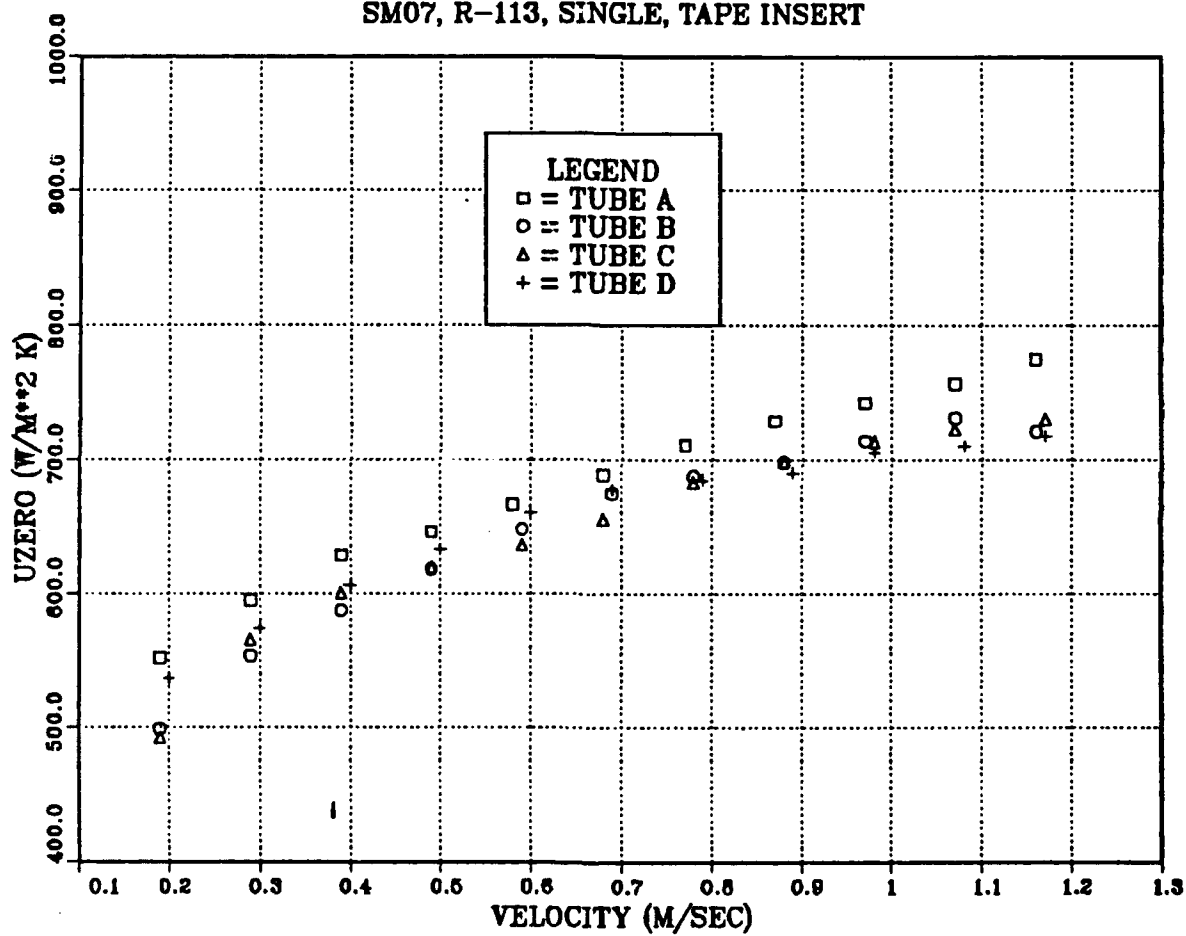


Figure 12. Smooth copper tubes with tape insert operated individually.

gued at the higher coolant velocities. This may reflect the fact that, at the higher coolant velocities, the inside resistance decreases while the outside resistance increases in importance. Anything which causes further increases in this resistance, such as condensate inundation, may cause noticeable effects in heat transfer.

As before, these same tubes with the HEATEX inserts installed were tested individually; the results are shown in Figure 14. The values of  $U_o$  for all four tubes are virtually identical and match the values for the top tube obtained during the bundle run (Figure 13). The values appear to be about 10% greater than for the tape insert experiments indicating that the HEATEX provides better tube-side enhancement.

While the preceding figures have shown the effect of inserts and also inundation on the heat transfer coefficient, two important questions must be addressed. First, what is the uncertainty associated with the calculated values for  $U_o$ . Secondly, the repeatability of the data must also be examined.

An uncertainty analysis was performed on  $U_o$  as shown in Appendix F based on the procedures of Kline and McClintock [Ref. 54]. At the low coolant velocities, the uncertainty was 5.2%. This uncertainty was based primarily on the uncertainty in the mass flow measurement. Here, one must include a scale interpolation term as well as a term to account for the time-wise jitter for the flowmeter. Since the flow rate is low for this coolant velocity, these two terms become more significant than at the higher flow rates. This is especially true if the magnitude of the time-wise jitter is the same for all flow rates which was the case in this study.

At high coolant velocities, the uncertainty in the value for  $U_o$  was about 5.6%. Here, the major factor driving this value is the uncertainty in the determination of temperature. The reason for this is that the  $\Delta T$  between the tube inlet and outlet is smaller than for low coolant velocities. Since the relative uncertainty for the thermocouples remains the same regardless of coolant velocities, uncertainty in the temperature measurement, specifically the LMTD, becomes the driving factor in determining the uncertainty in  $U_o$ .

The uncertainty analysis performed here was only for the overall heat transfer coefficient,  $U_o$ . In this analysis, any uncertainty in the correlations used to determine the physical properties of the ethylene glycol coolant or R-113 were neglected. Therefore, the level of uncertainty reported here is slightly conservative.

In order to examine the reproducibility of the data, repeat experiments were performed on the smooth copper tubes with the HEATEX elements installed. It is important to mention that during the time between the two runs, the tubes were removed



## UZERO SMOOTH COPPER TUBES

SM06, R-113, HEATEX, BUNDLE

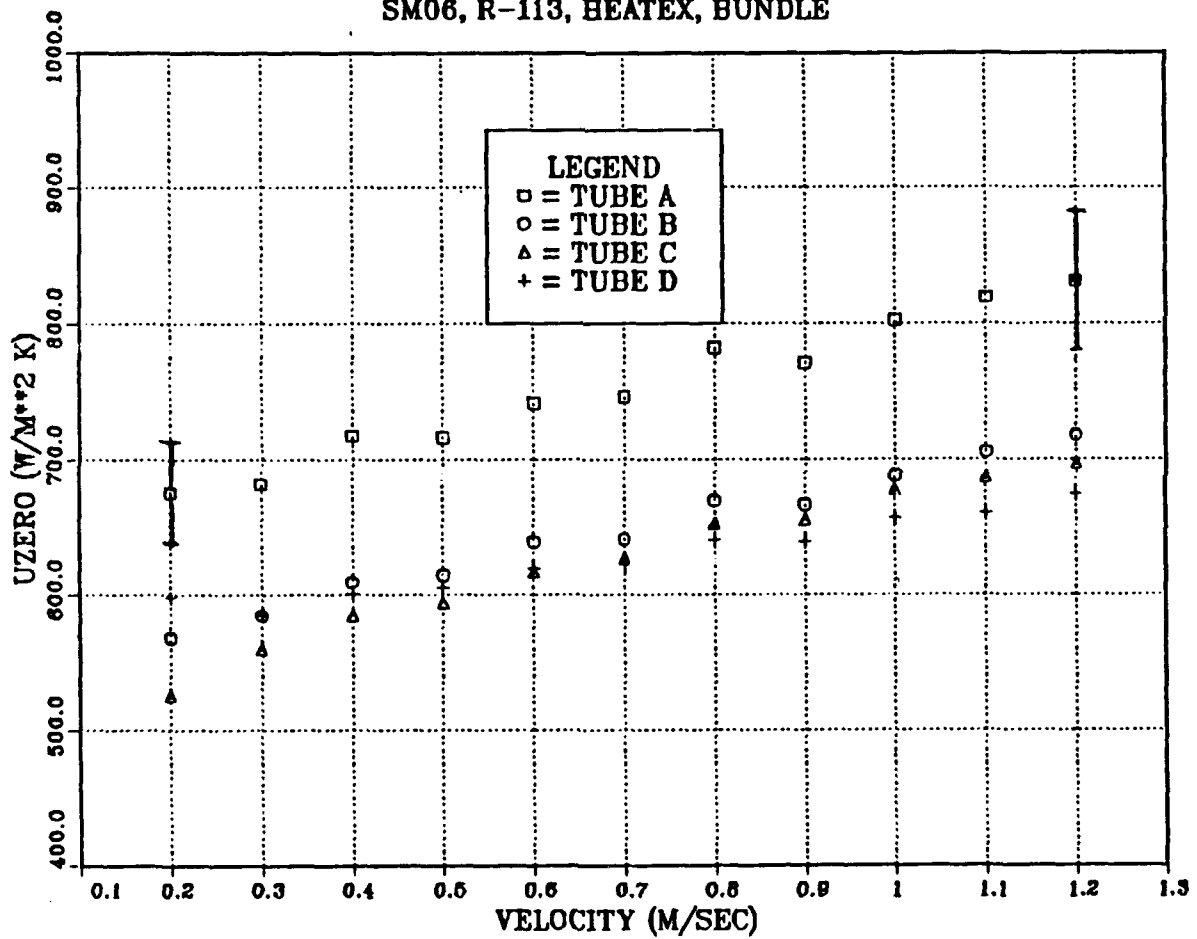


Figure 13. Smooth copper tubes with HEATEX inserts. Bundle operation.

## UZERO SMOOTH COPPER TUBES

SM06, R-113, HEATEX, SINGLE

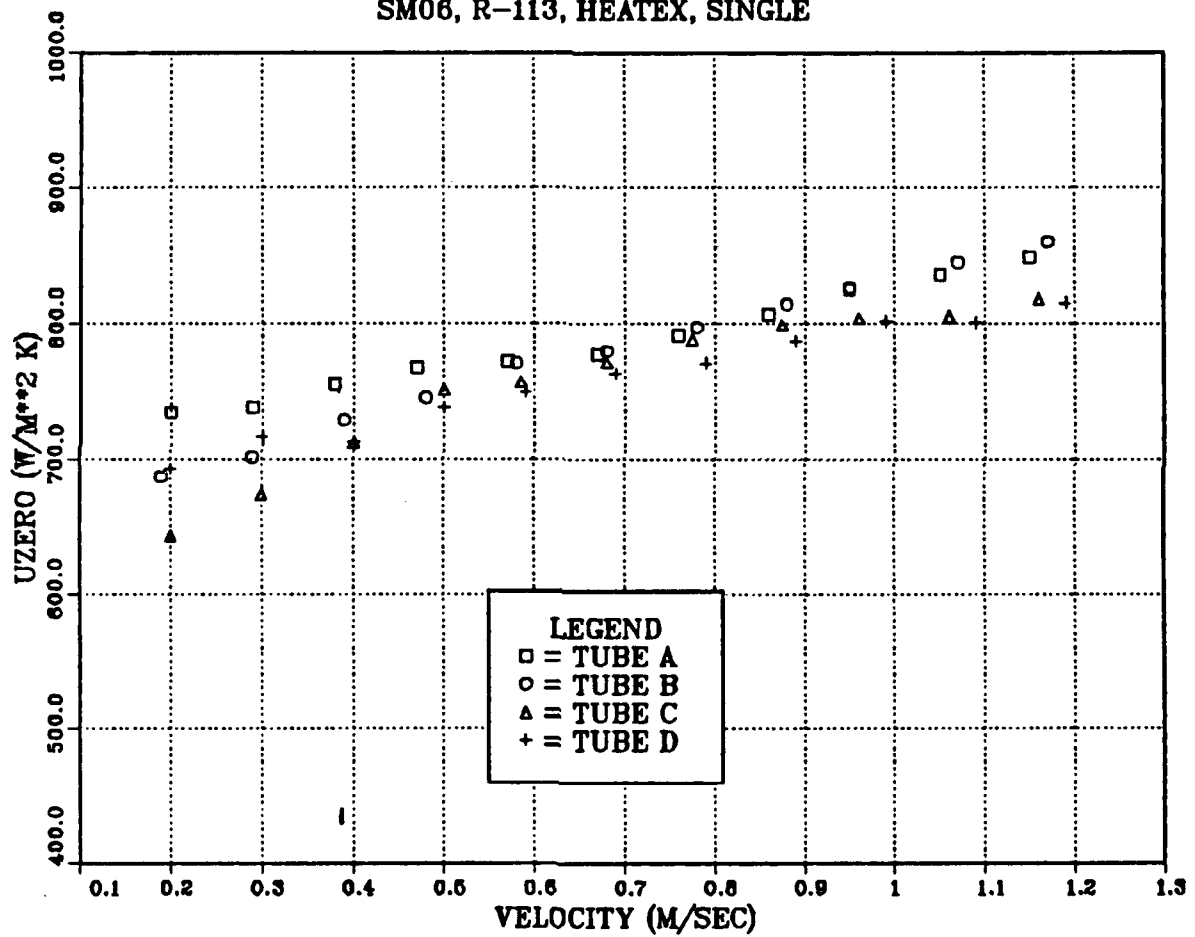


Figure 14. Smooth copper tubes with HEATEX installed. Individual operation.

from the condenser, cleaned and reinstalled. The results for the duplicate experiment are shown in Figure 15. When these values are compared to Figure 13, differences of the order of 3% is seen in the values of  $U_o$  for the top tube.  $U_o$  for the lower tubes are slightly larger with a more pronounced difference between the tubes. However, these differences all lie within the 6% uncertainty band indicating that the system gives good reproducibility.

In a similar manner, the results for a repeat experiment on the smooth copper tubes tested individually with the HEATEX installed is shown in Figure 16. When the values for  $U_o$  shown here are compared with those shown in Figure 14, no significant differences are seen. Again, this demonstrates the good reproducibility obtained by this system. However, a word of caution is in order. In all the experiments reported here, great care has been taken to control as many variables as possible. Of particular importance is to ensure that the heater power levels are set at the same level for each experiment. This will tend to keep vapor velocity in the condenser at similar levels for each experiment which will result in better repeatability.

The effects of having no insert as opposed to the twisted tape or HEATEX insert is shown in Figure 17. In this figure, the values for  $U_o$  for the top tube only have been plotted as a function of coolant velocity for the smooth copper tubes. As previously noted, without any insert, coolant flow is laminar and  $U_o$  is relatively constant up to about 0.7 m/s. When either the twisted tape or HEATEX inserts are installed,  $U_o$  increases markedly as coolant velocity increases. Interestingly, the HEATEX results in about a 10 to 14% increase in  $U_o$  when compared to the twisted tape inserts. Hence, from a heat transfer standpoint, the HEATEX element is the better insert. This is probably because the wire loops which make up the insert, touch much of the inside surface of the tube thereby "scrapping" the thermal boundary layer from the wall. With the twisted tape insert, mixing is provided only by inducing swirling which is probably not as an effective mechanism.

## **2. Copper/Nickel KORODENSE Tubes**

The results obtained for the overall heat transfer coefficient,  $U_o$ , for KORODENSE tubes operated as a bundle are shown in Figure 18. This series of experiments was performed without any inserts installed. Note the similarity between these results and those obtained under similar conditions with the smooth copper tubes (Figure 8). Again, values of  $U_o$  appear relatively constant for coolant velocities up to 0.7 m/s. As coolant velocity increases further, values of  $U_o$  increase dramatically. In addi-

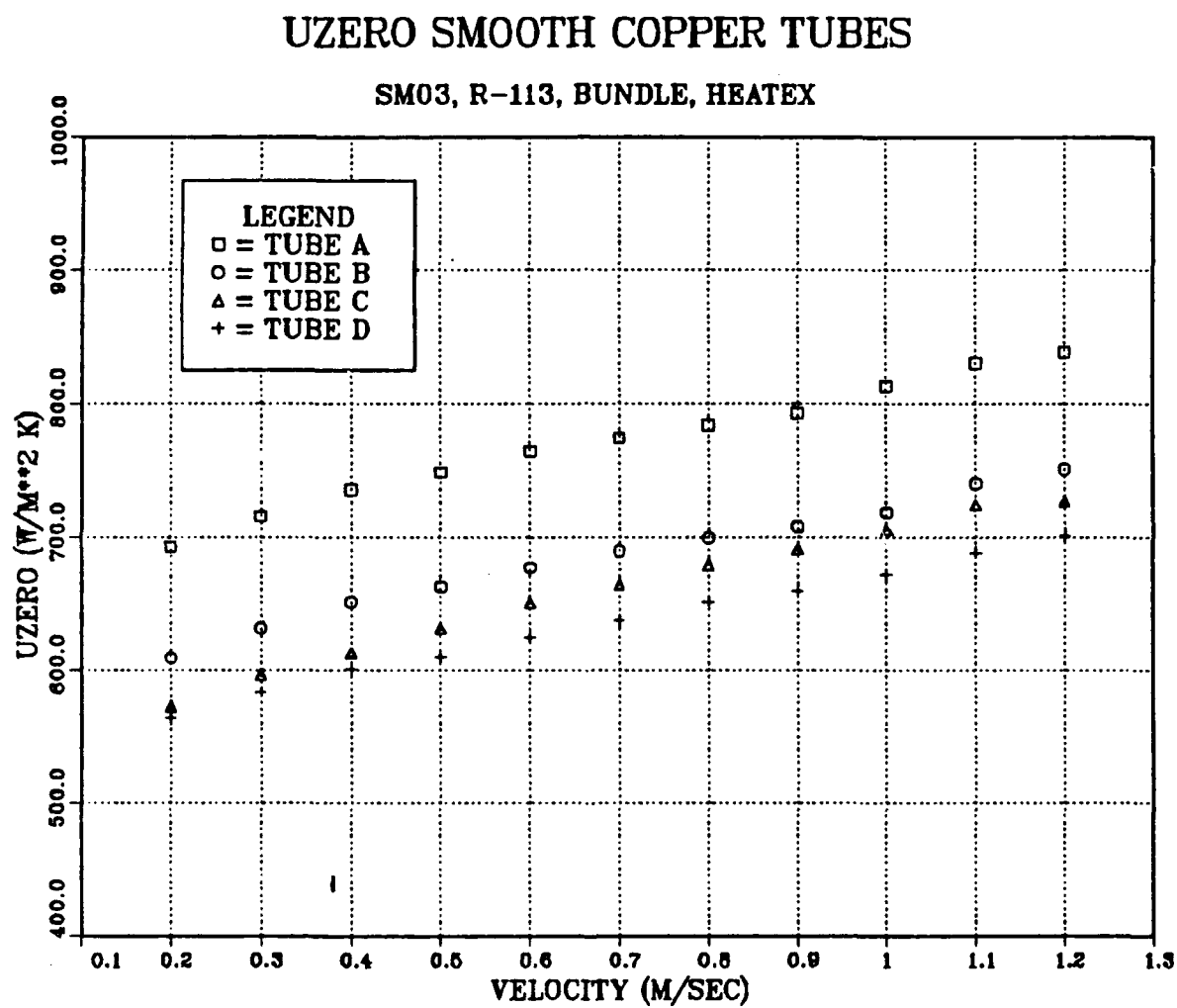


Figure 15. Repeat run on smooth copper tubes with HEATEX insert.

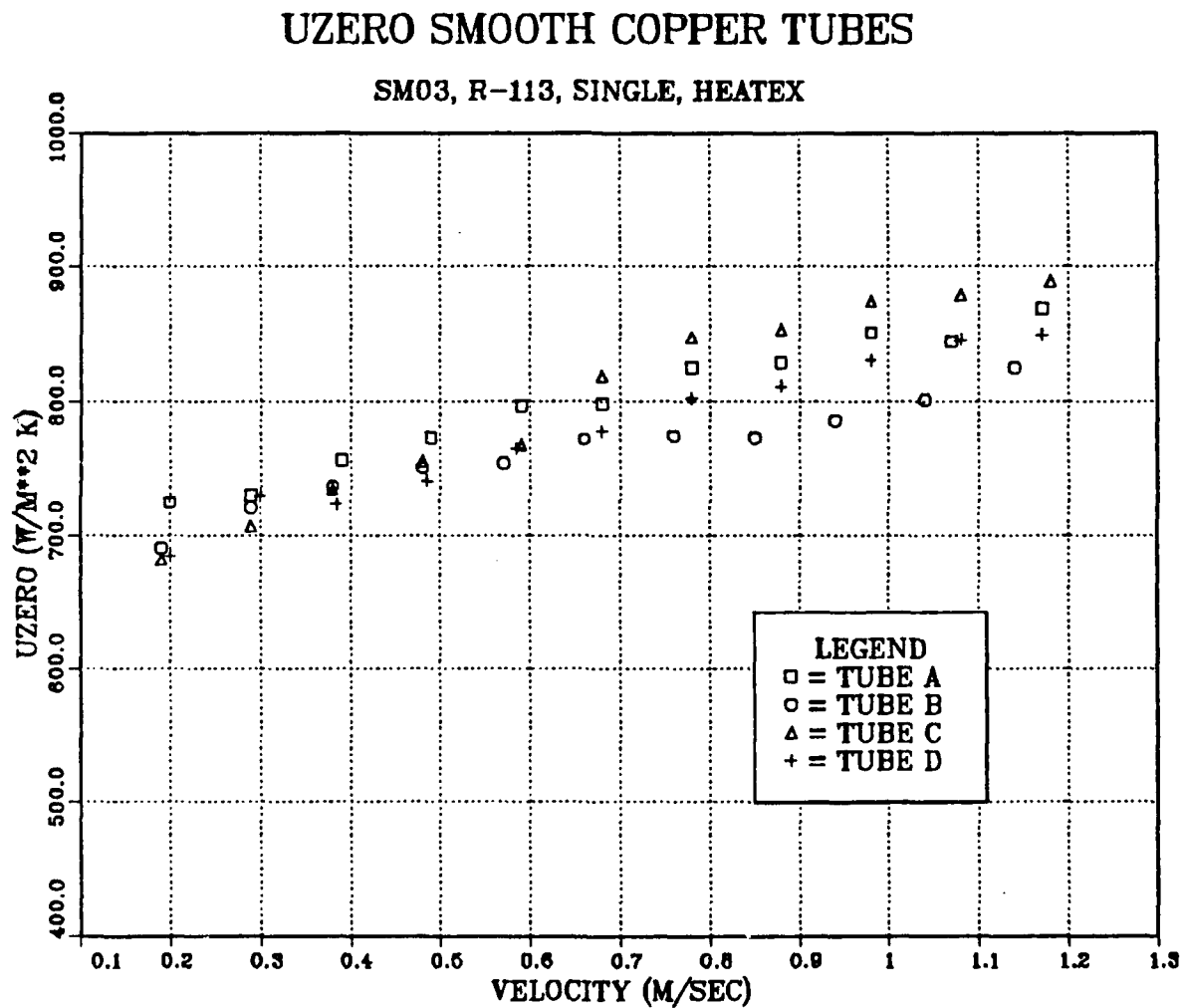


Figure 16. Repeat run on smooth copper tube with HEATEX. Individual runs.

## EFFECT OF INSERTS

SMOOTH COPPER TUBES

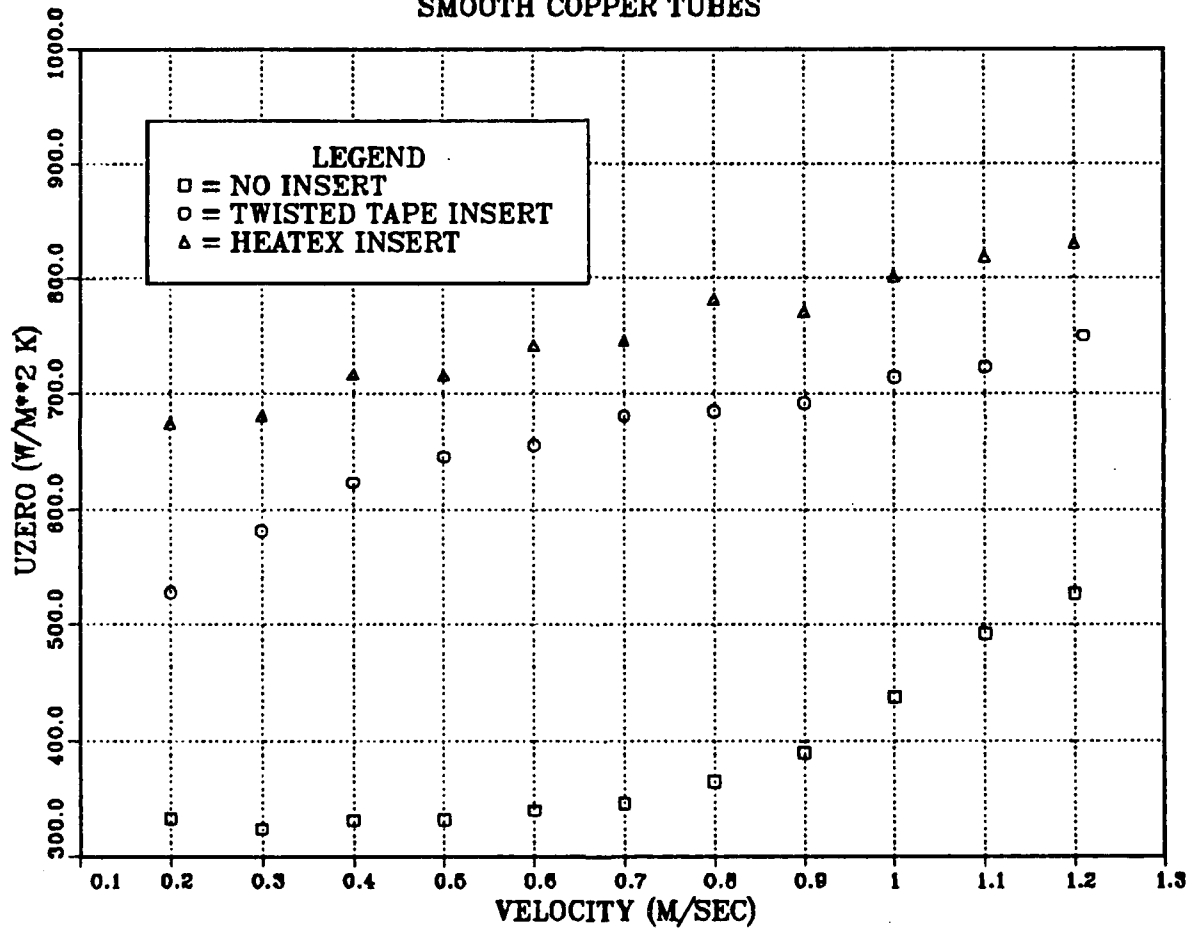


Figure 17. Effect of tube inserts on  $U_z$ .

tion, an effect of condensate inundation begins to be apparent at these higher coolant velocities.

Results obtained when these same tubes were operated individually are shown in Figure 19. Again, when there is no inundation, all tubes have similar behavior. In addition, the values obtained here match those obtained for the top tube during the bundle experiment (see Figure 18). Interestingly, the relative magnitude of  $U_o$  is remarkably similar to that obtained for the smooth copper tubes (Figure 9). This is somewhat surprising. The KORODENSE tubes are corrugated on both the inside as well as the outside. Therefore, one would have expected somewhat higher values for heat transfer with the KORODENSE than with the smooth copper tube.

Values of  $U_o$  for the KORODENSE tubes with the twisted tape inserts installed are shown in Figure 20. This data was obtained during bundle operation. As coolant velocity increased,  $U_o$  increased steadily. This was true for all four tubes. The effect of inundation reduced  $U_o$  by about 15% (tube B relative to tube A). There appeared to be more separation in the values of  $U_o$  for tubes B, C, and D than was the case for the smooth copper tubes (see Figure 10) suggesting a greater inundation effect. In comparison with the data obtained for the smooth copper tubes, the KORODENSE tubes resulted in a slight increase (about 6 to 8%) in  $U_o$ . This difference may be due to the fact that the insert reduces the inside heat transfer resistance so that the accuracy of the measurement is improved.

The results obtained for these same tubes operated individually are shown in Figure 21. As expected, all four tubes behave similarly when no inundation is present. In addition, the values for  $U_o$  match those obtained for the top tube during the bundle operation (Figure 20). In comparison to the smooth copper tube data (Figure 12), the data for the KORODENSE tubes appears somewhat higher (about 6 to 8%). However, given the known uncertainty, this difference is probably not significant.

Results obtained for the KORODENSE tubes during bundle operation with the HEATEX elements installed are shown in Figure 22. Note that  $U_o$  again increases markedly for all four tube as coolant velocity increases. An inundation effect can be seen for tubes B, C, and D which is similar to that seen in the twisted tape runs. Tube B shows approximately a 15% decrease in  $U_o$  compared to tube A. This effect is magnified at higher coolant velocities (condensation rates) as one would expect. When this data is compared to that obtained for the smooth copper tubes with HEATEX installed (see Figure 13), it can be seen that  $U_o$  is greater for the KORODENSE tubes. This suggests that roping of the tube provides some enhancement for the outside (and possibly the

## UZERO KORODENSE TUBES

KD02, R-113, BUNDLE, NO INSERT

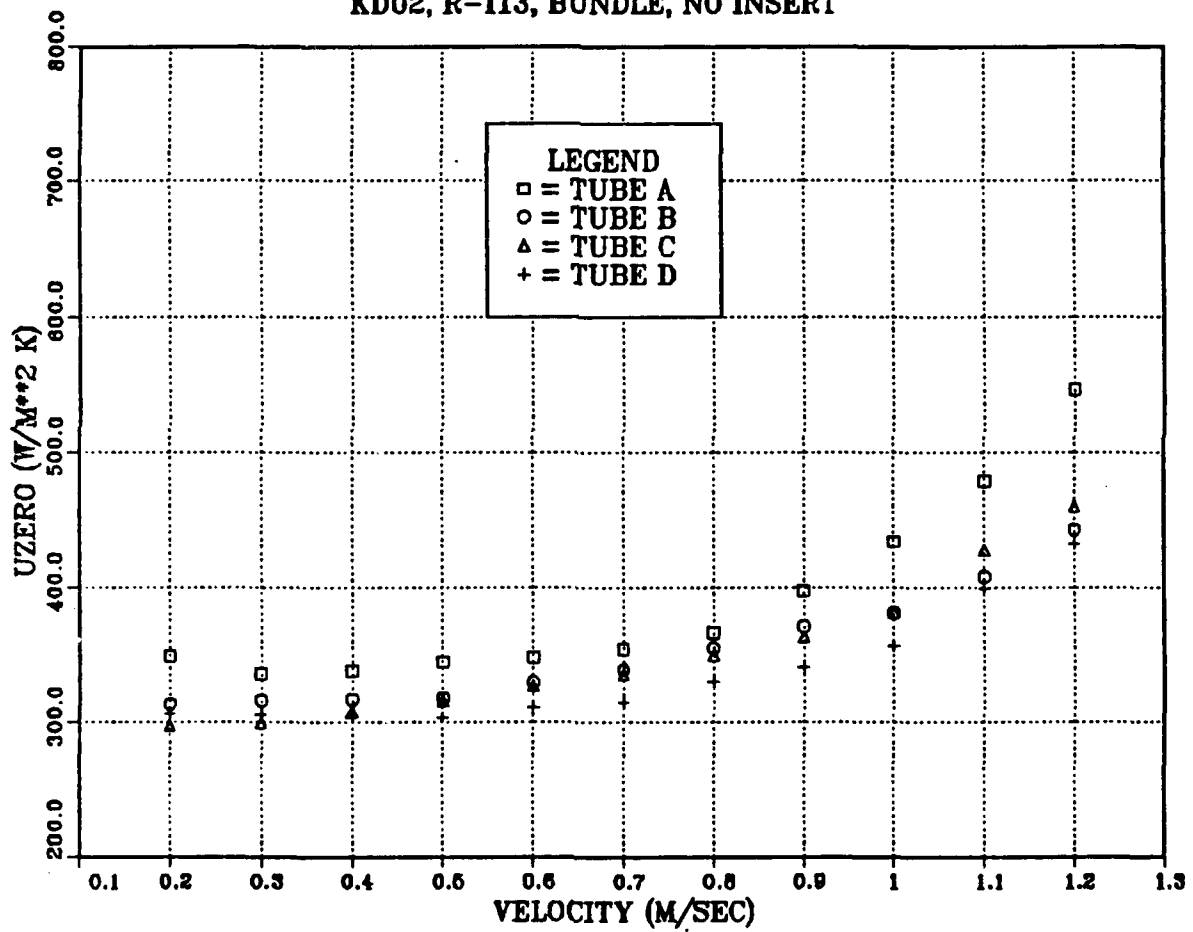


Figure 18. KORODENSE tubes with no insert, bundle operation.



## UZERO KORODENSE TUBES

KD02, R-113, SINGLE, NO INSERT

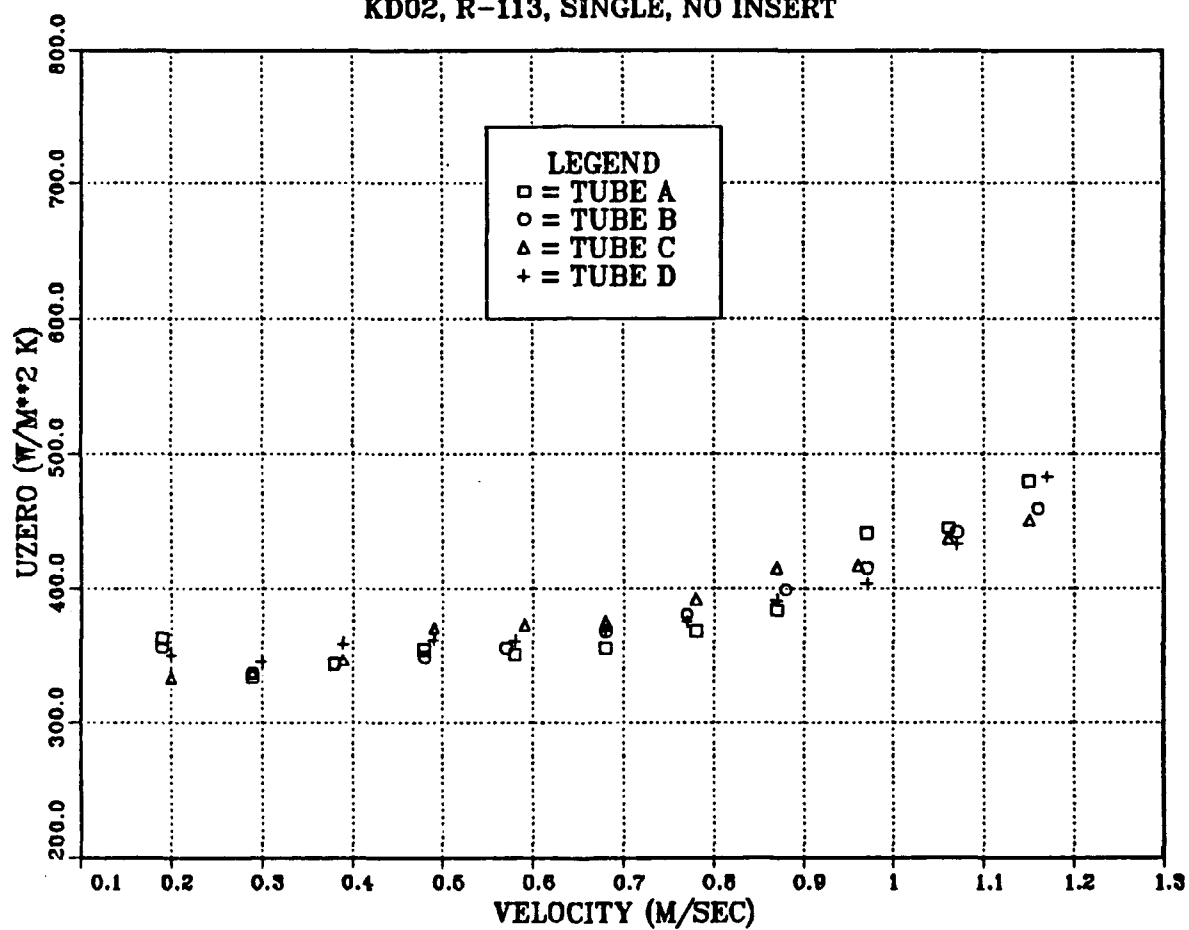


Figure 19. KORODENSE tubes operated individually, no inserts installed.

## UZERO KORODENSE TUBES

KD04, R-113, BUNDLE, TAPE INSERT

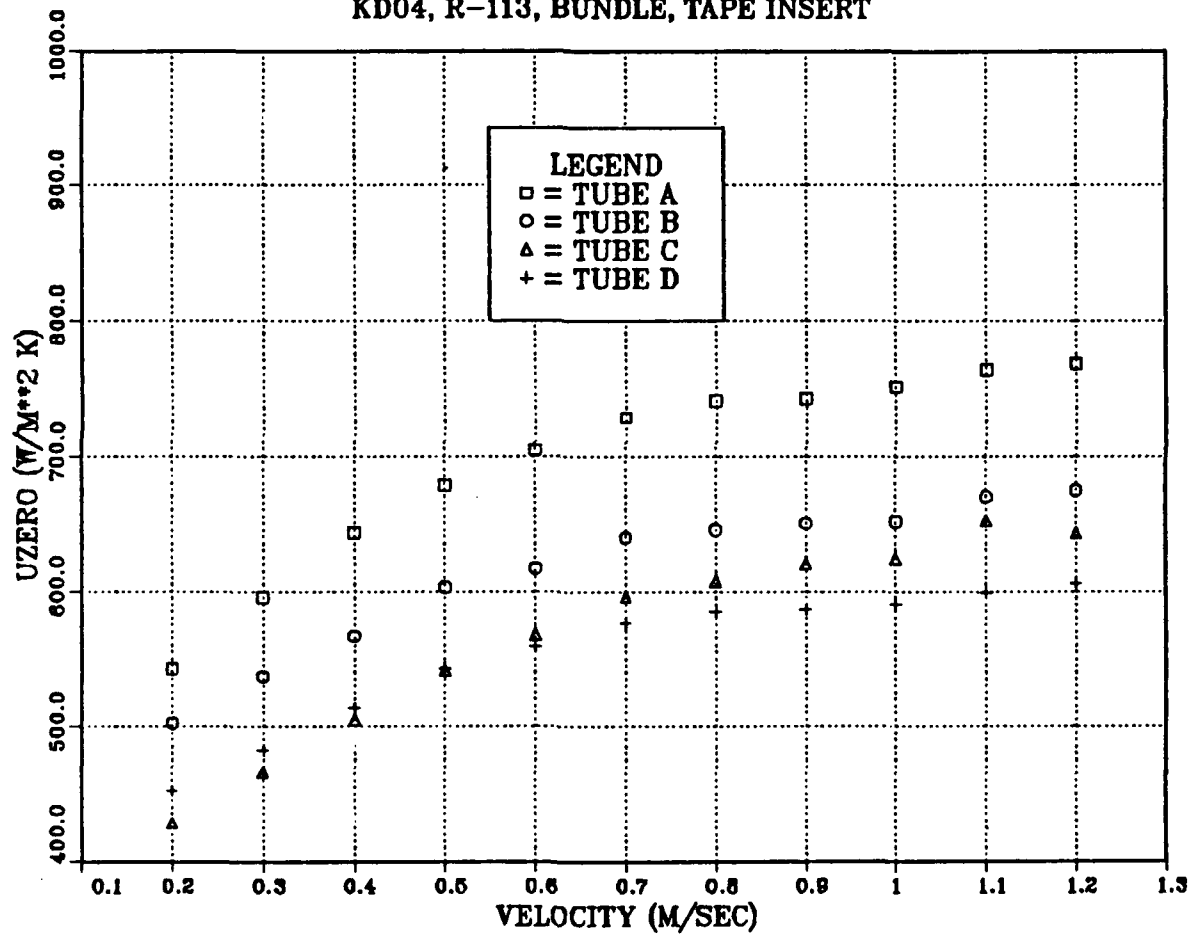


Figure 20. KORODENSE tubes with tape inserts, bundle operation.

## UZERO KORODENSE TUBES

KD04, R-113, SINGLE, TAPE INSERT

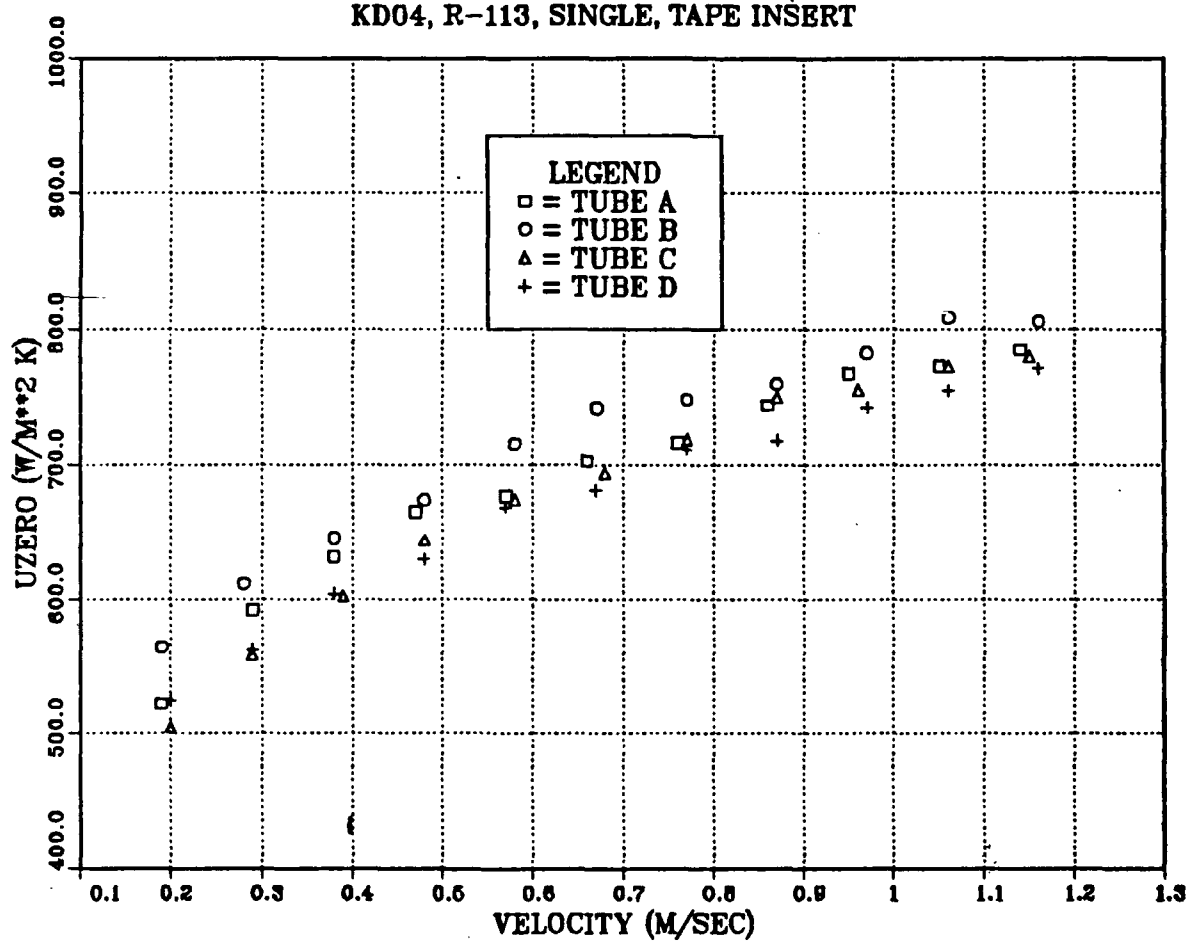


Figure 21. KORODENSE tubes with tape inserts, individual operation.

inside) heat transfer coefficients. While we expect some small difference, it must be pointed out that the differences observed here are at the bounds of the calculated uncertainty.

Results for these tubes tested individually are shown in Figure 23. As before, the values of  $U_o$  are similar for all four tubes and match the values obtained for the top tube during the bundle experiments (see Figure 22). In comparison to the data obtained for the smooth copper tubes, the values of  $U_o$  are somewhat higher as expected, but are still at the bounds of the calculated uncertainty.

The effect of using no insert, twisted tape and HEATEX on  $U_o$  can be seen in Figure 24. The data are for the top tube only. Note that, as with the smooth copper tubes (Figure 17), the HEATEX results in about a 10 to 14% increase in  $U_o$  in comparison to the twisted tape insert. Both provide significant enhancement in  $U_o$  when compared to no insert (almost 100% enhancement). As with the smooth copper tubes, when no insert is used,  $U_o$  appears relatively constant for coolant velocities over the range of 0.2 to 0.7 m/s indicating laminar flow.

### 3. Wire Wrapped KORODENSE Tubes

This series of experiments was performed to determine an optimum wire diameter as discussed in "Experimental Procedure". All tubes were tested individually and all had HEATEX mixing elements installed. Figure 25 shows  $U_o$  as a function of coolant velocity for the case of an ordinary KORODENSE tube together with tubes wrapped with 0.029", 0.049" and 0.0675" diameter wire, each tested in the top position (tube A). The 0.049" diameter wire gives the biggest enhancement in  $U_o$  (about 25%). While the other two wire diameters also provide enhancement in  $U_o$  (about 15%), it is below that of the 0.049" wire. The no wire case agrees with the previously obtained data (see Figure 22).

Figure 26 shows similar data but in this case for tube B. Again, the 0.049" diameter wire provides the greatest enhancement in  $U_o$  (again about 25%).

Figure 27 shows what happens when the different diameter wires are used on tube C. In this case an interesting fact can be observed. Here, both the 0.049" and 0.029" wire provide virtually the same degree of enhancement for  $U_o$  (about 20%) with both being better than the 0.0675" wire. Figure 28 shows the results obtained for tube D. Note that while the 0.049" wire again provides the greatest degree of enhancement for  $U_o$  (about 16%), the differences between the three different diameter wires are not as great.

## UZERO KORODENSE TUBES

KD03, R-113, BUNDLE, HEATEX

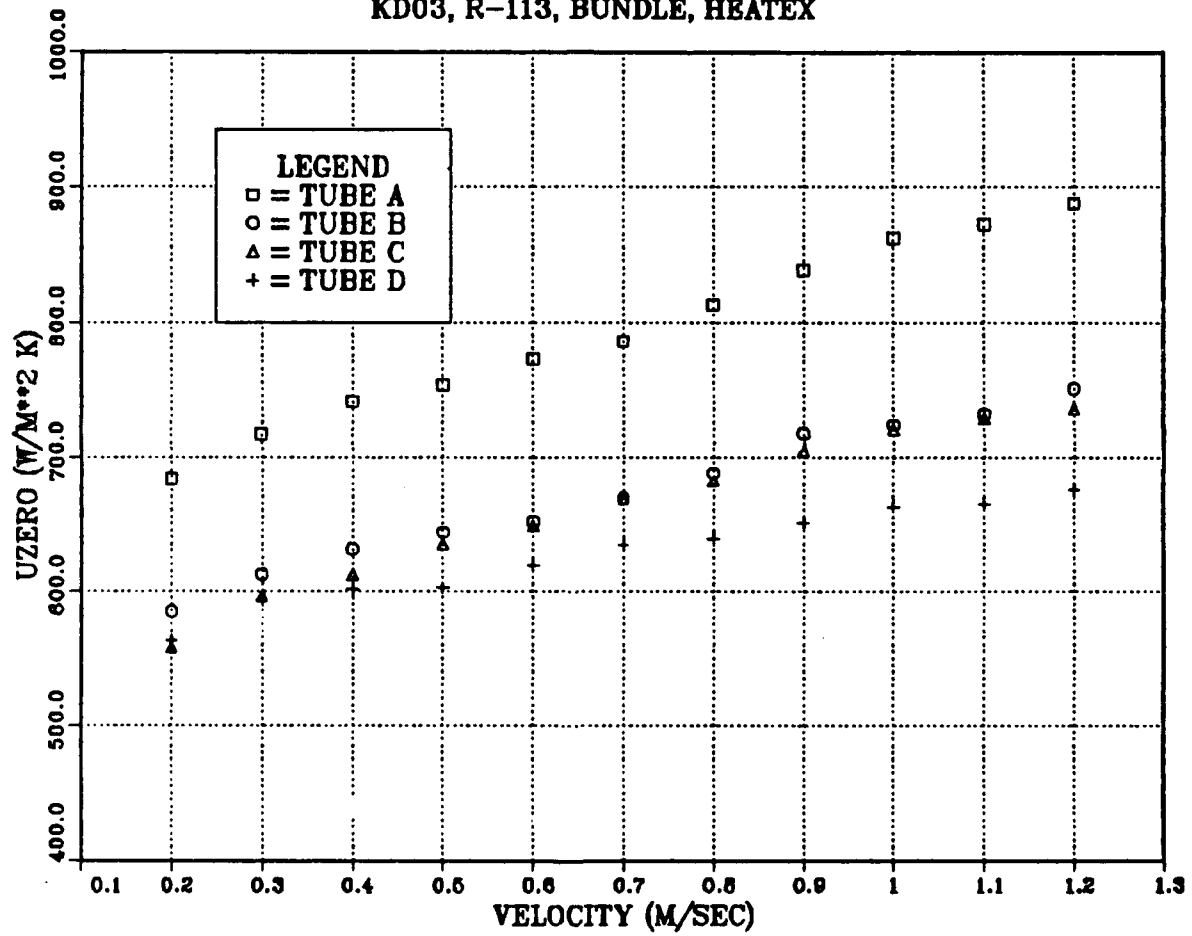


Figure 22. KORODENSE tubes with HEATEX inserts, bundle operation.

## UZERO KORODENSE TUBES

KD03, R-113, SINGLE, HEATEX

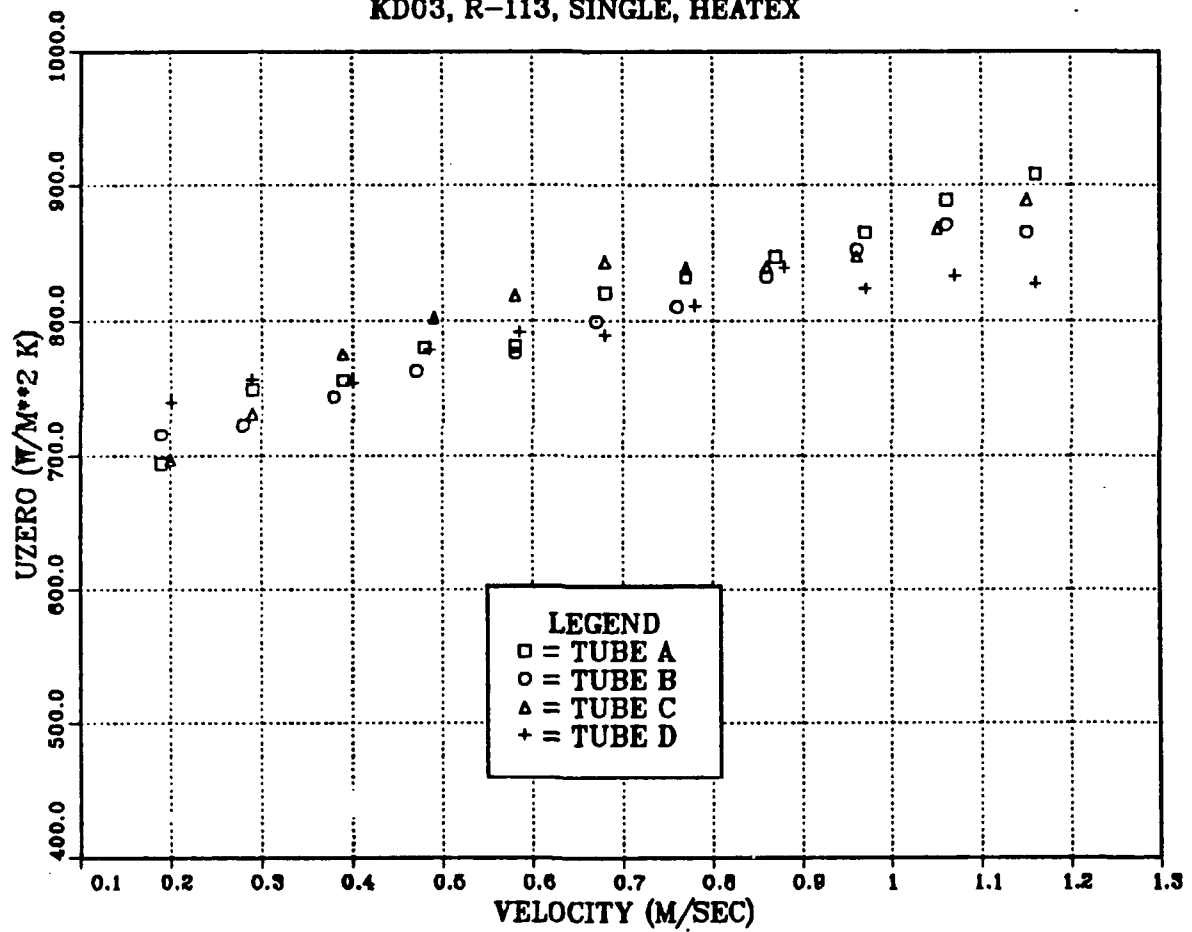


Figure 23. KORODENSE tubes with HEATEX inserts, individual operation.

## EFFECT OF INSERTS

KORODENSE CU/Ni TUBES

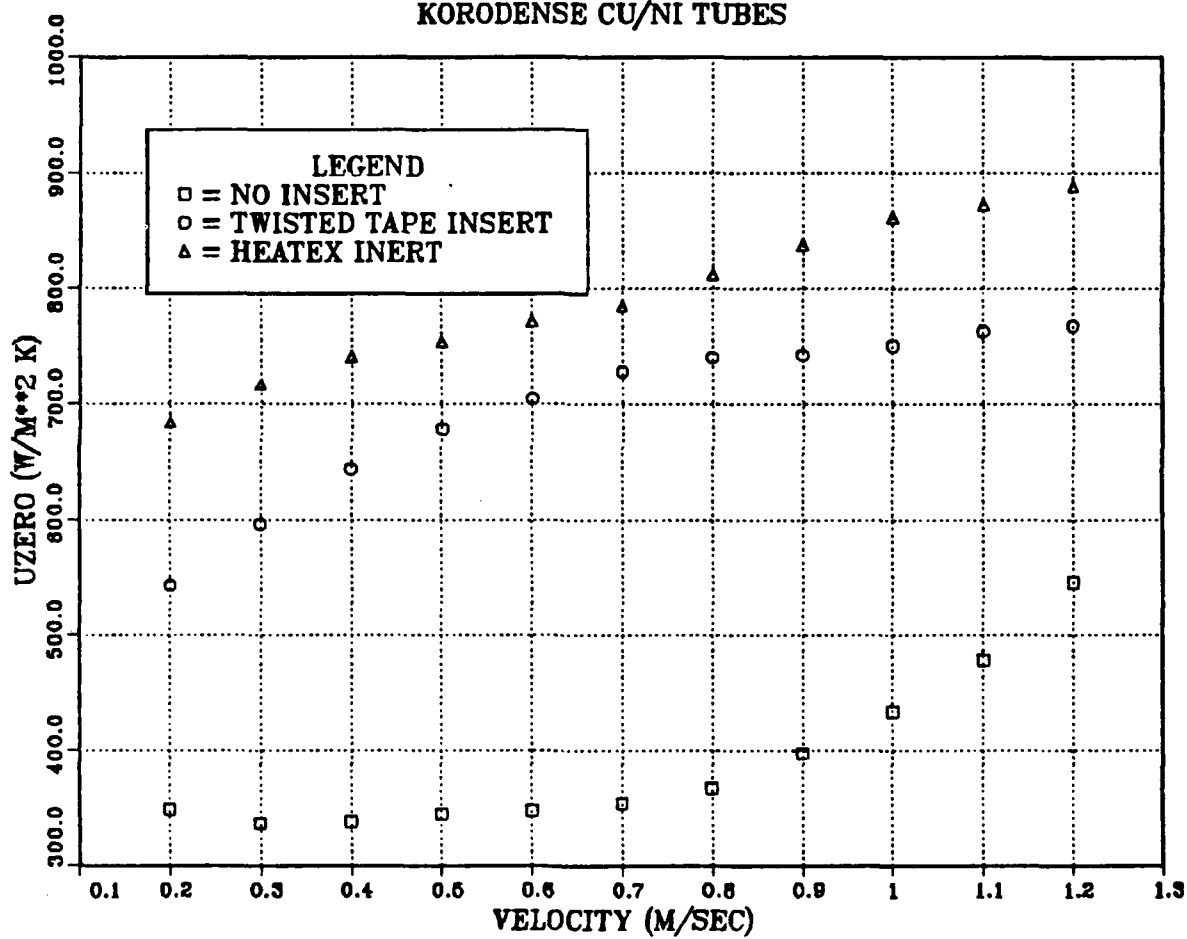


Figure 24. Effect of tube inserts on  $U_z$ .

# UZERO WIRE WRAPPED KORODENSE

TUBE A, R-113, HEATEX

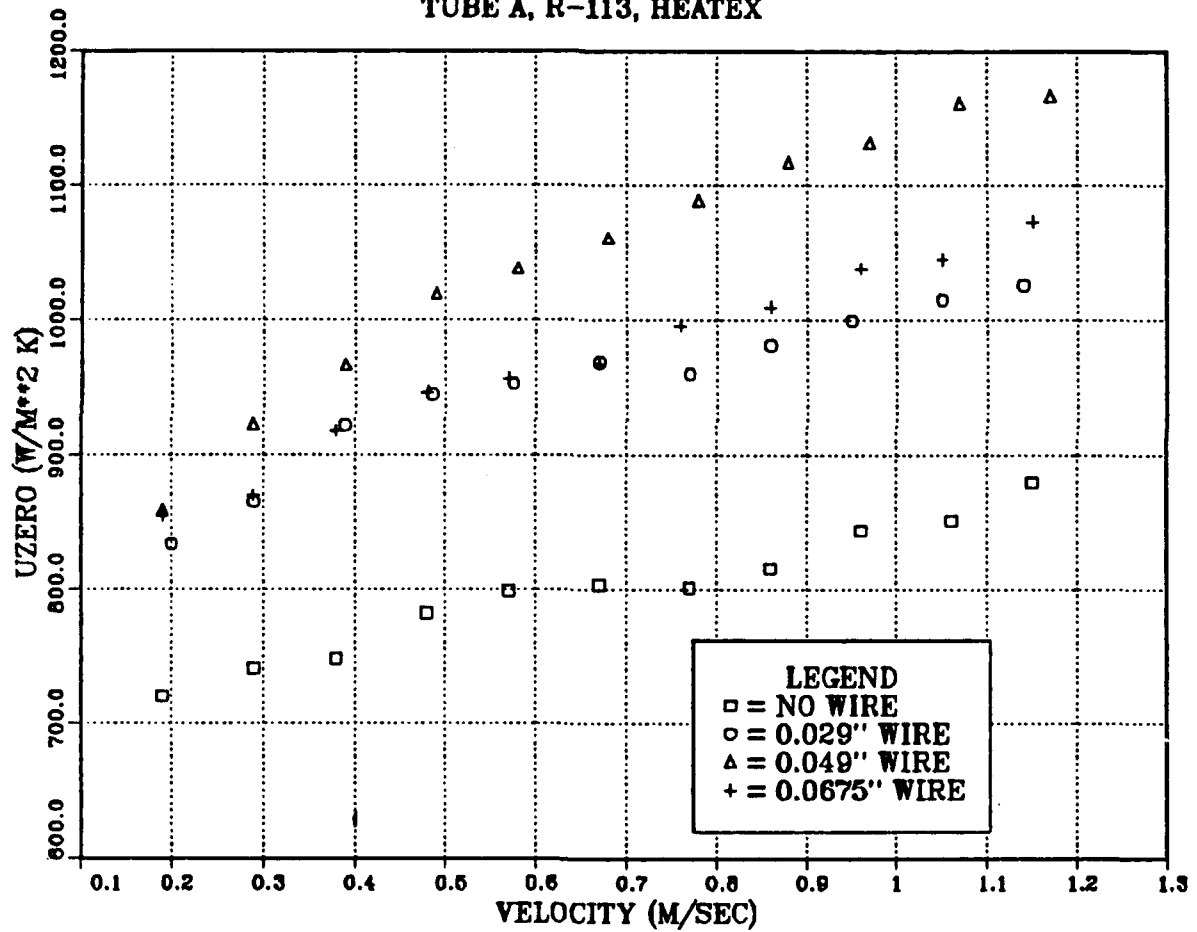


Figure 25. Effect of wire diameter on  $U_z$  for tube A.



# UZERO WIRE WRAPPED KORODENSE

TUBE B, R-113, HEATEX

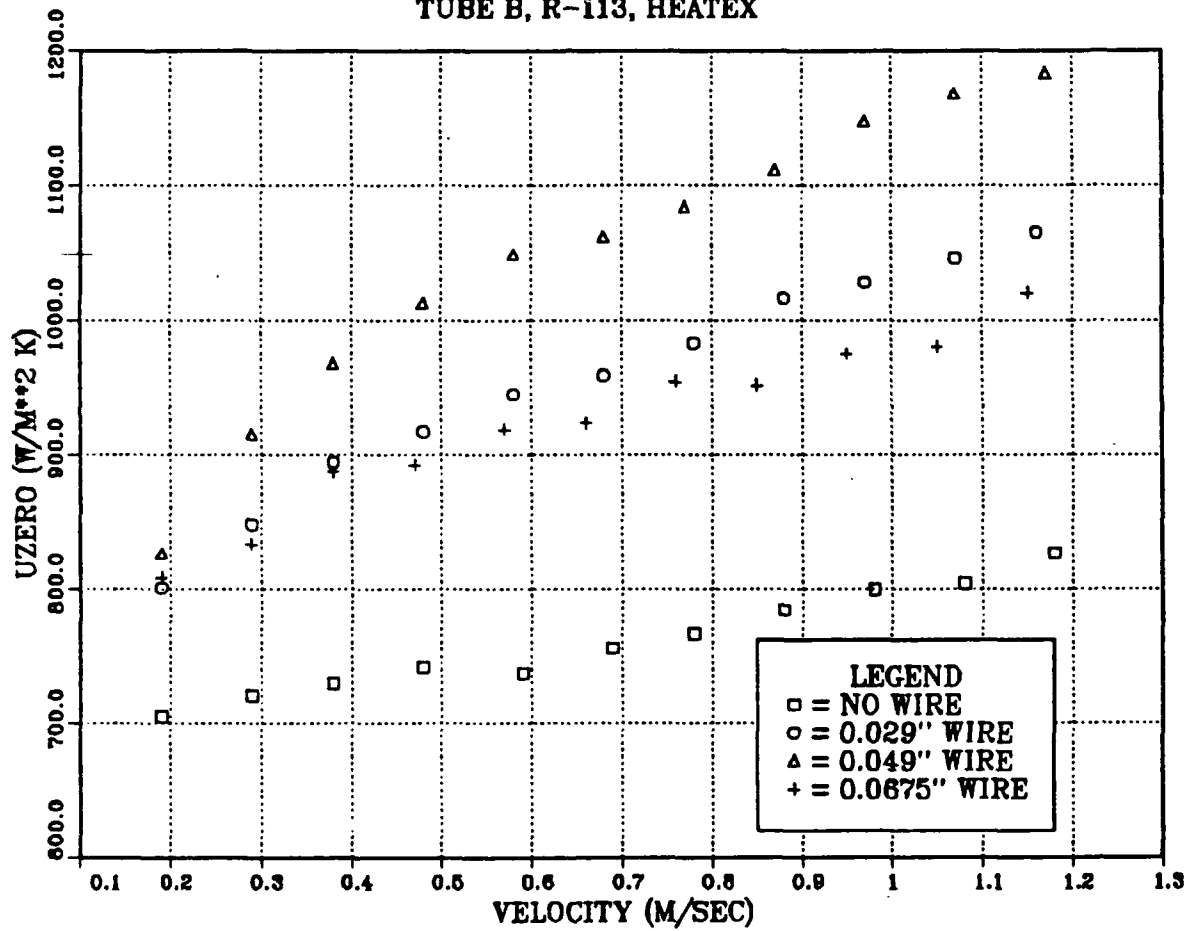


Figure 26. Effect of wire diameter on  $U_o$  for tube B.

# UZERO WIRE WRAPPED KORODENSE

TUBE C, R-113, HEATEX

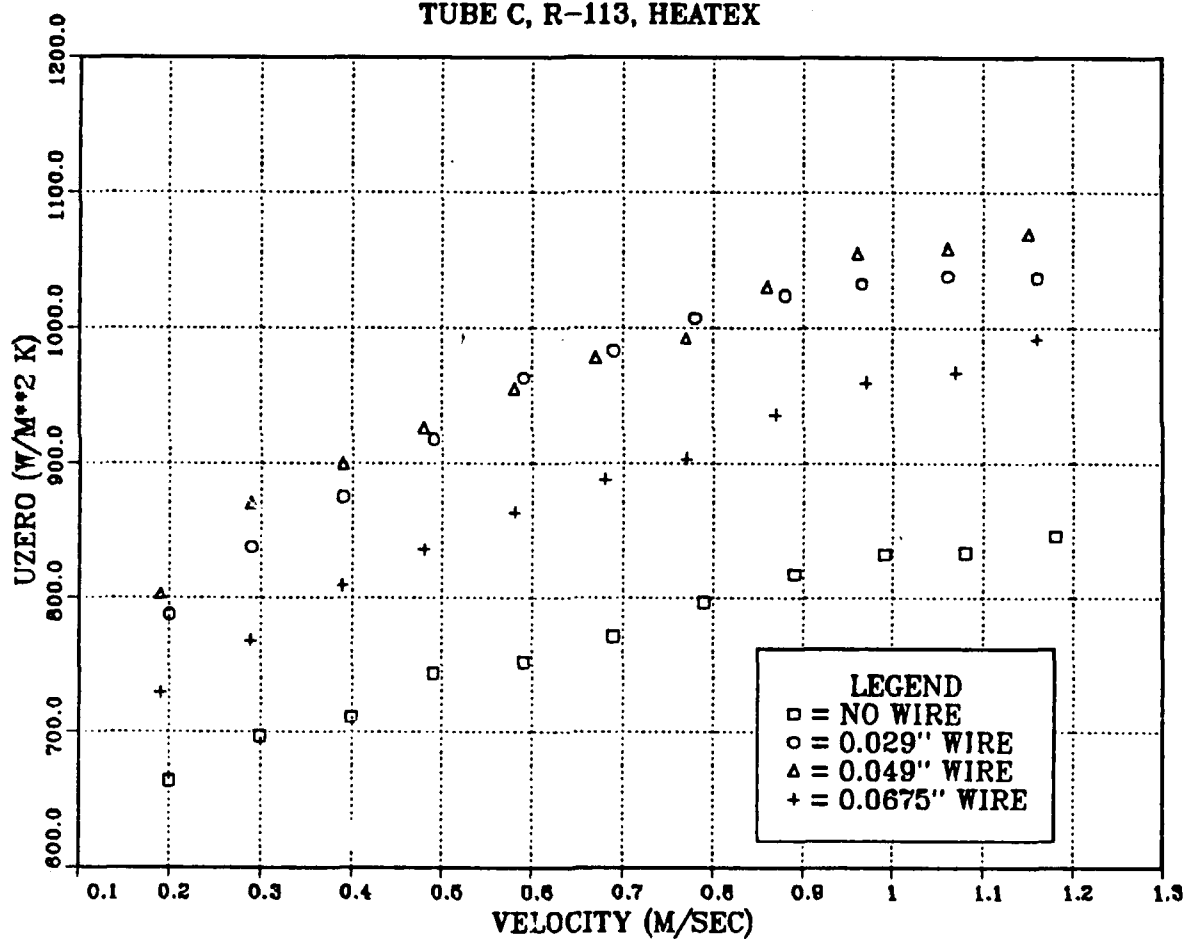


Figure 27. Effect of wire diameter on  $U_o$  for tube C.

# UZERO WIRE WRAPPED KORODENSE

TUBE D, R-113, HEATEX

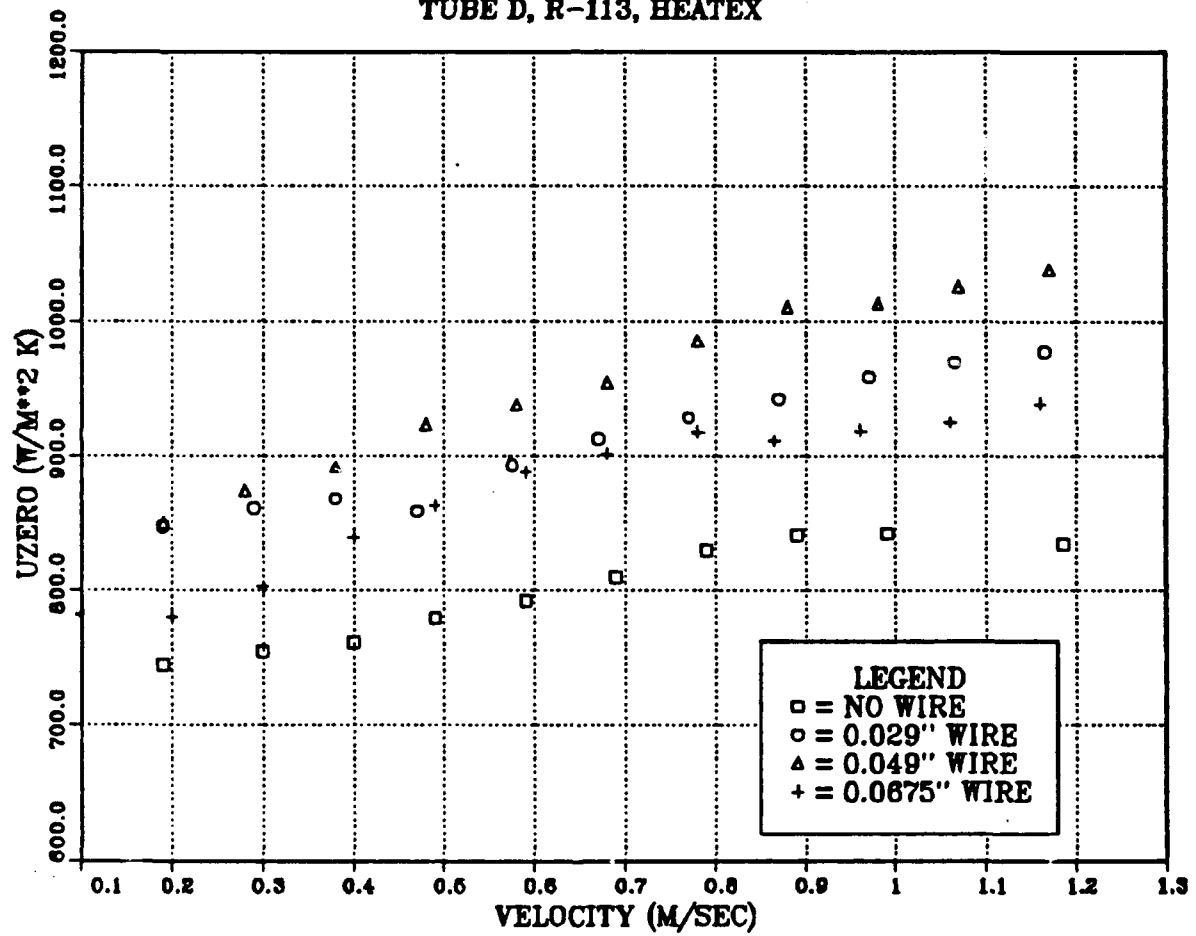


Figure 28. Effect of wire diameter on  $U_z$  for tube D.

Figure 27 and Figure 28 suggest that the position of the wire wrapped tube within the bundle may affect the overall heat transfer coefficient. In order to gain further insight on this, the data obtained from these experiments was replotted so that  $U_o$  for a given wire diameter was plotted as a function of coolant velocity for all four tube positions. The data for the tube without any wire is shown in Figure 29. The data is all very similar and no distinct trends are evident. Note that comparison of this data with Figure 23 again demonstrates the reproducibility of the system.

Figure 30 (0.029" wire diameter) shows that tubes A, B and C behave similarly. Tube D produces consistently lower values for  $U_o$  than the other tubes. Figure 31 (0.049" wire) demonstrates what appears to be a positional effect on  $U_o$ . The data for tube A and B is virtually identical and lies above that of tubes C and D which are also virtually identical. Figure 32 suggests that there is also a positional effect for the 0.0675" wire. The top tube seems to provide the greatest enhancement in  $U_o$ . The level of enhancement for tubes C and D are approximately the same, both being lower than tubes A and B.

Figure 33 shows  $U_o$  plotted as a function of wire diameter for an arbitrarily chosen coolant velocity of 1.0 m/s. Note that the strongest positional affect appears to be for the 0.049" wire. Also, it is clearly evident that the 0.049" wire provides the greatest enhancement for heat transfer.

The possible positional effect may be due to vapor velocity. Although the velocity of the vapor was very small in this study (approximately 0.1 m/s) there may still be an effect. As the vapor penetrates the tube bundle, it slows down. As its velocity is reduced, it can no longer help to strip condensate from the tubes. Hence, heat transfer is decreased. This effect looks much like an inundation effect. An interesting point is why this shows up in these experiments and not with the plain KORODENSE or smooth copper tubes. With the wire wrapped tubes, the condensate layer is presumably thin. Therefore, anything which could help to thin it further would be of importance in improving heat transfer. The loss of this small amount of vapor shearing may be important in this case.

In this study, the 0.049" diameter wire appears to give the best enhancement in heat transfer (see Figure 33). This yields a pitch to wire diameter ratio of 7.2. Fujii et al. [Ref. 33] found that for condensation of R-12 on wire wrapped smooth copper tubes, the optimal pitch-to-wire diameter ratio was on the order of 2. This difference could be due to our use of the KORODENSE tubes. For a pitch-to-wire diameter ratio of 2, we would have had to use wire which was of the order of 5 mm in diameter. This would have

# UZERO WIRE WRAPPED KORODENSE

NO WIRE, R-113, HEATEX

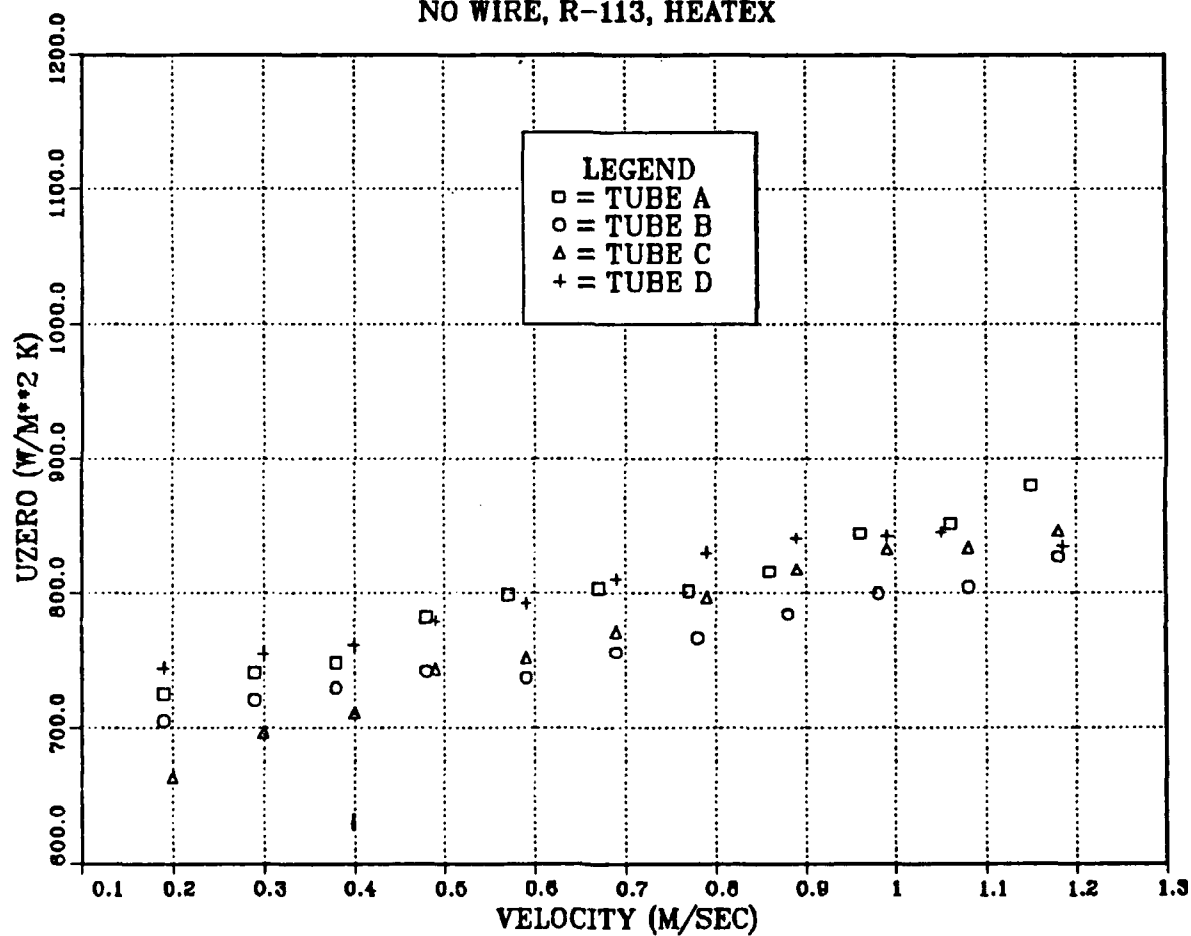


Figure 29. Effect of no wire on  $U_o$  for all tubes.

# UZERO WIRE WRAPPED KORODENSE

0.029" WIRE, R-113, HEATEX

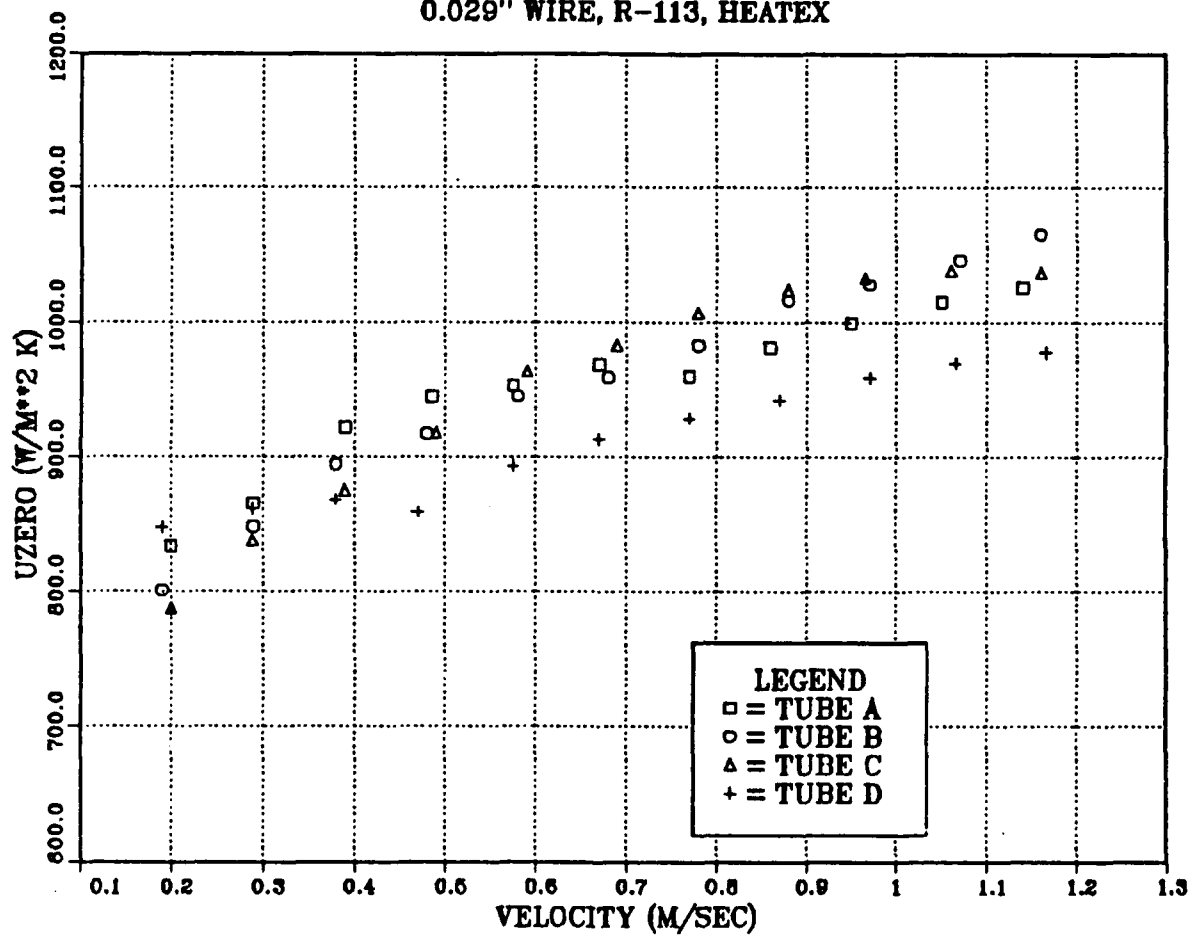


Figure 30. Effect of 0.029" wire on  $U_o$  for all tubes.

# UZERO WIRE WRAPPED KORODENSE

0.049" WIRE, R-113, HEATEX

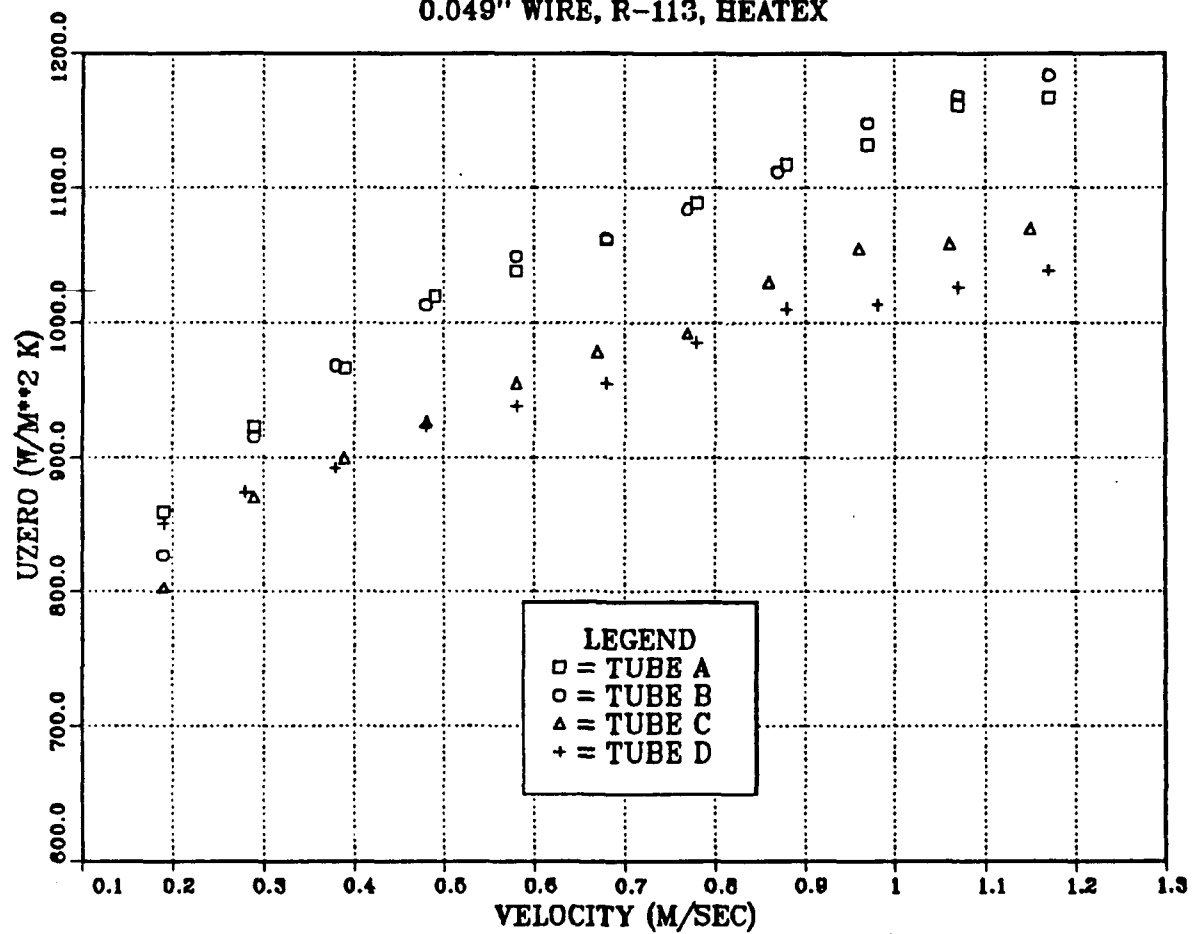


Figure 31. Effect of 0.049" wire on  $U_o$  for all tubes.

# UZERO WIRE WRAPPED KORODENSE

0.0675" WIRE, R-113, HEATEX

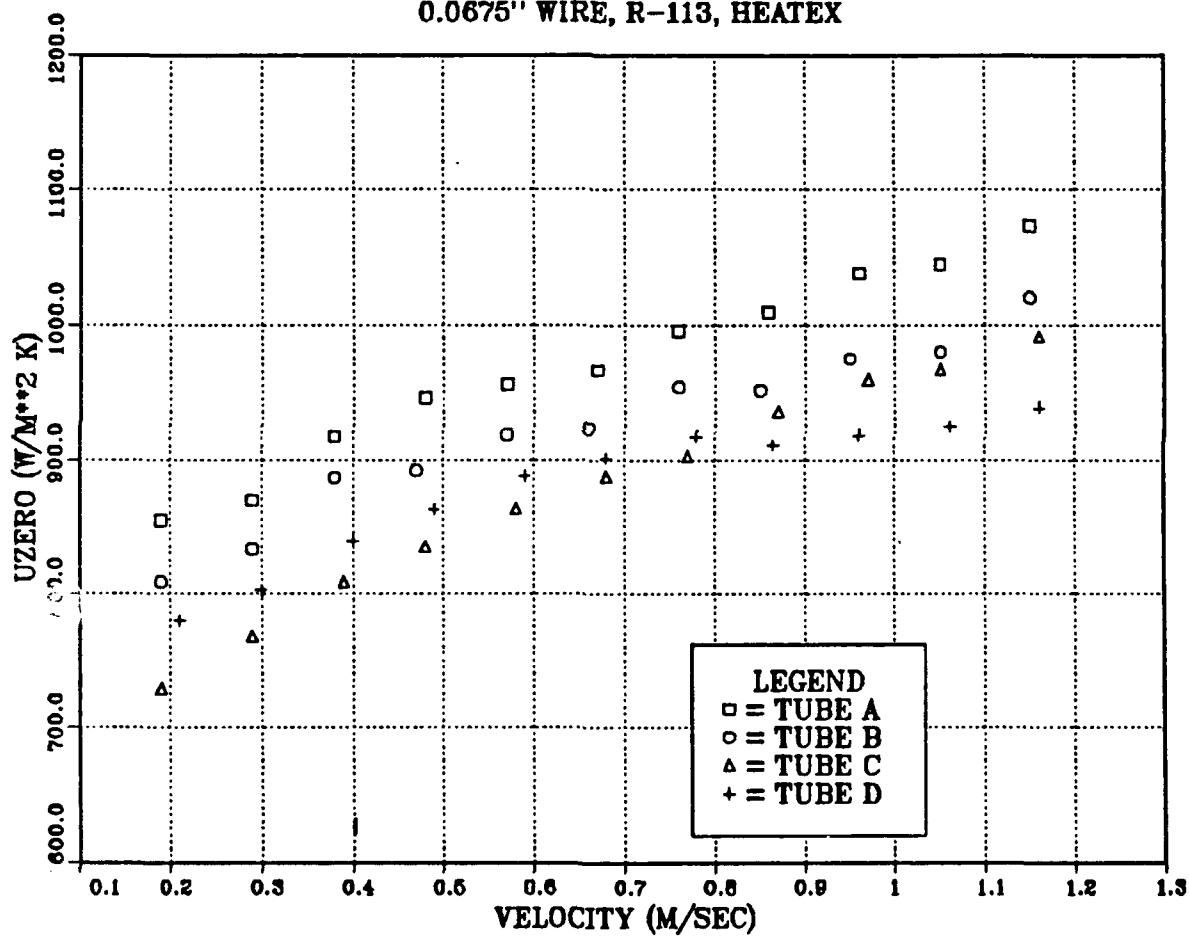


Figure 32. Effect of 0.0675" wire on  $U_o$  for all tubes.



## WIRE WRAPPED KORODENSE TUBES

COOLANT VELOCITY = 1 M/S

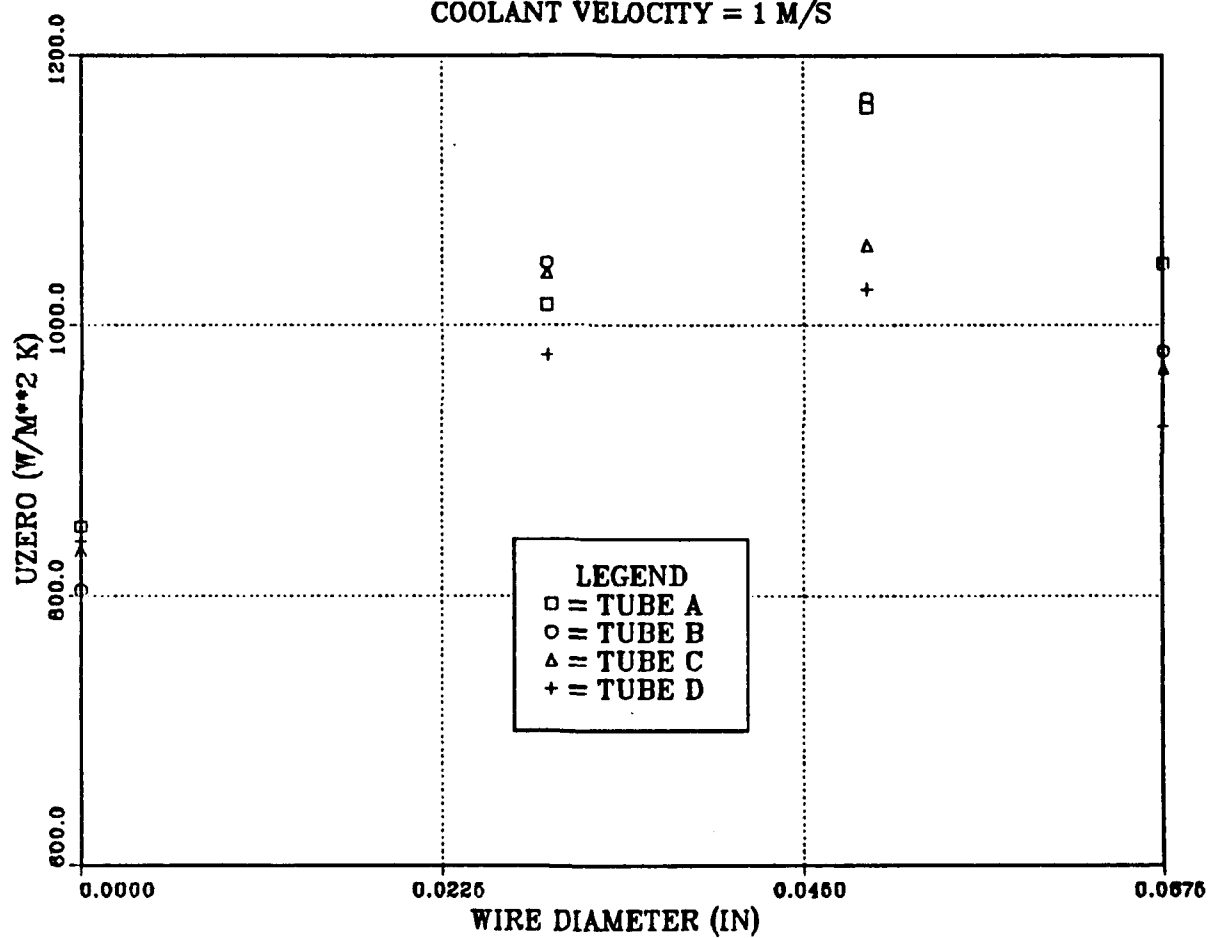


Figure 33.  $U_o$  as a function of wire diameter for the four tubes.

been unrealistic for our experiments. It may be that the optimal pitch-to-wire diameter may in fact be about 2. Additional experiments need to be performed with different pitch KORODENSE tubes.

#### **4. KORODENSE Tubes Wrapped with 0.049" Wire**

Once the optimal wire diameter had been determined, two identical experiments were performed on the KORODENSE copper/nickel tubes wrapped with the 0.049" diameter wire. The reason that two experiments were performed was to check the repeatability of the data. Figure 34 and Figure 35 show the results from these two experiments for bundle operation of the tubes. The two experiments show excellent repeatability. In comparing these results with the non-wire wrapped tubes (Figure 22), several interesting points can be made. The values of  $U_o$  for all four tubes are greater for the wire wrapped tubes than for the plain tubes (approximately 16% for the top tube). In addition, the inundation effect (seen as a lowering of  $U_o$ ) is reduced for the wire wrapped tubes. Finally, note that the differences between the tubes are more apparent than for the non-wire wrapped tubes. This suggests that the wire wrapping may have an effect upon condensate inundation. This will be addressed in more detail later.

Figure 36 and Figure 37 show the results obtained when the tubes wrapped with the 0.049" diameter wire were operated individually. All the tubes behave similarly and demonstrate good reproducibility between the two runs.

#### **5. Copper/Nickel Finned Tubes**

Figure 38 shows the results obtained when no insert was installed and the tubes were operated as a bundle. Comparison of these results with those shown in Figure 8 for the smooth tubes shows that the finned tubes yield higher heat transfer coefficients as expected (approximately 12%). Also, as with the smooth copper tubes, the top tube again displays the highest value of  $U_o$ , due to the fact that the lower tubes suffer from condensate inundation. The single tube data for the finned tubes is shown in Figure 39. All four tubes are virtually the same as the top tube during bundle operation.

Figure 40 and Figure 41 show the results obtained for the finned tubes with the tape insert installed during bundle and individual tube operation respectively. In bundle operation, the values of  $U_o$  are nearly double those obtained for both the smooth copper tubes (Figure 10) and the KORODENSE tubes (Figure 20) using similar inserts. As with the smooth and KORODENSE tubes, inundation again causes a reduction in  $U_o$ . This reduction for the second tube appears to be about 10%. Comparison of the single tube operation (Figure 41) with the bundle operation (Figure 40) shows that all four

## 0.049" WIRE WRAPPED KORODENSE

KD11, R-113, HEATEX, BUNDLE

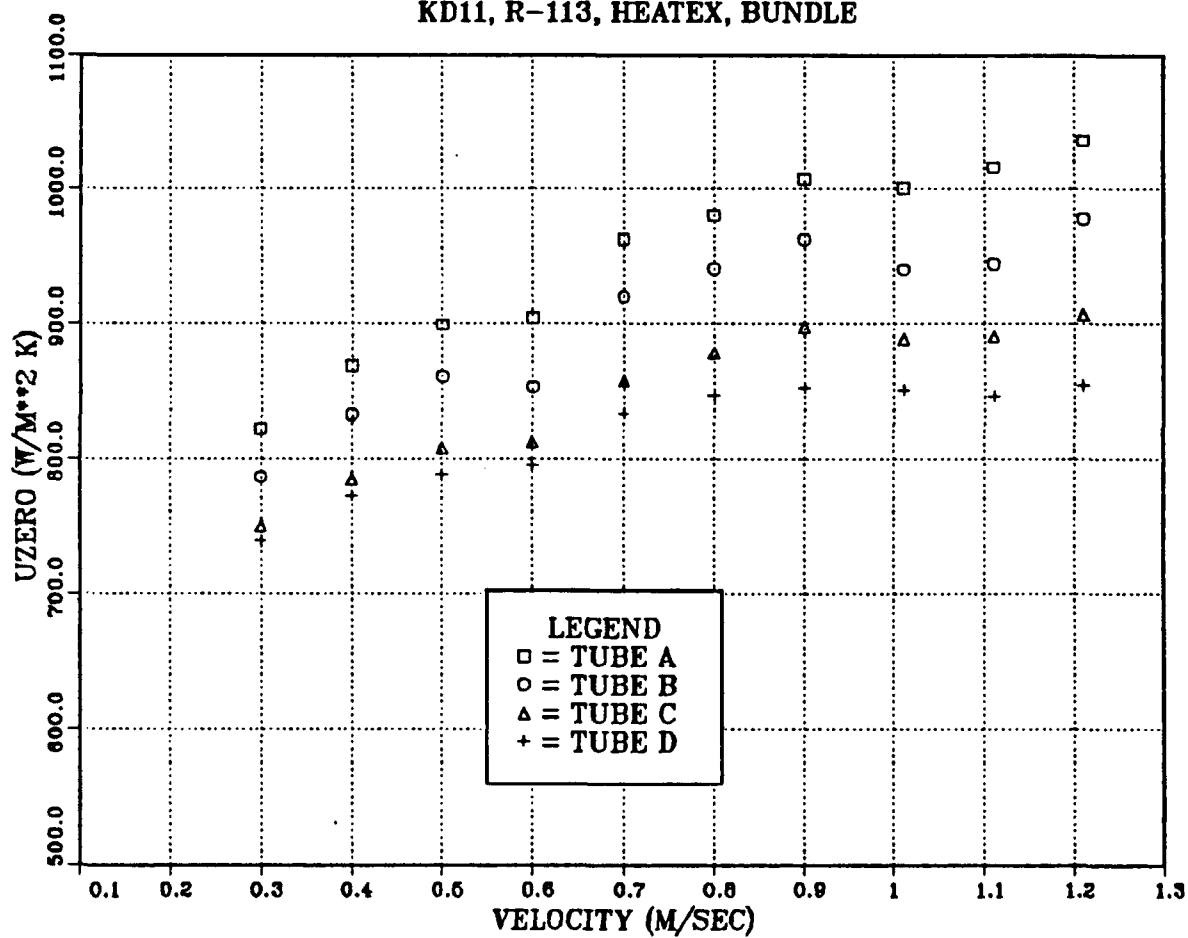


Figure 34. 0.049" wire wrapped KORODENSE tubes, bundle operation, expt. 1.

## 0.049" WIRE WRAPPED KORODENSE

KD12, R-113, HEATEX, BUNDLE

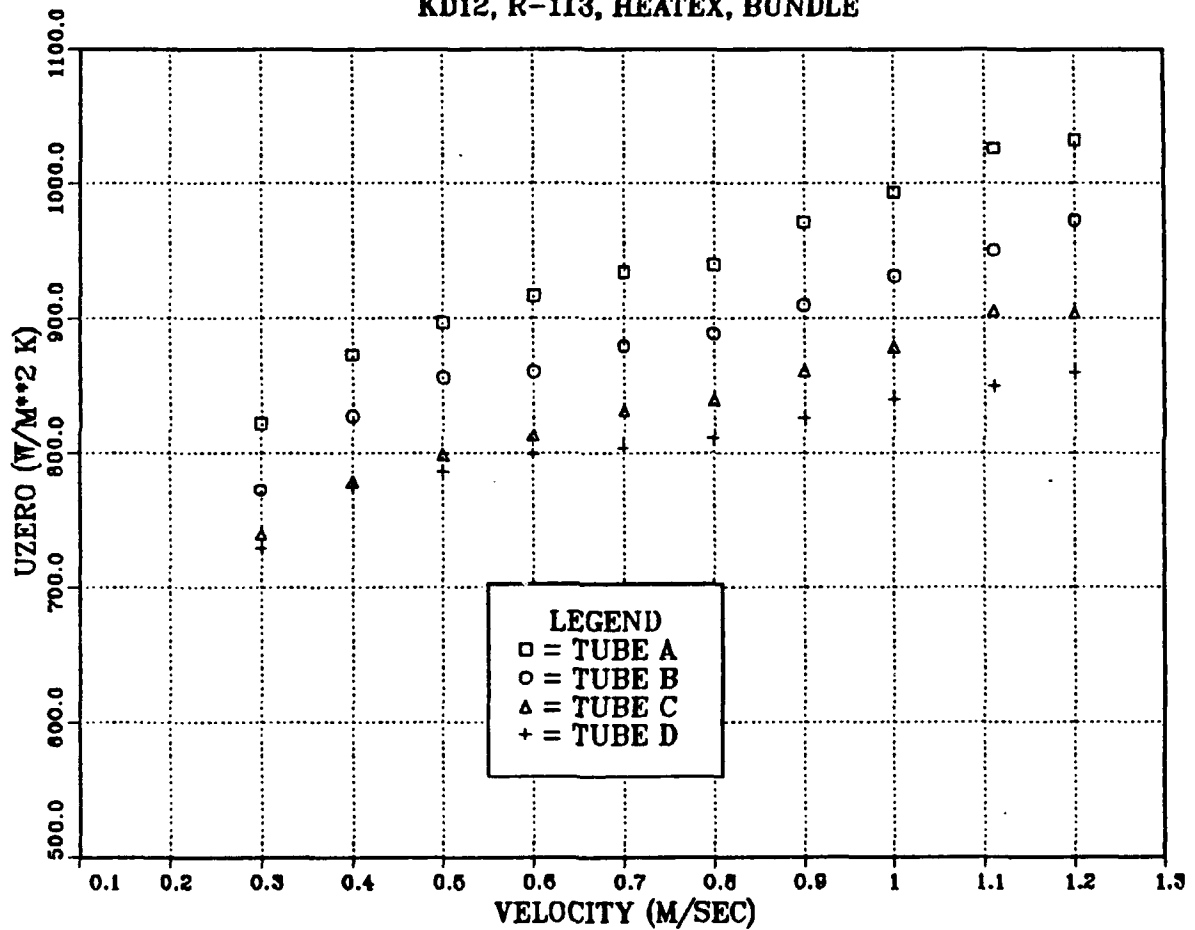


Figure 35. 0.049" wire wrapped KORODENSE tubes, bundle operation, expt. 2.

## UZERO WIRE WRAPPED KORODENSE

KD11, R-113, SINGLE, HEATEX

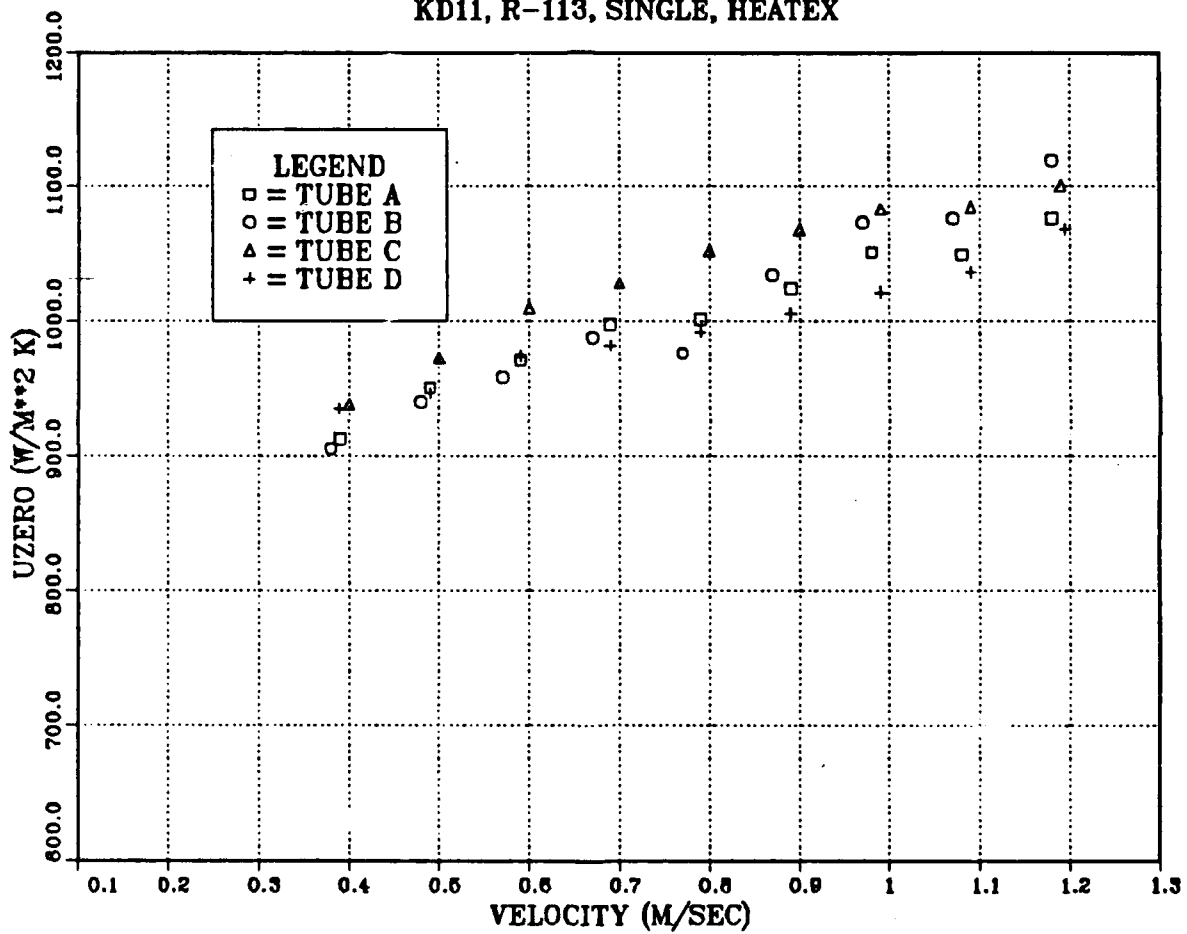


Figure 36. 0.049" wire wrapped KORODENSE tubes, individual operation.

## UZERO WIRE WRAPPED KORODENSE

KD12, R-113, SINGLE, HEATEX

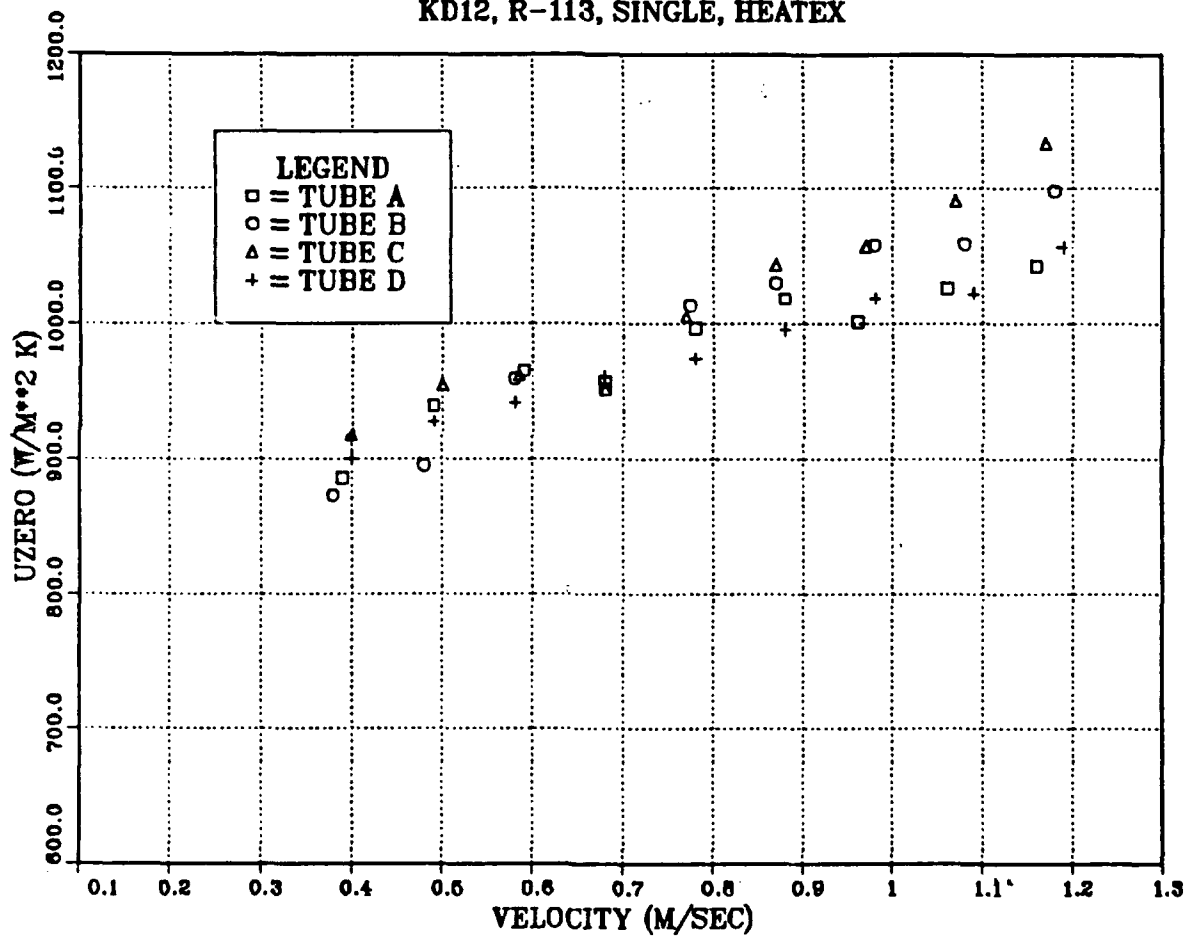


Figure 37. 0.049" wire wrapped KORODENSE tubes, individual operation.

# UZERO CU/NI FINNED TUBES

CF05, R-113, NO INSERT, BUNDLE

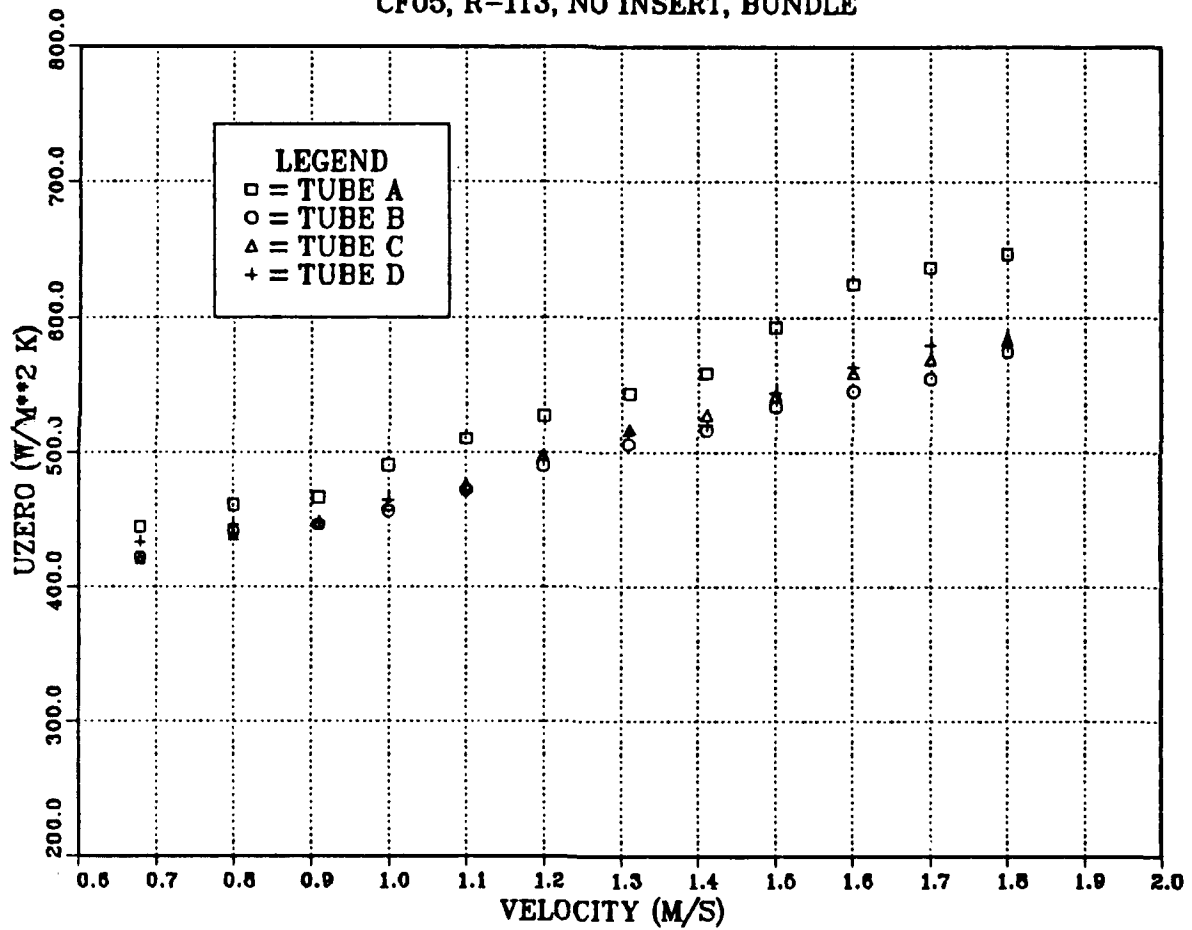


Figure 38. Copper/nickel finned tubes, no insert, bundle operation.

# UZERO CU/NI FINNED TUBES

CF05, R-113, NO INSERT, SINGLE

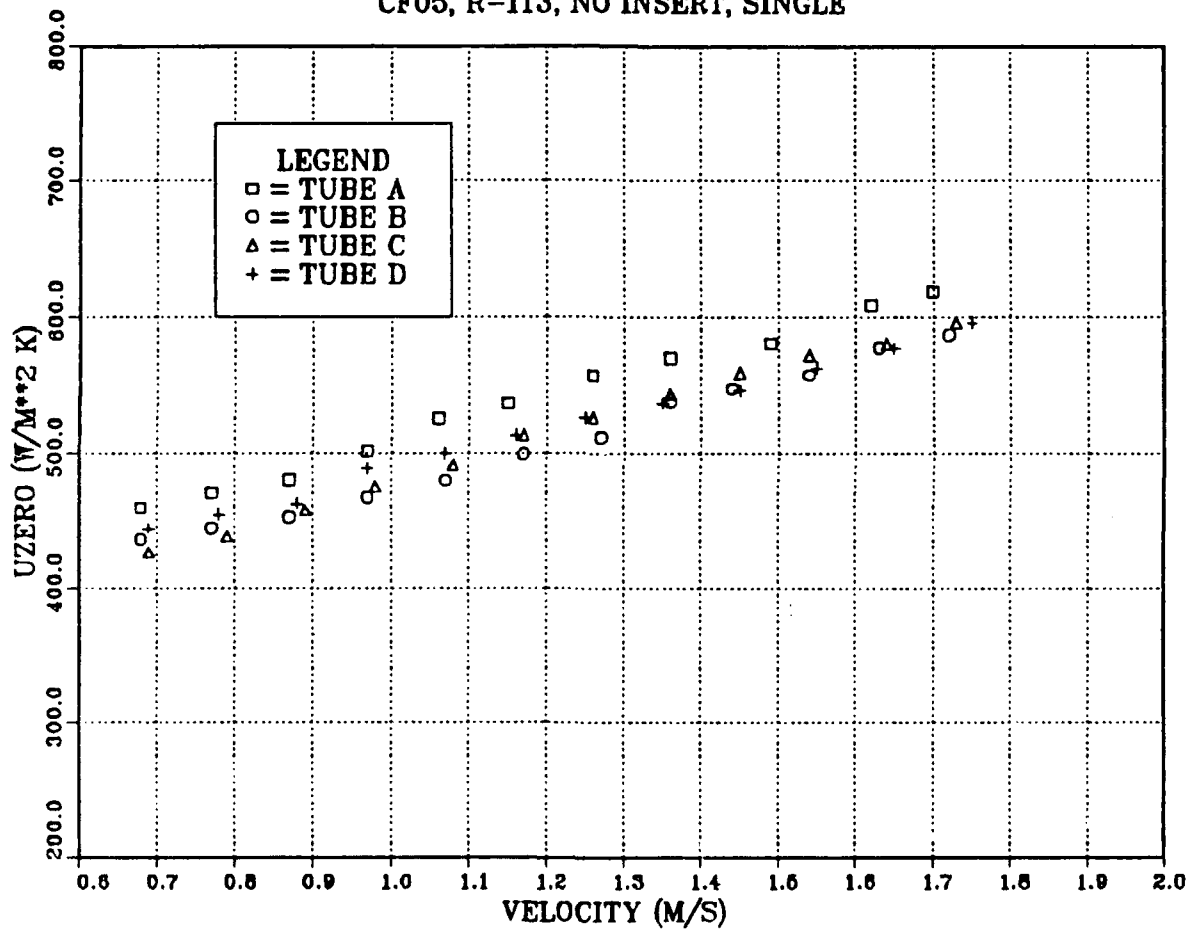


Figure 39. Copper/nickel finned tubes, no insert, individual operation.



tubes operated individually have approximately the same value of  $U_o$  as the top tube during the bundle operation.

Data obtained from experiments on the copper/nickel finned tubes with the HEATEX elements installed are shown in Figure 42 and Figure 43 for bundle and individual tube operation respectively. Note that in comparison with the tape insert experiments (Figure 40 and Figure 41), use of the HEATEX inserts results in about a 20% increase in  $U_o$  which again indicates the improvement afforded by using this type of insert. Again the inundation effect results in a decrement of 10 to 14%. During individual tube operation, all four tubes again behave like the top tube during the bundle operation.

As with the smooth copper tubes and the KORODENSE tubes, the effects of using different types of inserts can be summarized. This has been done in Figure 44. This data is for the top tube only. The similarity with data from the other tubes (see Figure 17 and Figure 24) is good with HEATEX yielding approximately a 20% increase in  $U_o$  over the twisted tape insert and a remarkable 200% increase over the case with no insert!

### C. OUTSIDE HEAT TRANSFER COEFFICIENT

The following figures deal with the outside heat transfer coefficient,  $h_o$ . In all cases, except as specifically noted, the outside heat transfer coefficient was determined using the modified Wilson Plot procedure. As before, tube A is the top tube with tube D being the bottom tube in the bundle. In addition, no values were obtained for  $h_o$  for experiments which had no insert. The reason for this is that, for the coolant velocities used, without inserts, the inside resistance was simply too large for any accurate results to be obtained for  $h_o$ .

#### 1. Smooth Copper Tubes

Figure 45 and Figure 46 show the values obtained for  $h_o$  for the smooth copper tubes with the tape insert installed during bundle and individual tube operation respectively. Several features deserve comment. First, values of  $h_o$  for the top tube are below those predicted by Nusselt theory. These differences range from about 15% at low coolant velocities to about 7% at the higher coolant velocities. In addition, note the inundation effect (seen as a reduction in  $h_o$  for tubes B, C, and D). Reductions in  $h_o$  range from 28% to 19% as coolant velocity increases from 0.2 to 1.2 m/s respectively. As was the case for the overall heat transfer coefficient, when the tubes were operated individ-

## UZERO COPPER/NICKEL FIN TUBES

CF03, R-113, TAPE INSERT, BUNDLE

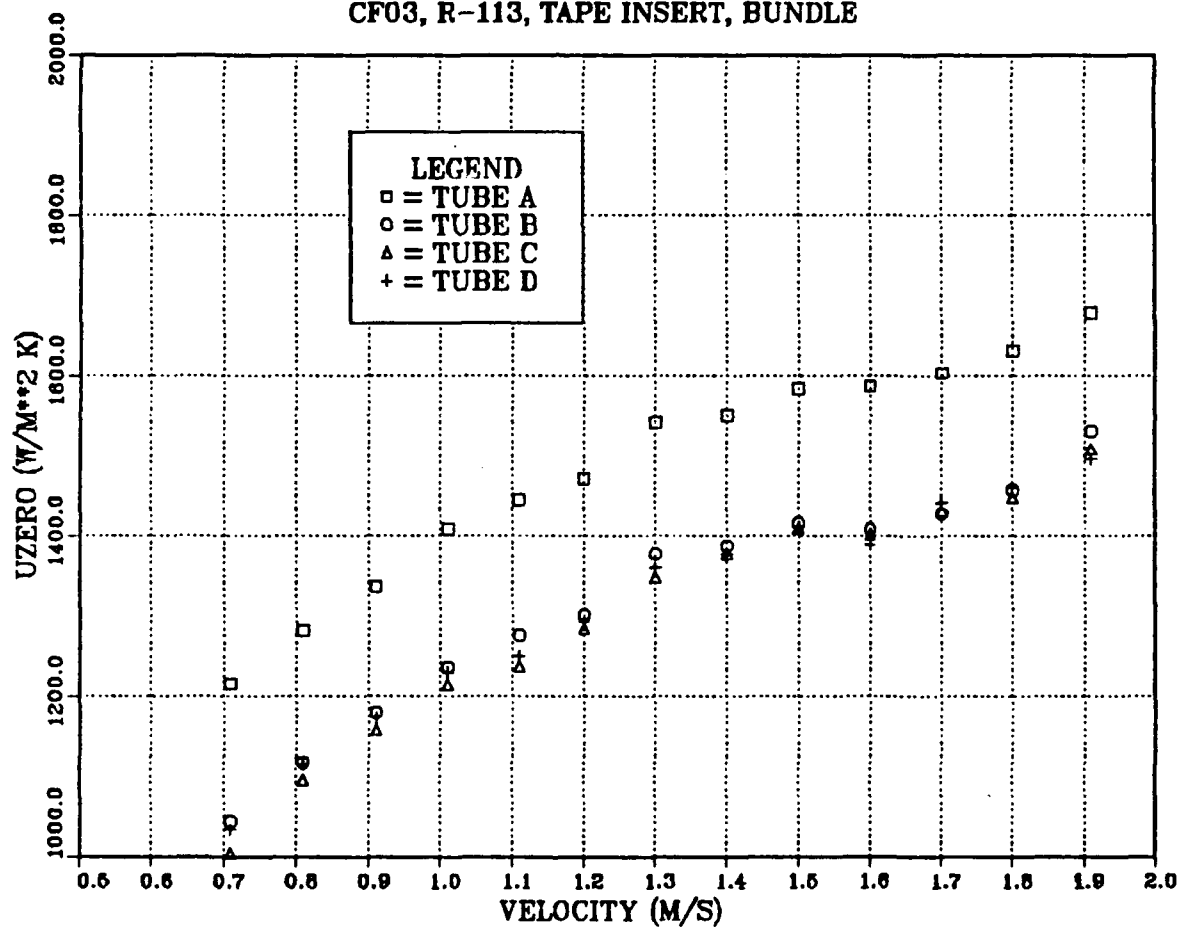


Figure 40. Copper/nickel finned tubes, tape insert, bundle operation.

## UZERO COPPER/NICKEL FIN TUBES

CF03, R-113, TAPE INSERT, SINGLE

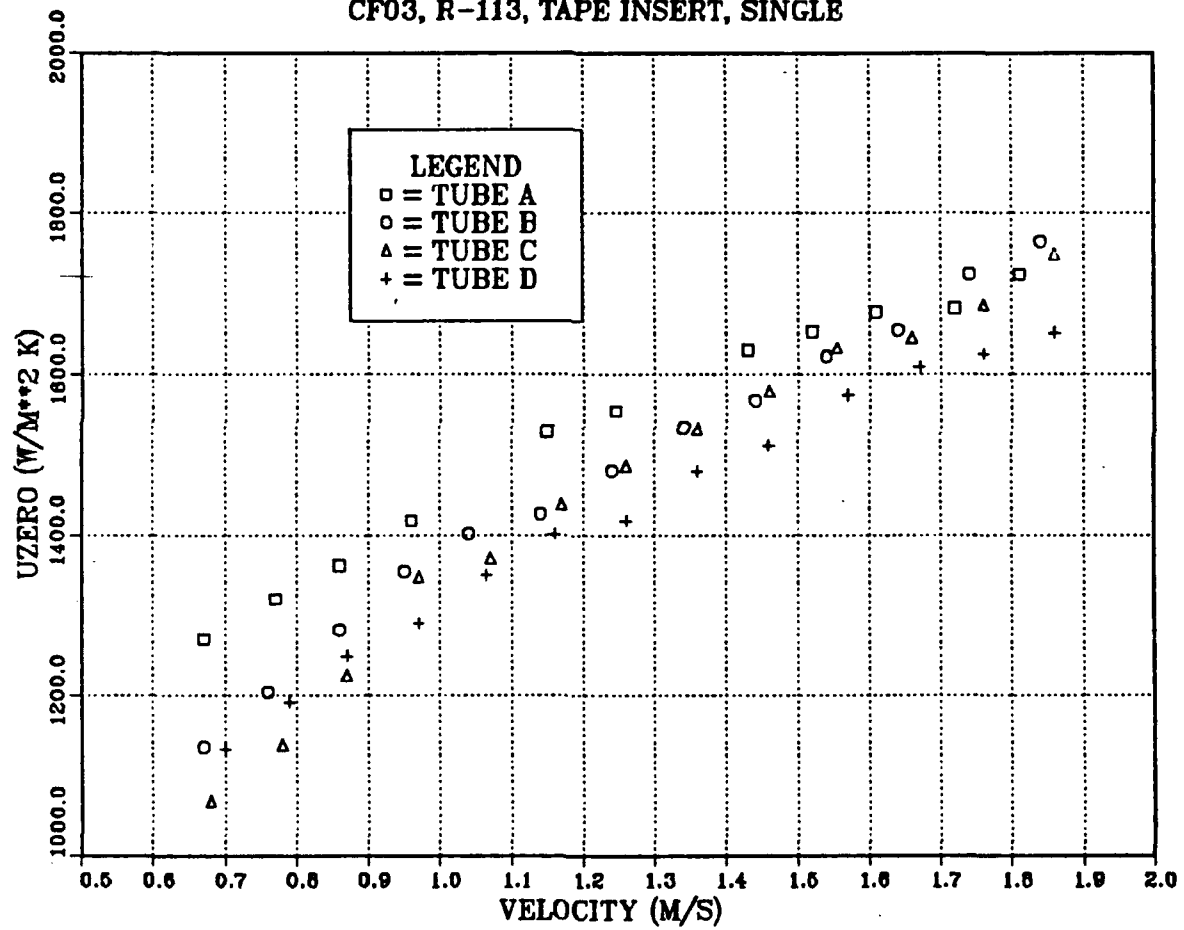


Figure 41. Copper/nickel finned tubes, tape insert, individual operation.

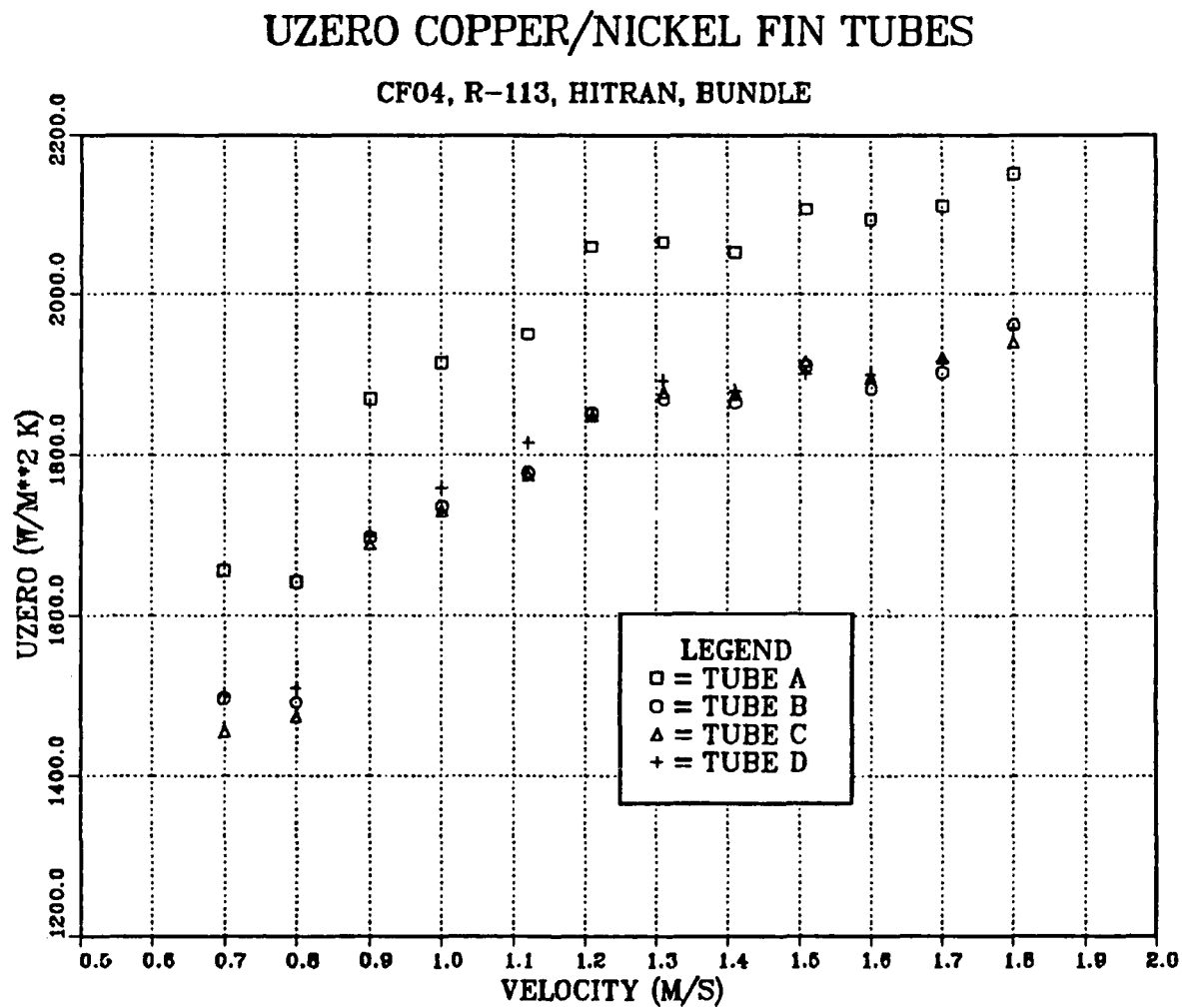


Figure 42. Copper/nickel finned tubes, HEATEX insert, bundle operation.

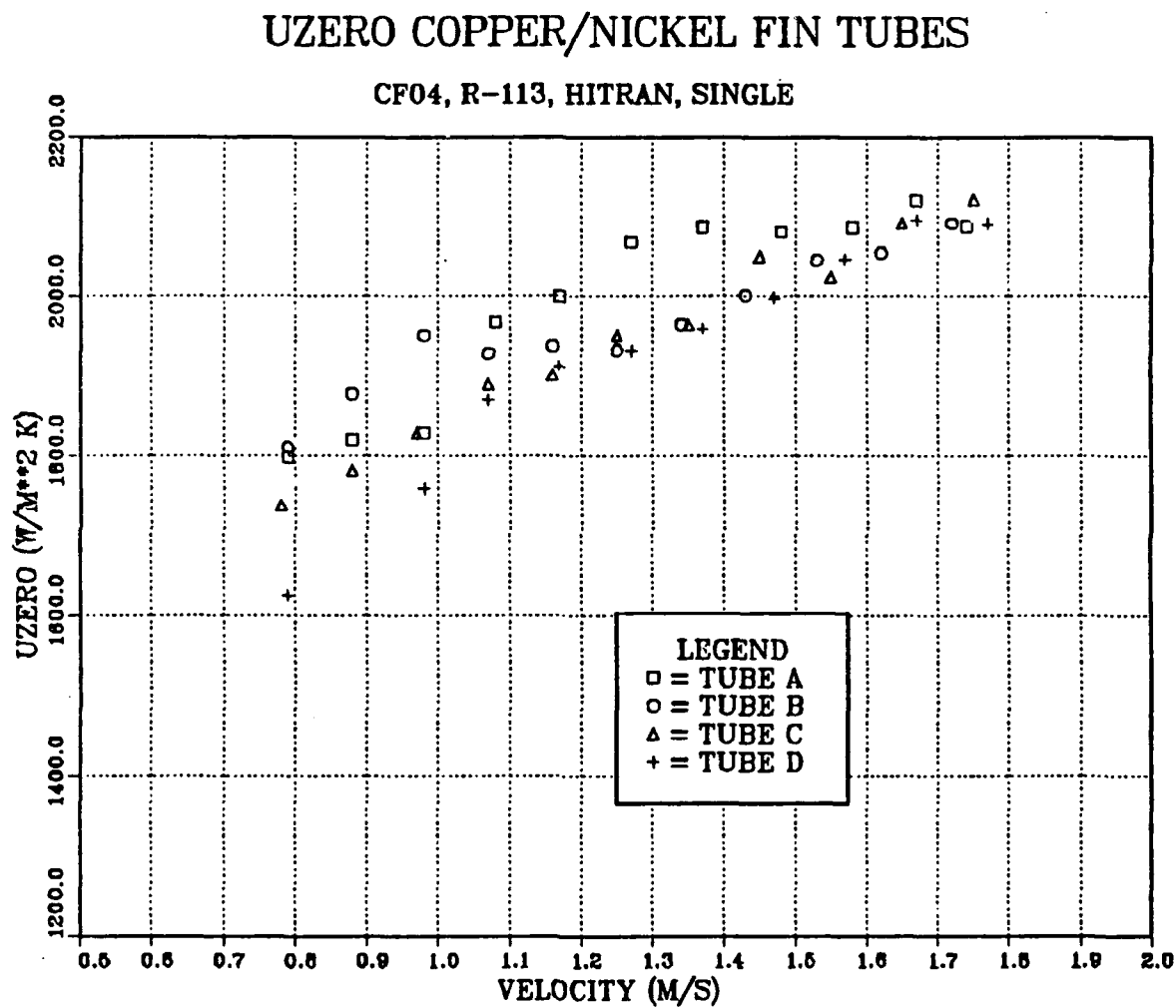


Figure 43. Copper/nickel finned tubes, HEATEX insert, individual operation.

# EFFECT OF INSERTS

CU/Ni FINNED TUBES

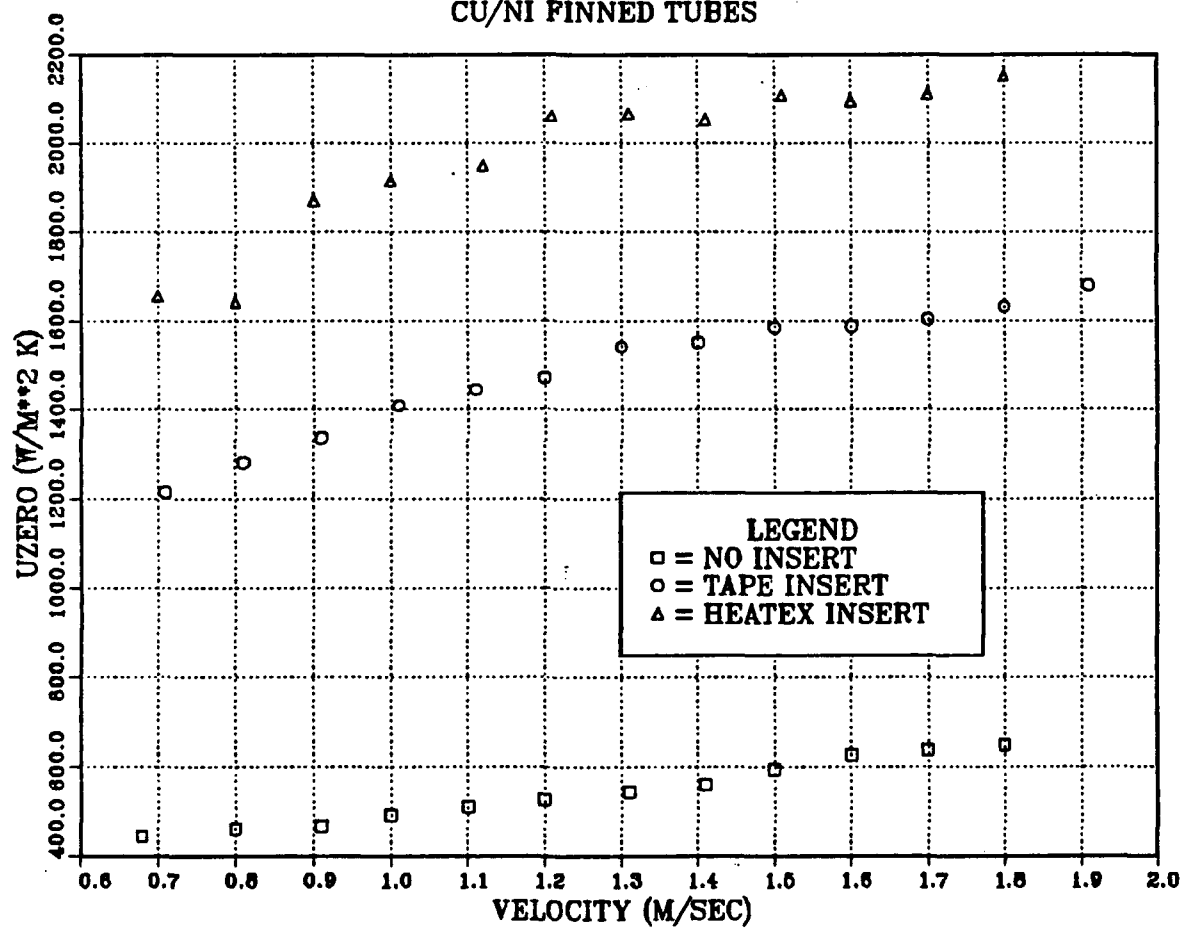


Figure 44. Summary of effect of tube inserts on  $U_z$ .

ually, all had values for  $h_o$  which were virtually identical to those obtained for the top tube during bundle operation.

Figure 47 and Figure 48 show values for  $h_o$  obtained when the HEATEX elements were installed in the copper tubes during bundle and individual tube operation respectively. As was the case for the tape insert, values of  $h_o$  range from about 10 to 14% below that predicted from Nusselt theory. Again, there is a substantial inundation effect which results in a 15 to 18% decrease in  $h_o$  when comparing the top tube to the second tube. Note that the values for  $h_o$  obtained for the individual tubes agree with those obtained for the top tube during bundle operation. Finally, comparison of the value for  $h_o$  obtained when the tape inserts were used as opposed to the HEATEX elements reveal no effect on  $h_o$  which is to be expected since we are examining the outside heat transfer coefficient.

It is interesting to note that Goto et al. [Ref. 5] found that values of  $h_o$  for R-113 condensing on long, smooth copper tubes were about 10% below that predicted by Nusselt theory. Marto et al. [Ref. 8] found that the vapor-side heat transfer coefficient for R-113 condensing on short (0.133m) smooth copper tubes was in relatively good agreement with Nusselt theory. This result was subsequently confirmed by Michael et al. [Ref. 32]. However, it is important to point out that both the latter reports used very short condenser tubes. The tubes used by Goto et al. were about 0.6 m in length, while the tubes used in this study had a condensing length of 1.2 m. Hence tube length may be an important consideration. The reason for this is as follows. The coolant enters the condenser tube with a given inlet temperature. As the coolant flows through the tube, the coolant temperature increases. The wall temperature is also changing down the length of the tube. At the tube entrance, the temperature difference between the tube wall and the vapor saturation temperature causes the formation of a thick condensate layer. This layer is thinner at the tube outlet due to the smaller wall-vapor saturation temperature difference. This causes condensate to flow in the axial direction. These factors taken together imply that the temperature difference is a function of the length of the tube. This factor is not taken into account in the Nusselt analysis. As coolant velocity increases, the difference between the coolant inlet and outlet temperatures is reduced. The wall temperature becomes more constant along the tube length so that values for  $h_o$  are in better agreement with those determined experimentally.

The effect of using the twisted tape and HEATEX insert on the inside and outside heat transfer coefficients is demonstrated in Figure 49 and Figure 50 respectively. In both cases, the values for  $h_o$  are virtually identical as expected. However, the

# HZERO SMOOTH COPPER TUBES

SM07, R-113, BUNDLE, TAPE INSERT

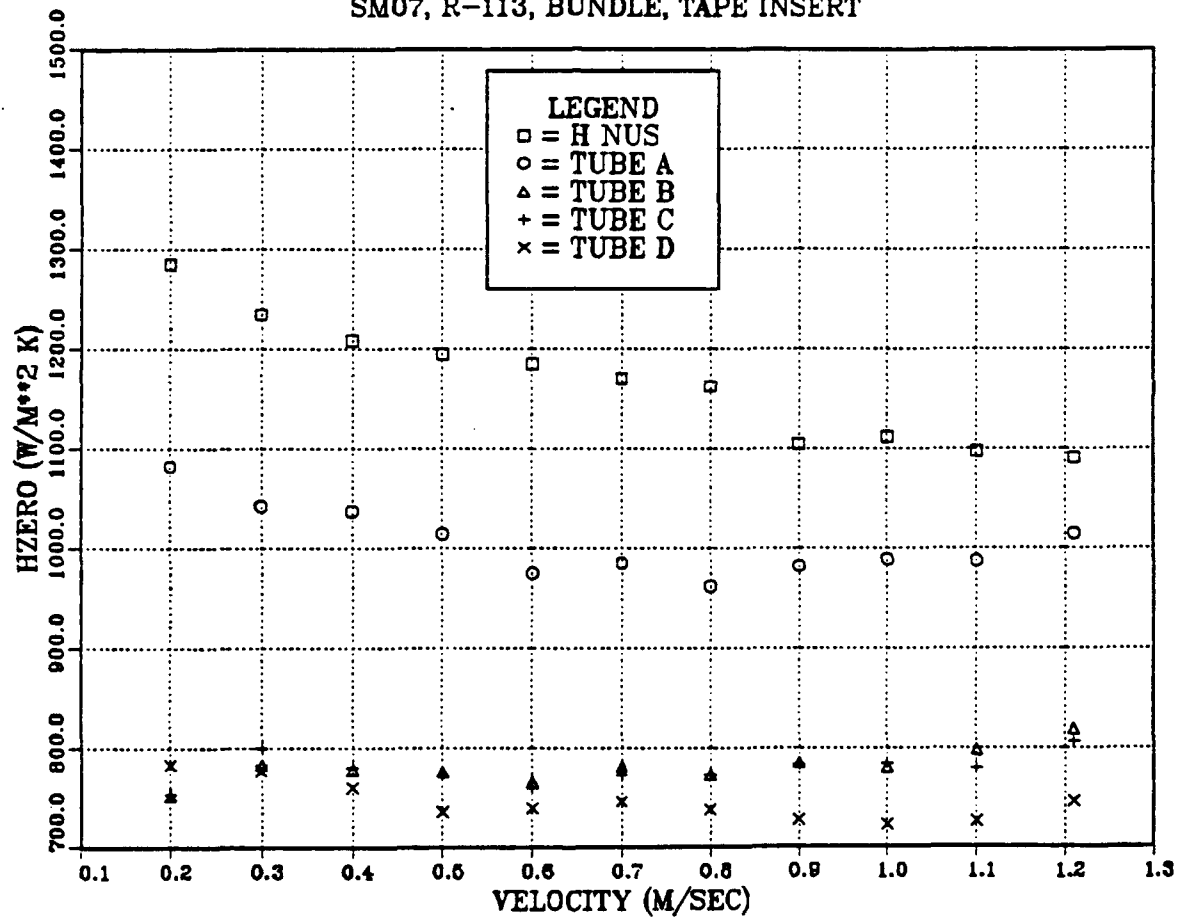


Figure 45. Smooth Copper tubes, tape insert, bundle operation.



## HZERO SMOOTH COPPER TUBES

SM07, R-113, SINGLE, TAPE INSERT

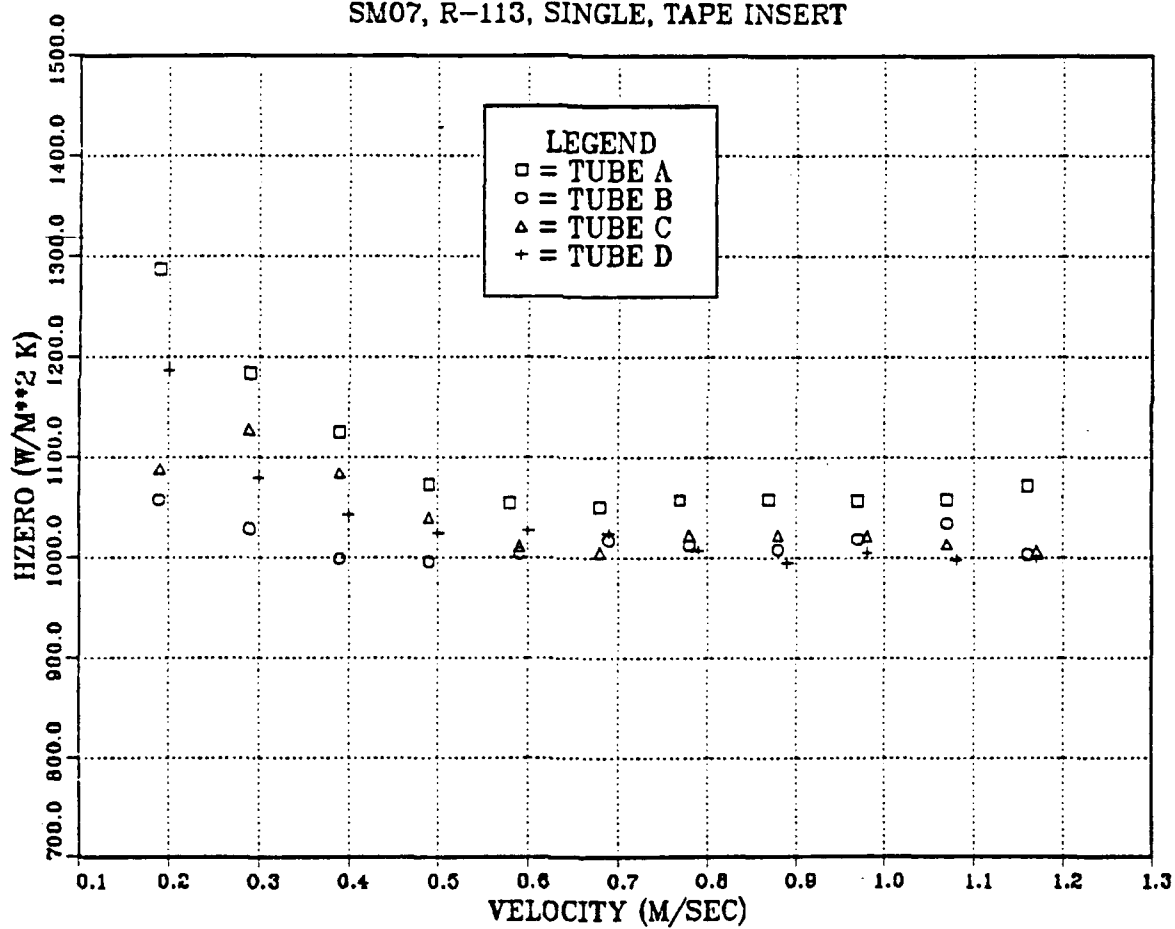


Figure 46. Smooth Copper tubes, tape insert, individual operation.

# 

SM06, R-113, HEATEX, BUNDLE

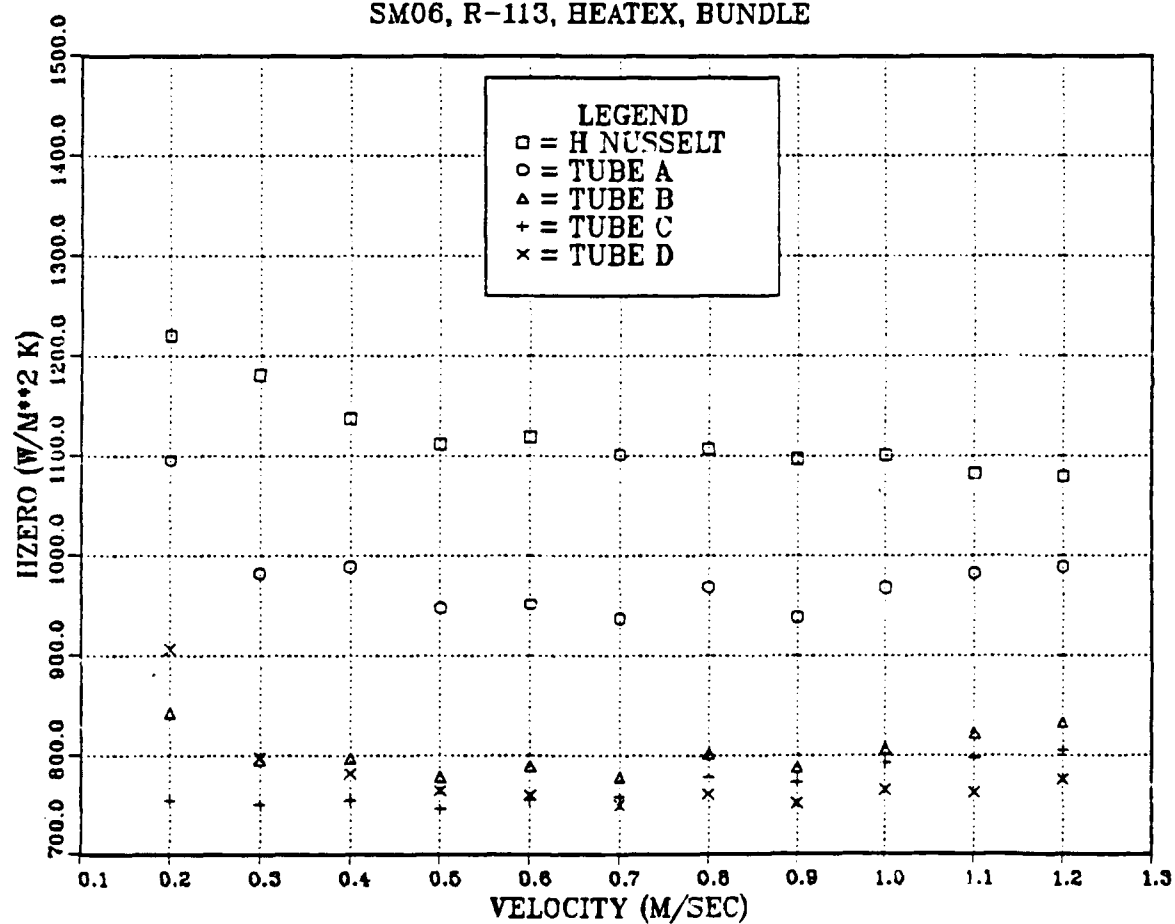


Figure 47. Smooth Copper tubes, HEATEX insert, bundle operation.

## HZERO SMOOTH COPPER TUBES

SM06, R-113, HEATEX, SINGLE

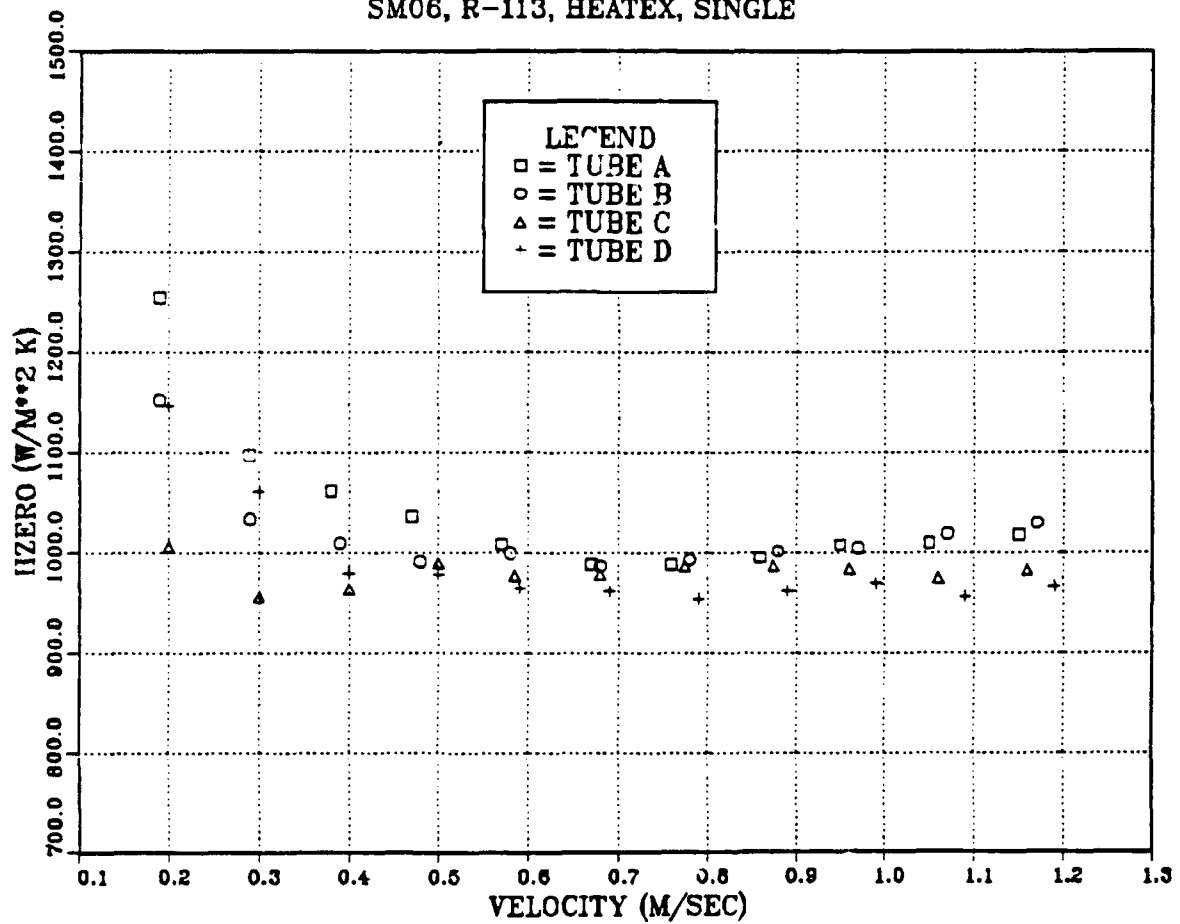


Figure 48. Smooth Copper tubes, HEATEX insert, individual operation.

HEATEX elements essentially double the inside heat transfer coefficient. This is what provides the improvement in overall heat transfer coefficient when the HEATEX elements are used.

The effects of inundation were examined by calculating an average and a local heat transfer coefficient. The local  $h_o$  is found by dividing the value for  $h_o$  for a given tube by the value for the top tube. Values obtained are then compared with Nusselt theory (Eq. 2-18) and the Kern model (Eq. 2-20). The average heat transfer coefficient is determined by taking an average value of  $h_o$  for the tube of interest plus the tubes above it and dividing this value by  $h_o$  for the top tube. Values obtained are then compared to Nusselt theory (Eq. 2-17), the Kern model (Eq. 2-19), or the Eissenberg model (Eq. 2-12). For both the local and average values, the flatter the curves, the less the effect of condensate inundation.

The effects of inundation on  $h_o$  for the smooth copper tubes are shown in Figure 51, Figure 52, Figure 53 and Figure 54 at three arbitrarily chosen coolant velocities. As expected, there is virtually no difference on the local or average values of the heat transfer coefficient when the tape insert is used as opposed to the HEATEX element. In addition, the values for the average heat transfer coefficient lie in between the values predicted by the Kern and Eissenberg models (equations 2-19, and 2-21). Values for the local heat transfer coefficient lie slightly above those predicted by the Kern model (equation 2-20). These results suggest that Nusselt theory is too conservative with regard to the effect of condensate inundation. It is interesting to note that the main inundation effect occurs for the second tube with little additional effect for subsequent tubes in the bundle. This again supports the notion that the smooth copper tubes can only support a limited amount of condensate

## 2. KORODENSE Tubes

Figure 55 and Figure 56 show values for  $h_o$  for the KORODENSE tubes with the tape inserts installed. The figures show data obtained when the tubes were operated as a bundle and individually respectively. The values of  $h_o$  for the top tube are above that predicted from Nusselt theory which is due to the small enhancement provided by the roping of the tubes. This enhancement is approximately 15 to 20% in comparison to the smooth copper tubes. As with the smooth copper tubes, there is again a substantial effect of inundation (on the order of 20% for the second tube compared to the top tube). There is also more separation between the values of  $h_o$  for tubes B, C, and D than for the smooth copper tubes indicating that the lower tubes may not be "saturated" with

## SMOOTH COPPER TUBES

TOP TUBE, TAPE INSERT

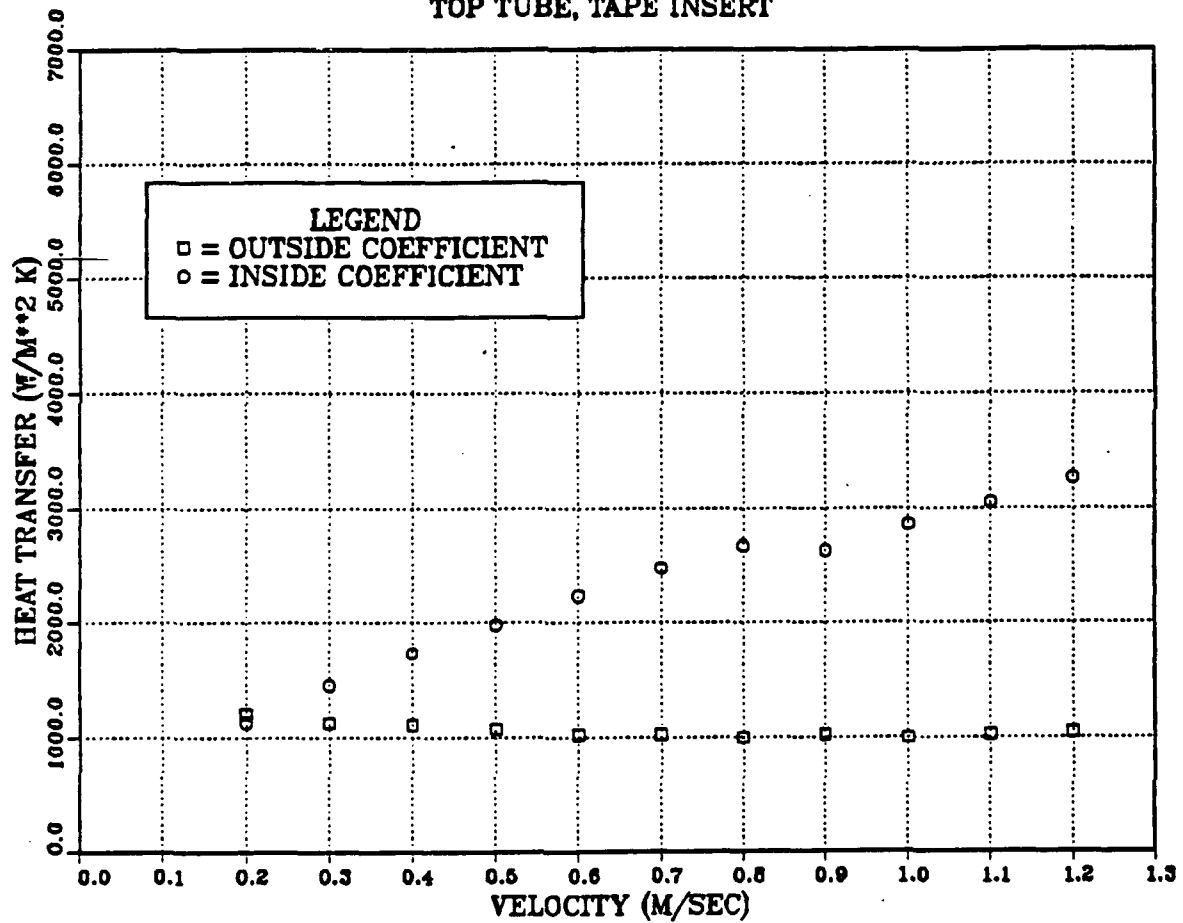


Figure 49. Effect of tape insert on  $h_o$  and  $h_i$

# SMOOTH COPPER TUBES

TOP TUBE, HEATEX INSERT

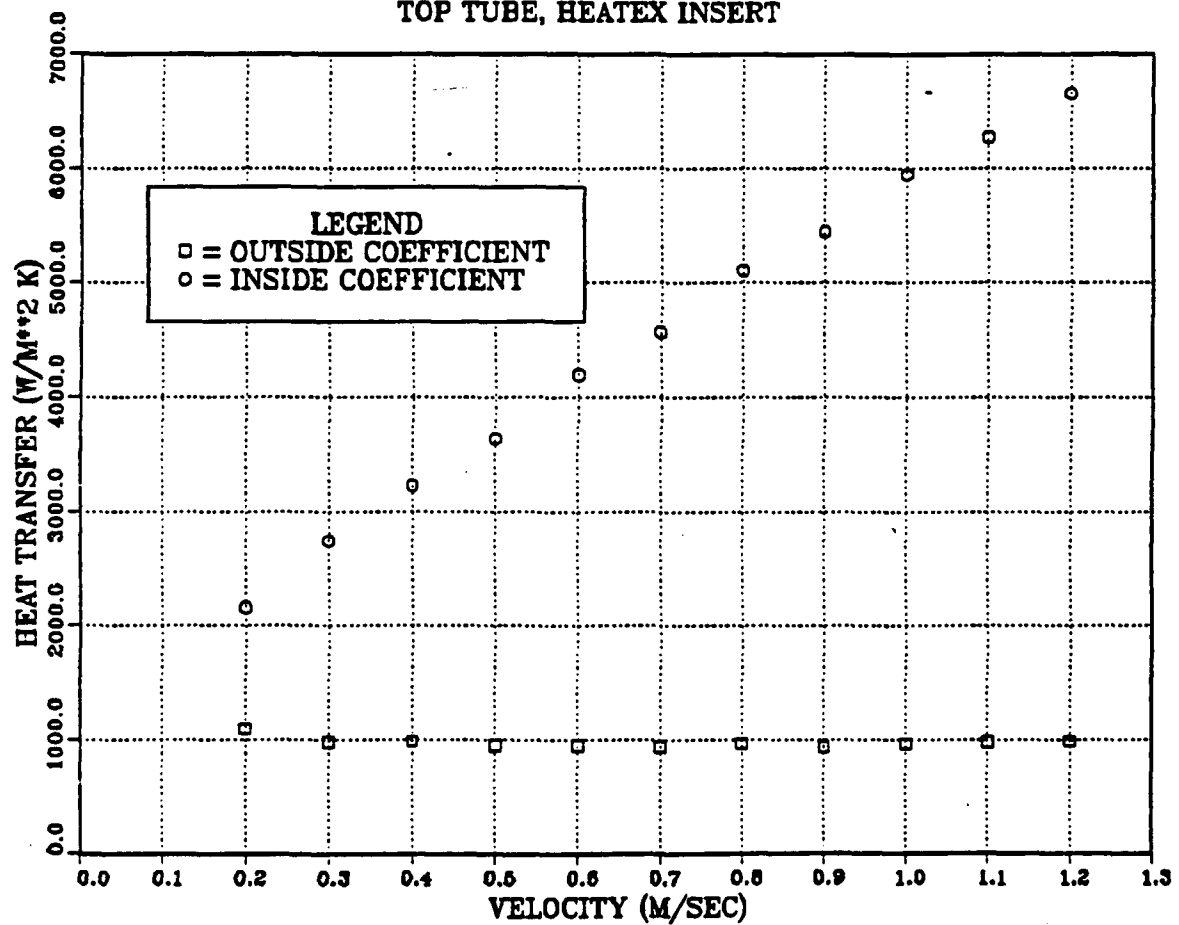


Figure 50. Effect of HEATEX insert on  $h_o$  and  $h_i$

# HEAT TRANSFER COEFFICIENT

## SMOOTH COPPER TUBES, TAPE INSERT

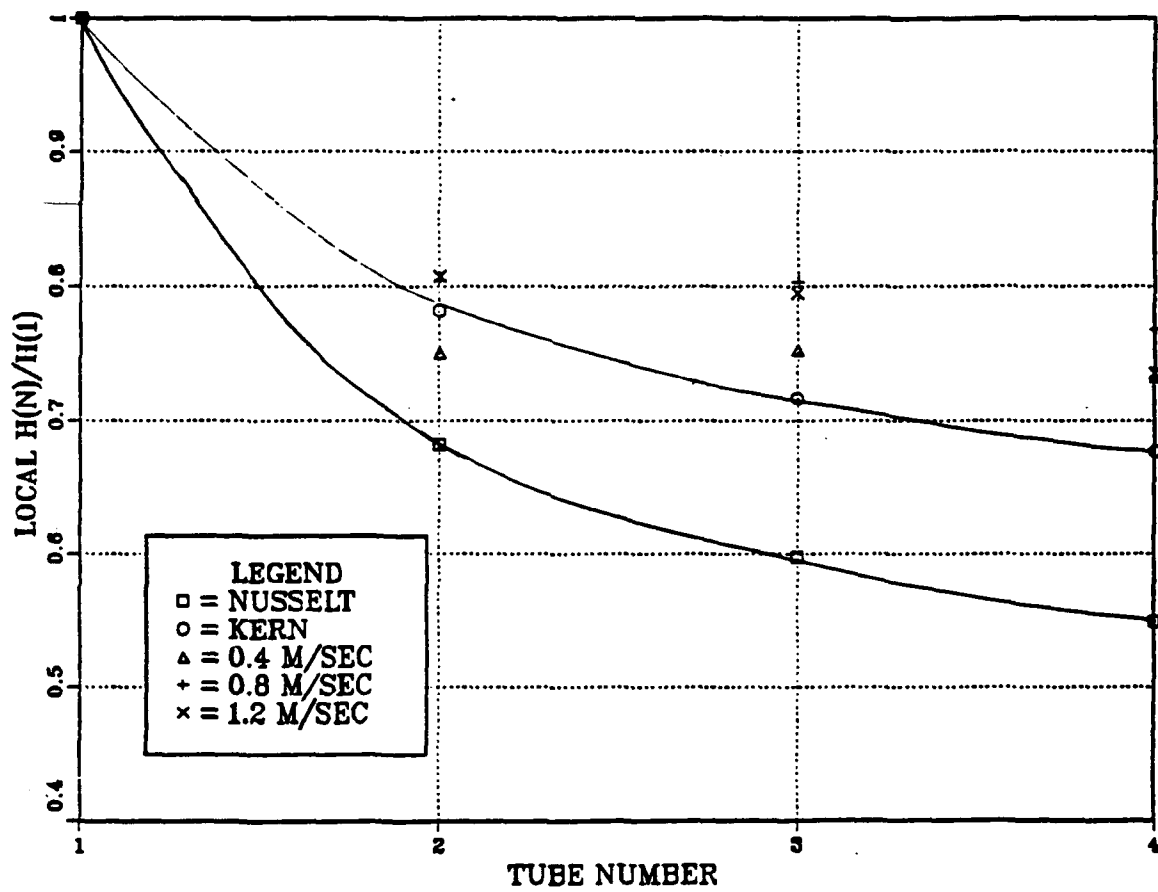


Figure 51. Local  $h$ , for tape insert.

## HEAT TRANSFER COEFFICIENT

SMOOTH COPPER TUBES WITH HEATEX

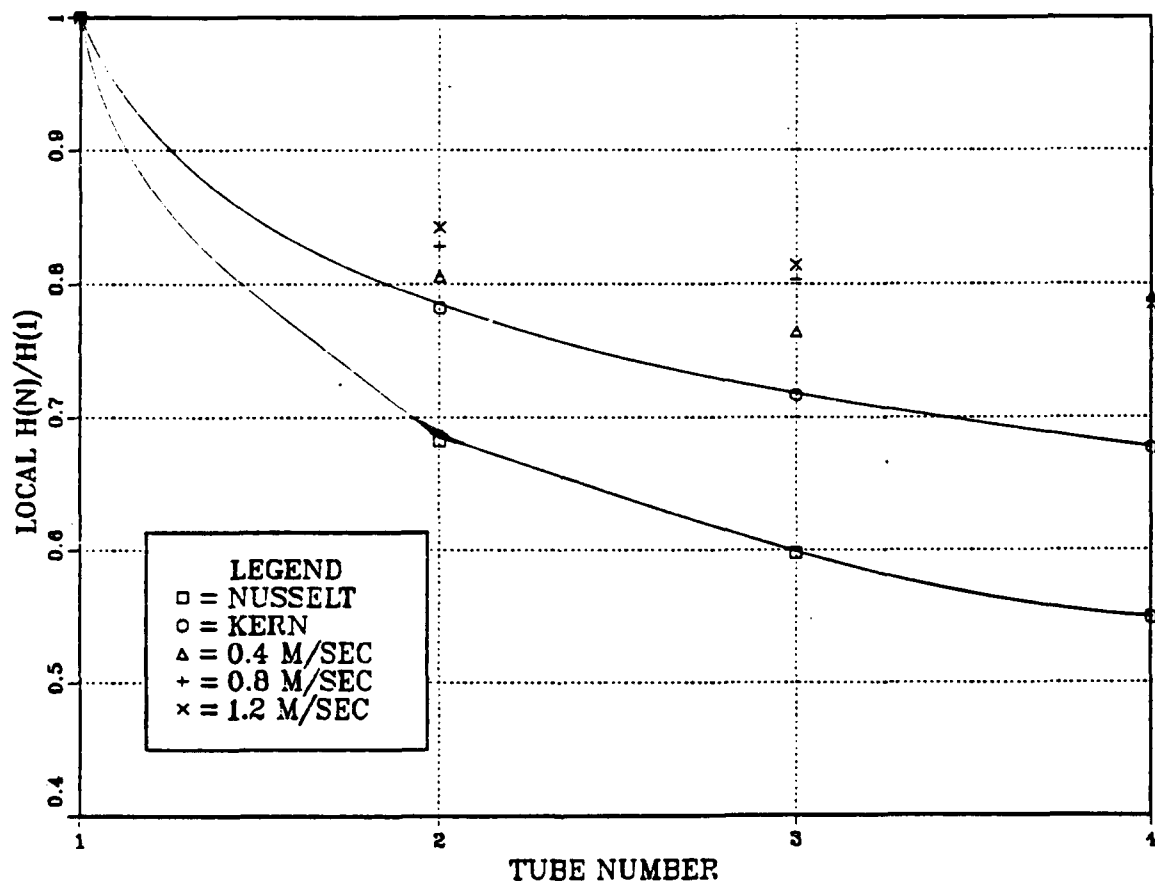


Figure 52. Local  $h$ , for HEATEX element.



# HEAT TRANSFER COEFFICIENT

SMOOTH COPPER TUBES, TAPE INSERT

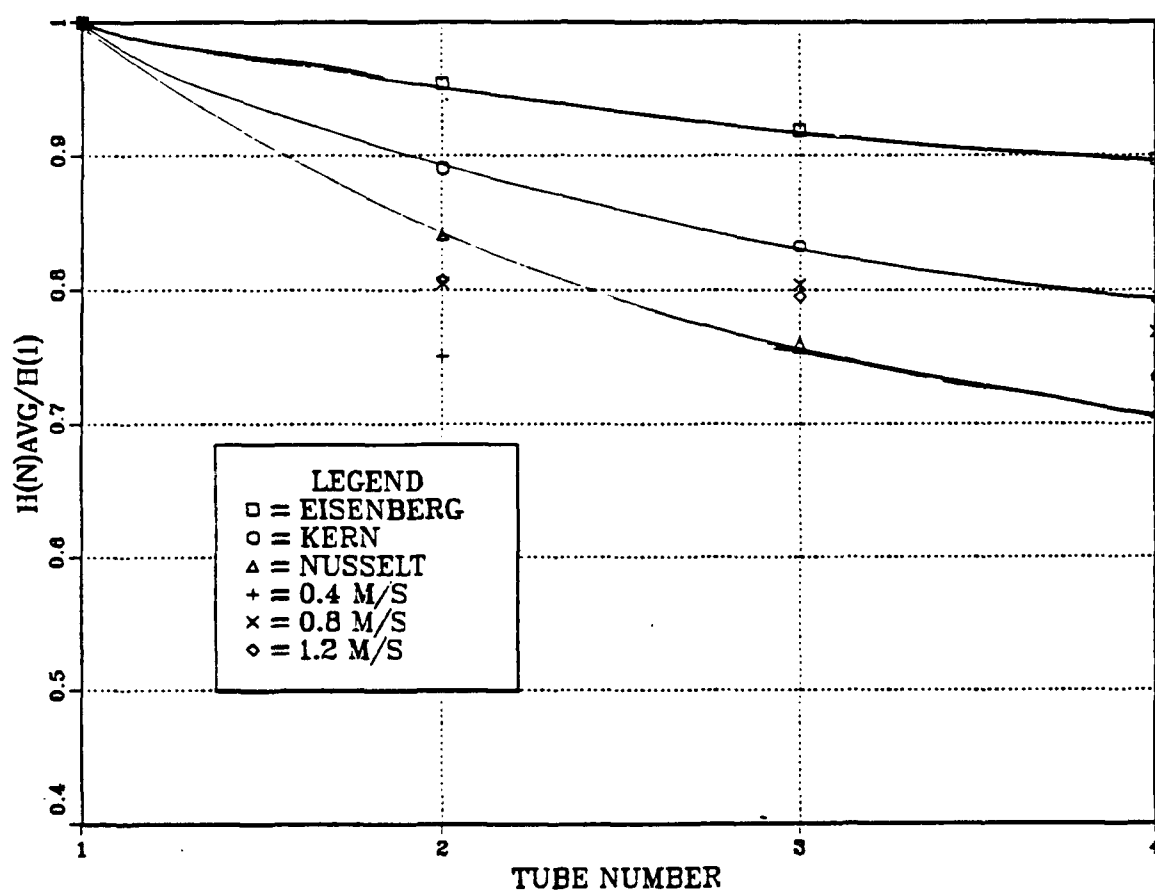


Figure 53. Average  $h$ , for tape insert.

# HEAT TRANSFER COEFFICIENT

## SMOOTH COPPER TUBES WITH HEATEX

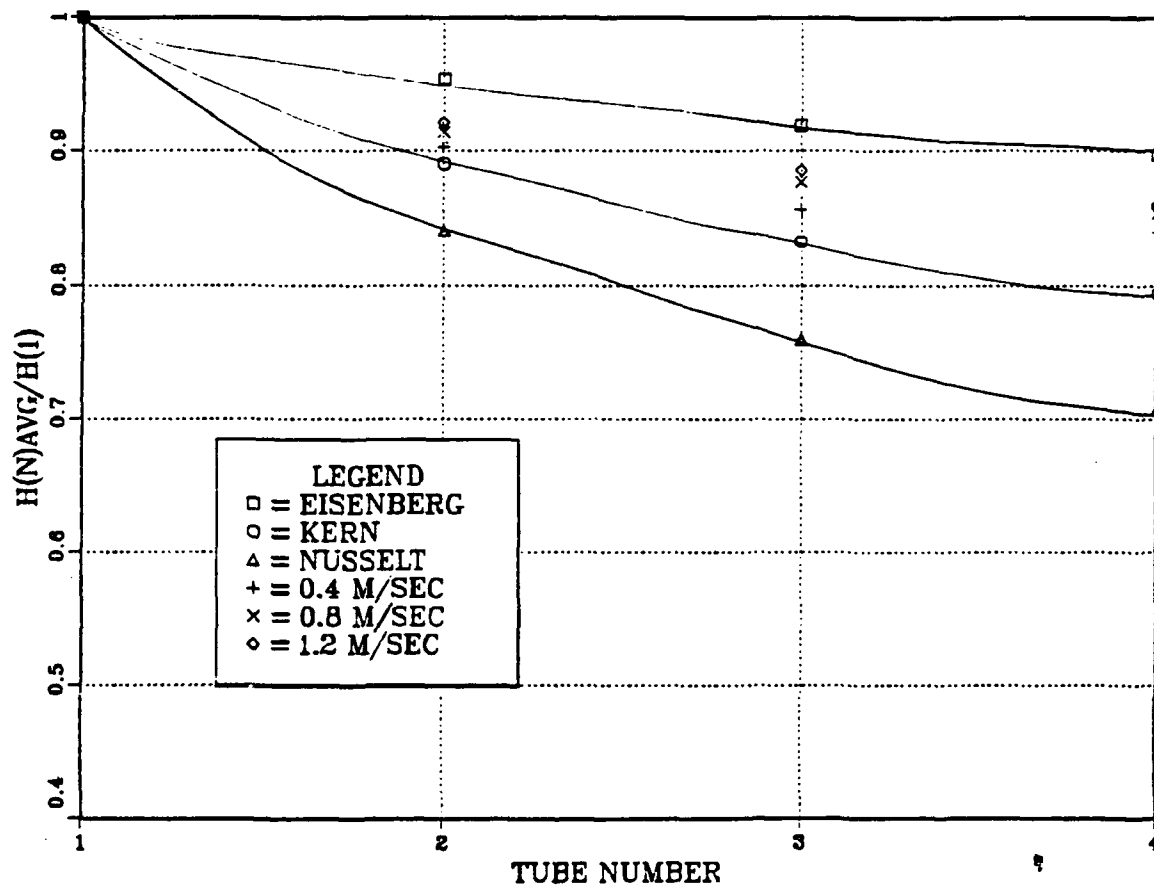


Figure 54. Average  $h$ , for HEATEX element.

condensate. Finally, note that the relative values for  $h_o$  for the KORODENSE tubes are about 10 to 15% higher than the corresponding values for the smooth copper tubes.

The data for the KORODENSE tubes operated individually show much more scatter than was seen for the smooth copper tubes especially at low coolant flow rates. Also, rather than being virtually identical with those obtained for the top tube during bundle operation, the values of  $h_o$  lay scattered between those for the top tube (bundle operation) and the values predicted by Nusselt theory. Presumably, this is due to either inaccuracies or uncertainty in the inside correlation especially at low coolant flow rates. At higher coolant velocities, the scatter appears to be within about 10%.

Values for  $h_o$  for the KORODENSE tubes obtained when the HEATEX elements were installed are shown in Figure 57 and Figure 58 for bundle and individual tube operation respectively. As with the experiments conducted with the tape inserts installed, values of  $h_o$  again lie above those predicted by Nusselt theory. The enhancement appears to be approximately 15 to 20%. Again there is a substantial inundation effect which is of the order of 20% for the second tube in comparison to the top tube. The data obtained for the individual tube operation shows less scatter. However, values for all the tubes again lie between those predicted by Nusselt theory and those obtained for the top tube during bundle operation.

As with the smooth copper tubes, the effects of changing inserts on the inside and outside heat transfer coefficients are shown in Figure 59 and Figure 60. The inside heat transfer coefficients are identical to those of the smooth copper tubes (Figure 49 and Figure 50). It was felt that the enhancement provided by the roping would be much less than the enhancement provided by the inserts. Therefore, the same correlations were used to determine the inside heat transfer coefficient. The values for  $h_i$  are slightly greater for the KORODENSE tubes than for the smooth copper tubes (approximately 5 to 10%).

Figure 61 and Figure 62 show the local heat transfer coefficient for the four tubes for the tape insert and the HEATEX elements. There is virtually no difference between the two. The values lie above the Kern estimate. Figure 63 and Figure 64 show the average heat transfer coefficient for the four tubes with both inserts. The differences for values using the tape inserts as opposed to the HEATEX elements are again negligible. The average values for  $h_o$  also lie just above the Kern model. This is in contrast to the smooth copper tubes where the average values lay near the Nusselt estimate. This suggests that the effect of condensate inundation is indeed less for the KORODENSE tubes.

# HZERO KORODENSE TUBES

KD04, R-113, BUNDLE, TAPE INSERT

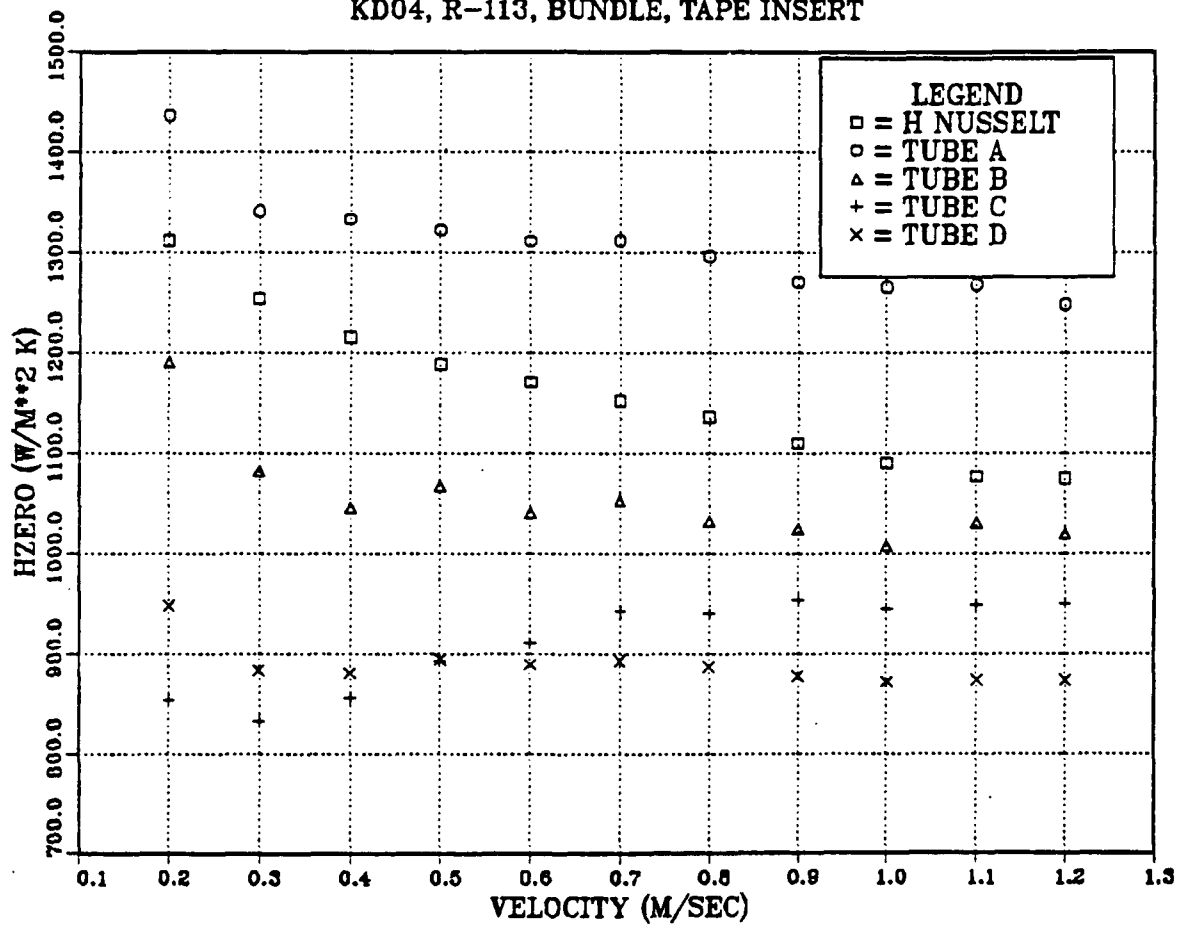


Figure 55. KORODENSE tubes, tape insert, bundle operation.

# HZERO KORODENSE TUBES

KD04, R-113, SINGLE, TAPE INSERT

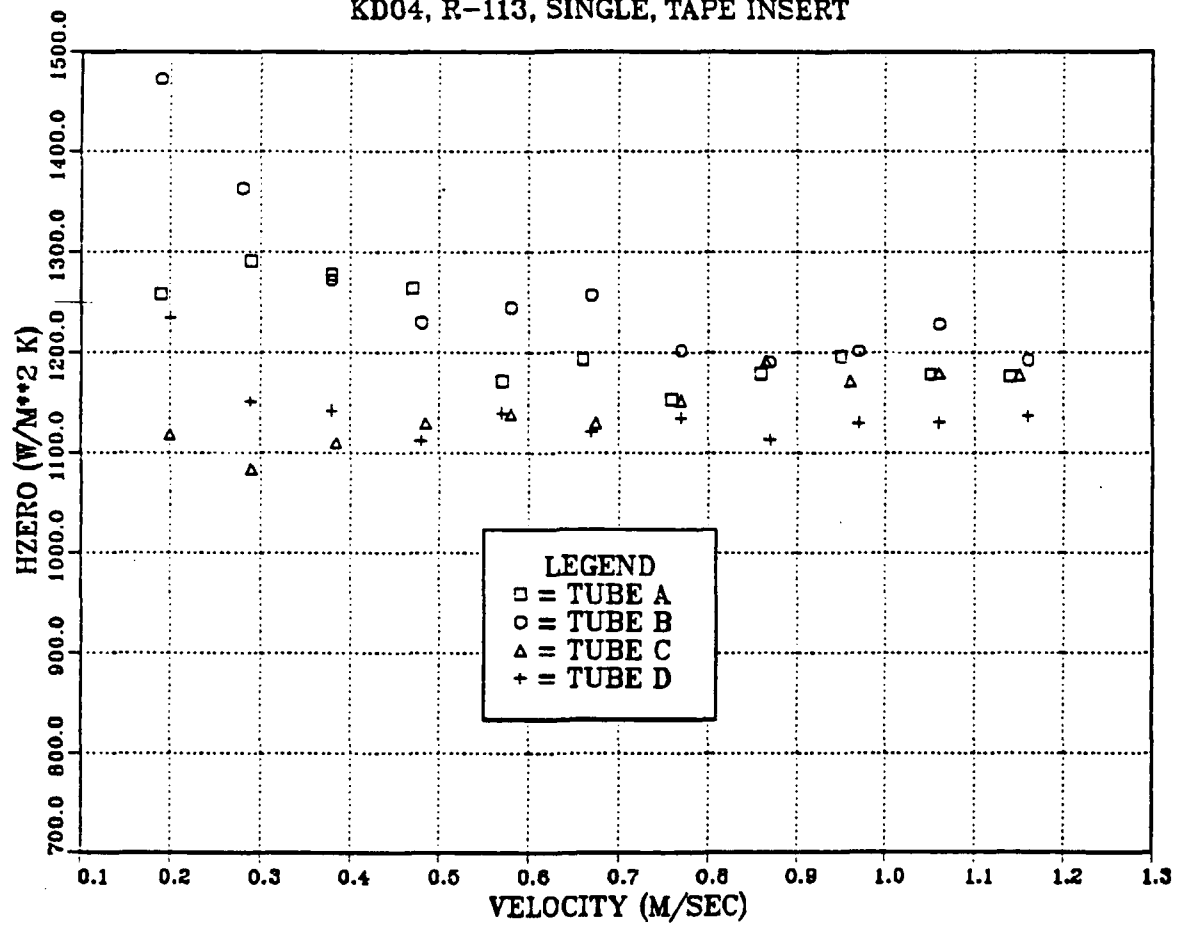


Figure 56. KORODENSE tubes, tape insert, individual operation.

# HZERO KORODENSE TUBES

KD03, R-113, BUNDLE, HEATEX

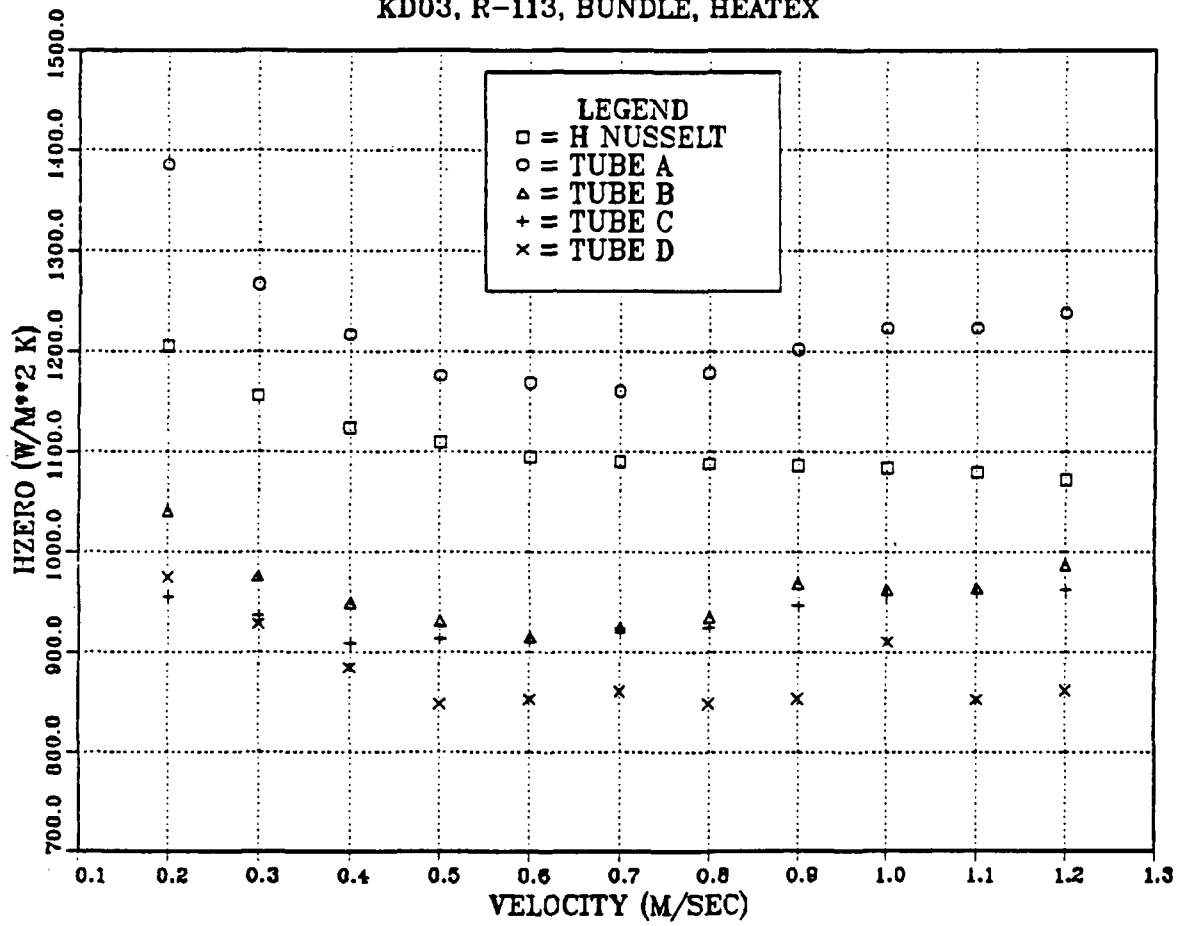


Figure 57. KORODENSE tubes, HEATEX insert, bundle operation.

# HZERO KORODENSE TUBES

KD03, R-113, SINGLE, HEATEX

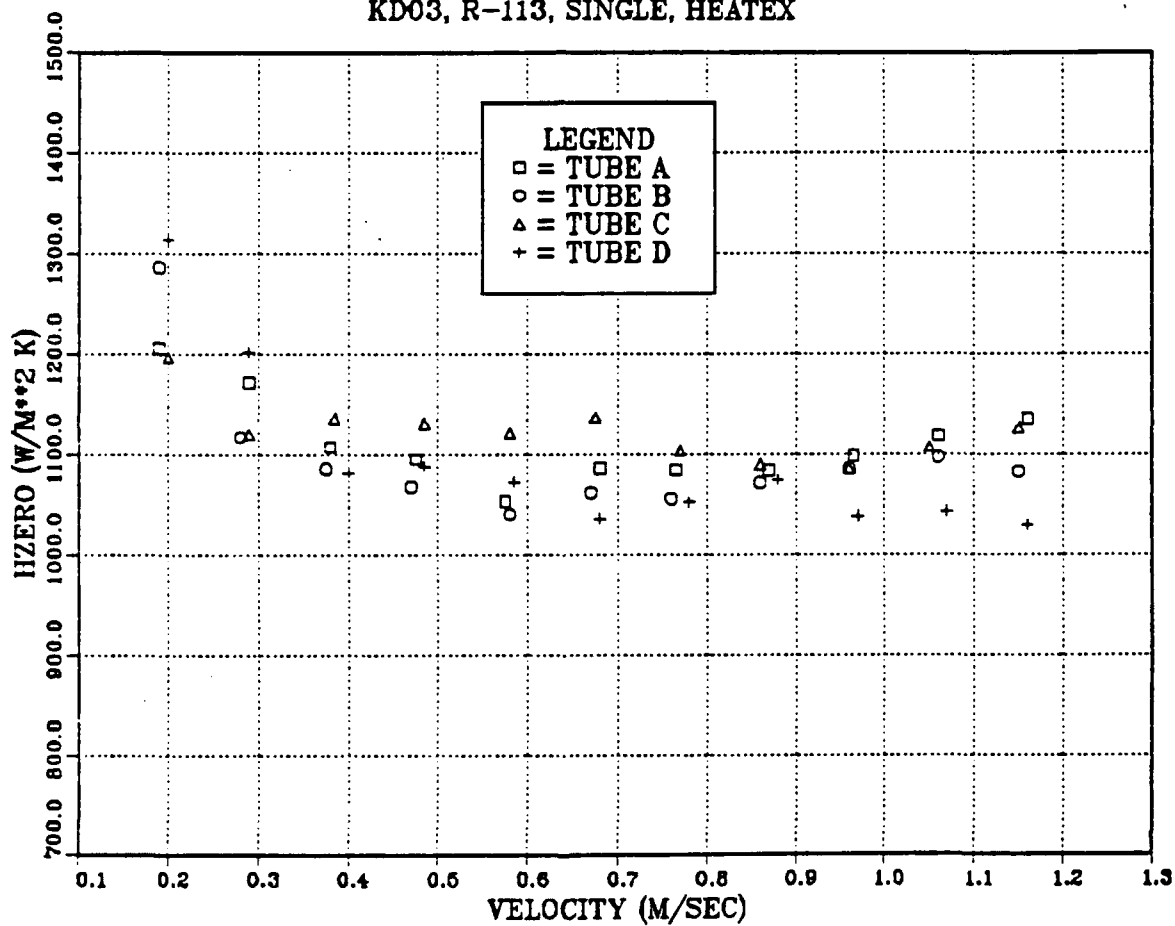


Figure 58. KORODENSE tubes, HEATEX insert, individual operation.

# KORODENSE COPPER/NICKEL TUBES

TOP TUBE, TAPE INSERT

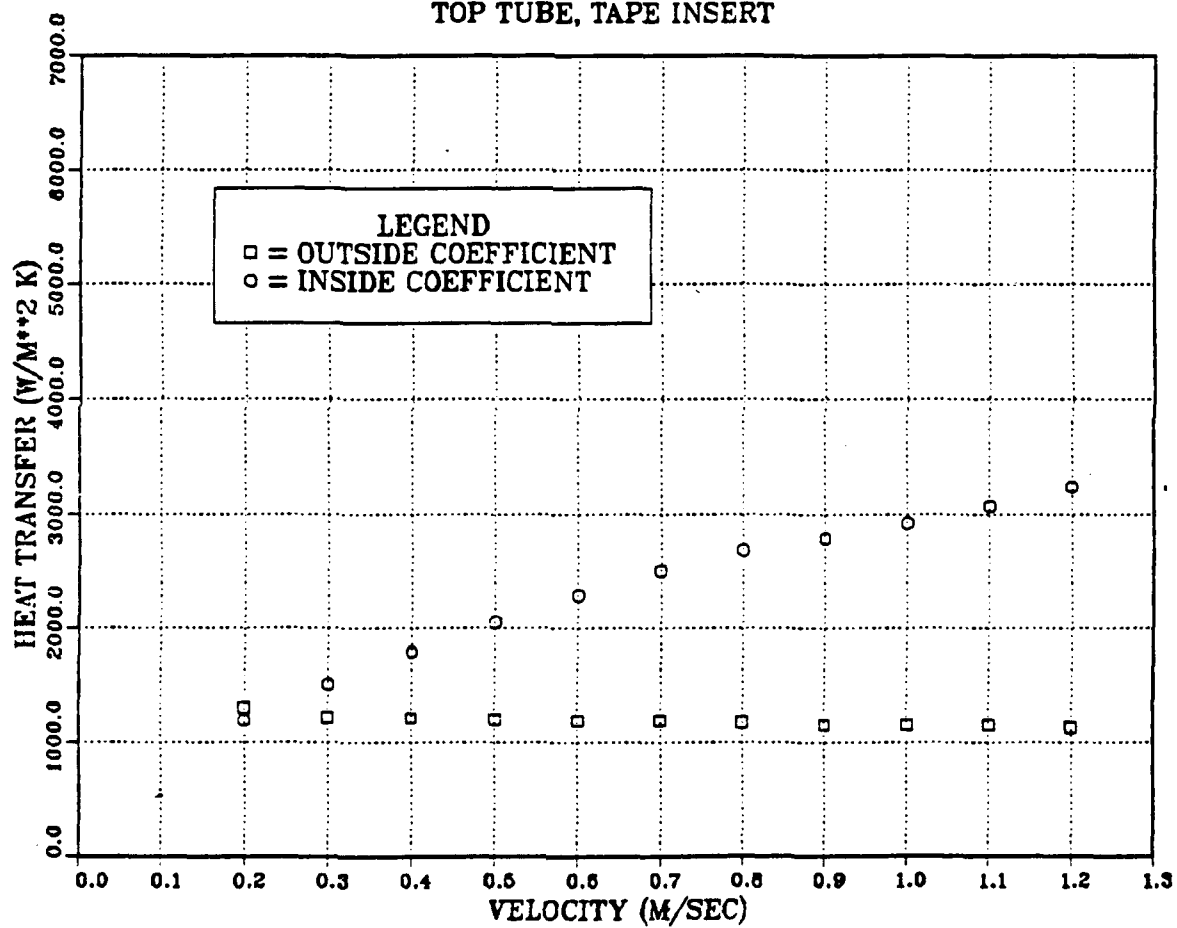


Figure 59. Effect of tape insert on  $h_o$  and  $h_i$



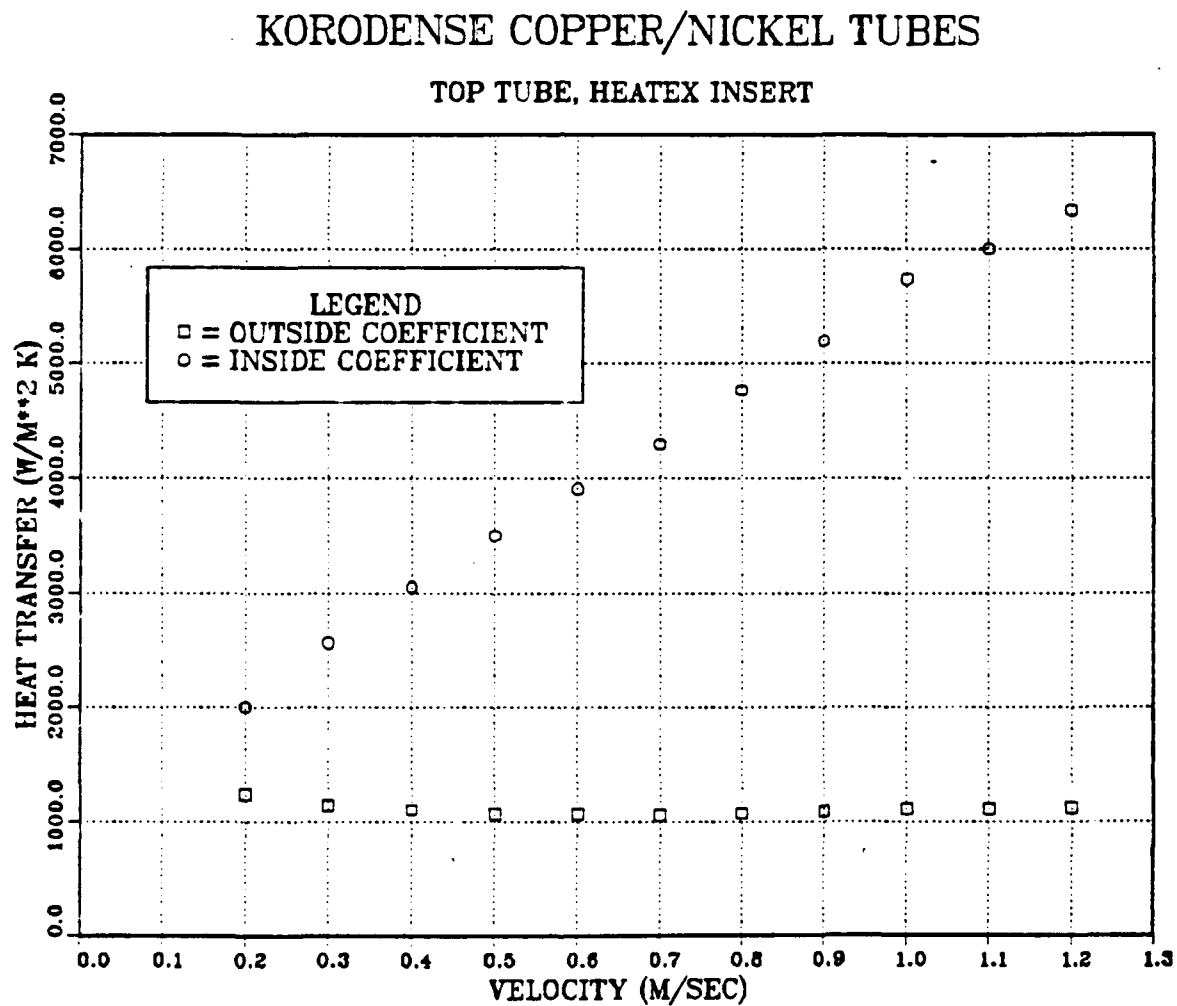


Figure 60. Effect of HEATEX insert on  $h_o$  and  $h_i$

# HEAT TRANSFER COEFFICIENT

KORODENSE TUBES, TAPE INSERTS

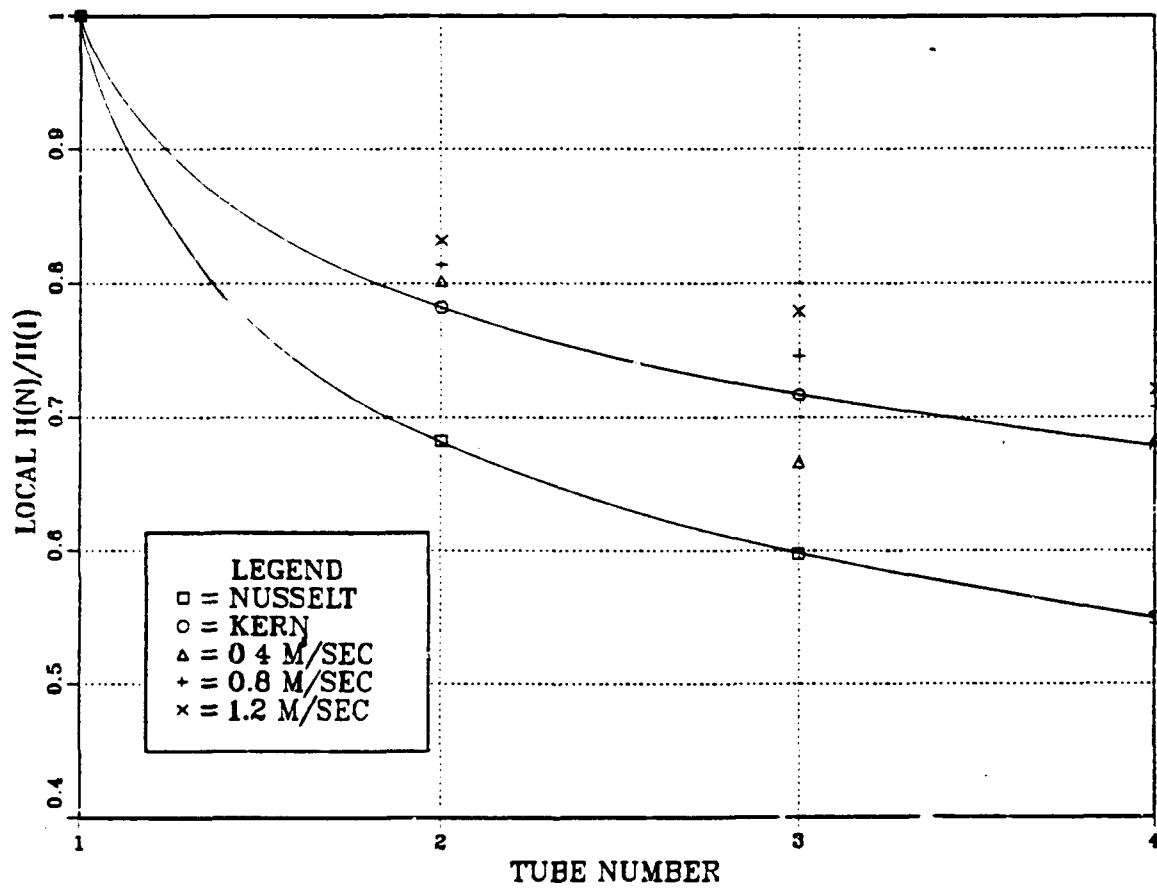


Figure 61. Local  $h$ , for tape insert.

# HEAT TRANSFER COEFFICIENT

## KORODENSE TUBES WITH HEATEX

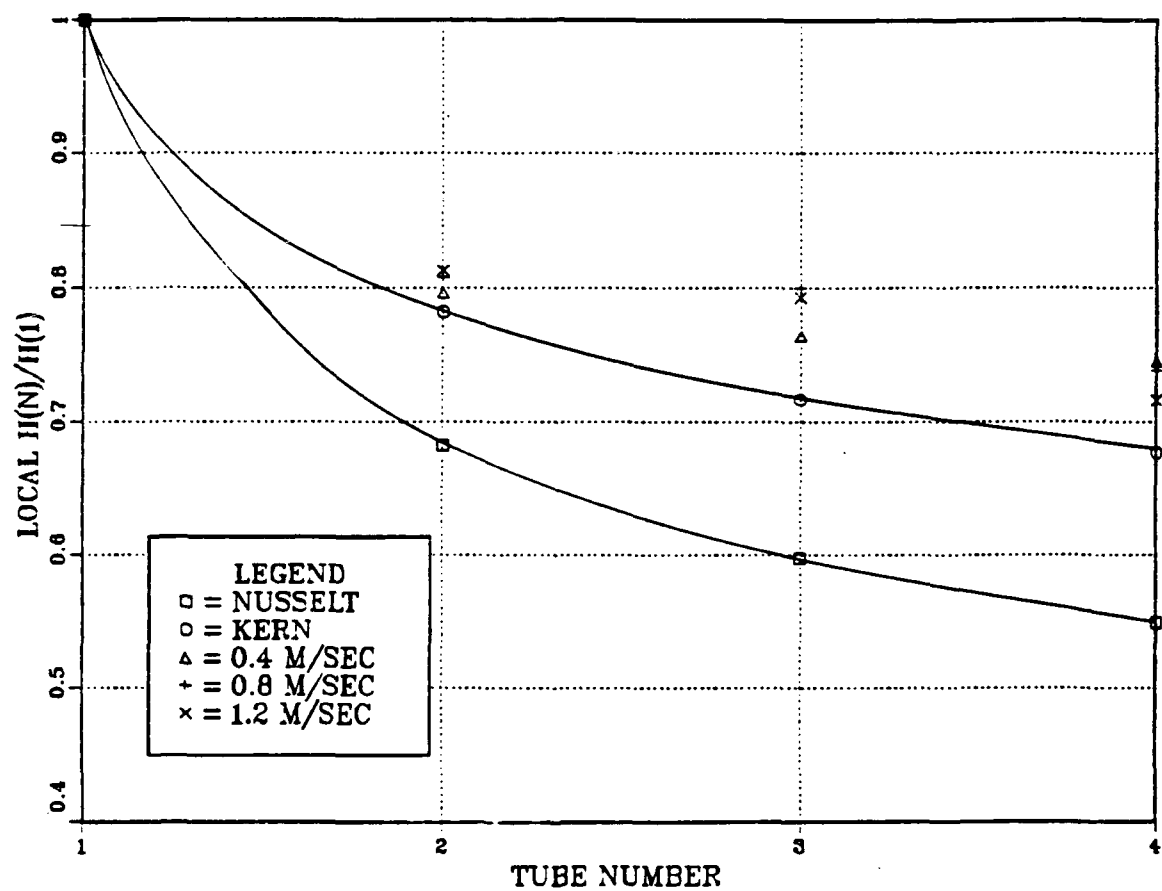


Figure 62. Local  $h$ , for HEATEX element.

# HEAT TRANSFER COEFFICIENT

KORODENSE TUBES, TAPE INSERT

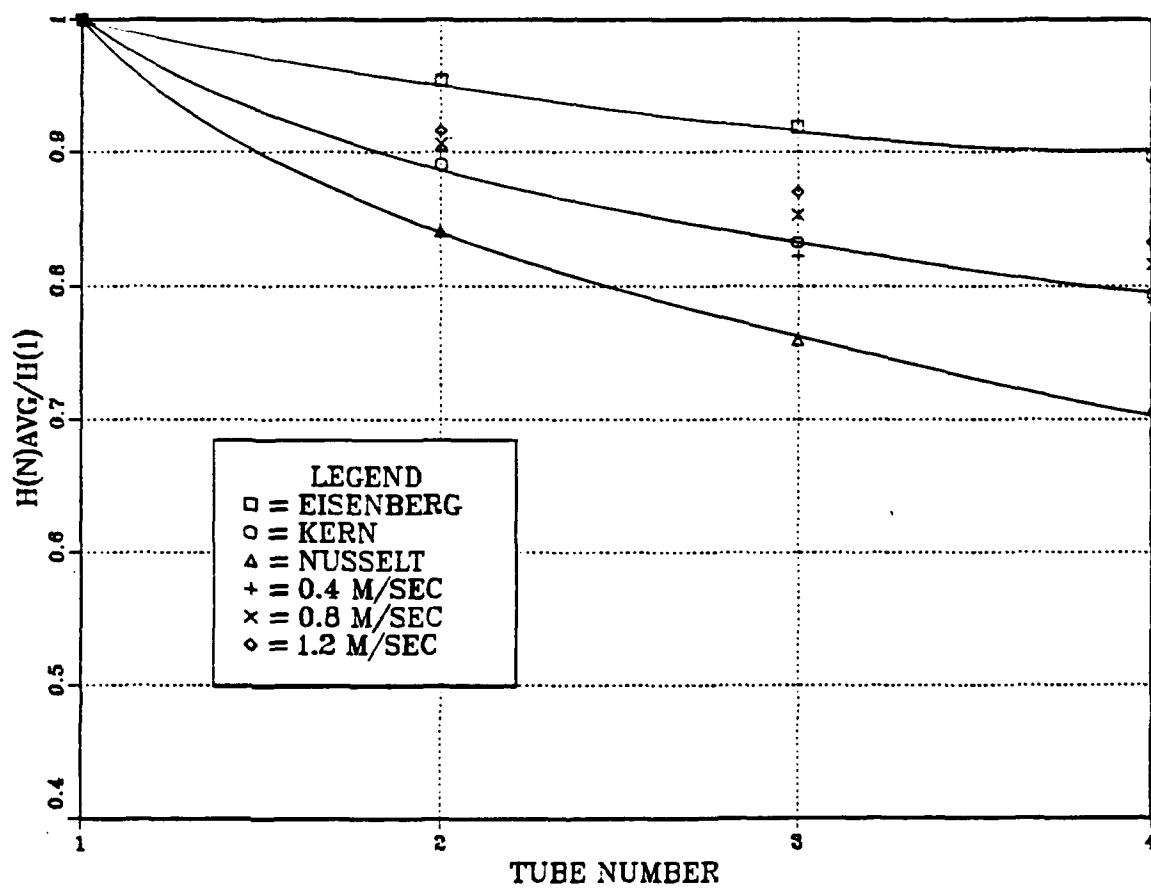


Figure 63. Average  $h$ , for tape insert.

# HEAT TRANSFER COEFFICIENT

## KORODENSE TUBES WITH HEATEX

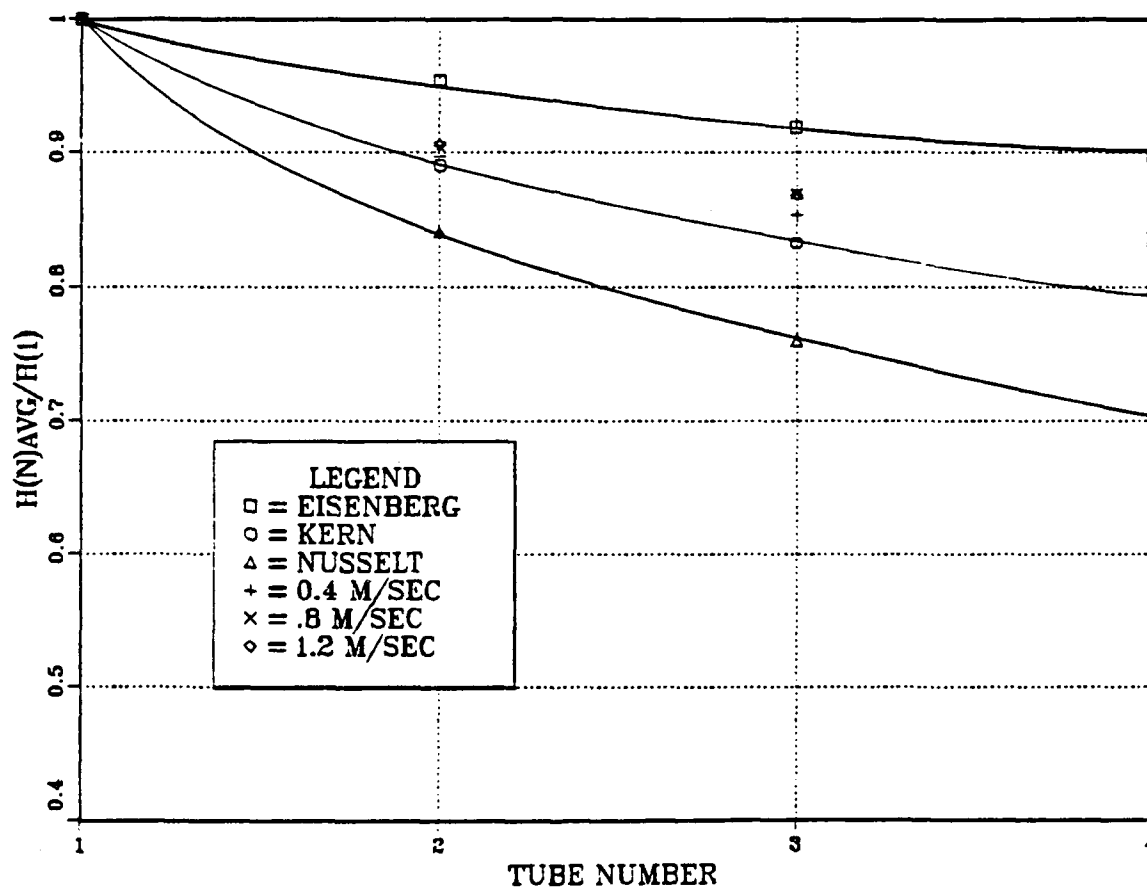


Figure 64. Average  $h_s$  for HEATEX element.

### 3. Wire Wrapped KORODENSE Tubes

The effect on  $h_o$  of wrapping wire around the KORODENSE tubes is shown in Figure 65, Figure 66, Figure 67 and Figure 68. In viewing these figures, one should remember that the values for the unwrapped KORODENSE tubes were about 10% greater than predicted from Nusselt theory and about 15% greater than for the smooth copper tubes. From the figures, it appears that the 0.049" diameter wire results in the greatest enhancement in  $h_o$  for all four tube positions. However, the relative magnitude of the enhancement decreases as lower tubes are examined. Since this data was obtained during individual tube operation, the results are not due to condensate inundation.

Values for  $h_o$  are shown for each wire diameter in all four tube positions in Figure 69, Figure 70, Figure 71 and Figure 72. When no wire is used, the results are the same as those shown in Figure 58. For the 0.029" wire, positions A and B are essentially identical with tube C showing the greatest enhancement and tube D the worst. The magnitude of the deviation is about 20%. The 0.049" diameter wire results in the best enhancement in  $h_o$  regardless of position. However, note that position D is not overwhelmingly greater than for the 0.029" wire. The data show that the level of enhancement depends upon bundle position. The top tube positions behave similarly while positions C and D show reduced levels of enhancement. Finally, the 0.0675" diameter wire yields values for  $h_o$  which are nearly the same although a positional effect appears evident. An interesting comparison are the values for  $h_o$  for the 0.049" and 0.0675" wire in the fourth position. Here it appears that the 0.0675" wire gives roughly the same level of enhancement especially at high coolant velocities.

### 4. KORODENSE Tubes Wrapped with 0.049" Wire

The effects on  $h_o$  of wrapping 0.049" diameter wire on KORODENSE tubes on are shown in Figure 73 and Figure 74. These two experiments are identical runs. In both cases, there is a substantial improvement in  $h_o$  for all tubes when compared to values predicted from Nusselt theory. It is interesting to note that even though tubes B, C, and D are all being inundated, the values for  $h_o$  are still well above Nusselt theory (32% for tube A, 28% for tube B, 22% for tube C and 16% for tube D). In comparison with the non-wire wrapped KORODENSE tubes, wrapping with the 0.049" diameter wire yields an increase of about 70% for tubes A and B and about a 30 to 50% increase for tubes C and D. Comparison with the top smooth tube yields almost a 90% increase in  $h_o$ .

The results for the single tube runs are shown in Figure 75 and Figure 76. Both runs demonstrate considerable scatter in the data of about  $\pm 22\%$ . It is also interesting

# HZERO WIRE WRAPPED KORODENSE

TUBE A, R-113, HEATEX

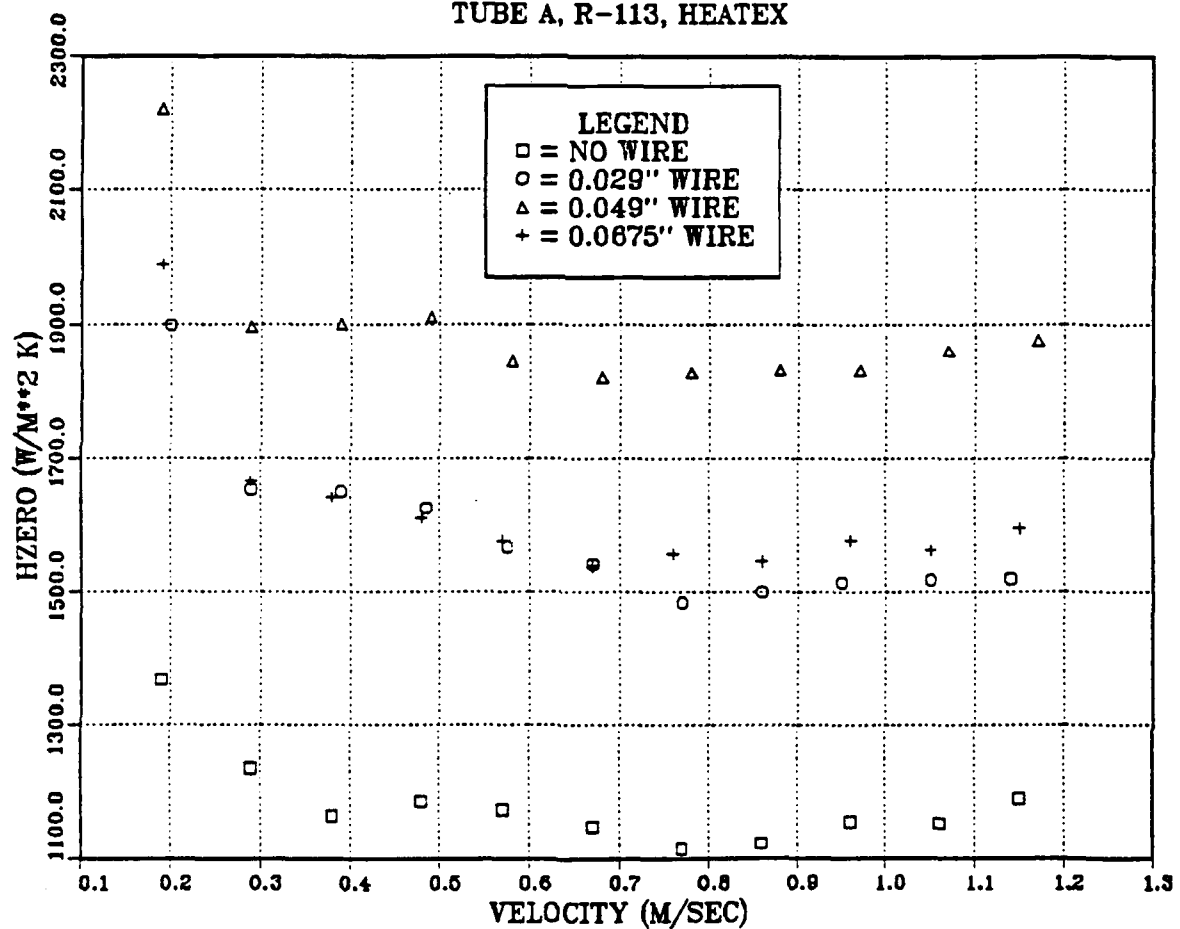


Figure 65. Effect of wire diameter on  $h_c$  for tube A.

# HZERO WIRE WRAPPED KORODENSE

TUBE B, R-113, HEATEX

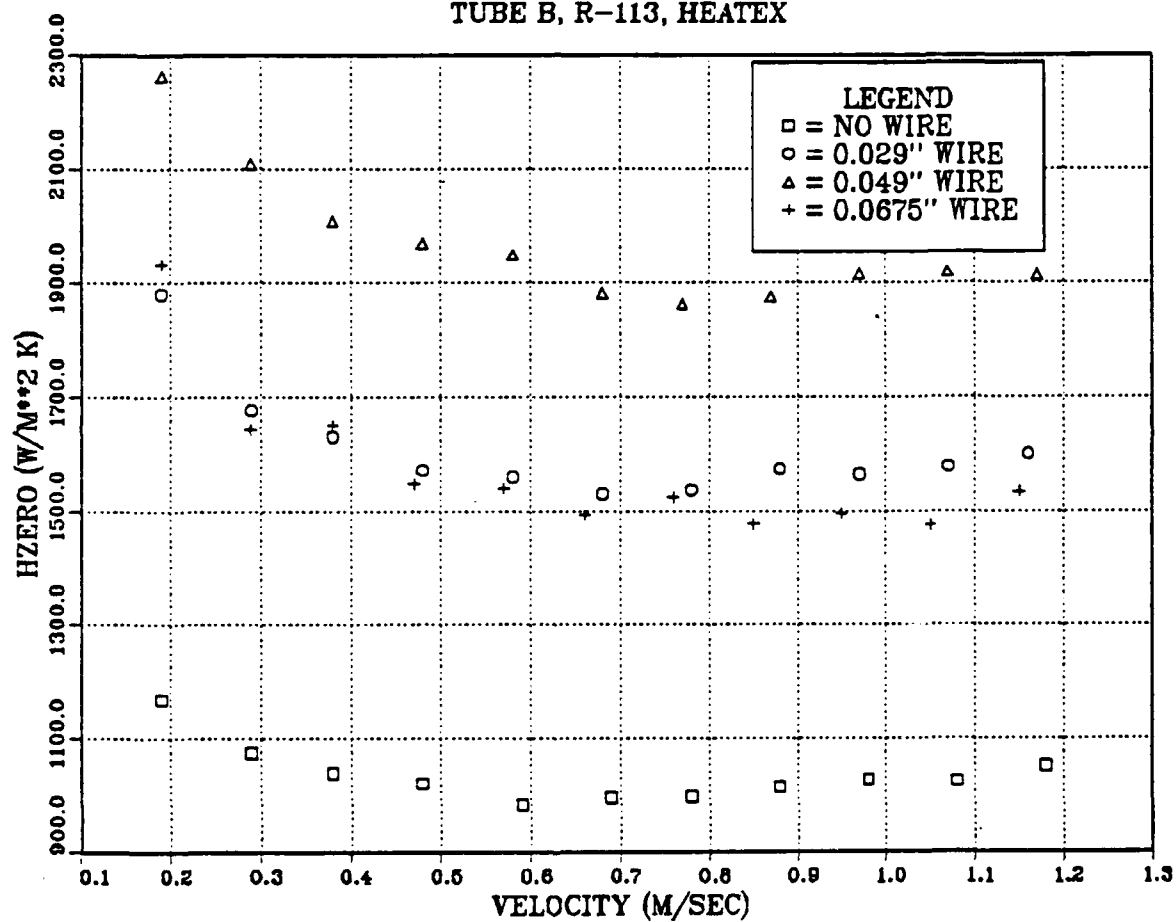


Figure 66. Effect of wire diameter on  $h_c$  for tube B.



# HZERO WIRE WRAPPED KORODENSE

TUBE C, R-113, HEATEX

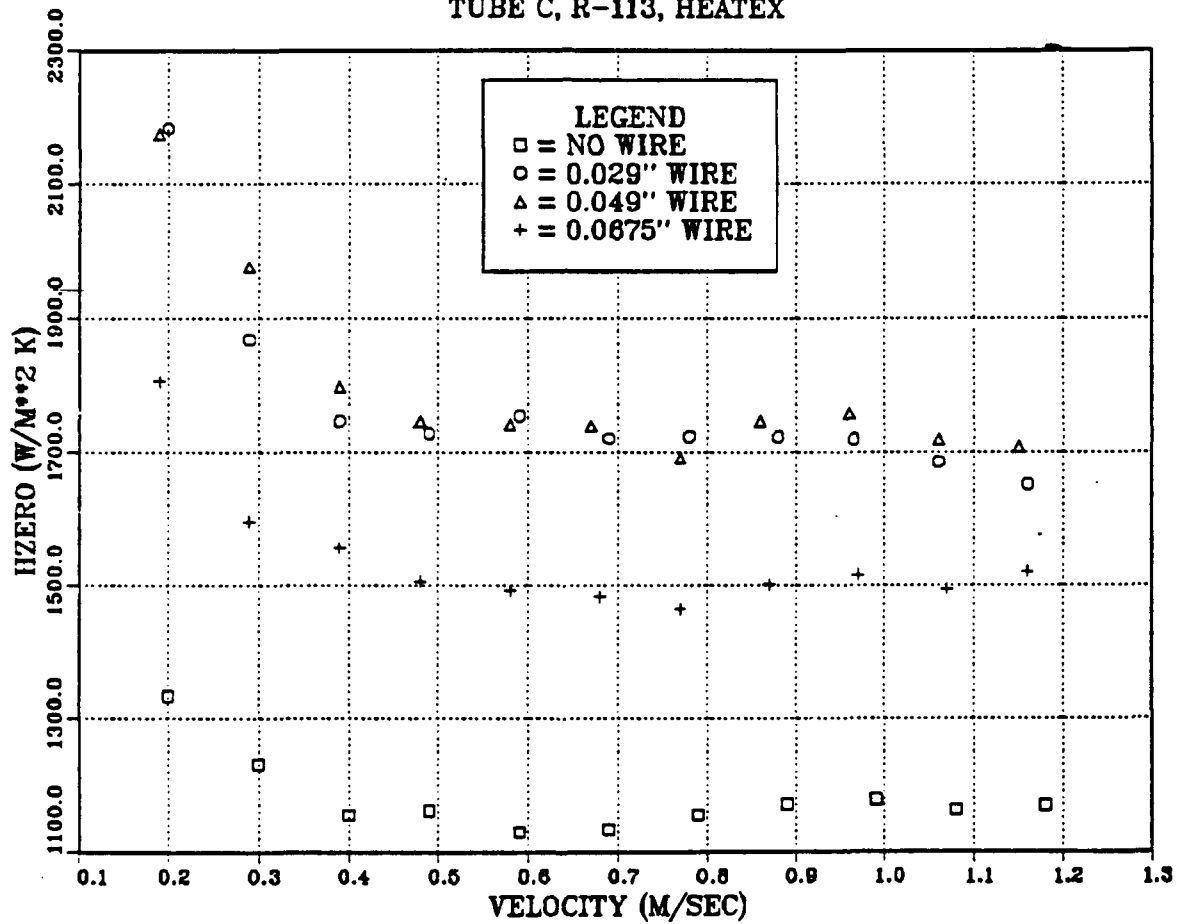


Figure 67. Effect of wire diameter on  $h$ , for tube C.

# HZERO WIRE WRAPPED KORODENSE

TUBE D, R-113, HEATEX

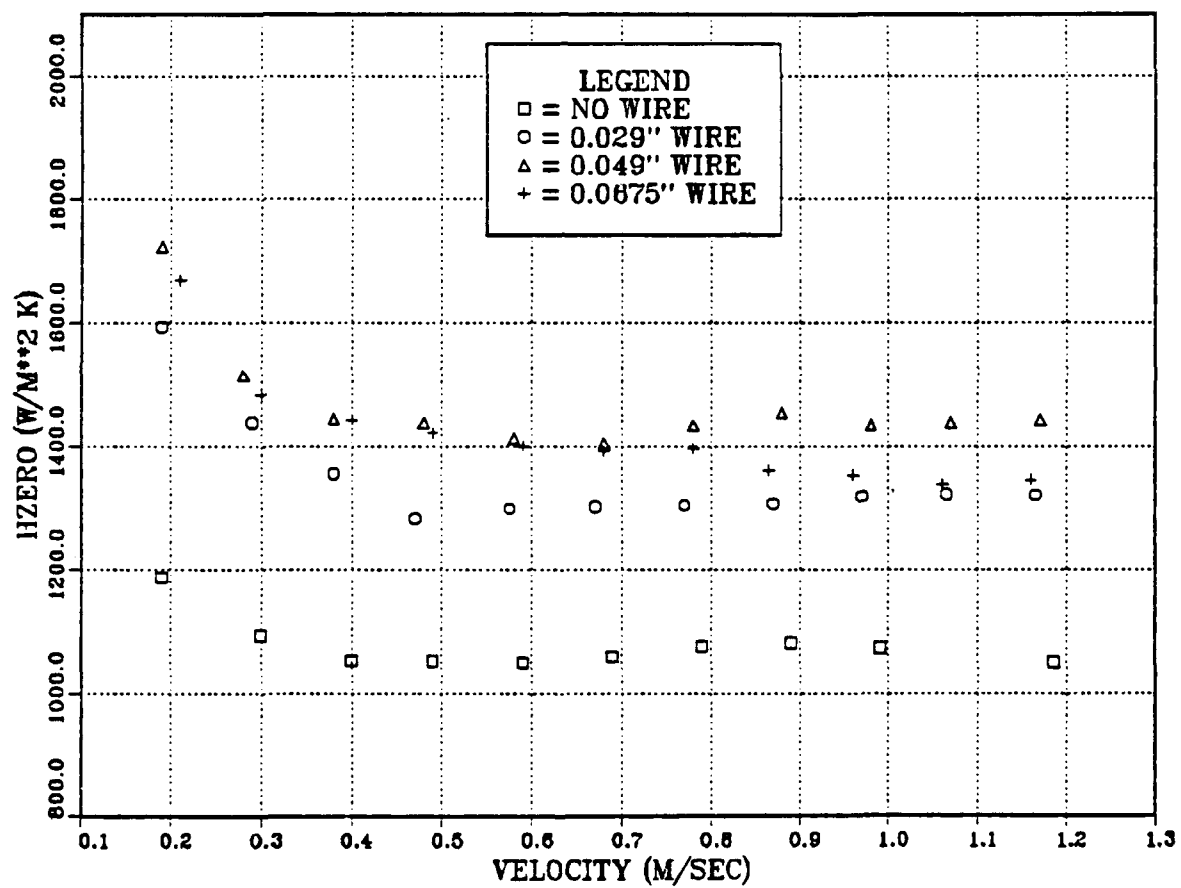


Figure 68. Effect of wire diameter on  $h_z$  for tube D.

# HZERO WIRE WRAPPED KORODENSE

NO WIRE, HEATEX

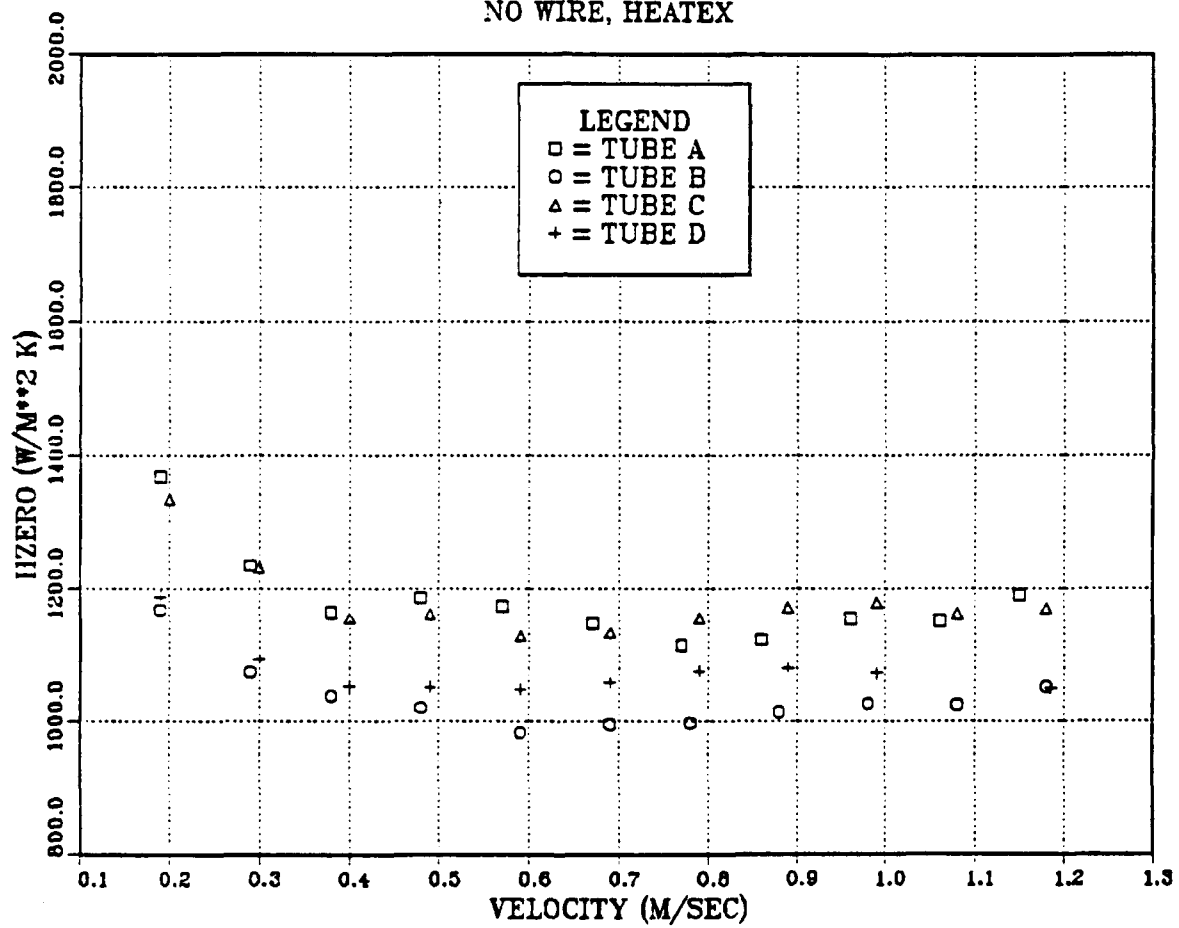


Figure 69. Effect of no wire on  $h_c$  for all tubes.

# HZERO WIRE WRAPPED KORODENSE

0.029" WIRE, HEATEX

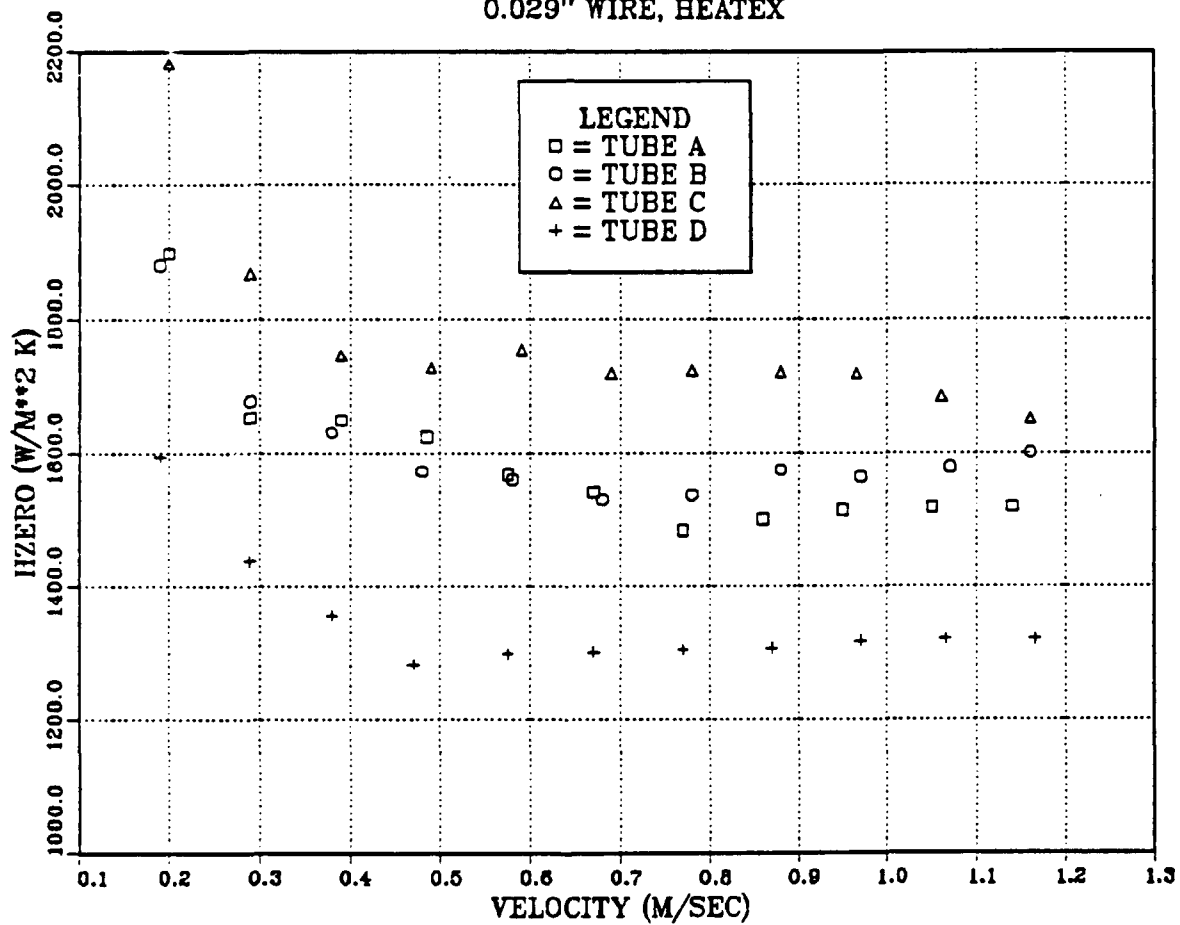


Figure 70. Effect of 0.029" wire on  $h_o$  for all tubes.

# HZERO WIRE WRAPPED KORODENSE

0.049" WIRE, HEATEX

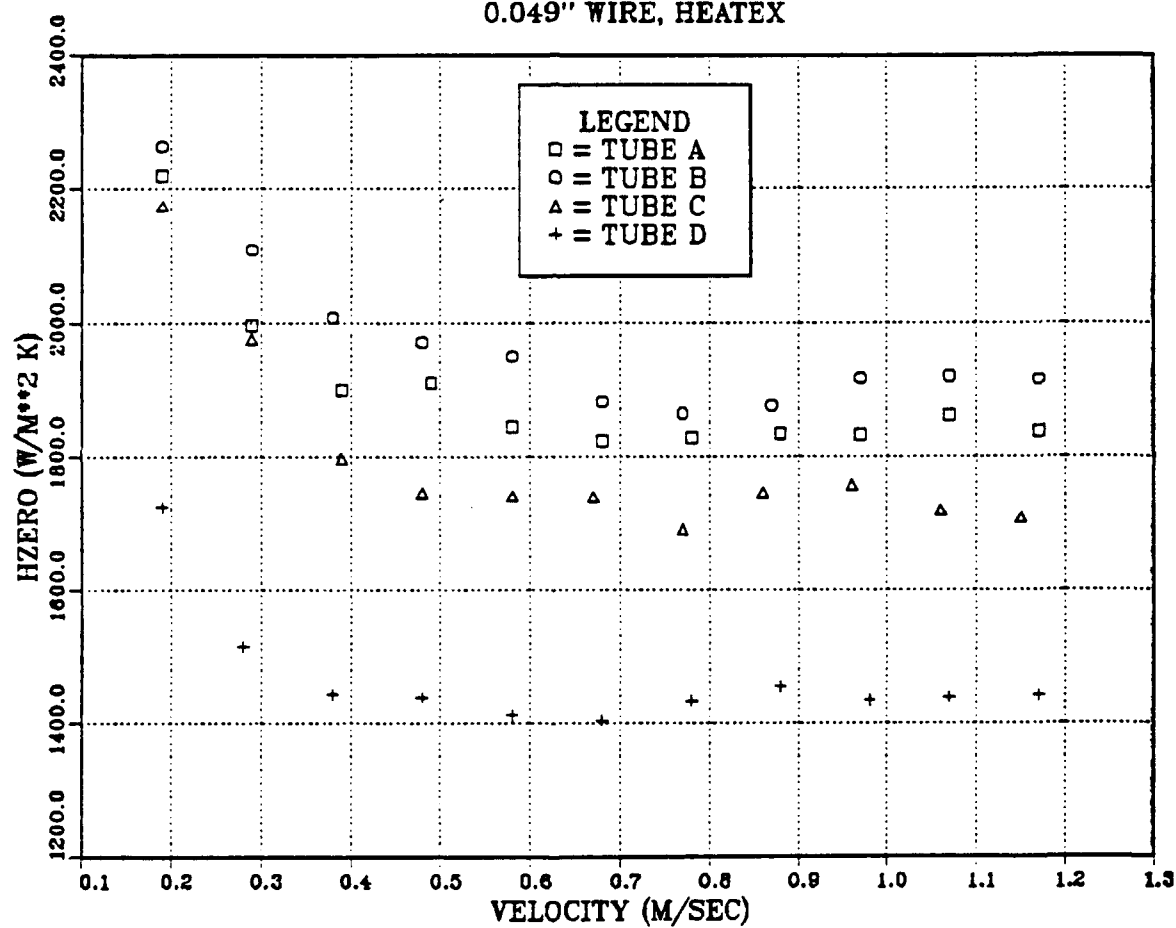


Figure 71. Effect of 0.049" wire on  $h_o$  for all tubes.

# HZERO WIRE WRAPPED KORODENSE

0.0675" WIRE, HEATEX

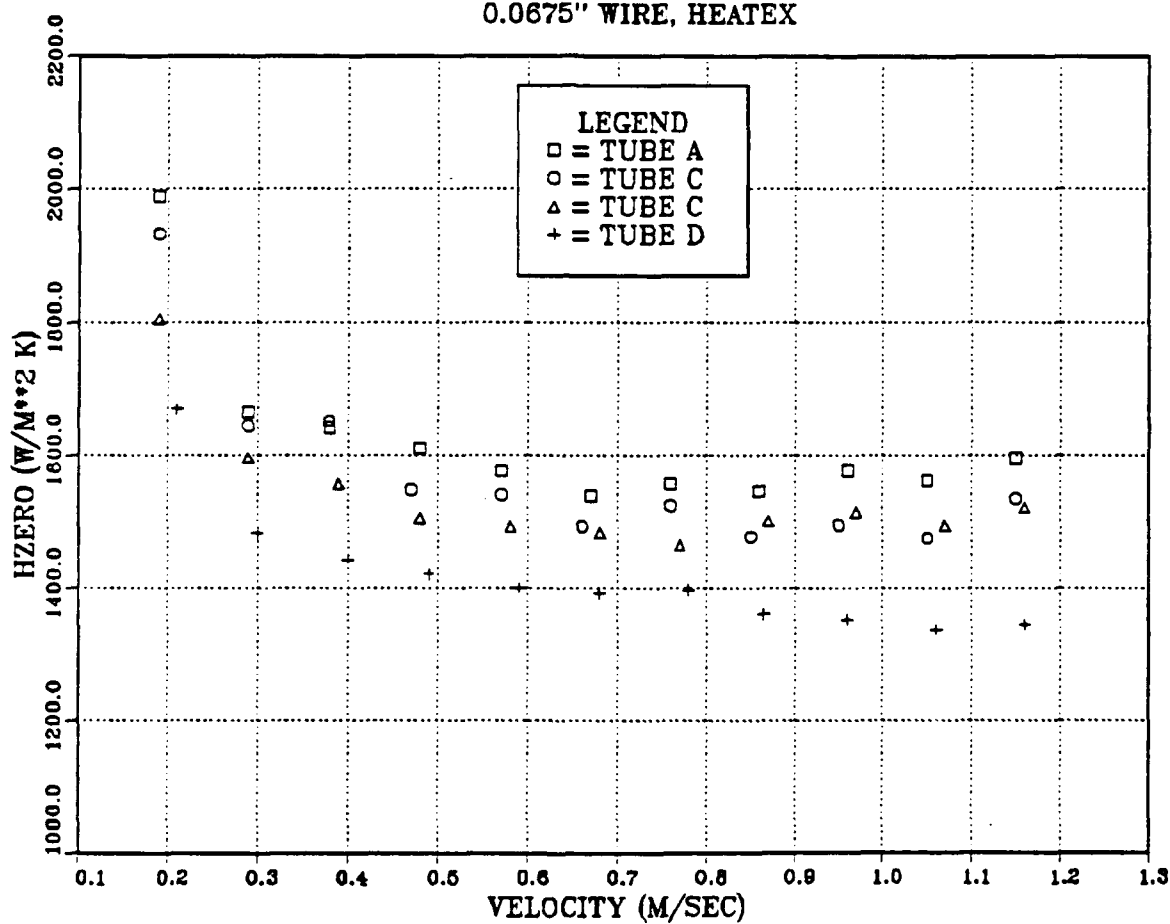


Figure 72. Effect of 0.0675" wire on  $h_c$  for all tubes.

# 0.049" WIRE WRAPPED KORODENSE

KD11, R-113, HEATEX, BUNDLE

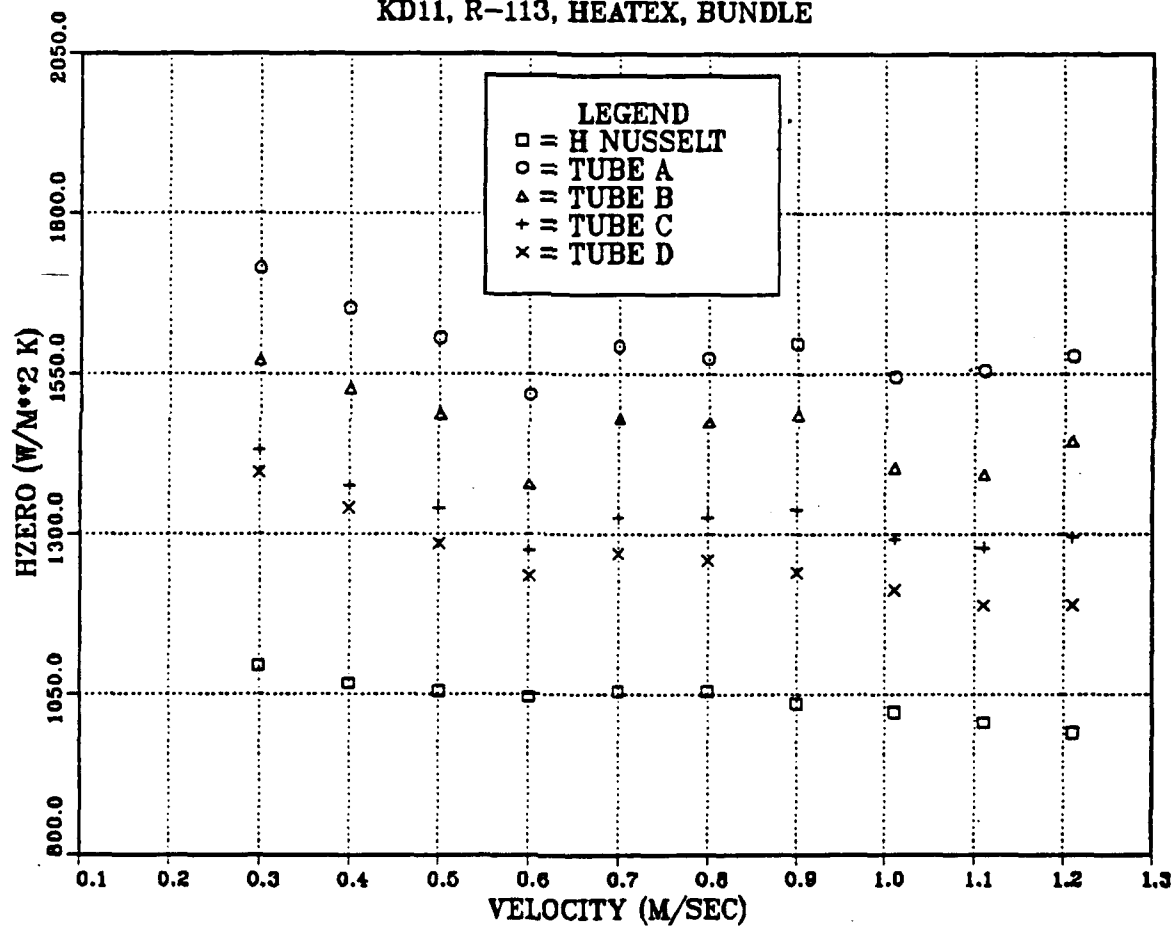


Figure 73. 0.049" wire wrapped KORODENSE tubes, bundle operation, expt. 1.

# 0.049" WIRE WRAPPED KORODENSE

KD12, R-113, HEATEX, BUNDLE

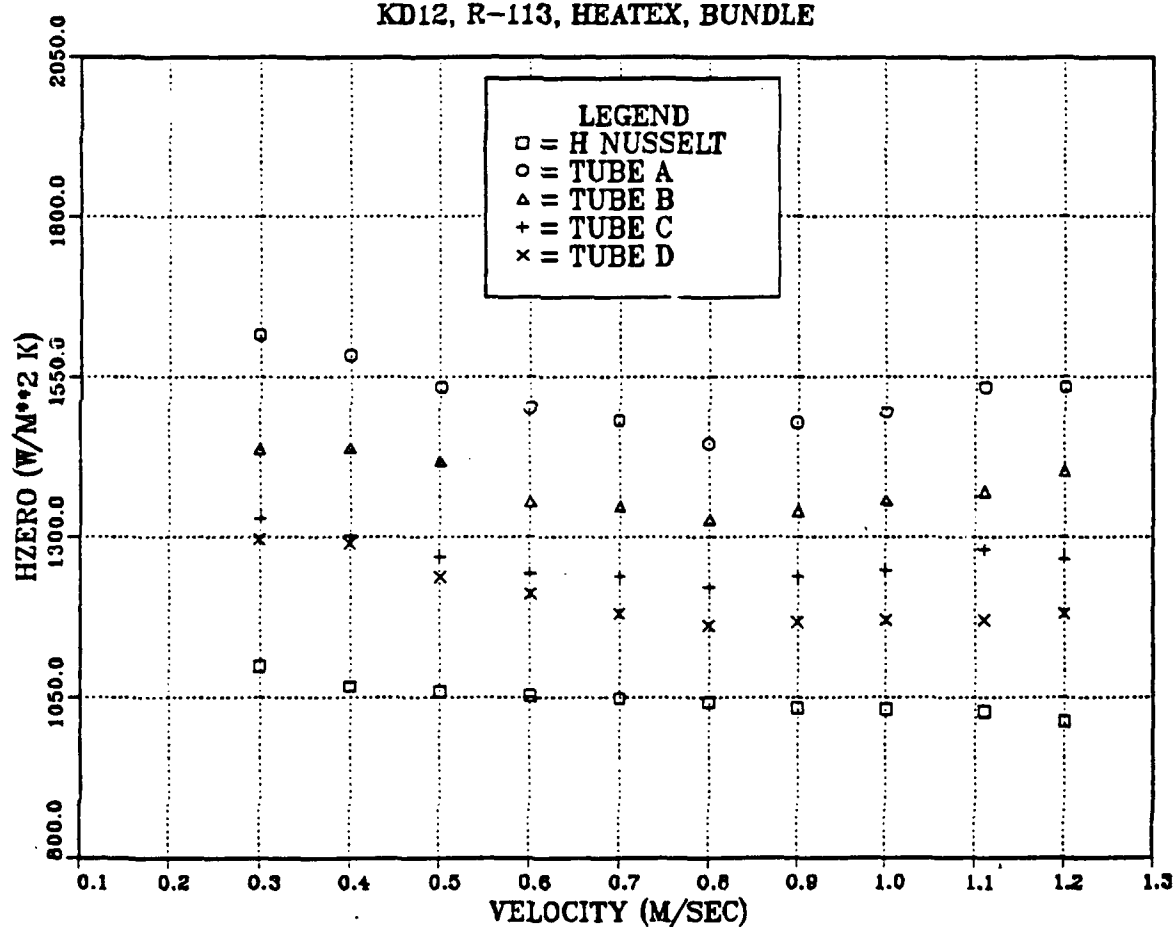


Figure 74. 0.049" wire wrapped KORODENSE tubes, bundle operation, expt. 2.



to note that the data for these single tube runs is somewhat higher than for the bundle runs (of the order of 11%). This may be due to uncertainty in the correlations used for  $h_i$  which are reflected in  $h_o$ .

The values for the average and local vapor-side heat transfer coefficients are shown in Figure 77, Figure 78, Figure 79 and Figure 80 for the two experiments conducted with the 0.049" wire wrapped KORODENSE tubes. The average vapor-side heat transfer coefficient is equal to that predicted by the Eissenberg model whereas the local vapor-side heat transfer coefficient is substantially above the Kern estimate. Recall that for the plain KORODENSE tubes, the average heat transfer coefficient was above the Kern estimate but below that predicted by the Eissenberg model. The local heat transfer coefficient was just above the Kern estimate. The differences between the plain and wire-wrapped KORODENSE tubes demonstrate that wrapping the tubes with wire substantially reduces the effects of condensate inundation.

### 5. Copper/Nickel Finned Tubes

The values for  $h_o$  obtained from experiments on copper/nickel finned tubes using the tape inserts are shown in Figure 81. The values obtained for the top tube are approximately 7 times greater than predicted by Nusselt theory. Condensate inundation caused about a 35% decrease in  $h_o$  for the second tube.

The values for  $h_o$  obtained using the same tubes but with the HEATEX elements are shown in Figure 82. In comparison to the values obtained for the tape inserts (see Figure 81), this data appears very scattered with enhancement over Nusselt theory of the order of 10 to 15 fold. This is a large discrepancy. It is possible that the correlation for the small diameter HEATEX element may be suspect. The data supplied by CAL GAVIN was collected on smooth copper tubes with a diameter similar to that of our copper/nickel finned tubes. This data was collected over a lower coolant velocity range than that used in this study. Therefore, the correlation for this HEATEX element may not be valid for the finned tube over the range of coolant velocities used here. This area needs to be studied further, perhaps even to gathering new experimental data which can be used to develop a new correlation.

The degree of inundation can be seen in Figure 83, Figure 84, Figure 85 and Figure 86. The data for the average vapor-side heat transfer coefficient for both HEATEX as well as tape inserts lie between the Nusselt and Kern models. This is also true for the local vapor-side heat transfer coefficients.

An interesting comparison is to look at the average and local heat transfer values for all tubes tested. Regarding the average heat transfer coefficient, for the smooth

# HZERO WIRE WRAPPED KORODENSE

KD11, R-113, SINGLE, HEATEX

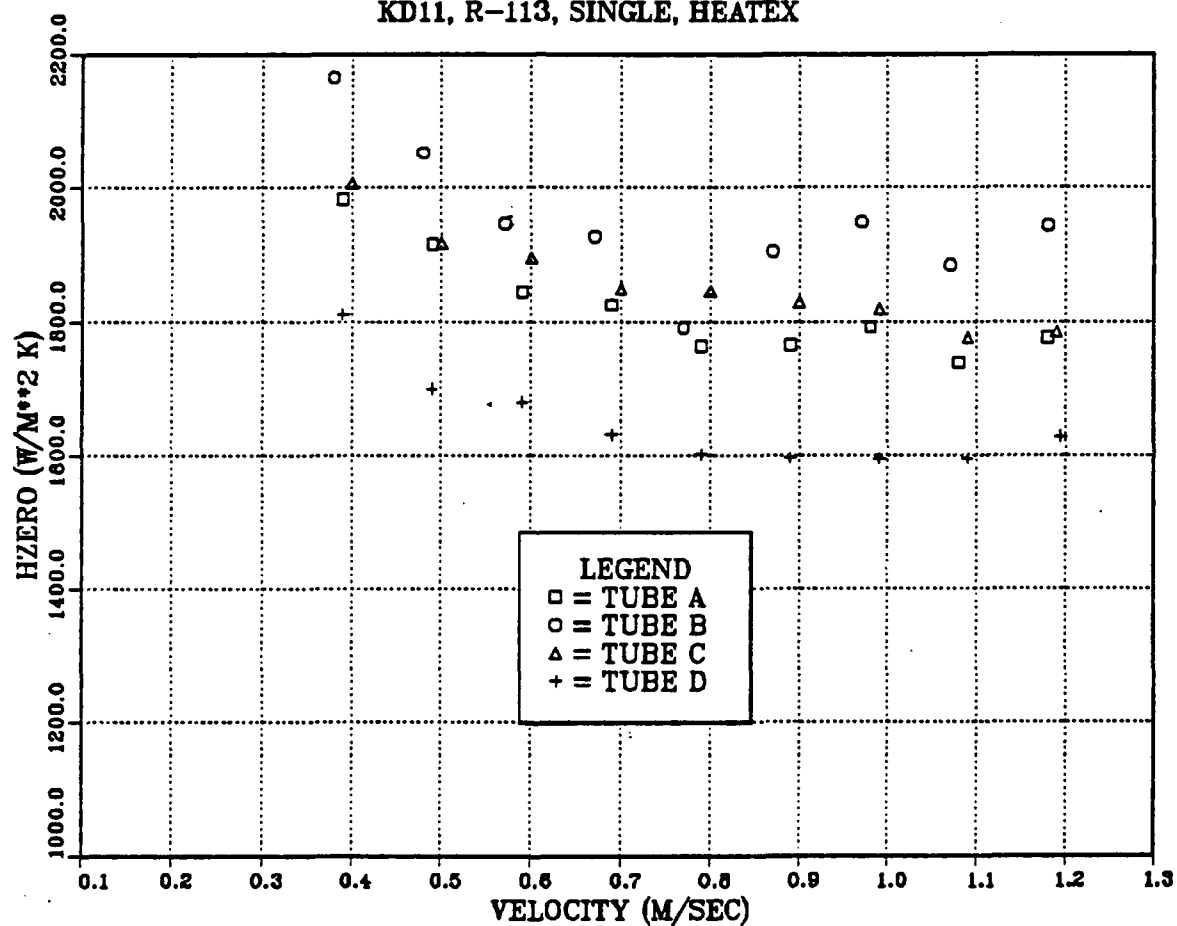


Figure 75. 0.049" wire wrapped KORODENSE, individual runs, expt. 1.

# 

KD12, R-113, SINGLE, HEATEX

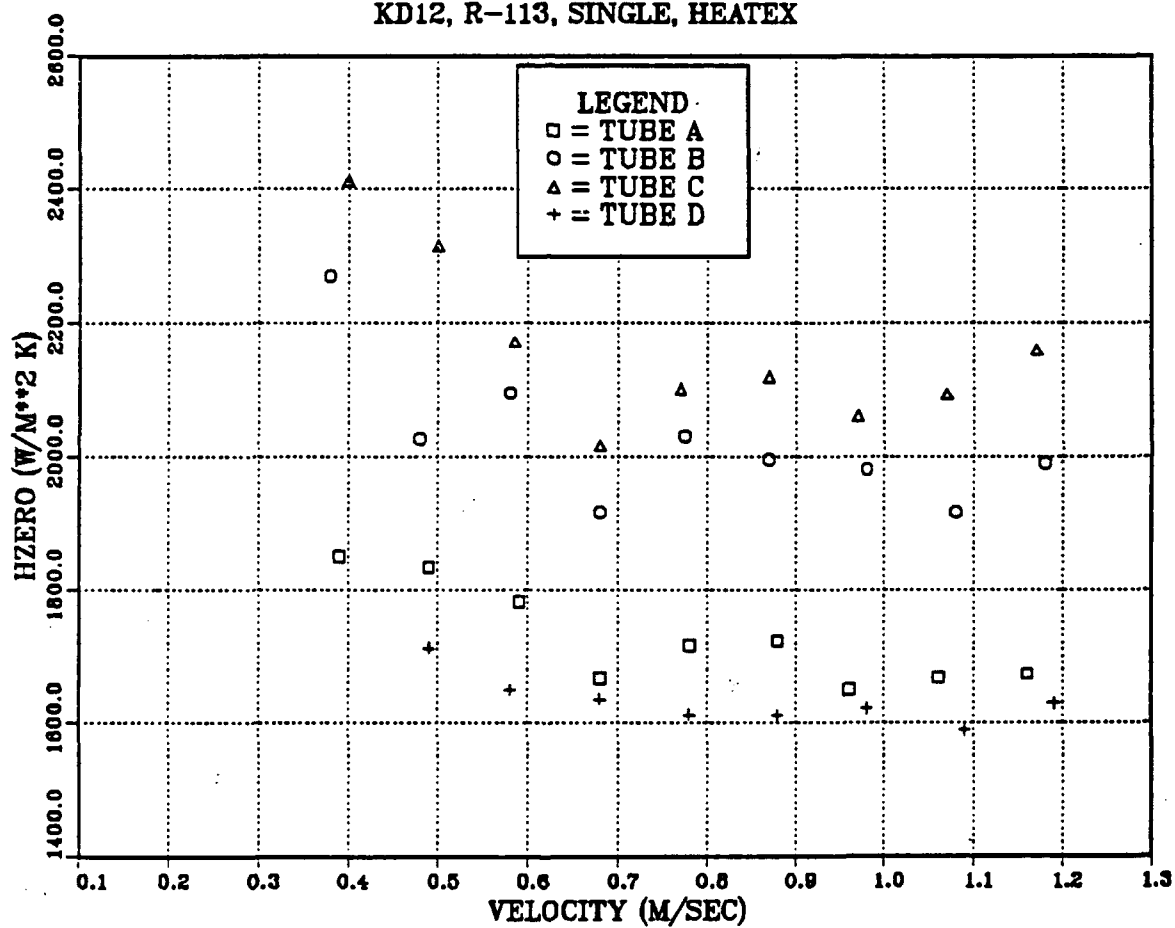


Figure 76. 0.049" wire wrapped KORODENSE, individual runs, expt. 2.

# HEAT TRANSFER COEFFICIENT

KD11, 0.049" WIRE, KORODENSE

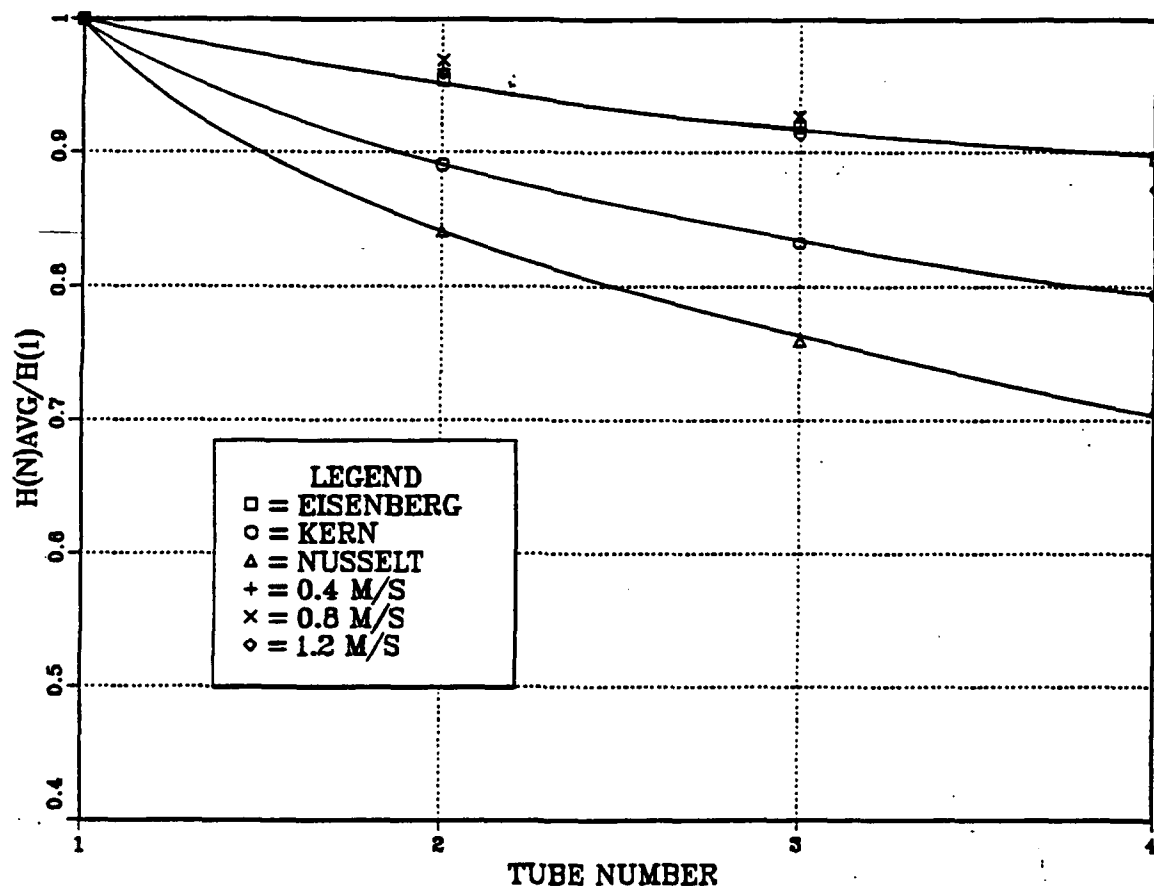


Figure 77. Average  $h$ , wire wrapped KORODENSE, expt. 1.

# HEAT TRANSFER COEFFICIENT

KD12, 0.049" WIRE, KORODENSE

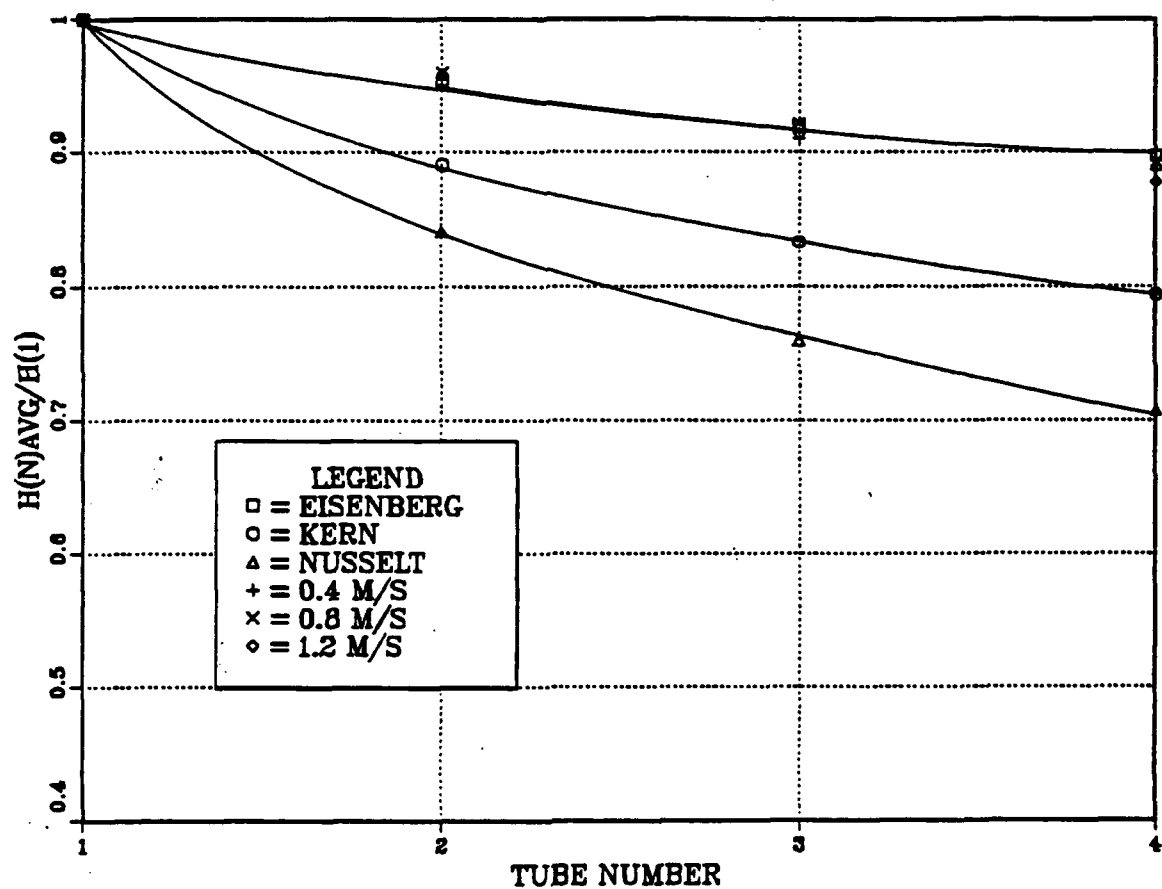


Figure 78. Average  $h$ , wire wrapped KORODENSE, expt. 2.

## HEAT TRANSFER COEFFICIENT

KD11, 0.049" WIRE, KORODENSE

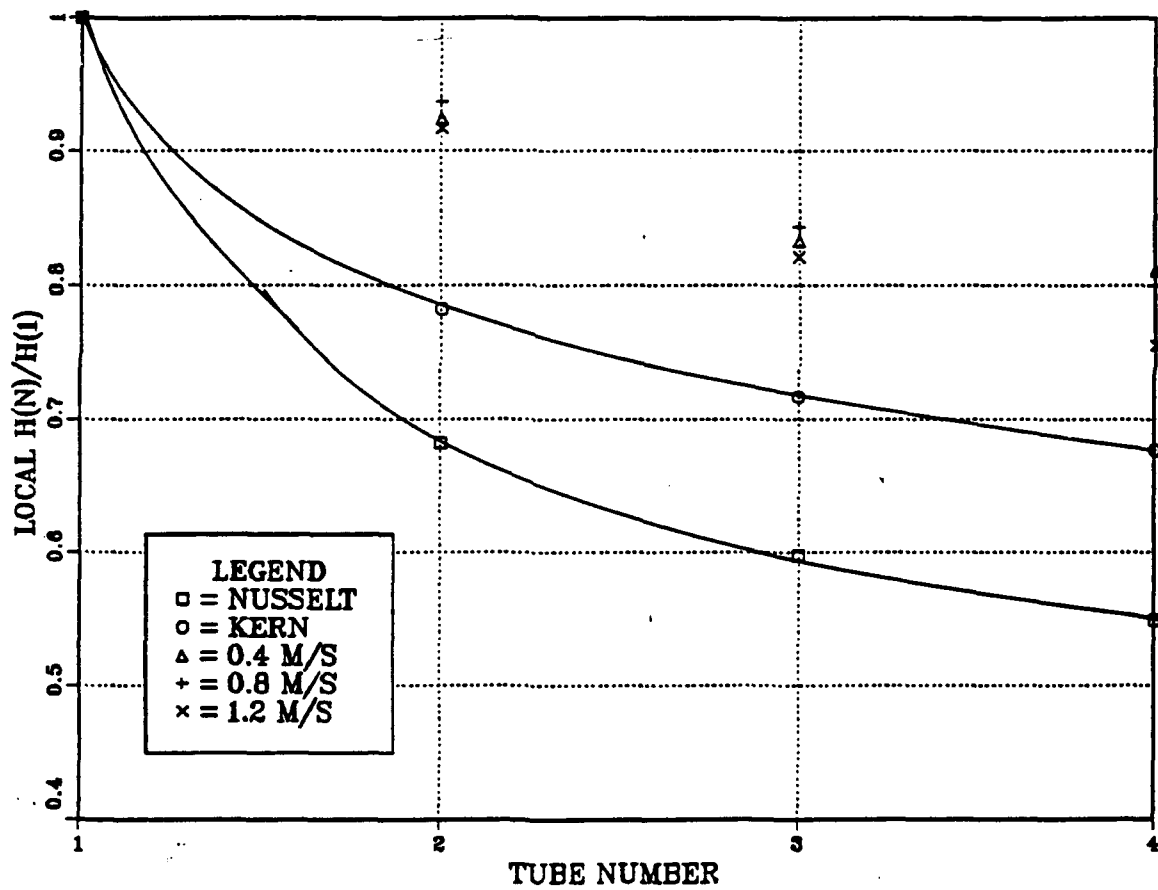


Figure 79. Local  $h$ , wire wrapped KORODENSE, expt. 1.

# HEAT TRANSFER COEFFICIENT

KD12, 0.049" WIRE, KORODENSE

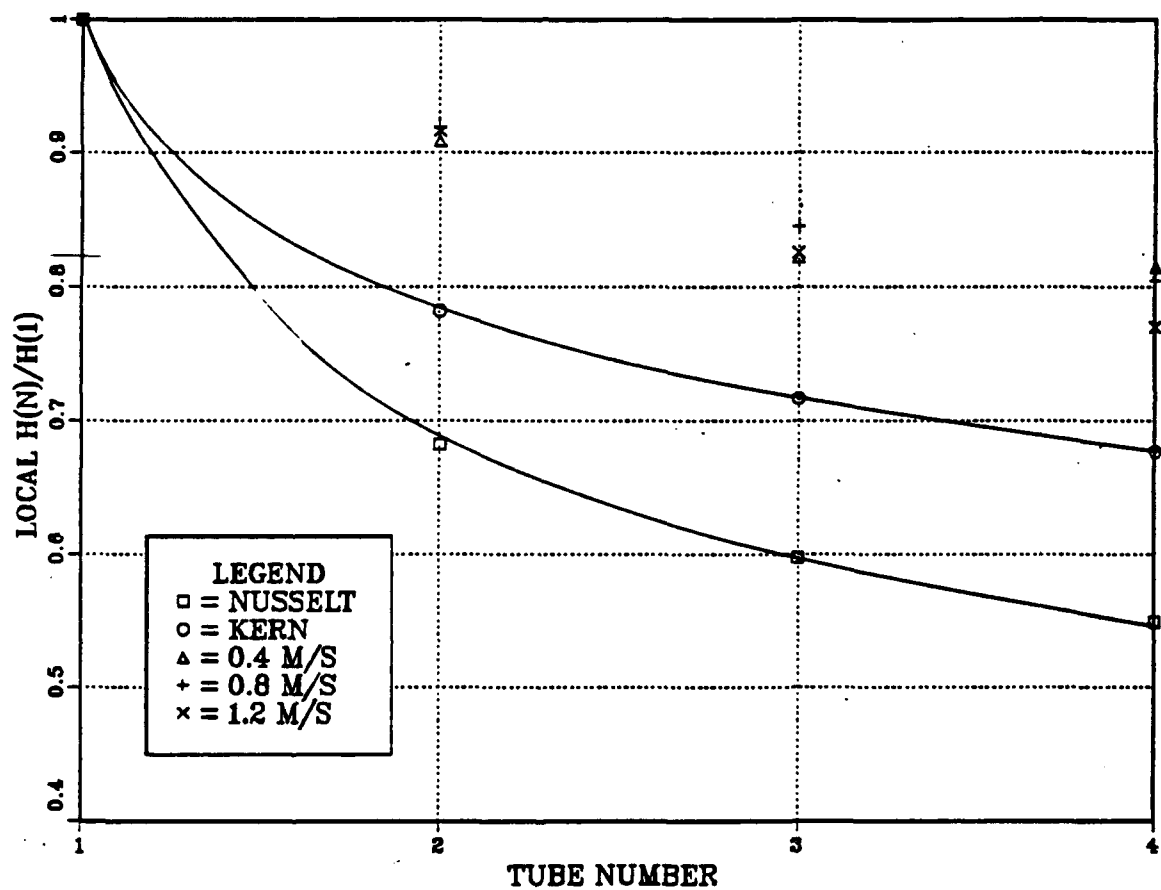


Figure 80. Local  $h$ , wire wrapped KORODENSE, expt. 2.

# HZERO COPPER/NICKEL FIN TUBES

CF03, R-113, TAPE INSERT, BUNDLE

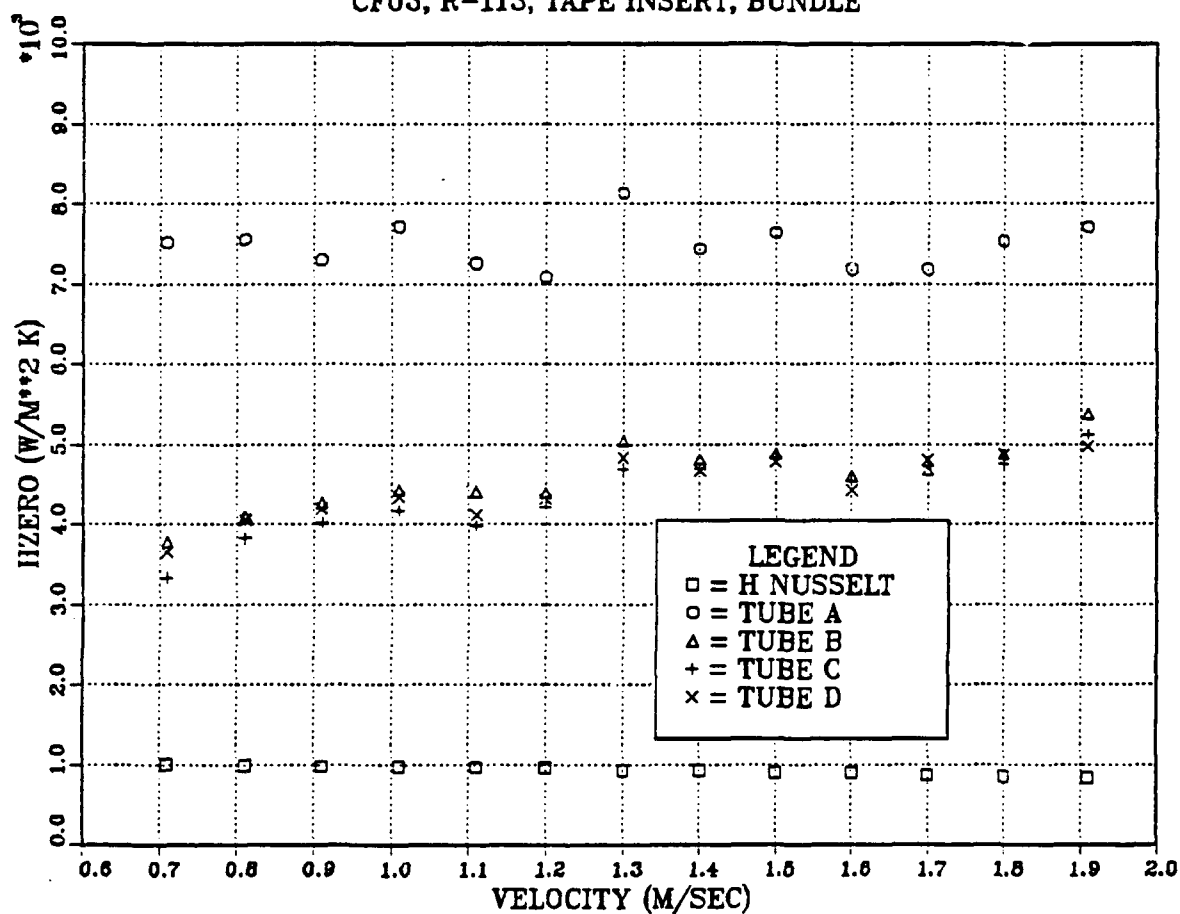


Figure 81.  $h_c$  for copper/nickel finned tubes, tape insert.



# HZERO COPPER/NICKEL FIN TUBES

CF04, R-113, HITRAN, BUNDLE

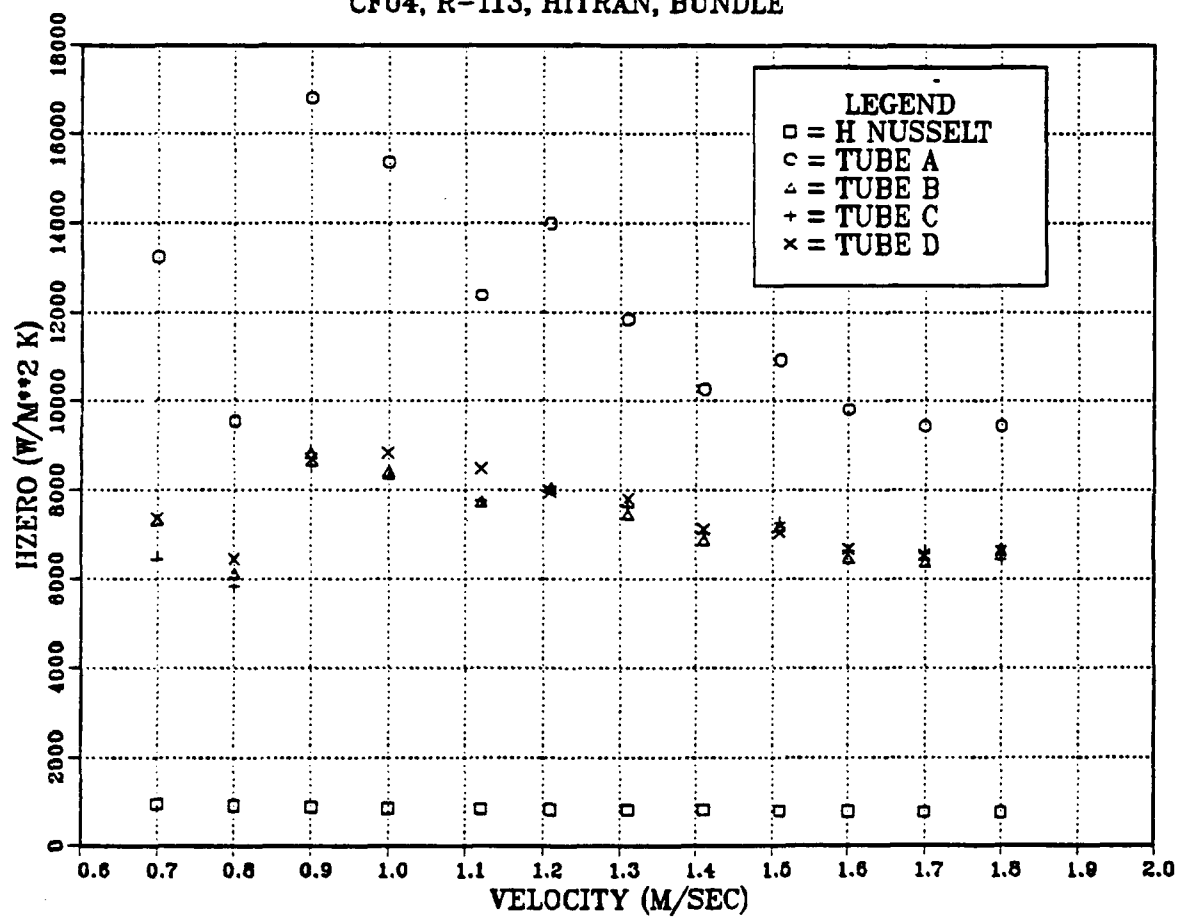


Figure 82.  $h_c$  for copper/nickel finned tubes, HEATEX insert.

copper tubes, the values lay between the Kern and Eissenberg estimates. The plain KORODENSE tubes had values similar to those for the smooth copper tubes while the 0.049" wire-wrapped KORODENSE had values which matched estimates based on Eissenberg's model. The copper/nickel finned tubes, on the other hand, had values which were between the Kern and Nusselt estimates. Since the lower the values the more condensate effect present, this data would imply that the effect of inundation is worse on the finned tubes and least on the wire-wrapped tubes. If the data for the local heat transfer coefficients is analyzed in a similar manner, the same conclusions are reached.

The wire wrapped KORODENSE tubes have the least effect of condensate inundation presumably because the wire serves to create a low pressure area at the base of the wire. This causes condensate to be pulled along the tube which enhances heat transfer. The values for the finned tubes are not in agreement with those of Honda et al. [Ref. 42]. These investigators found that the degree of inundation effect was substantially less than that reported here. There are two apparent reasons for this. The pitch-to-diameter ratio used by Honda et al. was 1.37 whereas in the present study it is 2.25. This difference may cause differences in the way condensate drains from one tube onto another. Alternatively, the correlations used to determine the heat transfer coefficient may be suspect. Hong and Bergles [Ref. 47] have reported that their correlation for the twisted tape has an uncertainty of about 15%. Therefore, it is possible that the large effect of condensate inundation is due more to uncertainty in the correlations than to a real phenomenon.

In order to assess the validity of the data obtained on the copper/nickel finned tubes, a comparison was made with the model of Beatty and Katz [Ref. 13]. In order to do this comparison, the fin efficiency had to be determined using equations from Incropera and DeWitt [Ref. 55]. It was assumed that the fins could be approximated as rectangular fins with adiabatic tips. The fin efficiency was then approximated by:

$$\eta_f = \frac{\tanh(mL_c)}{mL_c} \quad (6-1)$$

According to Incropera and DeWitt, the term  $mL_c$  can be approximated by [Ref. 55]:

$$mL_c = \left( \frac{2h}{kA_p} \right)^{\frac{1}{2}} L_c^{\frac{3}{2}} \quad (6-2)$$

# HEAT TRANSFER COEFFICIENT

CU/Ni FINNED TUBES, TAPE INSERT

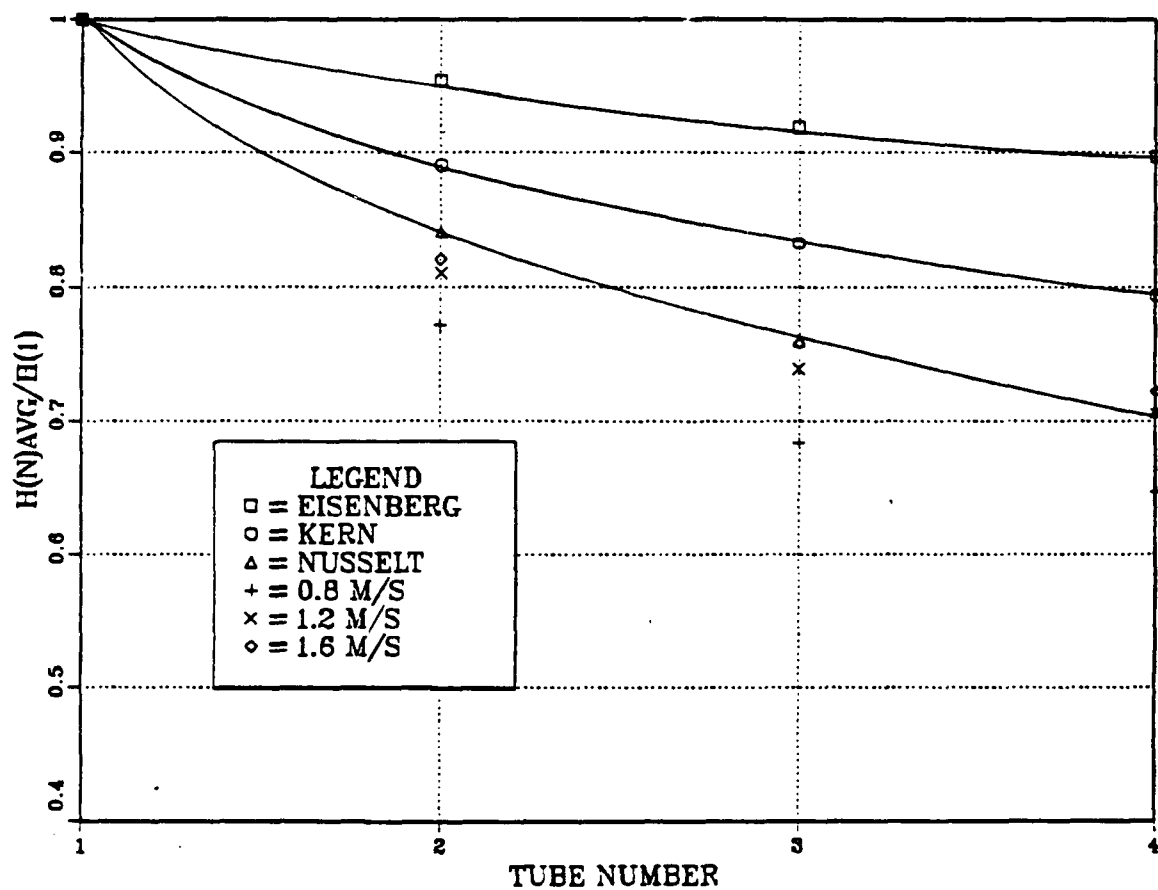


Figure 83. Average  $h$ , for Cu/Ni finned tubes, tape insert.

# HEAT TRANSFER COEFFICIENT

CU/Ni FINNED TUBES, HEATEX

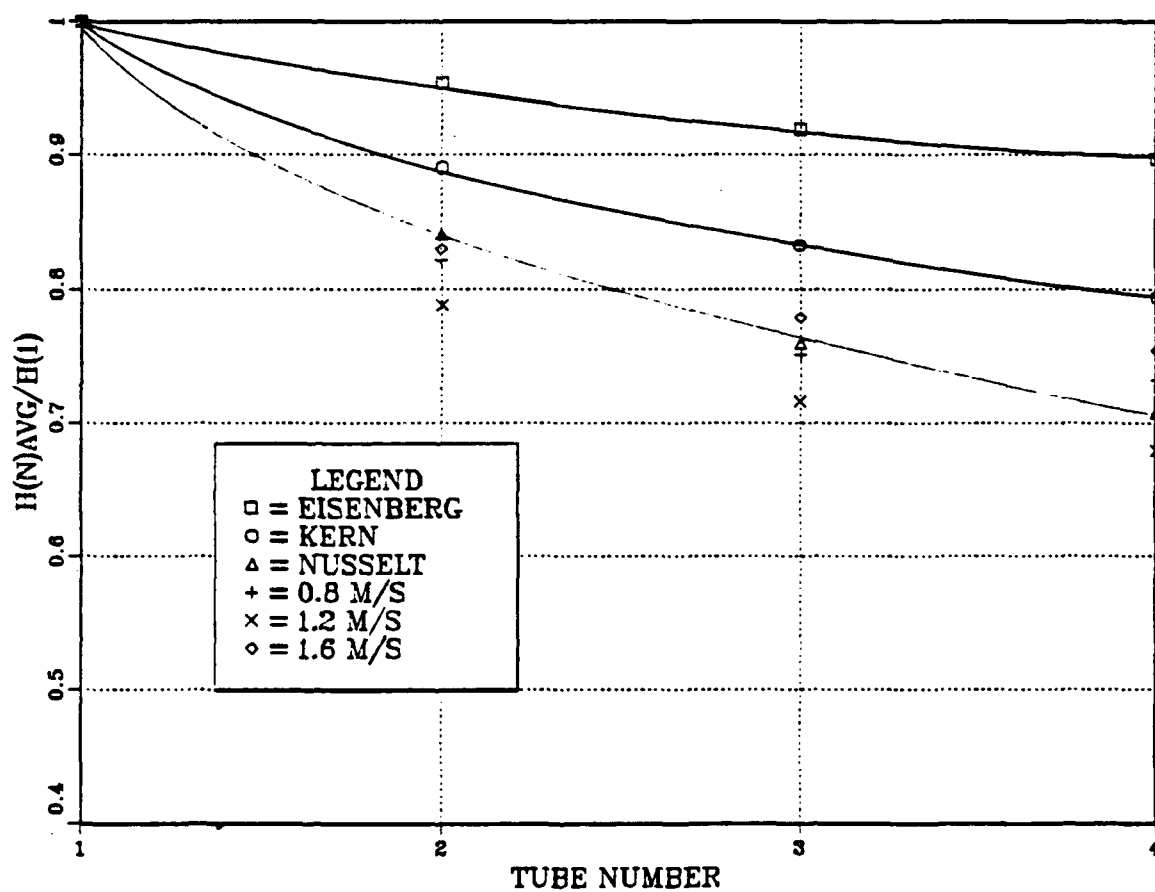


Figure 84. Average  $h$ , for Cu/Ni finned tubes, HEATEX insert.

# HEAT TRANSFER COEFFICIENT

CU/Ni FINNED TUBES, TAPE INSERT

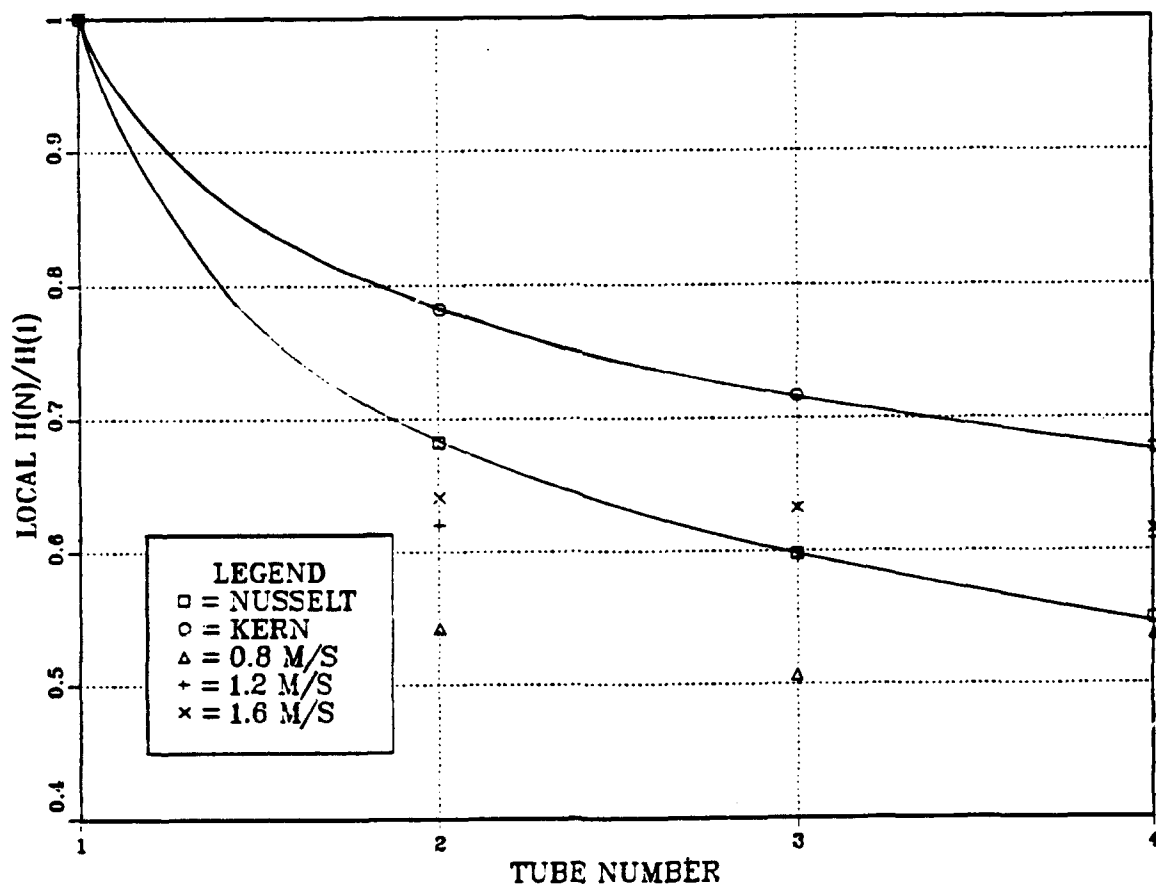


Figure 85. Local  $h$ , for Cu/Ni finned tubes, tape insert.

# HEAT TRANSFER COEFFICIENT

CU/NI FINNED TUBES, HEATEX

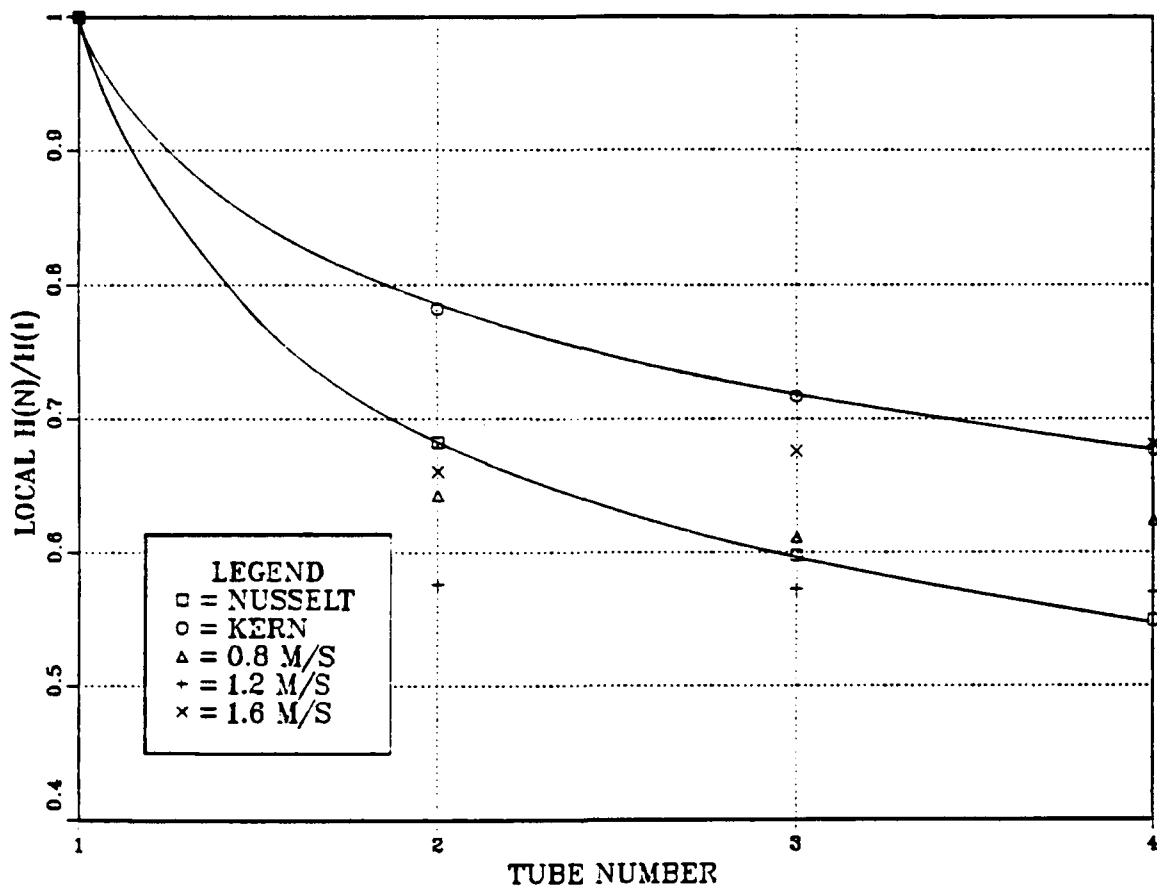


Figure 86. Local  $h$ , for Cu/Ni finned tubes, HEATEX insert.

where  $L_c$  is defined as:

$$L_c = L + \frac{t}{2} \quad (6-3)$$

Here,  $L$  is defined as the height of the fin and  $t$  is the fin thickness. The term  $A_p$  is defined as:

$$A_p = L_c t \quad (6-4)$$

In order to calculate a value for the fin efficiency,  $\eta_f$ , an iterative procedure was used. First, a value for  $h$  was guessed. Based on this value,  $\eta_f$  was calculated using equation (6-1). An effective area was then calculated from the following equation (Marto [Ref. 3]):

$$A_{ef} = \eta_f A_{fs} + \eta_f A_{ft} + A_u \quad (6-5)$$

where  $A_{fs}$  is the surface area of the fins sides,  $A_{ft}$  is the surface area of the fin tips and  $A_u$  is the interfin surface area. Using these values, the effective diameter,  $D_e$ , was determined from (Marto [Ref. 3]):

$$\left[ \frac{1}{D_e} \right]^{0.25} = 1.30 \eta_f \frac{A_{fs}}{A_{ef}} \frac{1}{\bar{L}^{0.25}} + \eta_f \frac{A_{ft}}{A_{ef}} \frac{1}{D_o^{0.25}} + \frac{A_u}{A_{ef}} \frac{1}{D_r^{0.25}} \quad (6-6)$$

where  $\bar{L}$  is defined as:

$$\bar{L} = \frac{\pi(D_o^2 - D_r^2)}{4D_o} \quad (6-7)$$

The heat transfer coefficient is then calculated from a modified version of the Beatty and Katz model (Eq. 2-2) which uses heat flux rather than the film temperature difference,  $\Delta T$ .

$$h_o = .6085 \left( \frac{k^3 \rho^2 g h_{fg}}{\mu D_e q''_o} \right)^{\frac{1}{3}} \quad (6-8)$$

The results of these calculations for the copper/nickel finned tubes with the tape inserts are shown in Figure 87. In this figure, the values of  $h_o$  predicted from the Beatty and Katz model have been expressed in terms of the smooth tube area, that is  $\pi d_s L$ . Also note that values for  $h_o$  have been calculated for copper, copper/nickel and titanium. It is important to note that the raw data lies below the predicted values for copper/nickel

finned tubes. The data obtained after reprocessing with the modified Wilson plot procedure lies somewhat above the prediction. However, both lie within  $\pm 20\%$  which is within the range of validity for the Beatty and Katz model. Therefore, it would appear that the data obtained in the present study for the copper/nickel finned tubes with the tape inserts are reasonable.

The results for the copper/nickel finned tubes with the HEATEX elements installed are not as good. These results are shown in Figure 88. This figure shows the tremendous amount of scatter in the data irrespective of whether the raw data or the data obtained from the modified Wilson plot procedure is used. In either case, it is apparent that the data do not match values predicted from the model of Beatty and Katz. The only difference in these two experiments is the type of insert used. The values for  $h_o$  are based on an experimentally determined value for  $U_o$  and a value for  $h_i$  which is obtained from a correlation. In this study, the correlations for the HEATEX elements were based on empirical data supplied from the manufacturer. This data was obtained on smooth copper tubes having the same diameter as the copper/nickel finned tubes used in this study. Another point which must be considered is that the range of velocity for which the empirical data was supplied was from 0.2 to 1.2 m/s. However, for the copper/nickel finned tubes used in this study, a coolant velocity of 0.7 to 2 m/s was used. These factors would suggest that the correlation used for the small diameter HEATEX element is in error. Further research will have to verify whether or not this is the case.

#### D. IMPLICATIONS OF PRESENT WORK

This study used R-113 as the refrigerant and a refrigerated ethylene glycol/water mixture as the coolant. However, Naval refrigeration systems use R-114 for the refrigerant and sea water as the condensing medium. Therefore, one must ask whether the results obtained from the present work can be extended to Naval applications. In order to perform the following analysis, the dimensions of the smooth copper tubes and copper/nickel finned tubes (26 fpi) used in this study were assumed. The inside heat transfer coefficient was calculated using the Dittus-Boelter correlation. For the smooth tubes,  $h_o$  was calculated using the Nusselt equation, modified to use heat flux rather than the film temperature difference,  $\Delta T$ . For the finned tube,  $h_i$  was again calculated using the Dittus-Boelter correlation. However,  $h_o$  was calculated using the modified Beatty and Katz equation (Eq. 6-8). The fin efficiency was assumed to be 1.0. The condenser design parameters were modeled after the requirements for the DDG-51. Hence, the refrigeration load was fixed at 242.7 tons. The number of condenser tubes was fixed at 340 tubes. Coolant inlet temperature was assumed to be 65 F (18.3 C) while the saturation temperature of R-114 was 107.8 F (42.1 C). The coolant velocity was held constant at 2 m/s.



# HEAT TRANSFER COEFFICIENT

CU/NI FINNED TUBES, TAPE INSERT

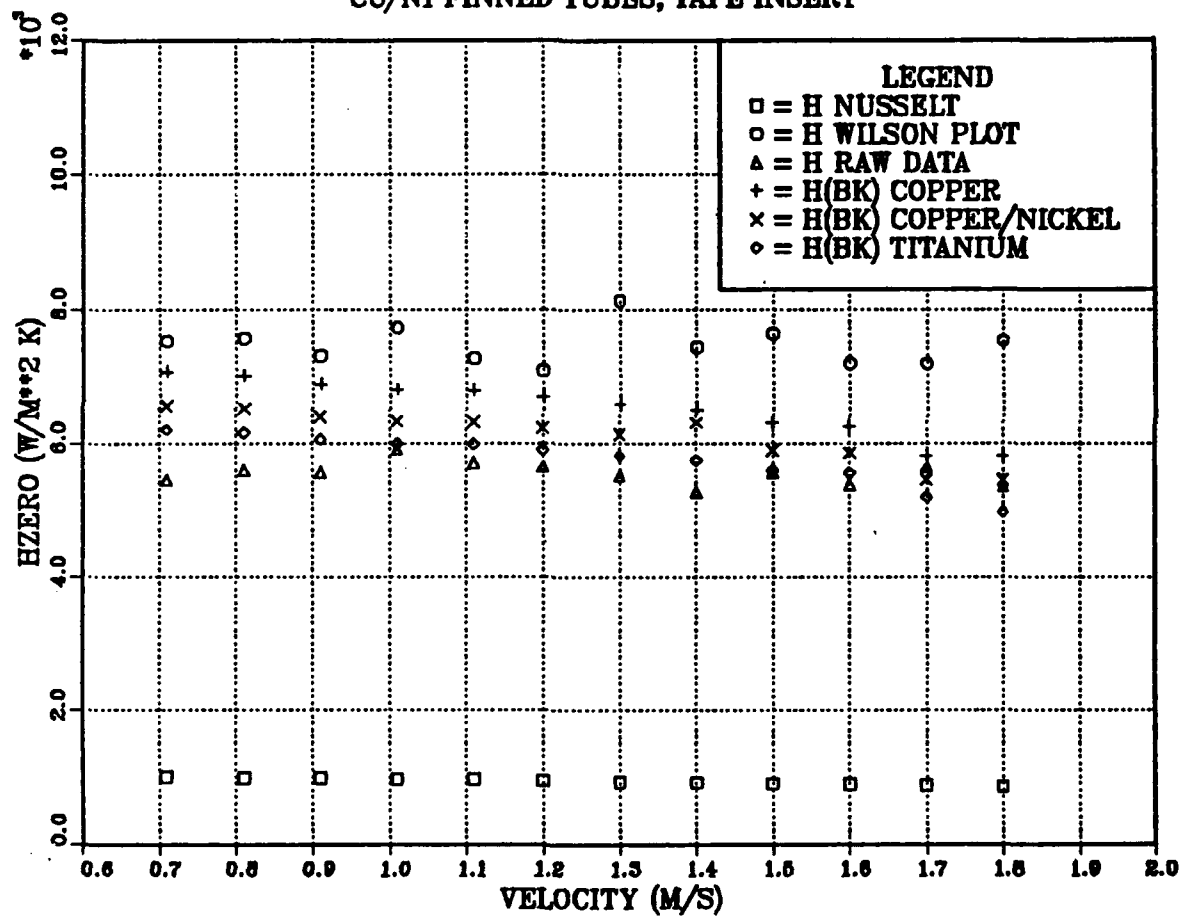


Figure 87. Experimental data (tape insert) vs. Beatty/Katz model.

# HEAT TRANSFER COEFFICIENT

CU/NI FINNED TUBES, HEATEX

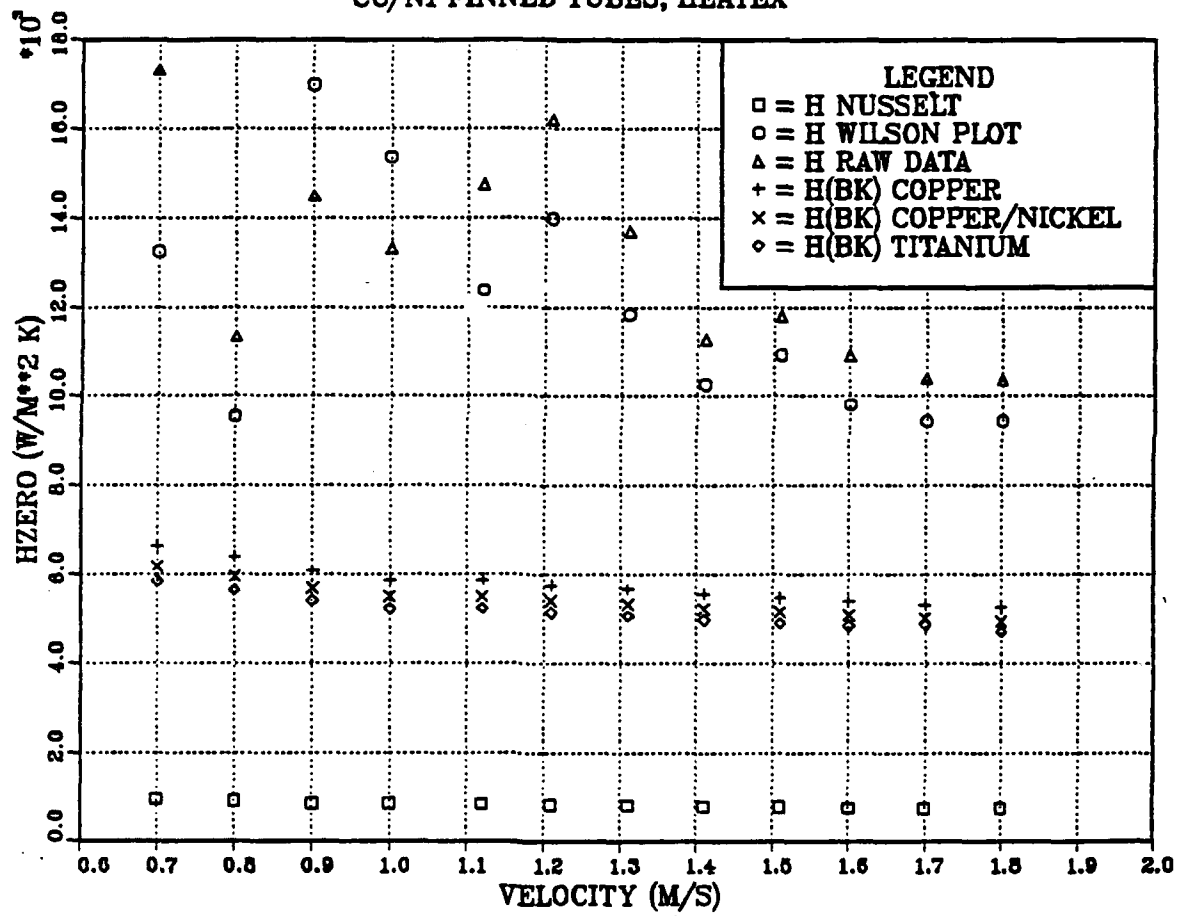


Figure 58. Experimental data (HEATEX insert) vs. Beatty/Katz model.

Ratios of the surface areas for finned to smooth tube and a finned KORODENSE tube to smooth tube were calculated. In order to carry out this calculation for the KORODENSE tube, some type of correlation must be used to calculate  $h_i$ . However, as shown by Cunningham and Ben Boudinar [Ref. 56] in their work on steam condensation on roped tubes, the enhancement due to the roping depends upon the type of groove cut into the tube. In this analysis, an enhancement of 1.6 for  $h_i$  was assumed for the KORODENSE tube over the finned tube. Once the area ratio is obtained, a condenser tube length can be calculated. This is done as follows. The area ratio can be expressed in terms of length by:

$$\frac{A_{o,f}}{A_{o,s}} = \frac{Na_f L_f}{Np i d_o L_s} \quad (6-9)$$

where  $A_{o,f}$  is the area of the finned tube,  $A_{o,s}$  is the area for the smooth tube, and  $N$  is the number of tubes. The term  $a_f$  is given by:

$$a_f = (A_f + A_o)N \quad (6-10)$$

where  $A_f$  and  $A_o$  are the finned and unfinned areas respectively.

Table 3 shows the results of this calculation. For the finned tube, the area ratio of 1.75 leads to a decrease in the condenser length of about 50%. On the other hand, if a roped KORODENSE tube could be manufactured which had fins on the outside surface, the reduction in length of the condenser tubes would be 58%. This could lead to even greater weight savings for refrigeration systems.

**Table 3. SUMMARY OF AREA RATIO CALCULATIONS**

	Smooth tube	Finned Tube	KORODENSE + Fins
$\frac{A_{o,f}}{A_{o,s}}$	1.0	1.75	1.51
$\frac{L_f}{L_s}$	1.0	0.497	0.42

## VII. CONCLUSIONS

The following conclusions can be made based on the results obtained in this study.

### A. GENERAL

1. The condenser/evaporator test platform is fully operational and shows no signs of the contamination problems reported by Mabrey [Ref. 2 ].
2. Values for outside heat transfer coefficient obtained using smooth copper tubes appear to be reasonable and agree with other published data.

### B. OVERALL HEAT TRANSFER COEFFICIENT

1. KORODENSE tubes provide enhancements of 6 to 8% over smooth copper tubes regardless of the type of insert used.
2. For the KORODENSE tubes used in this study, wire wrapping results in an enhancement in heat transfer.
3. The optimal pitch-to-wire diameter was about 7 for the KORODENSE tubes used in the present work.
4. Wrapping the KORODENSE tubes with 0.049" diameter wire resulted in an enhancement of 16% over the non wire-wrapped KORODENSE tubes and a 22 to 24% enhancement over the smooth copper tubes.
5. Copper/nickel finned tubes (26 fpi) yielded a doubling of the heat transfer in comparison to smooth copper tubes.
6. The use of HEATEX radial mixing elements yielded a 10 to 15% increase in comparison to the use of twisted tape inserts.

### C. OUTSIDE HEAT TRANSFER COEFFICIENT

1. The smooth tubes yielded values of  $h_o$  which were 7 to 15% below those estimated from Nusselt theory.
2. The KORODENSE tubes gave values of  $h_o$  which were about 15% greater than those estimated from Nusselt theory and approximately 25% greater than values obtained for the smooth copper tubes.
3. Wrapping the KORODENSE tube with 0.049" diameter wire resulted in a 90% increase in the outside heat transfer coefficient in comparison to the smooth copper tubes.
4. The copper/nickel finned tubes yielded a 7 fold increase in  $h_o$  over the smooth copper tubes.

### D. EFFECTS OF CONDENSATE INUNDATION

1. For smooth copper tubes, condensate inundation resulted is a 15 to 18% decrease in  $h_o$  for the second tube compared to the top tube.

2. KORODENSE tubes showed a 20% decrease in  $h_o$  for this same comparison.
3. Wrapping the KORODENSE tubes with 0.049" diameter wire resulted in a decrease of only 5 to 10% in  $h_o$  for the second tube compared to the top tube.
4. For the copper/nickel finned tubes, condensate inundation resulted in almost a 35% decrease in  $h_o$  for the second tube relative to the top tube. This large decrease is presumably due to uncertainty in the correlations used to determine the heat transfer coefficient.

## VIII. RECOMMENDATIONS

Based on the results of this study, the following recommendations are made:

### A. GENERAL RECOMMENDATIONS

1. The ball valves which control coolant flow to the flowmeters should be replaced with needle valves. This will provide better control of coolant flow.
2. The flowmeters should be replaced with larger capacity meters. This will allow investigation of heat transfer at higher coolant velocities and therefore higher condensation rates. This change will have to be accompanied by an increase in the diameter of the coolant return header in order to accommodate the increased coolant flow.
3. Extra lines from the top ends of the condenser to the cold trap need to be added. This will ensure that no isolated pockets of noncondensibles exist in the condenser.

### B. EXPERIMENTAL RECOMMENDATIONS

1. The correlation for the small diameter HEATEX element must be re-investigated. This may require obtaining additional data from CAL GAVIN or designing an experiment at the Naval Postgraduate School which can be used to obtain the required data.
2. The correlation used for the twisted tape insert also needs to be re-evaluated in light of the large inundation effects. As with the HEATEX, this may require that additional experiments be carried out at the Naval Postgraduate School.
3. Once a reliable correlation is obtained, the experiments conducted on the copper/nickel finned tubes need to be repeated.
4. Experiments need to be conducted using both titanium finned tubes as well as titanium KORODENSE tubes. This data can then be compared to that obtained with the copper/nickel finned tubes and the copper/nickel KORODENSE tubes to determine whether titanium tubes can deliver the required performance.
5. Smooth copper tubes should be wrapped with different wire diameters at different pitches in order to determine an optimal pitch-to-wire diameter ratio.
6. Experiments need to be conducted on wire wrapping of KORODENSE tubes which have a different pitch. These experiments should be based on results obtained from the smooth copper tube experiments.
7. Experiments need to be repeated using R-114 and possible alternate refrigerants that the Navy is interested in such as R-24.
8. A KORODENSE type tube which is roped on the inside and finned on the outside needs to be developed and tested since calculations have shown that this type of tube can lead to smaller condensers.

## APPENDIX A. FLOWMETER CALIBRATION

The flowmeters used to measure flow through the main condenser tubes were calibrated in the following manner. The meters were disconnected from the condenser tubes. An empty 55 gallon drum was placed on a scale (resolution 0.5 lbs). The condenser pump was started with flow through the bypass.

Flowmeters were calibrated at 0 °C and 24 °C. Each flowmeter was initially opened to maximum flow. The flow was then throttled back to 10%. The weight of fluid in the drum was recorded and the timer started. The weight was then recorded at the end of the calibration time. This procedure was repeated in 10% increments up to 100% flow. Flowmeter number 2 was only calibrated up to 90% flow since a mechanical stop prevented it from going to 100%. The calibration runs were then repeated from the maximum flow back to 10% flow in 10% increments. The mass flow rate was then calculated in kg/sec based on an average of the two readings. The data for the flowmeter calibrations as a function of nominal flow rate are shown in Table 4.

**Table 4. MASS FLOW RATE (KG/SEC) AT 0 AND 24 C.**

Nominal Flow Rate (%)	Flow Meter A		Flow Meter B		Flow Meter C		Flow Meter D	
	0°C	24°C	0°C	24°C	0°C	24°C	0°C	24°C
10	0.0149	0.0172	0.0127	0.0181	0.0141	0.0179	0.0253	0.0318
20	0.0363	0.0403	0.0308	0.0408	0.0374	0.0391	0.0513	0.0613
30	0.0544	0.0621	0.0531	0.0626	0.0566	0.0616	0.0798	0.0894
40	0.0794	0.0851	0.0739	0.0844	0.0793	0.0899	0.1129	0.1216
50	0.1003	0.112	0.0953	0.1102	0.1000	0.1103	0.1406	0.1555
60	0.1179	0.1339	0.1134	0.1295	0.1211	0.1318	0.1728	0.1823
70	0.1388	0.1556	0.1379	0.1506	0.1427	0.1552	0.1975	0.2114
80	0.1563	0.1769	0.1533	0.1715	0.1639	0.1716	0.2261	0.2409
90	0.1846	0.2028	0.1799	0.1912	0.1813	0.1975	0.2461	0.2667
100	0.2019	0.2151			0.2034	0.2183	0.2788	0.2924

A least squares linear regression was performed for each flowmeter at each of the two temperatures for which the calibration runs were carried out. The linear regression equation takes the following form:

$$\dot{m} = a + bN$$

where  $a$  is the y-intercept in kg/s,  $b$  is the slope in kg/s/% and  $N$  is the flowmeter setting in %. The results are shown in Table 5.

**Table 5. FLOWMETER CALIBRATION REGRESSION RESULTS.**

	Flow Meter A		Flow Meter B		Flow Meter C		Flow Meter D	
	0 °C	24 °C	0 °C	24 °C	0 °C	24 °C	0 °C	24 °C
Slope	0.00206	0.00225	0.00204	0.00216	0.00208	0.0022	0.0028	0.0029
Y intercept	-0.00414	-0.00329	-0.00615	-0.00138	-0.0036	-0.00211	-0.00122	0.0048

In order to obtain flowrates at any intermediate temperatures, a simplified interpolation procedure was used. The results of the calibrations for the four flowmeteres are shown in Figure 89, Figure 90, Figure 91, and Figure 92.



## FLOWMETER A

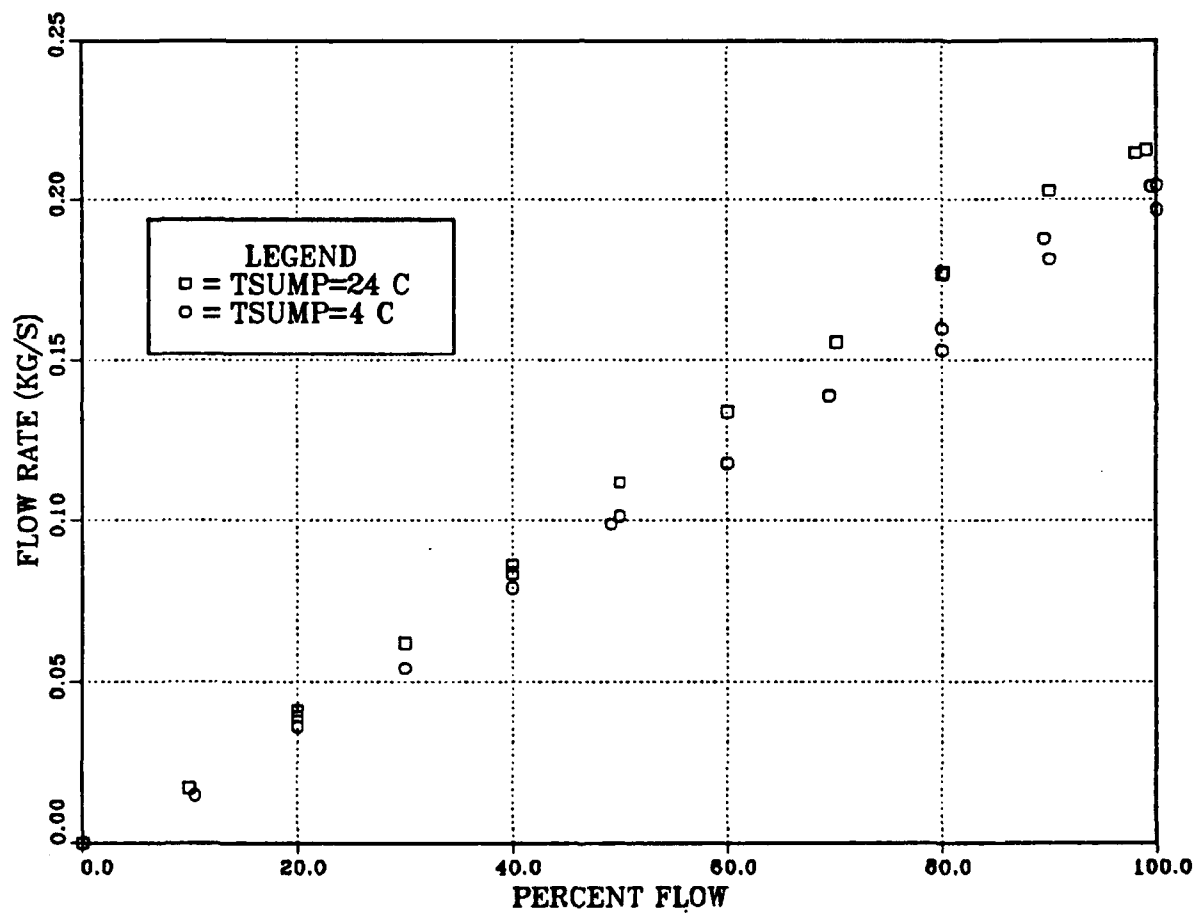


Figure 89. Calibration for flowmeter A.

## FLOWMETER B

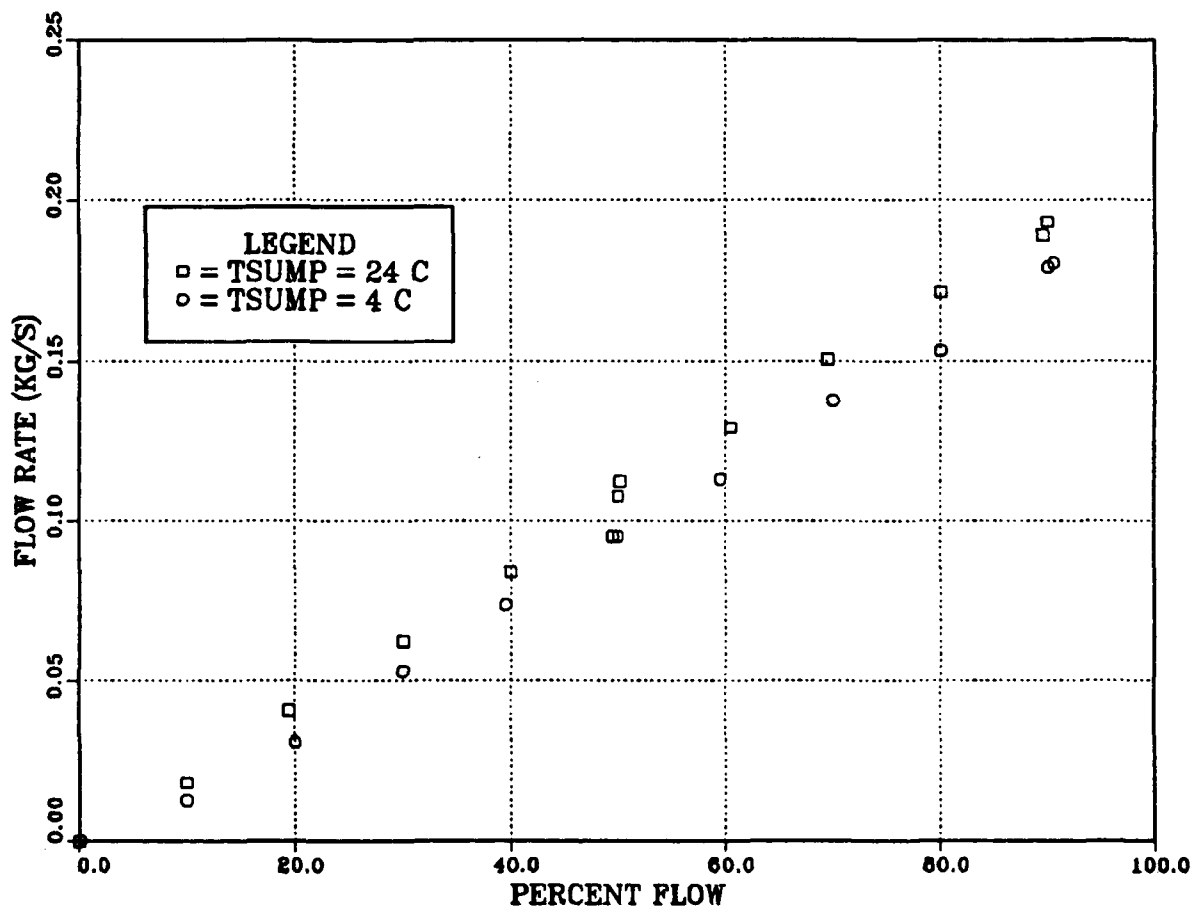


Figure 90. Calibration for flowmeter B.

## FLOWMETER C

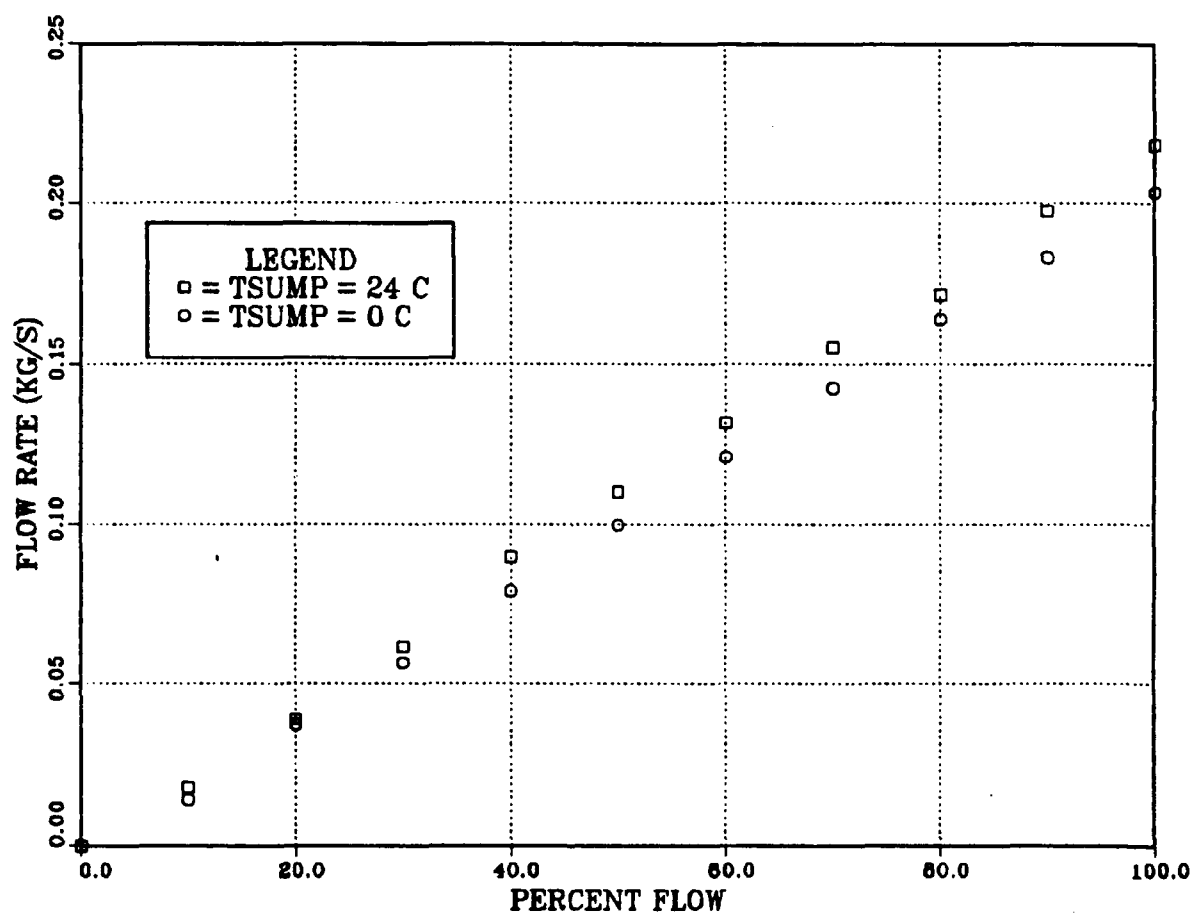


Figure 91. Calibration for flowmeter C.

## FLOWMETER D

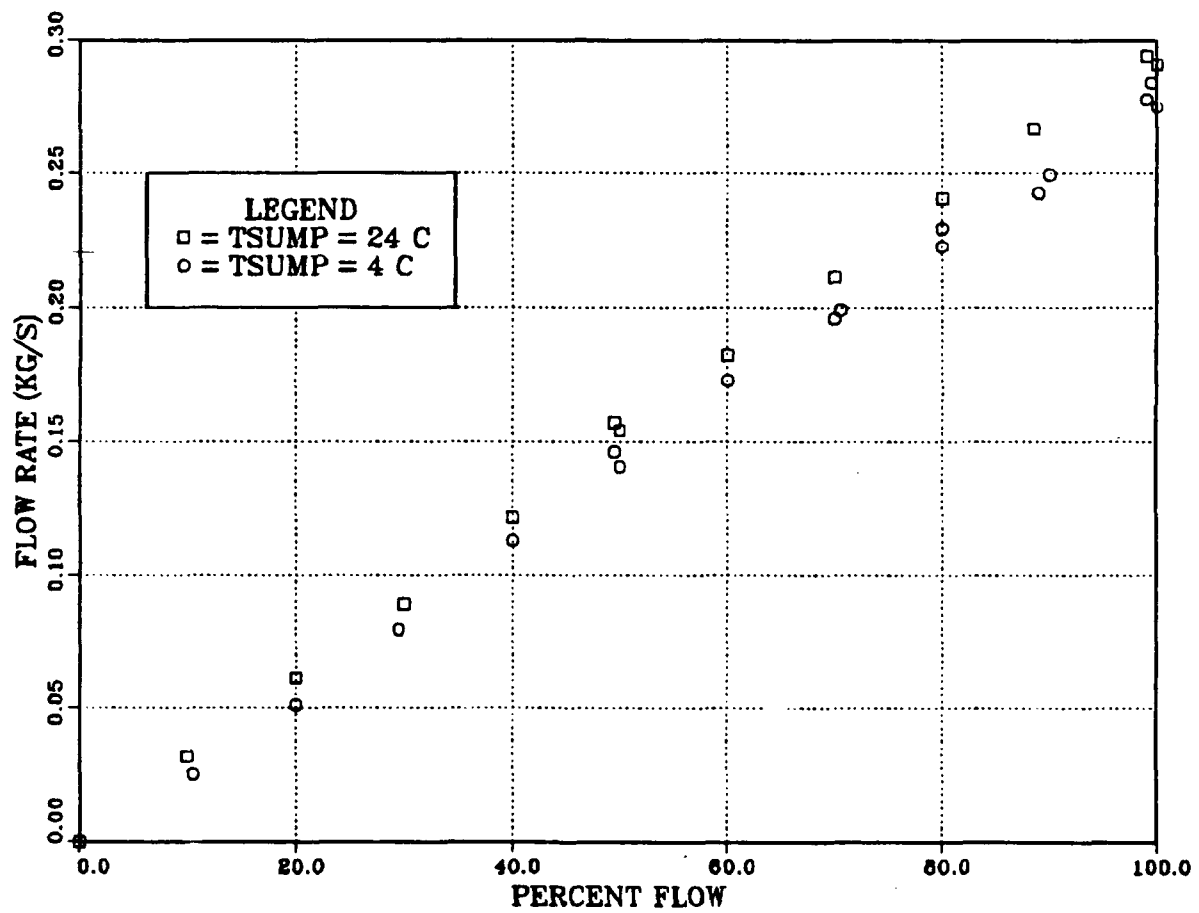


Figure 92. Calibration for flowmeter D.

## APPENDIX B. EMF VERSUS TEMPERATURE

The EMF read from the thermocouples must be converted into a temperature for purposes of calculation. This is accomplished using a 7<sup>th</sup> order polynomial which has the general form:

$$T = C(0) + C(1)V^1$$

where V is the EMF reading in volts, and I has values from 1 to 7. The leading coefficients are given in Table 6.

Figure 93 shows the relationship between EMF and temperature.

Table 6. LEADING COEFFICIENTS FOR CONVERSION OF EMF TO TEMPERATURE.

Leading Coefficient	Value
C(0)	0.10086
C(1)	25727.944
C(2)	-767345.8
C(3)	78025595.8
C(4)	-9247486589
C(5)	$6.977 \times 10^{11}$
C(6)	$-2.66 \times 10^{13}$
C(7)	$3.9 \times 10^{14}$

## EMF VERSUS TEMPERATURE

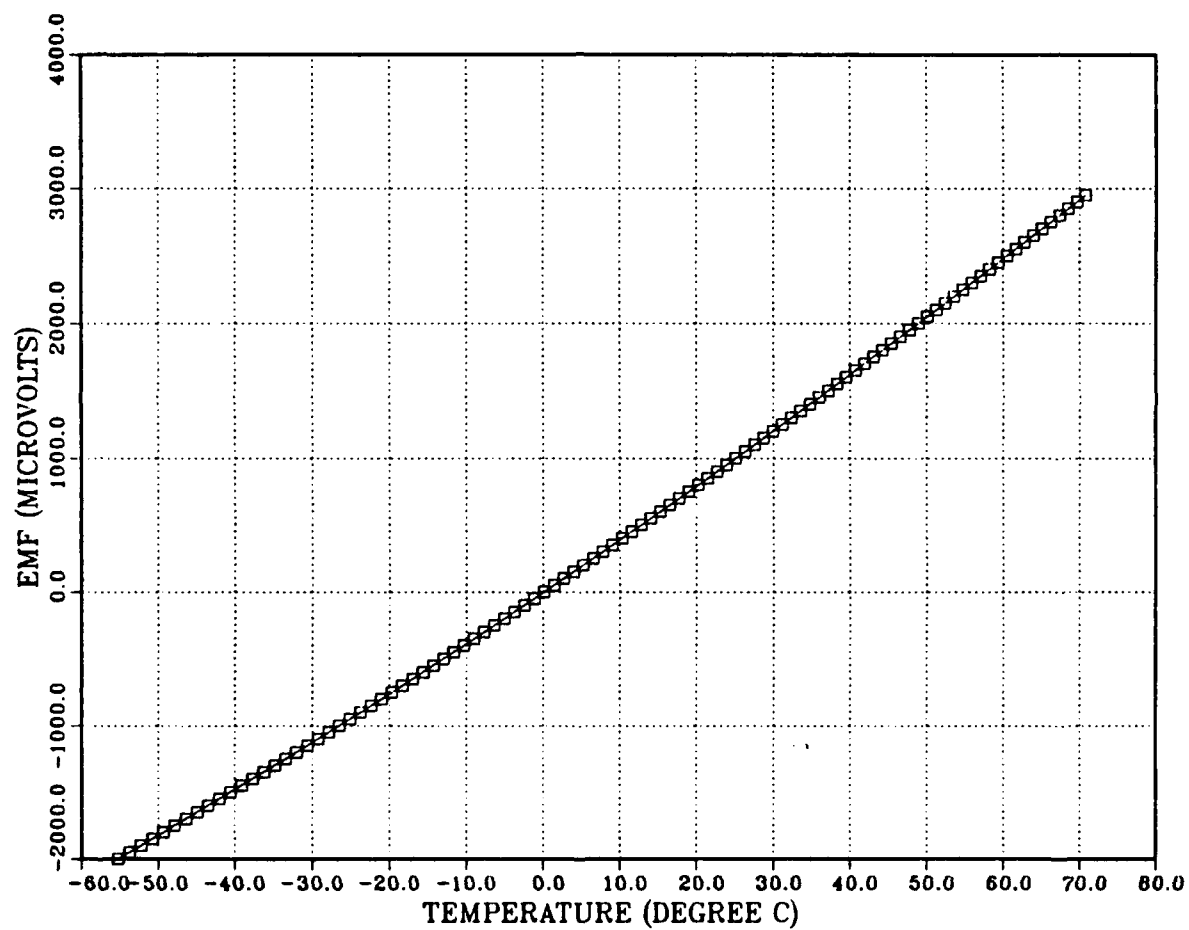


Figure 93. EMF versus temperature.

## APPENDIX C. PROPERTIES OF ETHYLENE GLYCOL/WATER MIXTURE

The physical and thermodynamic properties of the ethylene glycol/water mixture were determined using equations and figures from Cragoe [Ref. 56] and Gallant [Ref. 57].

The density of the ethylene glycol/water mixture is calculated in lines 2490 to 2530 of the computer program. Density as a function of temperature for various concentrations of ethylene glycol are shown in Figure 94.

The kinematic viscosity of the ethylene glycol/water mixture is calculated in lines 2370 to 2420. Figure 95 shows the kinematic viscosity plotted as a function of temperature for various ethylene glycol concentrations.

The heat capacity is calculated in lines 2430 to 2480. Figure 96 is a plot of heat capacity as a function of temperature for different ethylene glycol concentrations.

The thermal conductivity is calculated in lines 2560 to 2610 of the program. Values of the thermal conductivity as a function of temperature are plotted for various ethylene glycol concentrations in Figure 97.

# DENSITY

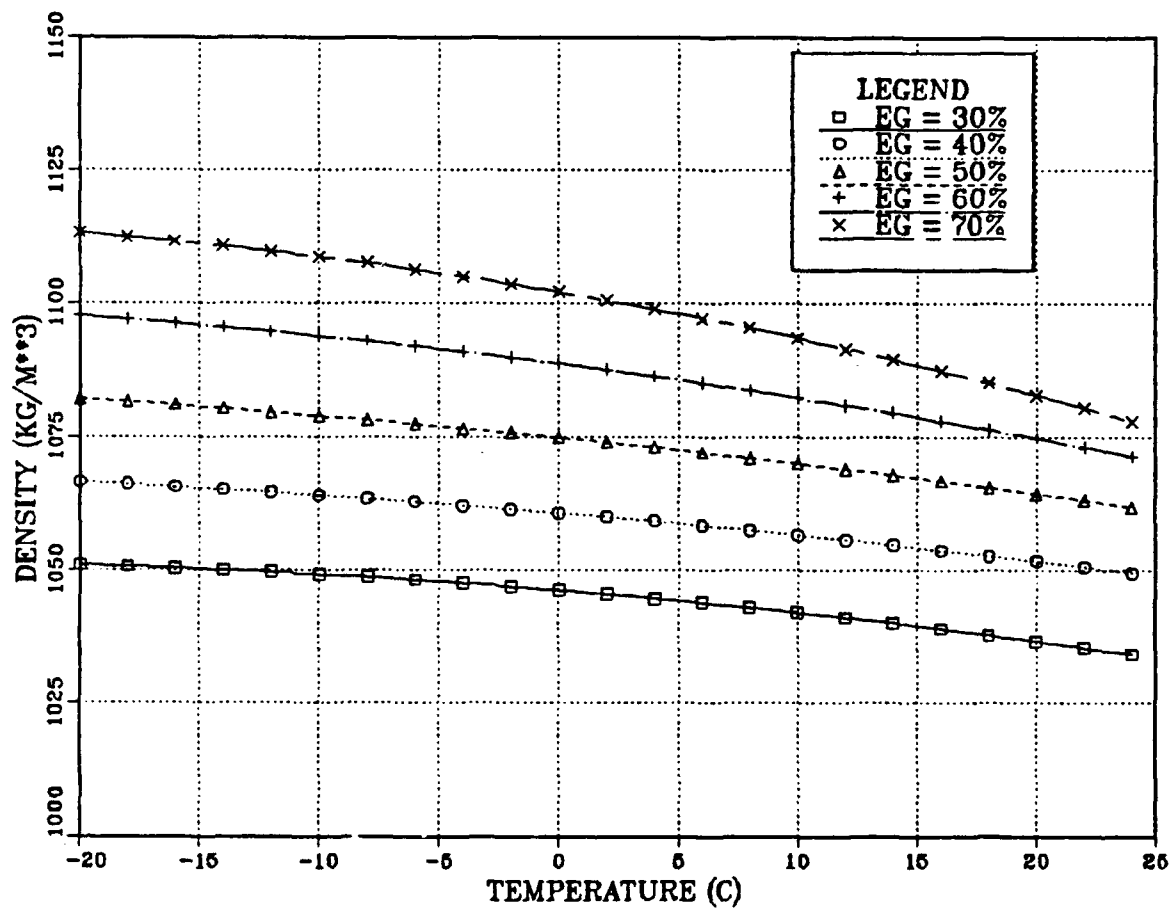


Figure 94. Density of ethylene glycol/water mixture.



## KINEMATIC VISCOSITY

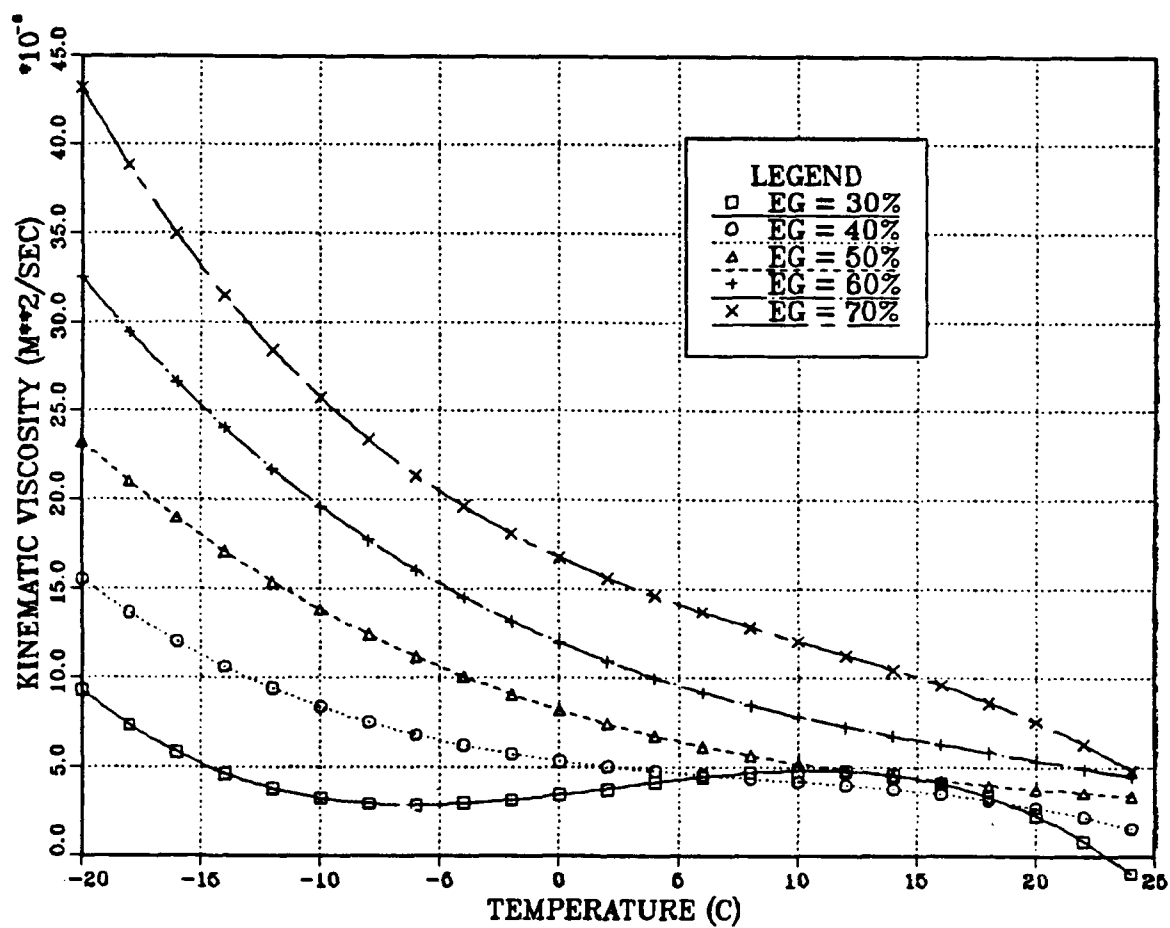


Figure 95. Kinematic viscosity of ethylene glycol/water mixture.

## HEAT CAPACITY

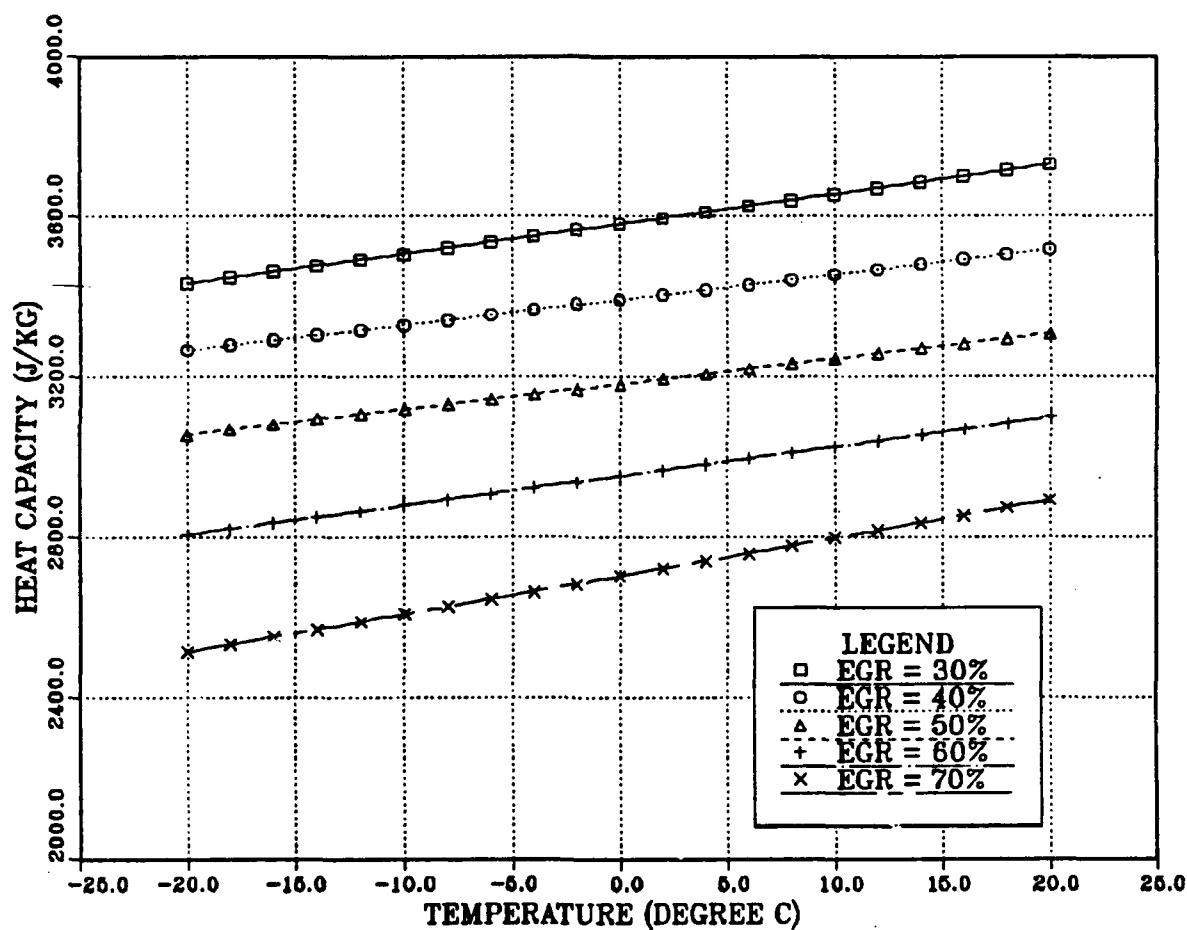


Figure 96. Thermal heat capacity of ethylene glycol/water mixture.

## THERMAL CONDUCTIVITY

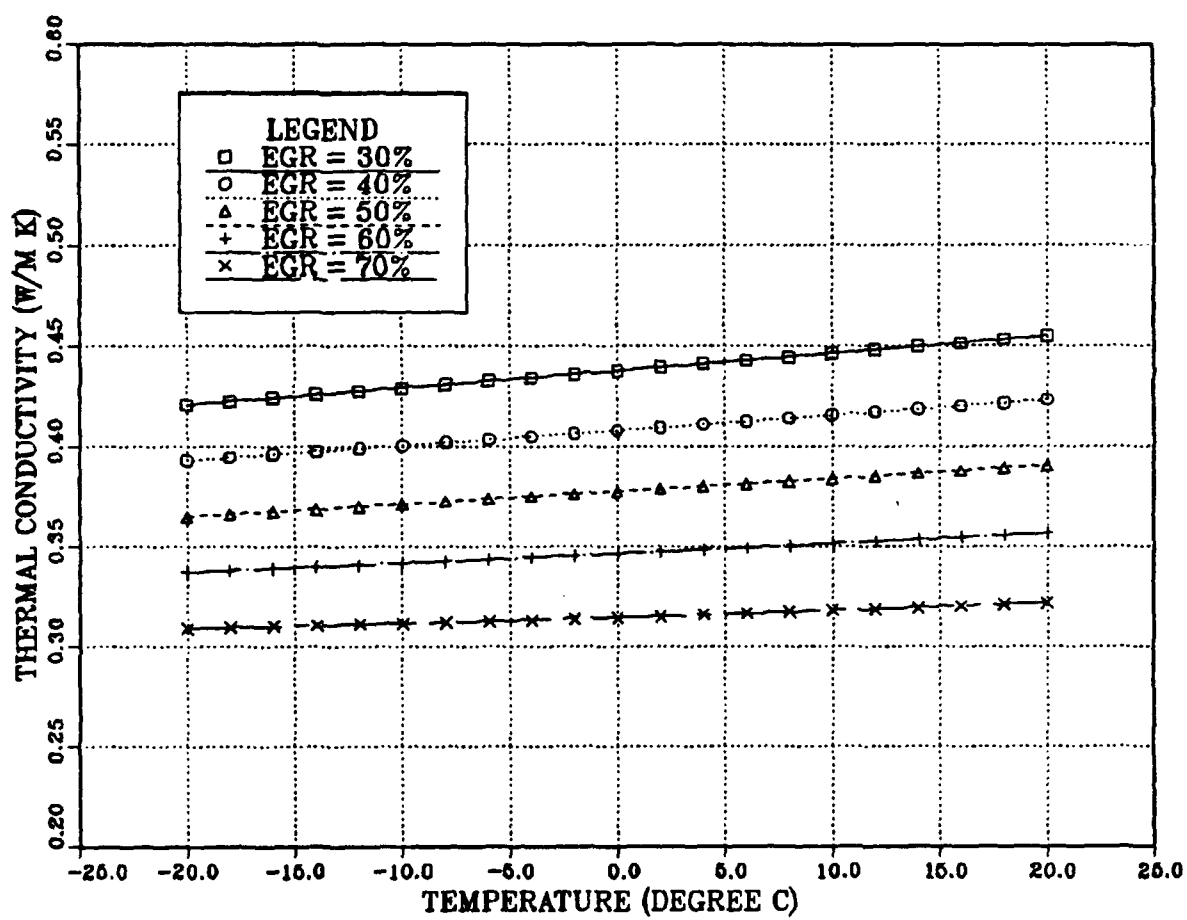


Figure 97. Thermal conductivity of ethylene glycol/water mixture.

## APPENDIX D. PHYSICAL AND THERMODYNAMIC PROPERTIES OF R-113

The physical and thermodynamic properties of R-113 were calculated based on equations supplied by Chapman [Ref. 58].

The heat capacity,  $C_p$ , of R-113 was calculated from the equation:

$$C_p = (929.0 + 1.03T)$$

where  $T$  is in  $^{\circ}\text{C}$  and  $C_p$  is in  $\text{kJ/kg K}$ . Figure 98 shows  $C_p$  as a function of temperature for R-113.

The dynamic viscosity for R-113 is calculated from the equation:

$$\mu = 1.34 \times 10^{-5} \times 10^{\frac{503}{(T-2.15)}}$$

where  $T$  is in  $\text{K}$  and  $\mu$  is given in  $\text{kg/m s}$ . The relationship between  $\mu$  and temperature is shown in Figure 99.

The thermal conductivity of R-113 can be calculated from:

$$k = 1.7308(4.846 \times 10^{-2} - T \times 6.57 \times 10^{-5})$$

where  $T$  is in  $^{\circ}\text{F}$  and  $k$  is in  $\text{W/m K}$ . Figure 100 shows the thermal conductivity as a function of temperature for R-113.

The density of R-113 can be calculated from:

$$\rho = 1.62 \times 10^3 - T \times (2.219 + T \times 2.358 \times 10^{-3})$$

where  $T$  is in  $^{\circ}\text{C}$  and  $\rho$  is in  $\text{kg/m}^3$ . Density of R-113 is shown as a function of temperature in Figure 101.

The latent heat of R-113 can be calculated from the equation:

$$h_{fg} = 2326.1(70.55 - t \times (0.04838 + 1.26 \times 10^{-4}T))$$

where  $T$  is in  $^{\circ}\text{F}$  and  $h_{fg}$  is in  $\text{J/kg}$ . Figure 102 shows the relationship between latent heat and temperature for R-113.

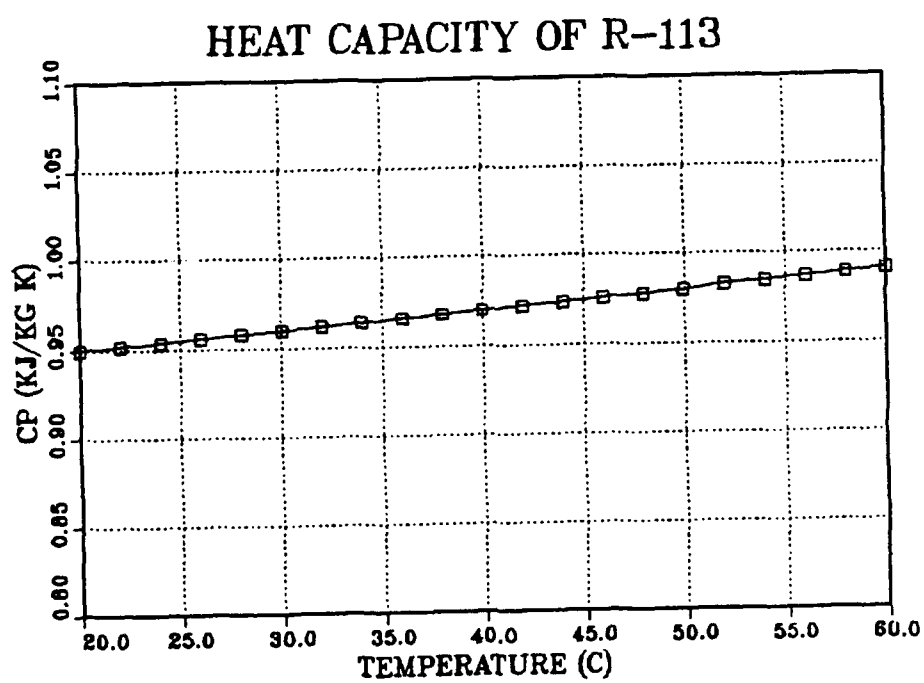


Figure 98. Heat capacity versus temperature for R-113.

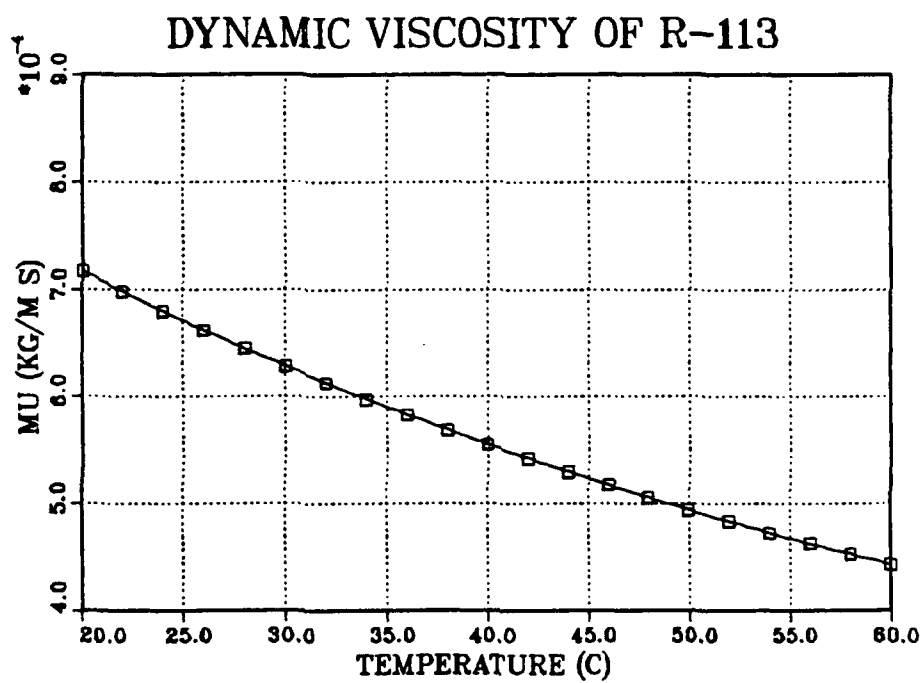


Figure 99. Viscosity as a function of temperature for R-113.

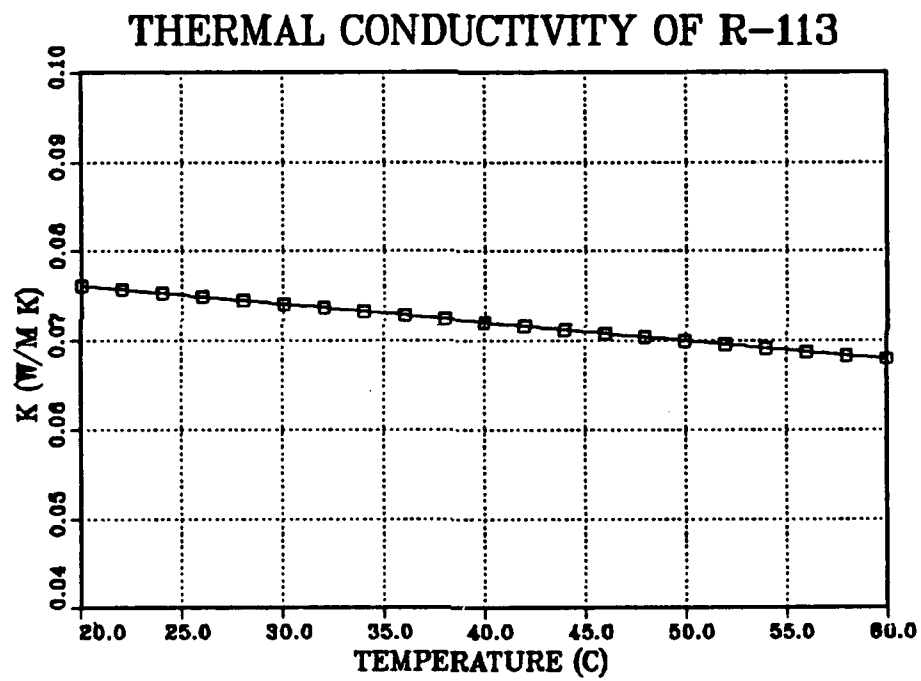


Figure 100. Thermal Conductivity of R-113 as function of temperature.

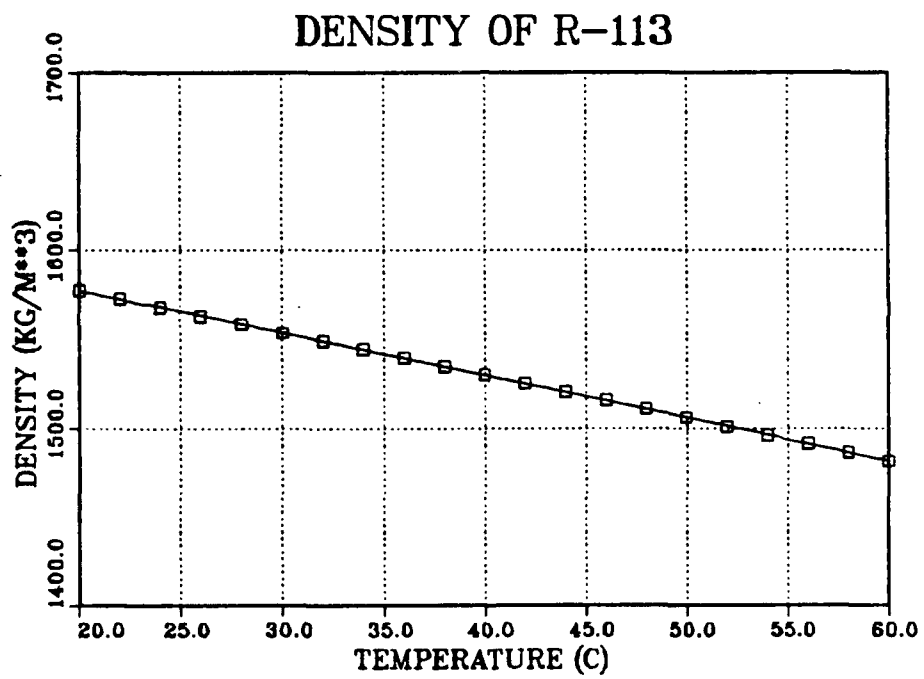


Figure 101. Density as a function of temperature for R-113.



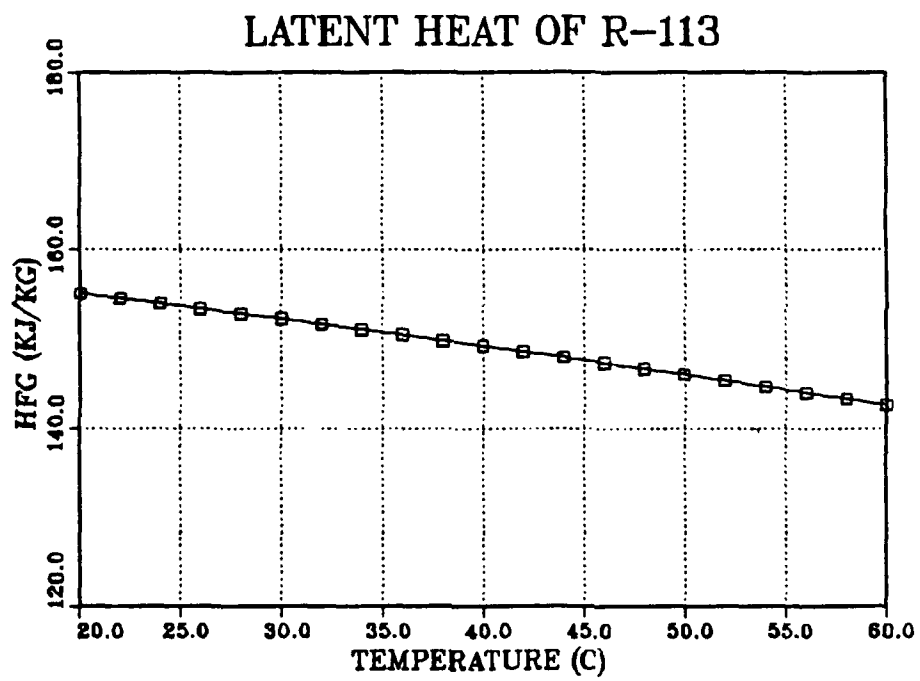


Figure 102. Latent heat versus temperature for R-113.

## APPENDIX E. SAMPLE CALCULATION

A sample calculation was conducted on run 1 of data set SM06. This run was carried out on smooth copper tubes with the HEATEX insert installed. The sample calculation was performed for the top tube only.

Temperatures were recorded as emf's using copper/constantan thermocouples. EMF values were converted to temperatures using the equation shown in Appendix B. Table 7 summarizes the results.

**Table 7. EMF AND TEMPERATURES FOR RUN 1 DATA SET SM06.**

Thermocouple	EMF (microvolts)	Temperature (C)
T(0)	1908	46.83
T(1)	1895	46.54
T(2)	1909	46.86
T(3)	1922	47.16
T(4)	1918	47.06
T(5)	1919	47.099
T(6)	367	9.44
T(7)	369	9.496
T(8)	370	9.52
T(9)	377	9.7
T(10)	893	22.52
T(11)	893	22.53
T(12)	831	20.99
T(13)	831	20.99
T(14)	798	20.18
T(15)	798	20.18
T(16)	853	21.54
T(17)	853	21.54

For tube A, the temperature differential is calculated by:

$$\Delta T = \frac{T(10) + T(11)}{2} - T(6) = 13.086 \text{ C}$$

The average temperature is then calculated from:

$$T_{avg} = T(6) + \Delta T \times 0.5 = 15.98 \text{ C}$$

Based on the ethylene glycol/water mixture physical properties (Appendix C), and using and average temperature of 15.98 C and an ethylene glycol concentration of 54%, the following fluid properties are obtained:

$$\begin{aligned}\rho_c &= 1071.3 \text{ kg/m}^3 \\ \mu_c &= 0.0051 \text{ kg/m s} \\ C_{p,c} &= 3196.99 \text{ J/kg K} \\ k_c &= 0.3742 \text{ W/m k} \\ Pr_c &= 43.57\end{aligned}$$

Based on the calibration curves for flowmeter A, the mass flowrate of coolant corresponding to a setting of 15.74 can be calculated. A simplified interpolation procedure is used to account for temperature differences. Based on this calculation, we obtain a mass flow rate of 0.2979 kg/s for this run.

The coolant velocity can be calculated from:

$$V_c = \frac{\dot{m}}{\rho_c A_i}$$

where the inside cross-sectional area is given by:

$$A_i = \frac{\pi}{4} d_i^2$$

$$A_i = \frac{\pi}{4} (0.013259)^2 = 0.000138 \text{ m}^2$$

and

$$V_c = \frac{0.02979}{(1071.3)(0.000138)} = 0.201 \text{ m/s}$$

The coolant Reynolds number,  $Re_c$ , is calculated from:

$$Re_c = \frac{V_c d_i}{\nu_c}$$

$$Re_c = \frac{(0.201)(0.013259)}{4.76 \times 10^{-6}} = 559.89$$

The heat transferred to the coolant is calculated from:

$$\dot{q} = \dot{m} C_{p,c} \Delta T = (0.02979)(3196.99)(13.085)$$

$$\dot{q} = 1246.19 \text{ W}$$

and the heat flux is then calculated from :

$$q''_o = \frac{\dot{q}}{A_o}$$

where

$$A_o = \pi d_o L = \pi(0.015875)(1.2192) = 0.0608 \text{ m}^2$$

where L is the condensing length of the tube. Based on this equation, we obtain:

$$q''_o = \frac{1246.19}{0.0608} = 20494.9 \text{ W/m}^2$$

In order to calculate the inside and outside heat transfer coefficients, the physical and thermodynamic properties of R-113 must be calculated (Appendix D). These fluid properties are based on a reference or condensate film temperature. In order to obtain this film temperature, the wall temperature is needed. To obtain this, an iteration is carried out with an initial value of  $h_o$  assumed (in this case  $1000 \text{ W/m}^2 \text{ K}$ ). The wall temperature is then calculated from:

$$T_{wall} = T_{sat} - \frac{q''_o}{h_o}$$

$$T_{wall} = 46.925 - \frac{20494.9}{1000} = 26.43^\circ \text{C}$$

The film temperature is then calculated from:

$$T_f = \frac{T_{sat}}{3} + \frac{2}{3} T_{wall}$$

or

$$T_f = \frac{46.925}{3} + \frac{2}{3} (26.43) = 33.26^\circ C$$

Based on the equations of fluid properties for R-113 (Appendix D), the following values were obtained for the condensate:

$$h_g = 147036.5 \text{ J/kg}$$

$$k = 0.0734 \text{ W/m K}$$

$$\rho = 1544.34 \text{ kg/m}^3$$

$$\mu = 6.029 \times 10^{-4} \text{ kg/m s}$$

Using these fluid properties together with equation (5-15), we obtain:

$$h_o = 1907.06 \text{ W/m}^2 K$$

Using an iterative procedure, we adjust the initial guess of  $h_o$  by taking the average of the calculated and guessed value of  $h_o$ . The wall and film temperatures are then recalculated and new fluid properties for R-113 are obtained. A new value of  $h_o$  is then calculated. This procedure continues until the newly calculated and previously calculated values are within 0.1%. For this run, we obtained:

$$h_o = 1251 \text{ W/m}^2 K$$

The next step is to find a value for the overall heat transfer coefficient,  $U_o$ , where:

$$U_o = \frac{q''_o}{LMTD}$$

where, for this run,

$$LMTD = 30.48^\circ C$$

and

$$U_o = \frac{20494.9}{30.48} = 672.5 \text{ W/m}^2 \text{ K}$$

The inside heat transfer coefficient,  $h_i$ , can be obtained from a correlation for the Nusselt number for single phase coolant flow in a tube. This Nusselt number is obtained from a correlation (in this case) for the HEATEX element where:

$$\text{Nu}_c = 0.226(\text{Re}_c)^{0.65}(\text{Pr}_c)^{0.46}$$

$$\text{Nu}_c = 0.226(559.89)^{0.65}(43.75)^{0.46} = 78.41$$

and

$$h_i = \frac{\text{Nu}_c k_c}{d_i} = \frac{(78.41)(0.3742)}{0.013259}$$

$$h_i = 2213.07 \text{ W/m}^2 \text{ K}$$

The outside heat transfer coefficient is calculated from equation (5-12) where:

$$h_o = \frac{1}{\frac{1}{U_o} - \frac{d_o}{d_i h_i} - R_m A_o}$$

The wall resistance,  $R_m$ , is defined as:

$$R_m = \frac{\ln\left(\frac{d_o}{d_i}\right)}{2Lk}$$

$$R_m = \frac{\ln\left(\frac{0.015875}{0.013259}\right)}{2(1.2192)(386)} = 1.91 \times 10^{-4} \text{ K/W}$$

Therefore,

$$h_o = \frac{1}{\frac{1}{672.49} - \frac{0.015875}{(0.013259)(2213.07)} - (1.91 \times 10^{-4})(0.0608)}$$

$$h_o = 1070.2 \text{ W/m}^2 \text{ K}$$

Figure 103 is a copy of the computer printout for this run. The small differences seen in the computer calculations versus these sample calculations are the result of roundoff error.

Data set number = 1

RESULTS FOR TUBE NO. 1

Mass flow rate = 2.980E-02  
Inlet temperature = 9.443E+00  
Saturation temp (Deg C) = 4.693E+01  
DELT temp Dif. = 1.307E+01  
Log. Mean temp Dif. = 3.048E+01  
Heat flux = 2.048E+04  
Resistance of Tube Metal = 1.913E-04  
Prandtl number = 4.359E+01  
Reynolds number = 5.608E+02  
Reynolds number H&B S = 6.745E+02  
Inside h.t.c. = 2.216E+03  
Inside NUSSULT NO. = 7.852E+01  
OVERALL H.t.c. (Uo) = 6.720E+02

TUBE	FM	VEG	DELT	Uo	HO	HNUS
#	(%)	(m/s)	(K)	(W/m^2.K)		
1	15.74	0.20	13.074	6.720E+02	1.068E+03	1.251E+03

Figure 103. Computer printout of results for run 1 data set SM06.



## APPENDIX F. UNCERTAINTY ANALYSIS FOR $U_o$

Run number 1 of data set SM06 was also chosen for the uncertainty analysis. The analysis was only conducted on  $U_o$ . The measured and calculated parameters found in the sample calculation (Appendix E) were therefore used in this section. In order to assess the effects of coolant velocity on the uncertainty in the measurement of  $U_o$ , an uncertainty analysis was also performed on run number 11 of data set SM06. This run had a coolant velocity of 1.2 m/s as opposed to 0.2 m/s in run number 1.

The uncertainty analysis utilizes the procedure suggested by Kline and McClintock [Ref. 54]. This procedure states that if

$$R = R(x_1, x_2, x_3, \dots, x_n)$$

then the uncertainty in R, namely,  $\delta R$  is given by the equation:

$$\delta R = \left[ \left( \frac{\partial R}{\partial x_1} \delta x_1 \right)^2 + \left( \frac{\partial R}{\partial x_2} \delta x_2 \right)^2 + \dots + \left( \frac{\partial R}{\partial x_n} \delta x_n \right)^2 \right]^{0.5}$$

where  $x_n$  is the measured variable and  $\delta x_n$  is the uncertainty in the measured variable.

The uncertainty in the temperature measurements is due to uncertainty in the voltage measured by the thermocouples. For the thermocouples used corresponds to 0.1 °C. The uncertainty in in this thesis, this value was assumed to be 4 microvolts or 0.1 C. The uncertainty in  $\Delta T$ ,  $T_{in}$  and coolant inlet and outlet temperatures,  $T_{ci}$  and  $T_{co}$ , can be calculated as follows:

$$T_{co} = \frac{T(10) + T(11)}{2}$$

Taking the partial derivatives we obtain:

$$\frac{\partial T_{co}}{\partial T(10)} = \frac{1}{2}$$

likewise,

$$\frac{\partial T_{co}}{\partial T(11)} = \frac{1}{2}$$

The uncertainty in the measurement of  $T_{co}$  is thus:

$$\delta T_{co} = \left[ \left( \frac{\partial T_{co}}{\partial T(10)} \delta T \right)^2 + \left( \frac{\partial T_{co}}{\partial T(11)} \delta T \right)^2 \right]^{0.5}$$

Based on the thermocouple uncertainty,  $\delta T = 0.1$  C, we obtain:

$$\delta T_{co} = 0.0778 \text{ C}$$

The coolant inlet temperature is calculated from a single thermocouple, number 6 for tube A. The uncertainty in this measurement is calculated as:

$$\frac{\partial T_{ci}}{\partial T(6)} = 1$$

and,

$$\delta T_{ci} = \left[ \left( \frac{\partial T_{ci}}{\partial T(6)} \delta T \right)^2 \right]^{0.5}$$

or,

$$\delta T_{ci} = 0.1 \text{ C}$$

Finally, the uncertainty in  $\Delta T$  is calculated from:

$$\delta \Delta T = [(\delta T_{co})^2 + (\delta T_{ci})^2]^{0.5}$$

and,

$$\delta \Delta T = 0.1347 \text{ C}$$

Coolant velocity is calculated from:

$$V_c = \frac{\dot{m}}{\rho_c A_t}$$

In this run,  $\dot{m}$  was calculated to be 0.02979 kg/s. The uncertainty in the reading of the flowmeter is defined as the scale interpolation. This value corresponds to one-half the value of the smallest marked increment. In this case, the scale interpolation factor,  $\delta_{it}$ ,

is 0.5% which corresponds to 0.00101 kg/s resolution. In addition, a time-wise jitter,  $\delta_{vj}$ , of 0.5% was noted during the runs. Therefore, the uncertainty in  $\dot{m}$  is given by:

$$\frac{\delta \dot{m}}{\dot{m}} = \left[ \left( \frac{\delta \dot{m}}{\dot{m}} \delta_{si} \right)^2 + \left( \frac{\delta \dot{m}}{\dot{m}} \delta_{vj} \right)^2 \right]^{\frac{1}{2}}$$

or

$$\frac{\delta \dot{m}}{\dot{m}} = 0.0479$$

The uncertainty in the cross-sectional area of the tubes was estimated from:

$$\frac{\delta A_i}{A_i} = \left[ 2 \times \left( \frac{\delta d_i}{d_i} \right)^2 \right]^{\frac{1}{2}}$$

where  $\delta d_i$  is given as 0.1 mm based on tolerances supplied from the manufacturer. Therefore,

$$\frac{\delta A_i}{A_i} = 0.0107 = 1.07 \%$$

The uncertainty in the coolant velocity is now given by:

$$\frac{\delta V_c}{V_c} = \left[ \left( \frac{\delta \dot{m}}{\dot{m}} \right)^2 + \left( \frac{\delta A_i}{A_i} \right)^2 \right]^{0.5}$$

or

$$\frac{\delta V_c}{V_c} = 0.049 = 4.9 \%$$

The uncertainty in the calculation of coolant Reynolds number is given by:

$$\frac{\delta Re_c}{Re_c} = \left[ \left( \frac{\delta V_c}{V_c} \right)^2 + \left( \frac{\delta d_i}{d_i} \right)^2 \right]^{0.5}$$

or substituting appropriate numbers we find

$$\frac{\delta Re_c}{Re_c} = 0.0497 = 4.97 \%$$

The uncertainty in the calculation of the heat transferred to the coolant is related to the uncertainty in the measurements of coolant mass flow rate and coolant temperature rise where:

$$\frac{\delta \dot{q}}{\dot{q}} = \left[ \left( \frac{\delta \dot{m}}{\dot{m}} \right)^2 + \left( \frac{\delta \Delta T}{\Delta T} \right)^2 \right]^{0.5}$$

or

$$\frac{\delta \dot{q}}{\dot{q}} = 0.0489 = 4.89 \%$$

The uncertainty in the heat flux is then:

$$\frac{\delta q''_o}{q''_o} = \left[ \left( \frac{\delta \dot{q}}{\dot{q}} \right)^2 + \left( \frac{\delta A_o}{A_o} \right)^2 \right]^{0.5}$$

where the uncertainty in  $A_o$  is given by:

$$\frac{\delta A_o}{A_o} = \left[ \left( \frac{\delta d_o}{d_o} \right)^2 + \left( \frac{\delta L}{L} \right)^2 \right]^{0.5}$$

Here, the uncertainty in the length of the tube,  $\delta L$ , is assumed to be 5 mm while  $\delta d_o$  is assumed to be 0.1 mm (again from given tolerances). Substitution of the appropriate numbers yields:

$$\frac{\delta q''_o}{q''_o} = 0.0496$$

Finally, since  $U_o$  is given by:

$$U_o = \frac{q''_o}{LMTD}$$

the uncertainty in the LMTD must be calculated. The LMTD is given by:

$$LMTD = \frac{\Delta T}{\ln \left[ \frac{T_{sat} - T_{c,i}}{T_{sat} - T_{c,o}} \right]}$$

In order to calculate the uncertainty in the measurement of the LMTD, the following equations were used:

$$\frac{\partial LMTD}{\partial \Delta T} = \frac{1}{\ln \left[ \frac{T_{sat} - T_{c,i}}{T_{sat} - T_{c,o}} \right]}$$

$$\frac{\partial LMTD}{\partial T_{sat}} = \frac{\Delta T [(T_{sat} - T_{c,o}) - (T_{sat} - T_{c,i})]}{\left[ \ln \left[ \frac{T_{sat} - T_{c,i}}{T_{sat} - T_{c,o}} \right] \right]^2 (T_{sat} - T_{c,i})(T_{sat} - T_{c,o})}$$

$$\frac{\partial LMTD}{\partial T_{c,o}} = - \frac{\Delta T}{\left[ \ln \left[ \frac{T_{sat} - T_{c,i}}{T_{sat} - T_{c,o}} \right] \right]^2 (T_{sat} - T_{c,o})}$$

$$\frac{\partial LMTD}{\partial T_{c,i}} = \frac{\Delta T}{\left[ \ln \left[ \frac{T_{sat} - T_{c,i}}{T_{sat} - T_{c,o}} \right] \right]^2 (T_{sat} - T_{c,i})}$$

The uncertainty in the LMTD is therefore given by:

$$\delta LMTD = \left[ \left( \frac{\partial LMTD}{\partial \Delta T} \delta \Delta T \right)^2 + \left( \frac{\partial LMTD}{\partial T_{sat}} \delta T_{sat} \right)^2 + \left( \frac{\partial LMTD}{\partial T_{c,o}} \delta T_{c,o} \right)^2 + \left( \frac{\partial LMTD}{\partial T_{c,i}} \delta T_{c,i} \right)^2 \right]^{\frac{1}{2}}$$

For the sample run with a coolant velocity of 0.2 m/s, the uncertainty in the measurement of the LMTD is:

$$\delta LMTD = \left[ [(2.329)(0.1347)]^2 + [(-1.0157)(0.0778)]^2 + [(-2.9097)(0.0778)]^2 + [(1.894)(0.1)]^2 \right]^{\frac{1}{2}}$$

or

$$\delta LMTD = 0.446 \text{ K}$$

and

$$\frac{\delta LMTD}{LMTD} = \frac{0.446}{30.48} = 0.0146 = 1.46 \%$$

The uncertainty in the overall heat transfer coefficient,  $U_o$ , is then given by:

$$\frac{\delta U_o}{U_o} = \left[ \left( \frac{\delta q''_o}{q''_o} \right)^2 + \left( \frac{\delta LMTD}{LMTD} \right)^2 \right]^{\frac{1}{2}}$$

or

$$\frac{\delta U_o}{U_o} = [(0.0496)^2 + (0.0146)^2]^{\frac{1}{2}}$$

and

$$\frac{\delta U_o}{U_o} = 0.052 = 5.2 \%$$

Table 7 summarizes the results of the uncertainty analysis for the smooth copper tubes with the HEATEX insert for coolant velocities of 0.2 and 1.2 m/s respectively.

The uncertainty analysis neglects any uncertainty in the physical properties of the coolant or the R-113. For the most part, this is probably a reasonable assumption. The exception to this may be the viscosity due to its sensitivity to temperature. Hence, the uncertainty reported here is an underestimate.

It is curious that the relative magnitudes of the uncertainty for the low and high coolant velocities are essentially the same. Two different mechanisms dominate in the calculated uncertainty at low and high coolant velocities. In terms of the mass flow rate, the time-wise jitter and scale interpolation terms are the same for both coolant velocities. However, the actual mass flow rate is less at the lower flow rates. Hence, the uncertainty in the mass flow rate calculation is more significant at the lower coolant velocities. At higher flow rates the uncertainty in the calculation of the LMTD becomes the dominant term. This is because the coolant temperature rise is smaller at high coolant velocities but the uncertainty in the temperature measurements remains the same. The mass flow

**Table 8. SUMMARY OF RESULTS FOR SAMPLE UNCERTAINTY ANALYSIS.**

Variable	$V_c = 0.2 \text{ m/s}$	$V_c = 1.2 \text{ m/s}$
$\delta T_{c,i}$	$0.1^\circ\text{C}$	$0.1^\circ\text{C}$
$\delta T_{c,o}$	$0.078^\circ\text{C}$	$0.078^\circ\text{C}$
$\delta T_{tot}$	$0.078^\circ\text{C}$	$0.078^\circ\text{C}$
$\delta \Delta T$	$0.135^\circ\text{C}$	$0.135^\circ\text{C}$
$\frac{\delta m}{m}$	0.048	0.008
$\frac{\delta A_i}{A_i}$	0.011	0.011
$\frac{\delta V_c}{V_c}$	0.049	0.013
$\frac{\delta Re_c}{Re_c}$	0.05	0.015
$\frac{\delta q}{q}$	0.05	0.015
$\frac{\delta A_o}{A_o}$	0.008	0.008
$\frac{\delta q''_o}{q''_o}$	0.05	0.017
$\frac{\delta LMTD}{LMTD}$	0.015	0.054
$\frac{\delta U_o}{U_o}$	0.052	0.057

rate goes up so that the uncertainty in the coolant mass flow rate calculation decreases. Thus, at the higher coolant velocities, the uncertainty in the calculation of the LMTD is the dominant term.

## APPENDIX G. PROGRAM LISTING



```

1000 ! FILE:      DRPCON7
1005 ! PURPOSE: This program collects and processes condensation data for the tube bundle.
1015 ! CREATED: NOVEMBER 2, 1988
1020 ! UPDATE1: APRIL 25 1991 (S. MEMORY)
1021 ! UPDATE2: May 17 1991 (S. MEMORY)
1022 ! UPDATE3: JULY 26, 1991 (R.W. MAZZONE)
1023 ! UPDATE4: 13 AUGUST 1991 (R.W. MAZZONE)
1024 ! UPDATE5: 10 OCTOBER 1991 (R.W. MAZZONE)
1026 ! CHANGE HOD=3 AND USING CALCULATED CI FROM WILSON
1030     BEEP
1035     PRINTER IS 1
1040     PRINT USING "4X,""SELECT OPTION""
1045     PRINT USING "6X,""0  TAKING DATA OR REPROCESSING PREVIOUS DATA""
1050     PRINT USING "6X,""1  PLOTTING H VS DELTA-T""
1055     PRINT USING "6X,""2  PLOTTING HRAT VS N""
1060     PRINT USING "6X,""3  PLOTTING WILSON""
1065     PRINT USING "6X,""4  PURGE FILES""
1070     PRINT USING "6X,""5  XYREAD""
1075     PRINT USING "6X,""6  NUSSELT ESTIMATE""
1080     PRINTER IS 701
1085     INPUT Icall
1090     IF Icall=0 THEN CALL Main
1095     IF Icall=1 THEN CALL Plot2
1100     IF Icall=2 THEN CALL Plot1
1105     IF Icall=3 THEN CALL Plot3
1110     IF Icall=4 THEN CALL Purge
1115     IF Icall=5 THEN CALL Xyread
1120     IF Icall=6 THEN CALL Nusselt
1125     END
1130     SUB Main
1135     COM /Cc/ C(7)
1140     COM /Fld/ Ifl
1145     COM /Nus/ Iin,Tsat,Qdpl,Hnus,Kf,Rhof,Hfg,Muf,Do,Itube
1150     COM /Wil1/ Doa(4),Dia(4),Kma(4),Iact,Droot(4)
1155     COM /Wil2/ Delta,Isat,Nsets,Hod,Cia(3,3),Alpaa(3)
1160     DIM Emf(17),Tp(4),T(17),Ho(4),Qdp(4),Uo(4),Pc(4)
1215     DATA 1.0,1.0,1.0,1.0
1216     DATA 5.172,5.172,5.172,5.172
1217     DATA 0.226,0.226,0.226,0.226
1218     DATA 0.063,0.063,0.063,0.063
1220     READ Cia(*)
1225     DATA 0.10086091,25727.94369,-767345.8295,78025595.81
1230     DATA -9247486589,6.97688E11,-2.66192E13,3.94078E14
1235     READ C(*)
1240     DATA 0.015875,0.014000,0.015798,0.0159,0.0
1245     DATA 0.013259,0.010160,0.012776,0.01346,0.0

```

```

1250 DATA 386.0,42.975,42.975,21.9,0.0
1251 DATA 0.0,0.014,0.0,.0141,0.0
1255 DATA 0.0005588,3
1260 READ Doa(*),Dia(*),Kma(*),Droot(*),Delta,Hod ! Hod=H/Di
1265 L=1.2192 ! Condensing length
1270 Jset=0
1271 Okacct=1
1275 BEEP
1280 INPUT "ENTER MONTH, DATE AND TIME (MM:DD:HH:MM:SS)",Dtg$
1285 OUTPUT 709;"TD";Dtg$
1290 BEEP
1295 INPUT "SELECT OPTION (0=DAQ, 1=FILE)",Im
1300 Ihard=1
1305 BEEP
1310 INPUT "WANT A HARDCOPY PRINTOUT (1=DEF=YES,0=N)",Ihard
1315 BEEP
1320 INPUT "SELECT (0=R-114,1=STEAM,2=R-113,3=EG)",Ift
1325 Iin=1
1330 Isat=2
1335 BEEP
1340 INPUT "SELECT SAT TEMP MODE (0=LIQ,1=VAP,2=(LIQ+VAP)/2=DEF)",Isat
1345 IF Ihard=1 THEN PRINTER IS 701
1350 IF Im=0 THEN
1355 BEEP
1360 INPUT "GIVE A NAME FOR THE NEW DATA FILE",File$
1365 CREATE BDAT File$,20
1370 ASSIGN @File TO File$
1375 BEEP
1380 INPUT "ENTER TUBE CODE (0=SMOOTH CU,1=FINNED CU,2=KORODENSE,3=TIT FIN
)",Itube
1381 BEEP
1382 INPUT "0=NO INSERT, 1=TWISTED TAPE, 2=HITRAN1, 3=HITRAN2",Insert
1385 BEEP
1390 INPUT "ENTER EG CONCENTRATION (WT PERCENT)",Egrat
1395 ENTER 709;Dtg$
1400 OUTPUT @File;Dtg$
1405 OUTPUT @File;Itube,Egrat,Dd1,Dd2,Dd3,Dd4,Dd5
1410 Iact=10
1415 BEEP
1420 INPUT "SELECT (0=TOP,1=SECOND,....,10=BUNDLE=DEFAULT)",Iact
1425 PRINT
1430 PRINT USING "10X,""FILE NAME: """,12A";File$
1435 PRINT
1440 ELSE
1445 BEEP
1450 INPUT "ENTER NAME OF EXISTING FILE",File$
1455 BEEP
1460 INPUT "ENTER NUMBER OF DATA SETS STORED",Nsets
1465 Iwil=1
1470 BEEP

```



```

1630      ASSIGN @Fout TO Fout$
1635      END IF
1640      !
1645      Do=Doa(Itube)
1646      Dol=Doa(Itube)
1650      Di=Dia(Itube)
1655      Km=Kma(Itube)
1660      Ax=PI*Di^2/4      ! Cross-sectional area
1665      Ao=PI*Do*L
1670      ! Rm=Do*LOG(Do/Di)/(2*Km)
1671      IF Itube=1 THEN
1672          Dol=Droot(Itube)
1673      END IF
1674      IF Itube=3 THEN
1675          Dol=Droot(Itube)
1676      END IF
1677      Ao=PI*Do*L
1679      Rm=LOG(Dol/Di)/(2*L*Km)
1680      Al=PI*Dol*L
1682      !
1683      IF Im=0 THEN
1685          PRINTER IS 1
1690          BEEP
1691          INPUT "WHAT IS REQUIRED NOMINAL COOLANT VELOCITY IN m/s (MAX. = 1.4 m
/s)?",Vegst
1694          OUTPUT 709;"AR AF6 ALS VRS"
1695          FOR I=6 TO 9
1696              OUTPUT 709;"AS SA"
1697              Vsum=0
1698              FOR J=1 TO 5
1699                  ENTER 709;E
1700                  Vsum=Vsum+E
1701              NEXT J
1702              Emf(I)=Vsum/5
1703              T(I)=FNTvsv(Emf(I))
1704          NEXT I
1705          Tavgl=(T(6)+T(7)+T(8)+T(9))/4
1706          IF Tavgl<0 OR Tavgl>24 THEN
1707              PRINT "COOLANT TEMP. NOT IN RANGE 0 TO 24 C"
1708              GOTO 1691
1709          END IF
1711          Rhoegl=FNRhoeg(Tavgl,Egrat)
1712          Mdot1=Rhoegl*Ax*Vegst
1713          Pca0=(Mdot1+.00414)/.00206
1714          Pca24=(Mdot1+.00329)/.00225
1715          Pcb0=(Mdot1+.00615)/.00204
1716          Pcb24=(Mdot1+.00138)/.00216
1717          Pcc0=(Mdot1+.0036)/.00208
1718          Pcc24=(Mdot1+.00301)/.00223
1719          Pcd0=(Mdot1+.00122)/.0028

```

```

1720      Pcd24=(Mdot1-.0048)/.0029
1721      Pc(0)=Pca0+(Tavg1*(Pca24-Pca0))/24
1722      Pc(1)=Pcb0+(Tavg1*(Pcb24-Pcb0))/24
1723      Pc(2)=Pcc0+(Tavg1*(Pcc24-Pcc0))/24
1724      Pc(3)=Pcd0+(Tavg1*(Pcd24-Pcd0))/24
1725      PRINT "SET FLOWMETER READINGS CORRESPONDING TO:"
1726      PRINT USING "6X, ""% OF METER A = "",DDD.D";Pc(0)
1727      PRINT USING "6X, ""% OF METER B = "",DDD.D";Pc(1)
1728      PRINT USING "6X, ""% OF METER C = "",DDD.D";Pc(2)
1729      PRINT USING "6X, ""% OF METER D = "",DDD.D";Pc(3)
1730      PRINT
1731      PRINT "HIT CONTINUE WHEN READY"
1733      PAUSE
1734 Repeat: !
1735 !      PRINTER IS 701
1736      Dtld=47.5 ! Desired temperature of liquid
1737      Ido=1
1738      ON KEY 0,15 RECOVER 1734
1739      PRINT USING "4X, ""SELECT OPTION ""
1740      PRINT USING "6X, ""0=TAKE DATA ""
1741      PRINT USING "6X, ""1=SET Tsat (DEFAULT) ""
1742      PRINT USING "4X, ""NOTE: KEY 0 = ESCAPE""
1743 !      Ido = desired option
1744      BEEP
1745      INPUT Ido
1746 !      Set default value for input
1747      IF Ido>1 THEN Ido=1
1748 !      Take data option
1749      IF Ido=0 THEN 1797
1750 !      Loop to check saturation temperature
1751      IF Ido=1 THEN
1752          INPUT "ENTER DESIRED Tsat (DEFAULT=47.5 C - R-113)",Dtld
1753 !      INPUT "ENTER DESIRED Tsat (DEFAULT=2.2 C - R-114)",Dtld
1754          Nn=1
1755          Nrs=Nn MOD 15
1756          Nn=Nn+1
1757          IF Nrs=1 THEN
1758              PRINT USING "4X, "" DTsat      Tld1      Tvab      Tvat      Del1      D
el2      Del3      Del4      ""
1759          END IF
1760 !      Read thermocouple voltages
1761          OUTPUT 709;"AR AF0 AL17 VRS"
1762          Nend=17
1763          FOR I=0 TO 5
1764              OUTPUT 709;"AS SA"
1765              Vsum=0
1766              FOR J=1 TO 5
1767                  ENTER 709;E
1768                  Vsum=Vsum+E
1769              NEXT J

```

```

1770         Emf(I)=Vsum/5
1771         T(I)=FNTvsv(Emf(I))
1772     NEXT I
1773     FOR I=6 TO Nend
1774         OUTPUT 709;"AS SA"
1775         Vsum=0
1776         FOR J=1 TO 20
1777             ENTER 709;E
1778             Vsum=Vsum+E
1779         NEXT J
1780         Emf(I)=Vsum/20
1781         T(I)=FNTvsv(Emf(I))
1782     NEXT I
1783     ! Compute average temperature of liquid
1784     Tliq=(T(3)+T(4))/2
1785     Tvap=(T(0)+T(1)+T(2))/3
1786     Tvat=(T(0)+T(1))/2
1787     Tliq1=T(5)
1788     Del1=((T(10)+T(11))/2)-T(6)
1789     Del2=((T(12)+T(13))/2)-T(7)
1790     Del3=((T(14)+T(15))/2)-T(8)
1791     Del4=((T(16)+T(17))/2)-T(9)
1792     PRINT USING "4X,8(MDD.DD,3X)";Dt1d,T(3),T(2),Tvat,Del1,Del2,Del3,De
1793     14
1794     WAIT 2
1795     GOTO 1755
1796     END IF
1797     TAKE DATA IF Im=0 LOOP
1798     PRINTER IS 701
1799     OUTPUT 709;"AR AF0 AL17 VR5"
1800     Nend=17 ! INCREASE TO 20 IF FIVE TUBES IN BUNDLE
1801     FOR I=0 TO 5
1802         OUTPUT 709;"AS SA"
1803         Vsum=0
1804         FOR J=1 TO 5
1805             ENTER 709;E
1806             Vsum=Vsum+E
1807         NEXT J
1808         Emf(I)=Vsum/5
1809     NEXT I
1810     FOR I=6 TO Nend
1811         OUTPUT 709;"AS SA"
1812         Vsum=0
1813         FOR J=1 TO 20
1814             ENTER 709;E
1815             Vsum=Vsum+E
1816         NEXT J
1817         Emf(I)=Vsum/20
1818     NEXT I
1819     ELSE

```

```

1830      ENTER @File:Pc(*),Emf(*),Tp(*)
1835      END IF
1840 !
1845 ! DATA ANALYSIS
1850 !
1855      Nend=17
1860      FOR I=0 TO Nend
1865          T(I)=FNTvsv(Emf(I))
1870      NEXT I
1875      Tvap=(T(0)+T(1)+T(2))/3
1880      Tliq=(T(3)+T(4))/2
1881      Tliq1=T(5)
1885      IF Isat=0 THEN
1890          Tsat=Tliq1
1895      END IF
1896      IF Isat=1 THEN
1900          Tsat=Tvap
1905      END IF
1906      IF Isat=2 THEN
1907          Tsat=(Tvap+Tliq)/2
1908      END IF
1925      Jset=Jset+1
1926      IF Okacpt=0 THEN Jset=Jset-1
1930      PRINT
1935      PRINT USING "10X," "Data set number = ",DD";Jset
1940      PRINT
1945      Ibeg=0
1950      Iend=3
1955      IF Iact<10 THEN
1960          Ibeg=Iact
1965          Iend=Iact
1970      END IF
1975      FOR I=Ibeg TO Iend
1980 !          Grad=FNGrad(Emf(I+6))
1981          Tout=(T(2*I+10)+T(2*I+11))/2
1985          Delt=Tout-T(I+6)
1990          Tavg=T(I+6)+Delt*.5
1991 !          IF I=Iend THEN
1992 !              Delt=T(10)-T(9)
1994 !              Tavg=T(10)-T(9)/2
1995 !          END IF
1996          Rhoeg=FNRhoeg(Tavg,Egrat)
2000          Nueg=FNNueg(Tavg,Egrat)
2005          Mueg=Nueg*Rhoeg
2010          Cpeg=FNCpeg(Tavg,Egrat)
2015          Keg=FNKeg(Tavg,Egrat)
2020          Preg=Cpeg*Mueg/Keg
2025          Mdot=FNFmc(I,T(I+6),Pc(I))
2030          Veg=Mdot/(Rhoeg*Ax)
2035          Reeg=Veg*D1/Nueg

```

```

2040 Res=4*Mdot/(PI*Mueg*(Di-4*Delta))
2045 Qdot=Mdot*Cpeg*Delt
2050 Qdp(I)=Qdot/Ao
2055 IF I=0 OR I=Iact THEN
2060     Qdp1=Qdp(I)
2065     CALL Nusselt
2070 END IF
2075 Lmtd=Delt/LOG((Tsats-T(I+6))/(Tsats-T(I+6)-Delt))
2080 Uo(I)=Qdp(I)/Lmtd
2081 Cpeg=1
2085 IF Reeg<4000 THEN
2086     IF Insert=0 THEN
2088         Bb1=.0668*(Di/L)*Reeg*Preg
2089         Bb2=1+.04*((Di/L)*Reeg*Preg)^.6666
2090         Nueg=3.66+(Bb1/Bb2)
2091     END IF
2092     IF Insert=1 THEN
2094         Nueg=1.86*(Preg*Reeg)^.333333*(Di/L)^.333333*Cpeg
2095         Nueg=Cia(Insert,I)*(1+5.484E-3*Preg^.7*(Res/Hod)^1.25)^.5
2096     END IF
2097     IF Insert=2 THEN
2098         Nueg=Cia(Insert,I)*(Reeg^.65)*Preg^.46
2099     END IF
2100     IF Insert=3 THEN
2101         Nueg=Cia(Insert,I)*(Reeg^.76)*Preg^.46
2102     END IF
2104 ELSE
2105     BEEP
2106     PRINT USING "10X","TURBULENT CORRELATION"
2110     Nueg=.027*Reeg^.8*Preg^.333333*Cpeg
2115 END IF
2120 Hi=Nueg*Keg/Di
2125 Ho(I)=1/(1/Uo(I)-Do/(Di*Hi))-Rm*A1)
2130 IF I=0 OR I=Iact THEN
2131     PRINT
2132     PRINT
2134     PRINT USING "10X","RESULTS FOR TUBE NO.",3D,I+1
2135     PRINT
2136     PRINT USING "10X","Mass flow rate" = "",M2.3DE";Mdot
2137     PRINT USING "10X","Inside Tube Dia. (m.)" = "",M2.3DE";Dia(Itube
)
2138     PRINT USING "10X","180 DEG OVER Dia. (HOD)" = "",M2.3DE";Hod
2140     PRINT USING "10X","Inlet temperature" = "",M2.3DE";T(I+6)
2145     PRINT USING "10X","Saturation temp (Deg C)" = "",M2.3DE";Tsats
2146     PRINT USING "10X","DELTA Tape Thickness" = "",M2.3DE";Delta
2147     PRINT USING "10X","DELT temp Dif." = "",M2.3DE";Delt
2148     PRINT USING "10X","Log. Mean temp Dif." = "",M2.3DE";Lmtd
2150     PRINT USING "10X","Heat flux" = "",M2.3DE";Qdp(I)
2151     PRINT USING "10X","Conductivity E.G." = "",M2.3DE";Keg
2152     PRINT USING "10X","Conductivity Tube Metal" = "",M2.3DE";Km

```



```

2153      PRINT USING "10X," "Resistance of Tube Metal= ",MZ.3DE":Rm
2155      PRINT USING "10X," "Prandtl number          = ",MZ.3DE":Preg
2160      PRINT USING "10X," "Reynolds number          = ",MZ.3DE":Reeg
2161      PRINT USING "10X," "Reynolds number H&B S     = ",MZ.3DE":Res
2165      PRINT USING "10X," "Inside h.t.c.            = ",MZ.3DE":Hi
2166      PRINT USING "10X," "Inside NUSSULT NO.        = ",MZ.3DE":Nueg
2167      PRINT USING "10X," "OVERALL H.t.c. (Uo)       = ",MZ.3DE":Uo(I)
2170      PRINT
2171      PRINT USING "10X," "KF                        = ",MZ.3DE":Kf
2172      PRINT USING "10X," "RHOF                     = ",MZ.3DE":Rhof
2173      PRINT USING "10X," "HFG                      = ",MZ.3DE":Hfg
2174      PRINT USING "10X," "MUF                      = ",MZ.3DE":Muf
2175      PRINT
2177      PRINT USING "10X," "TUBE          FM          VEG          DELT          Uo
      HO          HNUS""
2180      PRINT USING "10X," " #          (%)          (m/s)          (K)          (W/m^2.
      K)""
2185      PRINT USING "10X,3D,4X,3D.0D,3X,Z.0D,4X,0D.3D,2X,MZ.3DE,3X,MZ.3DE
      ,3X,MZ.3DE,3X";I+1,Pc(I),Veg,Delt,Uo(I),Ho(I),Hnus
2190      ELSE
2195      PRINT USING "10X,3D,4X,3D.0D,3X,Z.0D,4X,0D.3D,2X,MZ.3DE,3X,MZ.3DE
      ,3X";I+1,Pc(I),Veg,Delt,Uo(I),Ho(I)
2200      END IF
2205      NEXT I
2210      IF Im=0 THEN
2215          Okacct=1
2220          BEEP
2225          INPUT "OK TO ACCEPT THIS SET (1=DEFAULT=YES, 0=NO)?",Okacct
2230          IF Okacct=1 THEN OUTPUT @File:Pc(*),Emf(*),Tp(*)
2235      END IF
2240      IF (Okacct=1 OR Im=1) AND Iout=1 THEN
2245          FOR I=0 TO 2
2250              OUTPUT @Fout:Ho(I),Qdp(I)
2255          NEXT I
2260      END IF
2265      IF Im=0 THEN
2270          Okrpt=1
2275          BEEP
2280          INPUT "WILL THERE BE ANOTHER RUN (1=YES=DEFAULT,0=NO)",Okrpt
2285          IF Okrpt=1 THEN 1683
2290      ELSE
2295          IF Jset<Nsets THEN 1683
2300      END IF
2305      ASSIGN @File TO *
2310      IF Iout=1 THEN ASSIGN @File TO *
2315      SUBEND
2320      DEF FNGrad(T)
2325      Grad=-3.877857E-5-2*4.7142857E-8*T
2330      RETURN Grad
2335      FNEND

```

```

2340 DEF FNKcu(T)
2345 | OFHC COPPER 250 TO 300 K
2350 Tk=T+273.15
2355 K=434-.112*Tk
2360 RETURN K
2365 FNEND
2370 DEF FNNueg(Tc,Egr)
2375 | RANGE OF VALIDITY: -20 TO 20 DEG C
2380 Tk=Tc+273.15
2385 Nu1=7.1196507E-3-Tk*(7.4863347E-5-Tk*(2.6294943E-7-Tk*3.0833329E-10))
2390 Nu2=4.9237638E-3-Tk*(4.9213912E-5-Tk*(1.6437534E-7-Tk*1.8333331E-10))
2395 Nu3=8.6586293E-3-Tk*(8.8637902E-5-Tk*(3.0495032E-7-Tk*3.4999996E-10))
2400 A2=(Nu3-2*Nu2+Nu1)/200
2405 A1=(Nu2-Nu1-940*A2)/10
2410 A0=Nu1-42*A1-1764*A2
2415 Nu=A0+Egr*(A1+Egr*A2)
2420 RETURN Nu
2425 FNEND
2430 DEF FNCpeg(Tc,Egr)
2435 | RANGE OF VALIDITY: 0 TO 20 DEG C
2440 Tk=Tc+273.15
2445 Cp1=1.6701550E+3+Tk*6.3
2450 Cp2=1.4748125E+3+Tk*6.25
2455 Cp3=9.5800500E+2+Tk*7.3
2460 A2=(Cp3-2*Cp2+Cp1)/200
2465 A1=(Cp2-Cp1-900*A2)/10
2470 A0=Cp1-40*A1-1600*A2
2475 Cp=A0+Egr*(A1+Egr*A2)
2480 RETURN Cp
2485 FNEND
2490 DEF FNRhoeg(T,Egr)
2495 Ro1=1.0607093E+3-T*(3.7031283E-1+T*4.0837183E-3)
2500 Ro2=1.0748272E+3-T*(4.4266195E-1+T*4.0939706E-3)
2505 Ro3=1.0885934E+3-T*(5.7355653E-1+T*6.1281405E-3)
2510 A2=(Ro3-2*Ro2+Ro1)/200
2515 A1=(Ro2-Ro1-900*A2)/10
2520 A0=Ro1-40*A1-1600*A2
2525 Ro=A0+Egr*(A1+Egr*A2)
2530 RETURN Ro
2535 FNEND
2540 DEF FNPreg(T,Egr)
2545 Pr=FNCpeg(T,Egr)*FNNueg(T,Egr)*FNRhoeg(T,Egr)/FNKeg(T,Egr)
2550 RETURN Pr
2555 FNEND
2560 DEF FNKeg(Tc,Egr)
2565 | RANGE OF VALIDITY: -20 TO 20 DEG C
2570 Tk=Tc+273.15
2575 K1=2.2824708E-1+Tk*(5.5989286E-4+Tk*3.5714286E-7)
2580 K2=2.5846616E-1+Tk*(2.3978571E-4+Tk*7.1428571E-7)
2585 K3=3.2136902E-1-Tk*(3.0042857E-4-Tk*1.4285714E-6)

```

```

2590 A2=(K3-2*K2+K1)/200
2595 A1=(K2-K1-900*A2)/10
2600 A0=K1-40*A1-1600*A2
2605 K=A0+Egr*(A1+Egr*A2)
2610 RETURN K
2615 FNEND
2620 DEF FNTanh(X)
2625 P=EXP(X)
2630 Q=1/P
2635 Tanh=(P-Q)/(P+Q)
2640 RETURN Tanh
2645 FNEND
2650 DEF FNTvsv(V)
2655 COM /Cc/ C(7)
2660 T=C(0)
2665 FOR I=1 TO 7
2670 T=T+C(I)*V^I
2675 NEXT I
2680 RETURN T
2685 FNEND
2690 DEF FNBeta(T)
2695 Rop=FNRho(T+.1)
2700 Rom=FNRho(T-.1)
2705 Beta=-2/(Rop+Rom)*(Rop-Rom)/.2
2710 RETURN Beta
2715 FNEND
2720 DEF FNPsat(Tc)
2725 Q TO 80 deg F CURVE FIT OF Psat
2730 Tf=1.8*Tc+32
2735 Pa=5.945525+Tf*(.15352082+Tf*(1.4840963E-3+Tf*9.6150671E-6))
2740 Pg=Pa-14.7
2745 IF Pg>0 THEN I +=PSIG, -=in Hg
2750 Psat=Pg
2755 ELSE
2760 Psat=Pg*29.92/14.7
2765 END IF
2770 RETURN Psat
2775 FNEND
2850 SUB Xyread
2855 BEEP
2860 INPUT "ENTER FILE NAME",File$
2865 BEEP
2870 INPUT "ENTER NUMBER OF X,Y PAIRS",N
2875 ASSIGN @File TO File$
2880 FOR I=1 TO N
2885 ENTER @File:X,Y
2890 PRINT X,Y
2895 NEXT I
2900 SUBEND
2905 SUB Purge

```

```

2910 BEEP
2915 INPUT "ENTER FILE NAME TO BE DELETED",File$
2920 PURGE File$
2925 GOTO 2910
2930 SUBEND
2935 SUB Wilson
2940 COM /Wil1/ Doa(4),Dia(4),Kma(4),Iact,Droot(4)
2945 COM /Wil2/ Delta,Isat,Nsets,Hod,Cia(3,3),Alpaa(3)
2950 DIM Emf(17),T(17),Xa(100),Ya(100),Pc(4),Tp(4)
2955 BEEP
2960 INPUT "PLEASE RE-ENTER NAME OF FILE",File$
2965 ASSIGN @File TO File$
2970 INPUT "0=SMOOTH COPPER TUBE, 1=CUNI FIN, 2=KORODENSE, 3=FIN TITAN",Itube
2975 BEEP
2976 INPUT "0=NO INSERT, 1= TWISTED TAPE INSERT, 2=HITRAN1, 3=HITRAN2",Insert
2977 BEEP
2980 INPUT "GIVE A NAME FOR XY FILE",Xy$
2985 CREATE BDAT Xy$,20
2990 ASSIGN @Xy TO Xy$
2995 L=1.2192
3000 Do=Doa(Itube)
3005 D1=Dia(Itube)
3010 Km=Kma(Itube)
3015 Ax=PI*D1^2/4 ! Cross-sectional area
3020 Aa=PI*Do*L
3025 Rm=Do*LOG(Do/D1)/(2*Km)
3030 !
3035 ! Initial values
3040 Tf=Tsat
3045 Alpa=.655
3046 IF Insert=0 THEN
3050 C1=1.0
3051 END IF
3052 IF Insert=1 THEN
3053 C1=5.172
3054 END IF
3055 IF Insert=2 THEN
3056 C1=.226
3057 END IF
3058 IF Insert=3 THEN
3059 C1=.063
3060 END IF
3062 G=9.81
3063 Ibeg=0
3065 Iend=0 !CHANGE TO 4, IF FIVE TUBES IN BUNDLE
3070 IF Iact<10 THEN
3075 Ibeg=Iact
3080 Iend=Iact
3085 END IF
3090 !

```

```

3095     FOR I=Ibeg TO Iend
3100         Sx=0
3105         Sy=0
3110         Sxs=0
3115         Sxy=0
3120         Jset=0
3125         ASSIGN @File TO File$
3130         ENTER @File;Dtg$,Itube,Egrat,Dd1,Dd2,Dd3,Dd4,Dd5
3135         ENTER @File;Pc(*),Emf(*),Tp(*)
3140         FOR J=0 TO 17
3145             T(J)=FNTvsv(Emf(J))
3150         NEXT J
3155         Tvap=(T(0)+T(1)+T(2))/3
3160         Tliq=(T(3)+T(4))/2
3161         Tliq1=T(5)
3165         IF Isat=0 THEN
3170             Tsat=Tliq1
3175         ELSE
3180             Tsat=Tvap
3185         END IF
3190         Grad=FNGrad(T(I+6))
3191         Tout=(T(2*I+10)+T(2*I+11))/2
3195         Delt=Tout-T(I+6)
3200         Tavg=T(I+6)+Delt*.5
3201         IF I=Iend THEN
3202             Delt=T(10)-T(9)
3204             Tavg=(T(10)+T(9))/2
3205         END IF
3206
3210         Water/Ethylene Glycol Mixture Properties
3215         Rhoeg=FNRhoeg(Tavg,Egrat)
3220         Nueg=FNNueg(Tavg,Egrat)
3225         Mueg=Nueg*Rhoeg
3230         Cpeg=FNCPeg(Tavg,Egrat)
3235         Keg=FNKeg(Tavg,Egrat)
3240         Preg=Cpeg*Mueg/Keg
3245
3250         Mdot=FNFmcal(I,T(I+6),Pc(I))
3255         Veg=Mdot/(Rhoeg*Ax)
3260         Reeg=Veg*Di/Nueg
3265         Res=4*Mdot/(Mueg*(PI*Di-4*Delta))
3270         Qdot=Mdot*Cpeg*Delt
3275         Qdp=Qdot/Ao
3280         Lmtd=Delt/LOG((Tsat-T(I+6))/(Tsat-T(I+6)-Delt))
3285         Uo=Qdp/Lmtd
3286         IF Insert=0 THEN
3287             Bb1=.0668*((Di/L)*Reeg*Preg)
3288             Bb2=1+.04*((Di/L)*Reeg*Preg)^.6666
3289             Omega=3.66+(Bb1/Bb2)
3290         END IF

```

```

3291 IF Insert=1 THEN
3293 Omega=(1+5.484E-3*Preg^.7*(Res/Hod)^1.25)^.5
3294 END IF
3295 IF Insert=2 THEN
3296 Omega=(Reeg^.65)*(Preg^.46)
3297 END IF
3298 IF Insert=3 THEN
3299 Omega=(Reeg^.76)*(Preg^.46)
3300 END IF
3302 !
3303 ! R-114/R113 Properties
3305 Hfg=FNHfg(Tsat)
3310 Kf=FNK(Tf)
3315 Rhof=FNrho(Tf)
3320 Muf=FNmu(Tf)
3325 !
3330 F=(Kf^3*Rhof^2+6*Hfg/(Muf*Do*Qdp))^.33333
3335 Ho=Alpa*F
3340 Two=Tsat-Qdp/Ho
3345 Tf=Tsat/3+2*Two/3
3350 Y=(1/Uo-Rm)*F
3355 X=Do*F/(Keg*Omega)
3360 ! PRINT "OMEGA=";Omega;"F=";F;"X=";X;"Y=";Y
3365 Xa(Jset)=X ! INEFFICIENT (MODIFY LATER)
3370 Ya(Jset)=Y
3375 Sx=Sx+X
3380 Sy=Sy+Y
3385 Sxs=Sxs+X*X
3390 Sxy=Sxy+X*Y
3395 Jset=Jset+1
3400 IF Jset<Nsets THEN 3135
3405 ASSIGN @File TO *
3410 Slope=(Nsets*Sxy-Sx*Sy)/(Nsets*Sxs-Sx^2)
3415 Intcpt=(Sy-Slope*Sx)/Nsets
3420 Cic=1/Slope
3425 Alpac=1/Intcpt
3430 Cerr=ABS((Ci-Cic)/Cic)
3435 Aerr=ABS((Alpac-Alpa)/Alpac)
3440 IF Cerr>.001 OR Aerr>.001 THEN
3445 Alpa=(Alpa+Alpac)*.5
3450 Ci=(Ci+Cic)*.5
3455 ! PRINT "CIC=";Cic;"ALPA=";Alpa
3460 GOTO 3100
3465 END IF
3470 BEEP
3475 BEEP
3480 PRINTER IS 1
3485 PRINT "CIC=";Cic;"ALPA=";Alpa
3490 Cia(Insert,I)=Cic
3495 Alpa(I)=Alpac

```

```

3500     PRINTER IS 701
3505     FOR J=0 TO Nsets-1
3510         OUTPUT @Xy;Xa(J),Ya(J)
3515     NEXT J
3520     PRINTER IS 1
3525     NEXT I
3530     ASSIGN @Xy TO *
3535     SUBEND
3540     SUB Nusselt
3545     COM /Nus/ Iin,Tsat,Qdp,Hoc,Kf,Rhof,Hfg,Muf,Do,Itube
3550     Do=.0159
3555     Ho=1000
3560     IF Iin=0 THEN
3565         BEEP
3570         INPUT "ENTER TSAT AND HEAT FLUX",Tsat,Qdp
3575     END IF
3580     Hfg=FNHfg(Tsat)
3585     Two=Tsat-Qdp/Ho
3590     Tf=Tsat/3+2*Two/3
3595     Kf=FNK(Tf)
3600     Rhof=FNrho(Tf)
3605     Muf=FNmu(Tf)
3610     Hoc=.655*(Kf^3*Rhof^2*9.81*Hfg/(Muf*Do*Qdp))^.333333
3615     IF ABS((Ho-Hoc)/Hoc)>.001 THEN
3620         Ho=(Ho+Hoc)*.5
3625         GOTO 3585
3630     END IF
3635     IF Iin=0 THEN PRINT "HO=";Hoc
3640     SUBEND
3645     SUB Plot1
3650     DIM Yaa(4)
3655     PRINTER IS 705
3660     Idv=1
3665     BEEP
3670     INPUT "OK TO USE DEFAULT VALUES (1=DEF=Y,0=N)",Idv
3675     IF Idv=1 THEN
3680         Itn=2
3685         Xmin=1
3690         Xmax=5
3695         Xstep=1
3700         Ymin=0
3705         Ymax=2.0
3710         Ystep=.5
3715     ELSE
3720         BEEP
3725         INPUT "ENTER MINIMUM AND MAXIMUM X-VALUES",Xmin,Xmax
3730         BEEP
3735         INPUT "ENTER MINIMUM AND MAXIMUM Y-VALUES",Ymin,Ymax
3740         BEEP
3745         INPUT "ENTER STEP SIZE FOR X-AXIS",Xstep

```

```

3750      BEEP
3755      INPUT "ENTER STEP SIZE FOR Y-AXIS",Ystep
3760      END IF
3765      PRINT "IN:SP1:IP 2300,1800,8300,6800;"
3770      PRINT "SC 0,100,0,100;TL 2,0;"
3775      Sfx=100/(Xmax-Xmin)
3780      Sfy=100/(Ymax-Ymin)
3785      PRINT "PU 0,0 PD"
3790      FOR Xa=Xmin TO Xmax STEP Xstep
3795          X=(Xa-Xmin)*Sfx
3800          PRINT "PA";X,"",0; XT;"
3805      NEXT Xa
3810      PRINT "PA 100,0;PU;"
3815      PRINT "PU PA 0,0 PD"
3820      FOR Ya=Ymin TO Ymax STEP Ystep
3825          Y=(Ya-Ymin)*Sfy
3830          PRINT "PA 0,"";Y,"YT"
3835      NEXT Ya
3840      PRINT "PA 0,100 TL 0 2"
3845      FOR Xa=Xmin TO Xmax STEP Xstep
3850          X=(Xa-Xmin)*Sfx
3855          PRINT "PA";X,"",100; XT"
3860      NEXT Xa
3865      PRINT "PA 100,100 PU PA 100,0 PD"
3870      FOR Ya=Ymin TO Ymax STEP Ystep
3875          Y=(Ya-Ymin)*Sfy
3880          PRINT "PD PA 100,"",Y,"YT"
3885      NEXT Ya
3890      PRINT "PA 100,100 PU"
3895      PRINT "PA 0,-2 SR 1.5,2"
3900      FOR Xa=Xmin TO Xmax STEP Xstep
3905          X=(Xa-Xmin)*Sfx
3910          PRINT "PA";X,"",0;"
3915          PRINT "CP -2,-1;LB";Xa;"
3920      NEXT Xa
3925      PRINT "PU PA 0,0"
3930      FOR Ya=Ymin TO Ymax STEP Ystep
3935          Y=(Ya-Ymin)*Sfy
3940          PRINT "PA 0,"";Y,""
3945          PRINT "CP -4,-.25;LB";Ya;"
3950      NEXT Ya
3955      BEEP
3960      INPUT "SELECT MODE (0=HN/H1,1=HN(avg)/H1)",Ism
3965      Ism=Ism+1
3970      IF Idv=1 THEN
3975          IF Ism=1 THEN Ylabel$="HN/H1"
3980          IF Ism=2 THEN Ylabel$="HN(avg)/H1"
3985          Xlabel$="Tube Number"
3990      ELSE
3995          BEEP

```



```

4000     INPUT "ENTER X-LABEL",Xlabel$
4005     BEEP
4010     INPUT "ENTER Y-LABEL",Ylabel$
4015     END IF
4020     PRINT "SR 1.5,2;PU PA 50,-10 CP";-LEN(Xlabel$)/2;"0;LB";Xlabel$;"
4025     PRINT "PA -11,50 CP 0,";-LEN(Ylabel$)/2*5/6;"DI 0,1;LB";Ylabel$;"
4030     PRINT "CP 0,0 DI"
4035     Okp=1
4040     BEEP
4045     INPUT "WANT TO PLOT DATA FROM A FILE (1=DEF=Y,0=N)?",Okp
4050     IF Okp=1 THEN
4055         BEEP
4060         INPUT "ENTER THE NAME OF THE DATA FILE",Dfile$
4065         ASSIGN @File TO Dfile$
4070         BEEP
4075         INPUT "ENTER THE BEGINNING RUN NUMBER",Md
4080         BEEP
4085         INPUT "ENTER THE NUMBER OF X-Y PAIRS STORED",Nsets
4090         BEEP
4095         INPUT "SELECT A SYMBOL FOR THE PLOTTER (1=*,2=+,3=c,4=o,5=^)",Sy
4100         PRINT "PU DI"
4105         IF Sy=1 THEN PRINT "SM*"
4110         IF Sy=2 THEN PRINT "SM+"
4115         IF Sy=3 THEN PRINT "SMc"
4120         IF Sy=4 THEN PRINT "SMo"
4125         IF Sy=5 THEN PRINT "SM^"
4130         FOR I=1 TO Nsets
4135             FOR J=0 TO 3
4140                 ENTER @File;Yaa(J),D
4145                 IF J=0 THEN Ytop=Yaa(0)
4150                 Yaa(J)=Yaa(J)/Ytop
4155             NEXT J
4160             FOR J=0 TO 3
4165                 X=(J+1-Xmin)*Sfx
4170                 Y=Yaa(J)-Ymin)*Sfy
4175                 PRINT "PA",X,Y,"
4180             NEXT J
4185         NEXT I
4190         BEEP
4195         ASSIGN @File TO *
4200         GOTO 4040
4205     END IF
4210     BEEP
4215     INPUT "LIKE TO PLOT THE NUSSELT RELATION (1=Y,0=N)?",Oknus
4220     PRINT "PU;SM"
4225     IF Oknus=1 THEN
4230         FOR Xa=Xmin TO Xmax STEP Xstep/50
4235             X=(Xa-Xmin)*Sfx
4240             IF Ism=1 AND Xa>Xmin THEN Ya=Xa^.75-(Xa-1)^.75
4245             IF Ism=2 AND Xa>Xmin THEN Ya=Xa^(-.25)

```

```

4250         IF Xa=Xmin THEN Ya=1
4255         Y=(Ya-Ymin)*Sfy
4260         PRINT "PA",X,Y,"PD"
4265     NEXT Xa
4270     BEEP
4275     PRINT "PU"
4280     INPUT "MOVE THE PEN TO LABEL THE NUSSELT LINE",Ok
4285     PRINT "LBNusselt"
4290 END IF
4295 IF Ism=2 THEN
4300     BEEP
4305     INPUT "LIKE TO PLOT EXPTL CURVE (1=Y,0=N)",Okex
4310     Nq=0
4315     IF Okex=1 THEN
4320         BEEP
4325         INPUT "ENTER THE EXPONENT",Ex
4330         FOR Xa=Xmin TO Xmax STEP Xstep/10
4335             Nq=Nq+1
4340             Ya=Xa^(-Ex)
4345             X=(Xa-Xmin)*Sfx
4350             Y=(Ya-Ymin)*Sfy
4355             IF Nq MOD 2=0 THEN
4360                 PRINT "PA",X,Y,"PD"
4365             ELSE
4370                 PRINT "PA",X,Y,"PU"
4375             END IF
4380         NEXT Xa
4385         PRINT "PU"
4390         BEEP
4395         INPUT "MOVE PEN TO LABEL AND HIT ENTER",Ok
4400         PRINT "LBs=0"
4405         PRINT "PR -1 0"
4410         PRINT "LB";Ex;" "
4415         GOTO 4300
4420     END IF
4425 END IF
4430 GOTO 4510
4435 BEEP
4440 INPUT "LIKE TO PLOT KERN RELATIONSHIP (1=Y,0=N)?",Yes
4445 IF Yes=1 THEN
4450     FOR Xa=Xmin TO Xmax STEP Xstep/20
4455         Ya=Xa^(-1/6)
4460         X=(Xa-Xmin)*Sfx
4465         Y=(Ya-Ymin)*Sfy
4470         PRINT "PA",X,Y,"PD"
4475     NEXT Xa
4480     PRINT "PU"
4485     BEEP
4490     INPUT "MOVE THE PEN TO LABEL KERN RELATIONSHIP",Ok
4495     PRINT "LBKern:PU"

```

```

4500     END IF
4505     PRINT "PU PA 0,0"
4510     BEEP
4515     INPUT "LIKE TO PLOT EISSENBERG RELATION (1=Y,0=N)?",Okel
4520     IF Okel=1 THEN
4525         FOR Xa=Xmin TO Xmax STEP Xstep/10
4530             Ya=.6+.42*Xa^(-.25)
4535             X=(Xa-Xmin)*Sfx
4540             Y=(Ya-Ymin)*Sfy
4545             PRINT "PA",X,Y,"PD"
4550         NEXT Xa
4555         PRINT "PU"
4560         BEEP
4565         INPUT "MOVE THE PEN TO LABEL THE EISSENBERG LINE",Ok
4570         PRINT "LBEissenberg;PU"
4575     END IF
4580     PRINT "PU SP0"
4585     SUBEND
4590     DEF FNPvst(Tc)
4595     COM /Fld/ Ift
4600     DIM K(8)
4605     IF Ift=0 THEN
4610         BEEP
4615         PRINT "PVST CORRELATION NOT AVAILABLE FOR R-114"
4620         STOP
4625     END IF
4630     IF Ift=1 THEN
4635         DATA -7.691234564,-26.08023696,-168.1706546,64.23285504,-118.9646225
4640         DATA 4.16711732,20.9750676,1.E9,6
4645         READ K(*)
4650         T=(Tc+273.15)/647.3
4655         Sum=0
4660         FOR N=0 TO 4
4665             Sum=Sum+K(N)*(1-T)^(N+1)
4670         NEXT N
4675         Br=Sum/(T*(1+K(5)*(1-T)+K(6)*(1-T)^2))-(1-T)/(K(7)*(1-T)^2+K(8))
4680         Pr=EXP(Br)
4685         P=22120000*Pr
4690     END IF
4695     IF Ift=2 THEN
4700         Tf=Tc*1.8+32+459.6
4705         P=10^(33.0655-4330.98/Tf-9.2635*LGT(Tf)+2.0539E-3*Tf)
4710         P=P*101325/14.696
4715     END IF
4720     IF Ift=3 THEN
4725         A=9.394685-3066.1/(Tc+273.15)
4730         P=133.32*10^A
4735     END IF
4740     RETURN P
4745     FNPEND

```

```

4750 DEF FNHfg(T)
4755 COM /F1d/ Ift
4760 IF Ift=0 THEN
4765 Tf=T*1.8+32
4770 Hfg=6.1451558E+1-Tf*(6.951079E-2+Tf*(1.3988688E-4+1.9607843E-7*Tf))
4775 Hfg=Hfg*2326
4780 END IF
4785 IF Ift=1 THEN
4790 Hfg=2477200-2450*(T-10)
4795 END IF
4800 IF Ift=2 THEN
4805 Tf=T*1.8+32
4810 Hfg=7.0557857E+1-Tf*(4.838052E-2+1.2619048E-4*Tf)
4815 Hfg=Hfg*2326.1
4816 Hfg=(1.611-.0031*T)*1.0E+5
4820 END IF
4825 IF Ift=3 THEN
4830 Tk=T+273.15
4835 Hfg=1.35264E+6-Tk*(6.38263E+2+Tk*.747462)
4840 END IF
4845 RETURN Hfg
4850 FNEND
4855 DEF FNMu(T)
4860 COM /F1d/ Ift
4865 IF Ift=0 THEN
4870 Tk=T+273.15
4875 Mu=EXP(-4.4636+1011.47/Tk)*1.E-3
4880 END IF
4885 IF Ift=1 THEN
4890 A=247.8/(T+133.15)
4895 Mu=2.4E-5*10^A
4900 END IF
4905 IF Ift=2 THEN
4910 Mu=8.9629819E-4-T*(1.1094609E-5-T*5.566829E-8)
4911 Tk=T+273.15
4913 Mu=1.34E-5*10.0^(503.0/(Tk-2.15))
4915 END IF
4920 IF Ift=3 THEN
4925 Tk=1/(T+273.15)
4930 Mu=EXP(-11.0179+Tk*(1.744E+3-Tk*(2.80335E+5-Tk*1.12661E+8)))
4935 END IF
4940 RETURN Mu
4945 FNEND
4950 DEF FNUvst(Tt)
4955 COM /F1d/ Ift
4960 IF Ift=0 THEN
4965 BEEP
4970 PRINT "UVST CORRELATION NOT AVAILABLE FOR R-114"
4975 STOP
4980 END IF

```

```

4985     IF Ift=1 THEN
4990         P=FNPvst(Tt)
4995         T=Tt+273.15
5000         X=1500/T
5005         F1=1/(1+T*1.E-4)
5010         F2=(1-EXP(-X))^2.5*EXP(X)/X^.5
5015         B=.0015*F1-.000942*F2-.0004882*X
5020         K=2*P/(461.52*T)
5025         V=(1+(1+2*B*K)^.5)/K
5030     END IF
5035     IF Ift=2 THEN
5040         Tf=Tt*1.8+32
5045         V=13.955357-Tf*(.16127262-Tf*5.1726190E-4)
5050         V=V/16.018
5055     END IF
5060     IF Ift=3 THEN
5065         Tk=Tt+273.15
5070         P=FNPvst(Tt)
5075         V=133.95*Tk/P
5080     END IF
5085     RETURN V
5090     FNEND
5095     DEF FNCp(T)
5100     COM /F1d/ Ift
5105     IF Ift=0 THEN
5110         Tk=T+273.15
5115         Cp=.40118+Tk*(1.65007E-3+Tk*(1.51494E-6-Tk*6.67853E-10))
5120     END IF
5125     IF Ift=1 THEN
5130         Cp=4.21120858-T*(2.26826E-3-T*(4.42361E-5+2.71428E-7*T))
5135     END IF
5140     IF Ift=2 THEN
5145         Cp=9.2507273E-1+T*(9.3400433E-4+1.7207792E-6*T)
5146         Cp=(929.0+1.03*T)/1000.
5150     END IF
5155     IF Ift=3 THEN
5160         Tk=T+273.15
5165         Cp=4.1868*(1.6884E-2+Tk*(3.35083E-3-Tk*(7.224E-6-Tk*7.61748E-9)))
5170     END IF
5175     RETURN Cp*1000
5180     FNEND
5185     DEF FNRho(T)
5190     COM /F1d/ Ift
5195     IF Ift=0 THEN
5200         Tk=T+273.15
5205         X=1-(1.8*Tk/753.95)
5210         Ro=36.32+61.146414*X^(1/3)+16.418015*X+17.476838*X^.5+1.119828*X^2
5215         Ro=Ro/.062428
5220     END IF
5225     IF Ift=1 THEN

```

```

5230      Ro=999.52946+T*(.01269-T*(5.482513E-3-T*1.234147E-5))
5235      END IF
5240      IF Ift=2 THEN
5245          Ro=1.6207479E+3-T*(2.2186346+T*2.3578291E-3)
5246      Ro=1./((.617+.000647*T^1.1)*1.0E-3)
5250      END IF
5255      IF Ift=3 THEN
5260          Tk=T+273.15-338.15
5265          Vf=9.24848E-4+Tk*(6.2796E-7+Tk*(9.2444E-10+Tk*3.057E-12))
5270          Ro=1/Vf
5275      END IF
5280      RETURN Ro
5285      FNEND
5290      DEF FNPr(T)
5295      Pr=FNCp(T)*FNMu(T)/FNK(T)
5300      RETURN Pr
5305      FNEND
5310      DEF FNK(T)
5315      COM /Fld/ Ift
5320      IF Ift=0 THEN K=.071-.000261*T
5325      IF Ift=1 THEN
5330          X=(T+273.15)/273.15
5335          K=-.92247+X*(2.8395-X*(1.8007-X*(.52577-.07344*X)))
5340      END IF
5345      IF Ift=2 THEN
5350          K=8.2095238E-2-T*(2.2214286E-4+T*2.3809524E-8)
5351          K=.0802-.000203*T
5352          K=.071-.000261*T
5353          Tf=T*1.8+32
5354          K=4.8461905E-2-Tf*6.5714286E-5
5355          K=K*1.7308
5357      END IF
5360      IF Ift=3 THEN
5365          Tk=T+273.15
5370          K=4.1868E-4*(519.442+.320920*Tk)
5375      END IF
5380      RETURN K
5385      FNEND
5390      DEF FNHf(T)
5395      COM /Fld/ Ift
5400      IF Ift=0 THEN
5405          BEEP
5410          PRINT "HF CORRELATION NOT FOR R-114"
5415          STOP
5420      END IF
5425      IF Ift=1 THEN
5430          Hf=T*(4.203849-T*(5.88132E-4-T*4.55160317E-6))
5435      END IF
5440      IF Ift=2 THEN
5445          Tf=T*1.8+32

```

```

5450      Hf=8.2078571+Tf*(.19467857+Tf*1.3214286E-4)
5455      Hf=Hf*2.326
5460      END IF
5465      IF Ift=3 THEN
5470          Hf=250 ! TO BE VERIFIED
5475      END IF
5480      RETURN Hf*1000
5485      FNEND
5490      SUB Plot2
5495      COM /Dr1/ Star,Sym,Icon
5500      COM /Fld/ Ift
5505      DIM C(9),Xya(7),Doa(4)
5510      DATA 0.0158,0.0158,0.0158,0.0158
5515      READ Doa(*)
5520      Fw=1
5525      PRINTER IS 1
5530      BEEP
5535      PRINT USING "4X,""Select Option X-Y Limits: ""
5540      PRINT USING "6X,""0 Use default values ""
5545      PRINT USING "6X,""1 Use new values ""
5550      INPUT Okd
5555      BEEP
5560      INPUT "ENTER TUBE CODE",Icode
5565      Do=Doa(Itube)
5570      Iht=2
5575      BEEP
5580      PRINT USING "4X,""Select option: ""
5585      PRINT USING "6X,""0 h versus q ""
5590      PRINT USING "6X,""1 q versus Delta-T ""
5595      PRINT USING "6X,""2 h versus Delta-T (default) ""
5600      INPUT Iht
5605      PRINTER IS 705
5610      IF Okd=0 THEN !AXIS DEFAULT VALUES
5615          IF Iht=0 THEN !(h vs q)
5620              Ymin=0
5625              Ymax=60
5630              Ystep=10
5635              Xmin=.2
5640              Xmax=1.4
5645              Xstep=.2
5650          END IF
5655          IF Iht=1 THEN !(q vs t)
5660              Xmin=0
5665              Ymin=0
5670              Ymax=.5
5675              Xmax=15
5680              Xstep=3
5685              Ystep=.1
5690          END IF
5695          IF Iht=2 THEN !(h vs t)

```

```

5700         Xmin=0
5705         Ymin=0
5710         Xmax=50
5715         Ymax=6
5720         Xstep=10
5725         Ystep=1
5730     END IF
5735 END IF
5740 IF Okd=1 THEN
5745     BEEP
5750     INPUT "ENTER MINIMUM AND MAXIMUM X-VALUES",Xmin,Xmax
5755     BEEP
5760     INPUT "ENTER MINIMUM AND MAXIMUM Y-VALUES",Ymin,Ymax
5765     BEEP
5770     INPUT "ENTER STEP SIZE FOR X-AXIS",Xstep
5775     BEEP
5780     INPUT "ENTER STEP SIZE FOR Y-AXIS",Ystep
5785 END IF
5790 BEEP
5795 PRINT "IN:SP1:IP 2300,1800,8300,6800:"
5800 PRINT "SC 0,100,0,100:TL 2,0:"
5805 Sfx=100/(Xmax-Xmin)
5810 Sfy=100/(Ymax-Ymin)
5815 BEEP
5820 Icg=0
5825 INPUT "LIKE TO BY-PASS CAGE (1=Y,0=N=DEFAULT)?",Icg
5830 IF Icg=1 THEN 6175
5835 PRINT "PU 0,0 PD"
5840 FOR Xa=Xmin TO Xmax STEP Xstep
5845     X=(Xa-Xmin)*Sfx
5850     PRINT "PA":X,",",0: XT;"
5855 NEXT Xa
5860 PRINT "PA 100,0:PU;"
5865 PRINT "PU PA 0,0 PD"
5870 FOR Ya=Ymin TO Ymax STEP Ystep
5875     Y=(Ya-Ymin)*Sfy
5880     PRINT "PA 0,":Y,"YT"
5885 NEXT Ya
5890 PRINT "PA 0,100 TL 0 2"
5895 FOR Xa=Xmin TO Xmax STEP Xstep
5900     X=(Xa-Xmin)*Sfx
5905     PRINT "PA":X,",",100: XT"
5910 NEXT Xa
5915 PRINT "PA 100,100 PU PA 100,0 PD"
5920 FOR Ya=Ymin TO Ymax STEP Ystep
5925     Y=(Ya-Ymin)*Sfy
5930     PRINT "PD PA 100,":Y,"YT"
5935 NEXT Ya
5940 PRINT "PA 100,100 PU"
5945 PRINT "PA 0,-2 SR 1.5,2"

```



```

5950   FOR Xa=Xmin TO Xmax STEP Xstep
5955       X=(Xa-Xmin)*Sfx
5960       PRINT "PA":X,"",0:"
5965       IF Xa<1 AND Xa<>0 THEN PRINT "CP -1.5,-1:LB0:PR -1,0:LB":Xa:""
5970       IF Xa=0 THEN PRINT "CP -.5,-1:LB0"
5975       Xin=0
5980       IF Xa MOD 1=0 THEN Xin=1
5985       IF Xa>=10 THEN PRINT "CP -2,-1:LB":Xa:""
5990       IF Xa>1 AND Xa<10 AND Xin=1 THEN PRINT "CP -1.25,-1:LB":Xa:""
5995       IF Xa>1 AND Xin=0 THEN PRINT "CP -2,-1:LB":Xa:""
6000       IF Xa=1 THEN PRINT "CP -1,-1:LB1.0"
6005   NEXT Xa
6010   PRINT "PU PA 0,0"
6015   FOR Ya=Ymin TO Ymax STEP Ystep
6020       Y=(Ya-Ymin)*Sfy
6025       PRINT "PA 0,"":Y,""
6030       IF Iht=0 AND Ya>0 THEN PRINT "PR 2,0"
6035       IF Ya<1 AND Ya<>0 THEN PRINT "CP -4,-.25:LB0:PR -2,0:LB":Ya:""
6040       IF Ya=0 THEN PRINT "CP -2,-.25:LB0"
6045       IF Ya>1 AND Iht<2 THEN PRINT "CP -5,-.25:LB":Ya:""
6050       IF Ya>9 AND Iht=2 THEN PRINT "CP -4,-.25:LB":Ya:""
6055       IF Ya>0 AND Ya<10 AND Iht=2 THEN PRINT "CP -3,-.25:LB":Ya:""
6060       IF Ya=1 THEN PRINT "CP -4,-.25:LB1.0"
6065   NEXT Ya
6070   IF Ord=1 THEN
6075       BEEP
6080       INPUT "ENTER X-LABEL",Xlabels$
6085       BEEP
6090       INPUT "ENTER Y-LABEL",Ylabels$
6095   END IF
6100   IF Iht<>1 THEN
6105       PRINT "SR 1.5,2:PU PA -12,35:DI 0,1:LBh:PR 1,0.5:LB0:PR -1,0.5:LB/(
MW/m"
6110       PRINT "PR -1,0.5:SR 1,1.5:LB2:SR 1.5,2:PR .5,.5:LB.:PR .5,0:LBK)"
6115   ELSE
6120       PRINT "PA -12,39:DI 0,1:LBq/(MW/m:SR 1,1.5:PR -1,0.5:LB2:SR 1.5,2:P
R 1,0,0.5:LB)"
6125   END IF
6130   IF Iht=0 THEN
6135       PRINT "SR 1.5,2:PU PA 40,-10:DI:LBq/(MW/m:PR 0.5,1:SR 1,1.5:LB2:SR
1.5,2:PR .5,-1:LB)"
6140   ELSE
6145       PRINT "DI PA 38,-10:LB(T:PR .5,-1:LBs:PR .5,1:LB-T:PR -2.4,3 PD PR
2,0 PU:PR .5,-4:"
6150       PRINT "LBwo:PR .5,1:LB)/K"
6155   END IF
6160   PRINT "CP 0,0 DI"
6165   Xlg=1.E+6
6170   Xug=-1.E+6
6175   Xal=50

```

```

6180     Yal=95
6185     Nrun=0
6190     BEEP
6195     INPUT "WANT TO PLOT DATA FROM A FILE (1=Y,0=N)?",Ok
6200     X11=1.E+6
6205     Xul=-1.E+6
6210     Okp=0
6215     IF Ok=1 THEN
6220         BEEP
6225         INPUT "ENTER THE NAME OF THE PLOT DATA FILE",D_file$
6230         ASSIGN @File TO D_file$
6235         IF Icomb<>0 THEN 6265
6240         Sx=0
6245         Sy=0
6250         Sx2=0
6255         Sxy=0
6260         Md=1
6265         BEEP
6270         INPUT "ENTER THE BEGINNING RUN NUMBER (DEF=1)",Md
6275         Npairs=9
6280         BEEP
6285         INPUT "ENTER THE NUMBER OF X-Y PAIRS STORED (DEF=9)",Npairs
6290         Nrun=Nrun+Npairs
6295         PRINTER IS 1
6300         BEEP
6305         PRINT USING "4X," "Select a symbol:"
6310         PRINT USING "4X," " 1 Star    2 Plus sign"
6315         PRINT USING "4X," " 3 Circle  4 Square"
6320         PRINT USING "4X," " 5 Rombus"
6325         PRINT USING "4X," " 6 Right-side-up triangle"
6330         PRINT USING "4X," " 7 Up-side-down triangle"
6335         INPUT Sym
6340         BEEP
6345         INPUT "ENTER TUBE NUMBER FOR PLOTTING (0=TOP,1=SECOND,...)",Itube
6350         PRINTER IS 705
6355         IF Sym=1 THEN PRINT "SM*"
6360         IF Sym=2 THEN PRINT "SM+"
6365         IF Sym=3 THEN PRINT "SMo"
6370         IF Md>1 THEN
6375             FOR I=1 TO (Md-1)
6380                 ENTER @File:Xya(*)
6385             NEXT I
6390         END IF
6395         FOR I=1 TO Npairs
6400             ENTER @File:Xya(*)
6405             Ya=Xya(Itube*2)
6410             Xa=Xya(Itube*2+1)
6415             Yc=LOG(Xa)
6420             Xc=LOG(Xa/Ya)
6425             Sx=Sx+Xc

```

```

6430      Sy=Sy+Yc
6435      Sx2=Sx2+Xc^2
6440      Sxy=Sxy+Xc*Yc
6445      IF Iht=0 THEN
6450          Xt=Ya
6455          Ya=Ya/Xa
6460          Xa=Xt
6465          IF Xa/1.E+6>Xul THEN Xul=Xa/1.E+6
6470          IF Xa/1.E+6<Xll THEN Xll=Xa/1.E+6
6475      END IF
6480      IF Iht=0 THEN
6485          X=(Xa*1.E-6-Xmin)*Sfx
6490          Y=(Ya*1.E-3-Ymin)*Sfy
6495      END IF
6500      IF Iht=1 THEN
6505          X=(Xa-Xmin)*Sfx
6510          Y=(Ya*1.E-6-Ymin)*Sfy
6515      END IF
6520      IF Iht=2 THEN
6525          X=(Xa/Ya-Xmin)*Sfx
6530          Y=(Ya*1.E-3-Ymin)*Sfy
6535      END IF
6540      IF Y>100 OR Y<0 THEN 6585
6545      IF Sym>3 THEN PRINT "SM"
6550      IF Sym<4 THEN PRINT "SR 1.4,2.4"
6555      PRINT "PA",X,Y,""
6560      IF Sym>3 THEN PRINT "SR 1.2,1.6"
6565      IF Sym=4 THEN PRINT "UC2,4,99,0,-8,-4,0,0,8,4,0;"
6570      IF Sym=5 THEN PRINT "UC3,0,99,-3,-6,-3,6,3,6,3,-6;"
6575      IF Sym=6 THEN PRINT "UC0,5.3,99,3,-8,-6,0,3,8;"
6580      IF Sym=7 THEN PRINT "UC0,-5.3,99,-3,8,6,0,-3,-8;"
6585  NEXT I
6590  BEEP
6595  INPUT "WANT TO LABEL (1=Y,0=N)?",I1b1
6600  IF I1b1=1 THEN
6605      IF Sym>3 THEN PRINT "SM"
6610      IF Sym<4 THEN PRINT "SR 1.4,2.4"
6615      PRINT "PA",Xa1,Ya1,""
6620      IF Sym>3 THEN PRINT "SR 1.2,1.6"
6625      IF Sym=4 THEN PRINT "UC2,4,99,0,-8,-4,0,0,8,4,0;"
6630      IF Sym=5 THEN PRINT "UC3,0,99,-3,-6,-3,6,3,6,3,-6;"
6635      IF Sym=6 THEN PRINT "UC0,5.3,99,3,-8,-6,0,3,8;"
6640      IF Sym=7 THEN PRINT "UC0,-5.3,99,-3,8,6,0,-3,-8;"
6645      PRINT "SM"
6650      IF Sym<4 THEN PRINT "PR 2,0"
6655      PRINT "PR 2,-1.0;SR 1.0,1.8;LB";D_file$;"
6660      Yal=Yal-5
6665      BEEP
6670      INPUT "WANT TO ADD ANOTHER STRING (1=Y,0=N)?",Ias
6675      IF Ias=1 THEN

```

```

6680         BEEP
6685         INPUT "ENTER THE STRING",Label$
6690         PRINT "PR 2,0;SR 1.0,1.8;LB";Label$;" "
6695         GOTO 6665
6700     END IF
6705 END IF
6710 BEEP
6715 INPUT "WANT TO COMBINE ANOTHER FILE? (1=Y,0=N)",Icomb
6720 ASSIGN @File TO *
6725 X11=5
6730 Xul=45
6735 IF Icomb<>0 THEN 6220
6740 BEEP
6745 INPUT "WANT TO PLOT A LEAST-SQUARES LINE (1=Y,0=N)",Ils
6750 IF Ils=1 THEN
6755     BEEP
6760     INPUT "SELECT EXPONENT: 0=COMPUTE, 1=0.75",Iexp
6765     BEEP
6770     INPUT "SELECT CURVE TYPE (0=SOLID,1=DASHED)",Ilt
6775     Ilt=Ilt+1
6780     PRINT "SM"
6785     IF Iexp=0 THEN
6790         Bb=(Nrun*Sxy-Sy*Sx)/(Nrun*Sx2-Sx^2)
6795     ELSE
6800         Bb=.75
6805     END IF
6810     Aa=(Sy-Bb*Sx)/Nrun
6815     Aa=EXP(Aa)
6820     PRINTER IS 1
6825     PRINT USING "10X","a = ",Z.4DE;Aa
6830     PRINT USING "10X","n = ",Z.4DE;Bb
6835     PRINTER IS 705
6840     In=0
6845     IF Iht=0 THEN Xxstep=Xstep/40
6850     IF Iht>0 THEN Xxstep=Xstep/10
6855     FOR Xa=X11 TO Xul STEP Xxstep
6860         IF Xa>.99*Xmax THEN 6995
6865         IF Iht=1 THEN Ya=Aa*Xa^Bb
6870         IF Iht=0 THEN Ya=Aa^(1/Bb)*(Xa*1.E+6)^((Bb-1)/Bb)
6875         IF Iht=2 THEN Ya=Aa*Xa^(Bb-1)
6880         IF Iht=0 THEN
6885             Y=(Ya*1.E-3-Ymin)*Sfy
6890             X=(Xa-Xmin)*Sfx
6895         END IF
6900         IF Iht=1 THEN
6905             Y=(Ya*1.E-6-Ymin)*Sfy
6910             X=(Xa-Xmin)*Sfx
6915         END IF
6920         IF Iht=2 THEN
6925             Y=(Ya*1.E-3-Ymin)*Sfy

```

```

6930          X=(Xa-Xmin)*Sfx
6935      END IF
6940      IF Y<0 THEN Y=0
6945      IF Y>100 THEN G990
6950      IF Ilt=1 THEN
6955          PRINT "PA",X,Y,"PD"
6960      ELSE
6965          In=In+1
6970          Ir=In MOD Ilt
6975          IF Ir=1 THEN PRINT "PA",X,Y,"PD"
6980          IF Ir=0 THEN PRINT "PA",X,Y,"PU"
6985      END IF
6990      NEXT Xa
6995      PRINT "PU"
7000  END IF
7005      Icomb=0
7010      GOTO 6185
7015  END IF
7020  PRINT "PU SM"
7025  BEEP
7030  INPUT "WANT TO PLOT NUSSELT LINE (1=Y,0=N)?",Inp
7035  IF Inp=0 THEN 7125
7040  BEEP
7045  INPUT "ENTER TSAT (DEFAULT=18 DEG C)",Tsat
7050  Hfg=FNHfg(Tsat)
7055  X11=5
7060  Xul=45
7065  FOR Xa=X11 TO Xul STEP Xstep/50
7070      Tfilm=Tsats-Xa*.5
7075      Kf=FNK(Tfilm)
7080      Rhof=FNrho(Tfilm)
7085      Muf=FNmu(Tfilm)
7090      Ya=.728*(Kf^3*Rhof^2*9.81*Hfg/(Muf*Do*Xa))^.25
7095      X=(Xa-Xmin)*Sfx
7100      Y=(Ya*1.E-3-Ymin)*Sfy
7105      PRINT "PA",X,Y,"PD"
7110  NEXT Xa
7115  PRINT "PU PA 0,0"
7120  PRINT "PU PA 0,0 SP0"
7125  SUBEND
7130  SUB Plot3
7135  COM /Dr1/ Star,Sym,Icon
7140  COM /Fld/ Ift
7145  DIM C(9)
7150  Fw=1
7155  PRINTER IS 1
7160  BEEP
7165  PRINT USING "4X,""Select Option X-Y Limits: ""
7170  PRINT USING "6X,""0 Use default values ""
7175  PRINT USING "6X,""1 Use new values ""

```

```

7180 INPUT Okd
7185 PRINTER IS 705
7190 IF Okd=0 THEN
7195     Xmin=0
7200     Ymin=0
7205     Xmax=15
7210     Ymax=15
7215     Xstep=3
7220     Ystep=3
7225 ELSE
7230     BEEP
7235     INPUT "ENTER MINIMUM AND MAXIMUM X-VALUES",Xmin,Xmax
7240     BEEP
7245     INPUT "ENTER MINIMUM AND MAXIMUM Y-VALUES",Ymin,Ymax
7250     BEEP
7255     INPUT "ENTER STEP SIZE FOR X-AXIS",Xstep
7260     BEEP
7265     INPUT "ENTER STEP SIZE FOR Y-AXIS",Ystep
7270 END IF
7275 BEEP
7280 PRINT "IN:SP1;IP 2300,1800,8300,6800:"
7285 PRINT "SC 0,100,0,100;TL 2,0;"
7290 Sfx=100/(Xmax-Xmin)
7295 Sfy=100/(Ymax-Ymin)
7300 BEEP
7305 Icg=0
7310 INPUT "LIKE TO BY-PASS CAGE (1=Y,0=N=DEFAULT)?",Icg
7315 IF Icg=1 THEN 7620
7320 PRINT "PU 0,0 PD"
7325 FOR Xa=Xmin TO Xmax STEP Xstep
7330     X=(Xa-Xmin)*Sfx
7335     PRINT "PA";X,",",0; XT;"
7340 NEXT Xa
7345 PRINT "PA 100,0;PU;"
7350 PRINT "PU PA 0,0 PD"
7355 FOR Ya=Ymin TO Ymax STEP Ystep
7360     Y=(Ya-Ymin)*Sfy
7365     PRINT "PA 0,";Y,"YT"
7370 NEXT Ya
7375 PRINT "PA 0,100 TL 0 2"
7380 FOR Xa=Xmin TO Xmax STEP Xstep
7385     X=(Xa-Xmin)*Sfx
7390     PRINT "PA";X,",",100; XT"
7395 NEXT Xa
7400 PRINT "PA 100,100 PU PA 100,0 PD"
7405 FOR Ya=Ymin TO Ymax STEP Ystep
7410     Y=(Ya-Ymin)*Sfy
7415     PRINT "PD PA 100,";Y,"YT"
7420 NEXT Ya
7425 PRINT "PA 100,100 PU"

```

```

7430 PRINT "PA 0,-2 SR 1.5,2"
7435 FOR Xa=Xmin TO Xmax STEP Xstep
7440   X=(Xa-Xmin)*Sfx
7445   PRINT "PA";X,"",0;"
7450   IF Xa<1 AND Xa<>0 THEN PRINT "CP -1.5,-1;LB0;PR -1,0;LB";Xa;"
7455   IF Xa=0 THEN PRINT "CP -.5,-1;LB0"
7460   Xin=0
7465   IF Xa MOD 1=0 THEN Xin=1
7470   IF Xa>=10 THEN PRINT "CP -2,-1;LB";Xa;"
7475   IF Xa>1 AND Xa<10 AND Xin=1 THEN PRINT "CP -1.25,-1;LB";Xa;"
7480   IF Xa>1 AND Xin=0 THEN PRINT "CP -2,-1;LB";Xa;"
7485   IF Xa=1 THEN PRINT "CP -1,-1;LB1.0"
7490 NEXT Xa
7495 PRINT "PU PA 0,0"
7500 Iht=2 ! MODIFY
7505 FOR Ya=Ymin TO Ymax STEP Ystep
7510   Y=(Ya-Ymin)*Sfy
7515   PRINT "PA 0,";Y,""
7520   IF Iht=0 AND Ya>0 THEN PRINT "PR 2,0"
7525   IF Ya<1 AND Ya<>0 THEN PRINT "CP -4,-.25;LB0;PR -2,0;LB";Ya;"
7530   IF Ya=0 THEN PRINT "CP -2,-.25;LB0"
7535   IF Ya>1 AND Iht<2 THEN PRINT "CP -5,-.25;LB";Ya;"
7540   IF Ya>9 AND Iht=2 THEN PRINT "CP -4,-.25;LB";Ya;"
7545   IF Ya>0 AND Ya<10 AND Iht=2 THEN PRINT "CP -3,-.25;LB";Ya;"
7550   IF Ya=1 THEN PRINT "CP -4,-.25;LB1.0"
7555 NEXT Ya
7560 IF Okd=0 THEN
7565   Xlabel$="X"
7570   Ylabel$="Y"
7575 ELSE
7580   BEEP
7585   INPUT "ENTER X-LABEL",Xlabel$
7590   BEEP
7595   INPUT "ENTER Y-LABEL",Ylabel$
7600 END IF
7605 PRINT "SR 1.5,2 PU PA 50,-10 CP";-LEN(Xlabel$)/2;"0;LB";Xlabel$;"
7610 PRINT "PA -11,50 CP 0,";-LEN(Ylabel$)/2*5/6;"DI 0,1;LB";Ylabel$;"
7615 PRINT "CP 0,0 DI"
7620 Nrun=0
7625 BEEP
7630 INPUT "WANT TO PLOT DATA FROM A FILE (1=Y,0=N)?",Ok
7635 Okp=0
7640 IF Ok=1 THEN
7645   BEEP
7650   INPUT "ENTER THE NAME OF THE PLOT DATA FILE",D_file$
7655   ASSIGN @File TO D_file$
7660   IF Icomb<>0 THEN 7690
7665   Sx=0
7670   Sy=0
7675   S>2=0

```

```

7680 Sxy=0
7685 Md=1
7690 BEEP
7695 INPUT "ENTER THE BEGINNING RUN NUMBER (DEF=1)",Md
7700 Npairs=9
7705 BEEP
7710 INPUT "ENTER THE NUMBER OF X-Y PAIRS STORED (DEF=9)",Npairs
7715 BEEP
7720 INPUT "SELECT TUBE NUMBER (0=TOP,1=SECOND,...)",Itube
7725 Nrun=Nrun+Npairs
7730 PRINTER IS 1
7735 BEEP
7740 PRINT USING "4X,""Select a symbol:"""
7745 PRINT USING "4X,"" 1 Star 2 Plus sign""
7750 PRINT USING "4X,"" 3 Circle 4 Square""
7755 PRINT USING "4X,"" 5 Rombus""
7760 PRINT USING "4X,"" 6 Right-side-up triangle""
7765 PRINT USING "4X,"" 7 Up-side-down triangle""
7770 INPUT Sym
7775 PRINTER IS 705
7780 IF Sym=1 THEN PRINT "SM*"
7785 IF Sym=2 THEN PRINT "SM+"
7790 IF Sym=3 THEN PRINT "SMo"
7795 Md=Itube*9
7800 IF Md>1 THEN
7805     FOR I=0 TO (Md-1)
7810         ENTER @File;X,Y
7815     NEXT I
7820 END IF
7825 FOR I=1 TO Npairs
7830     ENTER @File;Xa,Ya
7835     Sx=Sx+Xa
7840     Sy=Sy+Ya
7845     Sx2=Sx2+Xa^2
7850     Sxy=Sxy+Xa*Ya
7855     X=(Xa-Xmin)*Sfx
7860     Y=(Ya-Ymin)*Sfy
7865     IF Y>100 OR Y<0 THEN 7910
7870     IF Sym>3 THEN PRINT "SM"
7875     IF Sym<4 THEN PRINT "SR 1.4,2.4"
7880     PRINT "PA",X,Y,""
7885     IF Sym>3 THEN PRINT "SR 1.2,1.6"
7890     IF Sym=4 THEN PRINT "UC2,4,99,0,-8,-4,0,0,8,4,0;"
7895     IF Sym=5 THEN PRINT "UC3,0,99,-3,-6,-3,6,3,6,3,-6;"
7900     IF Sym=6 THEN PRINT "UC0,5.3,99,3,-8,-6,0,3,8;"
7905     IF Sym=7 THEN PRINT "UC0,-5.3,99,-3,8,6,0,-3,-8;"
7910 NEXT I
7915 BEEP
7920 INPUT "WANT TO LABEL (1=Y,0=N)?",Ilb1
7925 IF Ilb1=1 THEN

```



```

7930      IF Sym>3 THEN PRINT "SM"
7935      IF Sym<4 THEN PRINT "SR 1.4,2.4"
7940      PRINT "PA",Xal,Yal,""
7945      IF Sym>3 THEN PRINT "SR 1.2,1.6"
7950      IF Sym=4 THEN PRINT "UC2,4,99,0,-8,-4,0,0,8,4,0;"
7955      IF Sym=5 THEN PRINT "UC3,0,99,-3,-6,-3,6,3,6,3,-6;"
7960      IF Sym=6 THEN PRINT "UC0,5.3,99,3,-8,-6,0,3,8;"
7965      IF Sym=7 THEN PRINT "UC0,-5.3,99,-3,8,6,0,-3,-8;"
7970      PRINT "SM"
7975      IF Sym<4 THEN PRINT "PR 2,0"
7980      PRINT "PR 2,-1.0;SR 1.0,1.8;LB";D_file$:""
7985      Yal=Yal-5
7990      BEEP
7995      INPUT "WANT TO ADD ANOTHER STRING (1=Y,0=N)?",Ias
8000      IF Ias=1 THEN
8005          BEEP
8010          INPUT "ENTER THE STRING",Label$
8015          PRINT "PR 2,0;SR 1.0,1.8;LB";Label$:""
8020          GOTO 7990
8025      END IF
8030      END IF
8035      BEEP
8040      INPUT "WANT TO COMBINE ANOTHER FILE? (1=Y,0=N)",Icomb
8045      ASSIGN @File TO *
8050      IF Icomb<>0 THEN 7645
8055      IIs=1
8060      BEEP
8065      INPUT "WANT TO PLOT A LEAST-SQUARES LINE (1=DEF=YES,0=NO)",IIs
8070      IF IIs=1 THEN
8075          BEEP
8080          INPUT "SELECT CURVE TYPE (0=SOLID,1=DASHED)",IIt
8085          IIt=IIt+1
8090          PRINT "SM"
8095          IF Iexp=0 THEN
8100              Bb=(Nrun*Sxy-Sy*Sx)/(Nrun*Sx2-Sx^2)
8105          ELSE
8110              Bb=.75
8115          END IF
8120          Aa=(Sy-Bb*Sx)/Nrun
8125          PRINTER IS 1
8130          PRINT USING "10X,""a = "",MZ.3DE";Aa
8135          PRINT USING "10X,""n = "",MZ.3DE";Bb
8140          PRINTER IS 705
8145          In=0
8150          FOR Xa=Xmin TO Xmax STEP (Xmax-Xmin)
8155              Ya=Aa+Xa*Bb
8160              Y=(Ya-Ymin)*Sfy
8165              X=(Xa-Xmin)*Sfx
8170              IF Y<0 THEN Y=0
8175              IF Y>100 THEN GOTO 8220

```

```

8180             IF Ilt=1 THEN
8185                 PRINT "PA",X,Y,"PD"
8190             ELSE
8195                 In=In+1
8200                 Ir=In MOD Ilt
8205                 IF Ir=1 THEN PRINT "PA",X,Y,"PD"
8210                 IF Ir=0 THEN PRINT "PA",X,Y,"PU"
8215             END IF
8220             NEXT Xa
8225             PRINT "PU"
8230         END IF
8235         Icomb=0
8240         GOTO 7620
8245     END IF
8250     PRINT "PU PA 0,0"
8255     PRINT "PU PA 0,0 SP0"
8260     SUBEND
8270     DEF FNFmcal(I,T,Pc)
8280     IF I=0 THEN
8290         Mdot0=.00206*Pc-.00414
8300         Mdot24=.00225*Pc-.00329
8320     END IF
8330     IF I=1 THEN
8340         Mdot0=.00204*Pc-.00615
8350         Mdot24=.00216*Pc-.00138
8370     END IF
8380     IF I=2 THEN
8390         Mdot0=.00208*Pc-.0036
8400         Mdot24=.00223*Pc-.00301
8420     END IF
8430     IF I=3 THEN
8440         Mdot0=.0028*Pc-.00122
8450         Mdot24=.0029*Pc+.0048
8460     END IF
8470     Mdt=(T*(Mdot24-Mdot0)/24)+Mdot0
8480     RETURN Mdt
8490     FNEND

```

## LIST OF REFERENCES

1. Zebrowski, D.S., *Condensation Heat Transfer Measurements of Refrigerants on Externally Enhanced Surfaces*, M.S. Thesis, Naval Postgraduate School, Monterey, California, September 1987.
2. Mabrey, B.D., *Condensation of Refrigerants on Small Tube Bundles*, M.S. Thesis, Naval Postgraduate School, Monterey, California, December 1988.
3. Marto, P.J., *Heat Transfer in Condensation*, Boilers, Evaporators and Condensers, ed. by S. Kakal, John Wiley and Sons, pp. 525-570, 1991.
4. Nusselt, W., *The Condensation of Steam on Cooled Surfaces*, Z.d. Ver. Deut. Ing., Vol. 60, pp. 541-546 and pp. 569-575, 1916. (Translated into English by F. Fullarton in Chem. Eng. Fund., Vol. 1, No. 2, pp. 6-19, 1982).
5. Goto, M., Hotta, H. and S. Tezuka, *Film Condensation of Refrigerant Vapors on a Horizontal Tube*, Int. J. of Refrig., Vol. 3, No. 3, pp. 161-166, 1980.
6. Masuda, H. and J.W. Rose, *An Experimental Study of Condensation of Refrigerant 113 on Low Integral-fin Tubes*, Proc. Int. Symp. on Heat Transfer, Beijing, PRC, Vol. 2, paper 32, Tsinghua Univ. Press, Oct. 1985.
7. Masuda, H., *Film Condensation Heat Transfer on Low Integral-Fin Tube*, Ph.D Thesis, Queen Mary College, University of London, July 1985.
8. Marto, P.J., Zebrowski, D., and A.S. Wanniarachchi, *An Experimental Study of R-113 Film Condensation on Horizontal Integral-Fin Tubes*, J. Heat Transfer, Vol. 112, pp. 758-767, 1990.
9. Marto, P.J., *An Evaluation of Film Condensation on Horizontal Integral-fin Tubes*, Journal of Heat Transfer, Vol.110, No.4B, pp.1287-1305, 1988.

10. Marto, P.J., *Recent Progress in Enhancing Film Condensation Heat Transfer on Horizontal Tubes*, Heat Trans. Engrg., Vol. 7, pp.61-71, 1986.
11. Webb, R.L., *Enhancement of Film Condensation*, Int. Comm. Heat Mass Transfer, Vol. 15, pp. 475-507, 1988.
12. Sukhatme, S.P., *Condensation on Enhanced Surface Horizontal Tubes*, Proc. 9th Int. Heat Transfer Conference, Vol. 1, pp. 305-327, 1990.
13. Beatty, K.D. and D.L. Katz, *Condensation of Vapors on Outside Finned Tubes*, Chem. Eng. Prog., Vol. 44, No. 1, pp. 55-70, 1948.
14. Rudy, T.M. and R.L. Webb, *Condensate Retention of Horizontal Integral-finned Tubing*, Advances in Enhanced Heat Transfer, HTD-Vol. 18, pp. 35-41, 20th National Heat Transfer Conference, Milwaukee, Wisconsin, August, 1981.
15. Webb, R.L., Keswani, S.T. and T.M. Rudy, *Investigation of Surface Tension and Gravity Effects in Film Condensation*, Proc. 7th Int. Heat Transfer Conf., Vol. 5, pp. 175-180, 1982.
16. Owen, R.G., Sardesai, R.G., Smith, R.A. and W.C. Lee, *Gravity Controlled Condensation on Low Integral-Fin Tubes*, Proc. Symp. on Condensers: Theory and Practice, I. Chem. E. Symp. Ser. No. 75, pp. 415-428, 1983.
17. Webb, R.L., Rudy, T.M. and M.A. Kedzierski, *Prediction of the Condensation Coefficient on Horizontal Integral-Fin Tubes*, J. Heat Transfer, Vol. 107, pp. 369-376, 1985.
18. Adamek, T., *Rechenmodell der Filmkondensation an engberippten Kondensatorrohren*, Wärme-und Stoffübertragung, Vol. 19, pp. 145-157, 1985.
19. Honda, H. and S. Nozu, *A Prediction Method for Heat Transfer During Film Condensation on Horizontal Low Integral-Fin Tubes*, ASME J. Heat Transfer, Vol. 109, pp. 218-225, 1987.

20. Honda, H., Nozu, S. and B. Uchima, *A Generalized Prediction Method for Heat Transfer During Film Condensation on a Horizontal Low Finned Tube*, Proc. 2nd ASME-JSME Thermal Engineering Joint Conference, P.J. Marto and I. Tanasawa, eds., JSME, Vol. 4, pp. 385-392, 1987.
21. Katz, D.L., Hope, R.E., Datsko, S.C., and D.B. Robinson, *Condensation of Freon-12 with Finned Tubes, Part I. Single Horizontal Tubes*, J. Am. Soc. Refrigerating Engineers, Vol. 53, pp. 211-217, 1947.
22. Katz, D.L., Hope, R.E., Datsko, S.C., and D.B. Robinson, *Condensation of Freon-12 with Finned Tubes, Part II. Multitube Condensers*, J. Am. Soc. Refrigerating Engineers, Vol. 53, pp. 315-319, 352-354, 1947.
23. Karkhu, V.A. and V.P. Borovkov, *Film Condensation of Vapor at Finely Finned Horizontal Tubes*, Heat Transfer-Soviet Research, Vol. 3, pp. 183-191, 1971.
24. Arai, N., Fukushima, T., Arai, A., Nakajima, T., Fujie, K., and Y. Nakayama, *Heat Transfer Tubes Enhancing Boiling and Condensation in Heat Exchangers of a Refrigerating Machine*, Trans. ASHRAE, Vol. 83, pp. 58-70, 1977.
25. Kisaragi, t., Enya, S., Ochiai, J., Kuwahara, K., and I. Tanasawa, *On the Improvement of Condensation Heat Transfer on Horizontal Tubes*, JSME paper No. 780-1, pp. 1-5, 1978.
26. Carnavos, T.C., *An Experimental Study: Condensing R-11 on Augmented Tubes*, ASME Paper No. 80-HT-54, 1980.
27. Rudy, T.M., *A Theoretical and Experimental Study of Condensation on Single, Integral-Fin Tubes*, Ph.D. Thesis, The Pennsylvania State University, University Park, Pa, 1982.
28. Honda, H., Nozu, S. and K. Mitsumori, *Augmentation of Condensation on Horizontal Finned Tubes by Attaching a Porous Drainage Plate*, Proc. ASME-JSME Thermal Eng. Joint Conf., Vol. 3, pp. 289-296, 1983.

29. Kabov, O.A., *Film Condensation of Vapor on a Horizontal Finned Cylinder*, Heat Transfer-Soviet Research, Vol. 16, pp. 76-83, 1984.
30. Lin, C.C. and J. Berghmans, *R-11, R-113 and R-114 Condensation on an Enhanced Tube*, Proc. 4th Miami Int. Symp. on Multi-phase Transport and Particulate Phenomena, 15-17 December, 1986.
31. Sukhatme, S.P., Jagadish, B.S. and P. Prabhakaran, *Film Condensation of R-11 Vapor on Single Horizontal Enhanced Condenser Tubes*, J. Heat Transfer, Vol. 112, pp. 229-234, 1990.
32. Michael, A.G., Marto, P.J., Wanniarachchi, A.S. and J.W. Rose, *Filmwise Condensation of R-113 on Horizontal Integral-Fin Tubes of Different Diameters*, Proc. 9th Int. Heat Transfer Conf., Vol. 3, pp. 15-20, 1990.
33. Fujii, T., Wang, W. Ch., Koyama, Sh. and Y. Shimizu, *Heat Transfer Enhancement for Gravity Controlled Condensation on a Horizontal Tube by a Coiled Wire*, Proc. Int. Symp. on Heat Transfer, Beijing, China, 1985.
34. Kern, D.Q., *Mathematical Development of Loading in Horizontal Condensers*, Journal of the American Institute of Chem. Eng., Vol. 4, pp. 157-160, 1958.
35. Eissenberg, D.M., *An Investigation of the Variables Affecting Steam Condensation of the Outside of a Horizontal Tube Bundle*, Ph.D. Thesis, Univ. of Tennessee, Knoxville, December, 1972.
36. Butterworth, D., *Developments in the Design of Shell and Tube Condensers*, ASME Winter Meeting, Atlanta, ASME Preprint 77-WA/HT-24, 1977.
37. Young, F.L. and W.J. Wohlenberg, *Condensation of Saturated Freon-12 Vapor on a Bank of Horizontal Tubes*, Trans. ASME., Vol. 64, pp. 787-794, 1942.
38. Katz, D.L. and J.M. Geist, *Condensation on Six Finned Tubes in a Vertical Row*, Trans. ASME, Vol. 70, pp. 907-914, 1948.

39. Smirnov, G.F. and I.I. Lukanov, *Study of Heat Transfer from Freon-11 Condensing on a Bundle of Finned Tubes*, Heat Transfer-Soviet Research, Vol. 4, pp. 51-56, 1972.
40. Honda, H., S. Nozu and Y. Takeda, *Flow Characteristics of Condensate on a Vertical Column of Horizontal Low Finned Tubes*, Proc. 2nd ASME-JSME Thermal Eng. Joint Conf., Vol. 1, pp. 517-524, 1987.
41. Webb, R.L. and C.G. Murawski, *Row Effect for R-11 Condensation on Enhanced Tubes*, Trans. ASME, Vol. 112, pp. 768-776, 1990.
42. Honda, H., Uchima, B., Nozu, S., Nakata, H. and E. Torgoe, *Film Condensation of R-113 on In-line Bundles of Horizontal Finned Tubes*, J. Heat Transfer, Vol. 113, pp. 479-486, 1991.
43. Honda, H. and S. Nozu, *Effects of Bundle Depth and Working Fluid on the Optimal Fin Geometry of a Horizontal Low Finned Condenser Tube*, Proc. 2nd Int. Symp. Condensers and Condensation, HTFS, pp. 407-416, 1990.
44. Honda, H., Nozu, S. and Y. Takeda, *A Theoretical Model of Film Condensation in a Bundle of Horizontal Low Finned Tubes*, J. Heat Transfer, Vol. 111, pp. 525-532, 1989.
45. Murphy, T.J., *Pool Boiling of R-114/Oil Mixtures from Single Tubes and Tube Bundles*, M.S. Thesis, Naval Postgraduate School, Monterey, California, September 1987.
46. Chilman, S.V., *Nucleate Boiling Characteristics of R-113 in a Small Enhanced Tube Bundle*, M.S. Thesis, Naval Postgraduate School, Monterey, California, September 1991.
47. Hong, S.W. and A.E. Bergles, *Augmentation of Laminar Flow Heat Transfer in Tubes by Means of Twisted Tape Insert*, J. Heat Transfer, Vol. 98, No. 2, 1976, pp. 251-256.

48. Saha, S.K., U.N. Gaitonoe and A.W. Date, *Heat Transfer and Pressure Drop Characteristics of Laminar Flow in a Circular Tube fitted with Regularly Spaced Twisted Tape Elements*, Experimental Heat Transfer, Fluid Mechanics and Thermodynamics, ed. by R.K. Shah, E.N. Ganic and K.T. Yang, Elsevier Science Publishing Company, pp. 511-518, 1988.
49. Hausen, H., *Darstellung des Wamneuberganges in Rohren durch verallgemeinerte Potenzbeziehungen*, VDI Z., No. 4, p. 91, 1943.
50. Gough, M.J. and J.V. Rodgers, *Reduced Fouling by Enhanced Heat Transfer using Wire Matrix Radial Mixing Elements*, A. I. Ch. Eng., Vol. 83, No. 257, pp. 16-21, 1987.
51. Olivier, D.R. and R.W.J. Aldington, *Enhancement of Laminar Flow Heat Transfer using Wire Matrix Turbulators*, 8th International Heat Transfer Conference, Vol. 6, pp. 2897-2902, 1986.
52. Oliver, D.R. and R.W.J. Aldington, *Heat Transfer Enhancement in Round Tubes using Wire Matrix Turbulators: Newtonian and Non-Newtonian Liquids*, Chem. Eng. Res. Des., Vol.66, pp. 555-565, 1988.
53. Gough, M.J., J.V. Rodgers, and G.M.B. Russell, *The Development of a Practical Answer to the Improvement of Tube-side Heat Transfer*, 12th HTFS Res. Symp., Univ. Warwick, United Kingdom, pp. 123-134, 1982.
54. Kline, S.J. and F.A. McClintock, *Describing Uncertainties in Single Sample Experiments*, Mechanical Engineering, Vol. 78, pp. 3-8, 1953.
55. Incropera, F.P. and D.P. DeWitt, *Introduction to Heat Transfer*, 2nd edition, published by John Wiley and Sons, New York, pp. 127-133, 1990.
56. Cragoe, C.S., *Properties of Ethylene Glycol and its Aqueous Solutions*, Cooperative Research Council, New York, Unpublished.



57. Gallant, R. W., *Ethylene Glycols* , Physical Properties of Hydrocarbons, Golf Publishing Co., Houston, Texas, Chapter 13, pp. 109-123, 1968.
58. Chapman, R.H., *Saturated Pool and Flow Boiling Studies with Freon-113 and Water at Atmospheric Pressure* , ORNL-4987, pp. 217-220, November, 1974.

## INITIAL DISTRIBUTION LIST

		No. Copies
1.	Defense Technical Information Center Cameron Station Alexandria, VA 22304-6145	2
2.	Library, Code 52 Naval Postgraduate School Monterey, CA 93943-5002	2
3.	Department Chairman, Code 69 Department of Mechanical Engineering Naval Postgraduate School Monterey, California 93943-5000	1
4.	Professor Paul Marto Department of Mechanical Engineering Naval Postgraduate School Monterey, California 93943-5000	3
5.	Professor Stephen B. Memory Department of Mechanical Engineering Naval Postgraduate School Monterey, California 93943-5000	3
6.	Curricular Officer, Code 34 Department of Mechanical Engineering Naval Postgraduate School Monterey, California 93943-5000	1
7.	Mr. James Hanrahan, Code 2722 David Taylor Research Center Annapolis, Maryland 21402	1
8.	Mr. R. Helmick, Code 2722 David Taylor Research Center Annapolis, Maryland 21402	1
9.	LT. R.W. Mazzone 5156 Pacifica Dr. San Diego, California 92109	2